I-35W BRIDGE OVER THE MISSISSIPPI RIVER: COLLAPSE INVESTIGATION

BRIDGE NO. 9340
MINNEAPOLIS, MINNESOTA

FINAL REPORT
NOVEMBER 2008
WJE No. 2007.3702

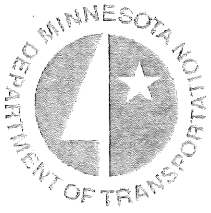

Prepared for:
Minnesota Department of Transportation
Bridge Office
Oakdale, Minnesota

WJE

Prepared by:
Wiss, Janney, Elstner Associates, Inc.
330 Pfingsten Road
Northbrook, Illinois 60062

Howard J. Hill
Jonathan C. McGormley
Michael J. Koob
William J. Nugent

Consultant's Report

WJE

I-35W BRIDGE OVER THE MISSISSIPPI RIVER
Collapse Investigation

Minneapolis, Minnesota

Howard J. Hill, Ph.D.
Principal

Jonathan C. McGormley
Associate Principal

Michael J. Koob
Senior Principal

William J. Nugent
President
State of Minnesota License No. 41787

Final Report
November 2008
WJE No. 2007.3702

Prepared for:
Minnesota Department of Transportation
Bridge Office
Oakdale, Minnesota

WJE

Prepared by:
Wiss, Janney, Elstner Associates, Inc.
330 Pfingsten Road
Northbrook, Illinois 60062
847.272.7400 tel | 847.291.4813 fax

EXECUTIVE SUMMARY

The deck truss portion of the I-35W Bridge in downtown Minneapolis, Minnesota collapsed on the warm, calm summer evening of August 1, 2007. Bridge deck overlay work was underway at the time of the collapse with four of the eight traffic lanes closed to traffic. Approximately 110 vehicles including construction equipment and materials were on the structure at the time of the collapse. Thirteen people were killed and 145 people were injured. Wiss, Janney, Elstner Associates, Inc. (WJE) was retained by the Minnesota Department of Transportation (MnDOT) at the request of the Governor of Minnesota to lead an investigation into the cause of the I-35W Bridge collapse.

At the time of the collapse, gravity loading on the bridge consisted of:

- Self weight (including overlay material and other items that had been added to the bridge following the original construction)
- Construction materials and equipment in the four lanes that were closed to traffic as part of an ongoing construction project
- Vehicle traffic in the four open lanes

The construction material included large quantities of coarse aggregate and sand for an overlay that was scheduled to have been placed the night of the collapse. This material was located in the southwest quadrant of the deck truss main span, along with several heavy pieces of construction equipment. The construction material and equipment was placed on the bridge approximately 2 to 3 hours before the collapse. Evaluation of the main span loading at the time of the collapse revealed the following:

- Forces in the most severely loaded deck truss members were nearly equal to the original design service loads.
- As designed, the deck truss members themselves were capable of carrying the construction loading and the original AASHO design lane loads in the open lanes, with an appropriate factor of safety.

Visible portions of the collapsed structure were examined and documented, after which the entire bridge was carefully taken apart. While demolition proceeded, the conditions of exposed elements were thoroughly documented as they were moved to storage areas. During this time, samples of steel and concrete elements were tested to verify key structural properties. Information obtained via the examination and testing was used to evaluate the collapsed structure. This evaluation revealed the following:

- Construction of the deck truss structure was consistent with the design documents.
- The as-built capacities of the gusset plates at the U10, U10', L11 and L11' nodes of the main span were roughly half of the capacities required by the governing design code.
- Prior to the collapse, the U10 and U10' gusset plates had not experienced any significant damage or deterioration.
- Although other elements of the structure had experienced measurable section loss due to corrosion – including some of the L11 and L11' gusset plates – at the time of the collapse, the U10 gusset plates were the most critically loaded elements in the deck truss structure and had no measurable section loss.
- The as-built ultimate capacity of the U10 gusset plates in the vicinity of the L9-U10 compression diagonals was essentially identical to the demands that existed at the time of the collapse.

- The failure mode of the U10 gusset plates predicted by non-linear finite element modeling involved substantial inelastic deformation of the plates and was consistent with the condition of the actual plates observed after the collapse.
- If the deck truss roller bearings did not move as intended, variation in the temperature of the deck truss structure, consistent with ambient temperature fluctuations and the influence of direct sunlight, would likely cause significant changes in the forces in the members framing into the U10 gusset plates.

Photographs that were taken as part of a pre-collapse inspection showed bowing in the vertical edges of the U10 and U10' gusset plates located above the L9-U10 compression diagonals. To assess the significance of this bowing, finite element models were developed that included:

- Comparable bowing in the gusset plates at comparable loads
- Gusset plate properties matching those used on the bridge (i.e. plates with about half of the required capacity)
- Gusset plates conforming to the original AASHO design requirements

The results of this effort verified that properly designed plates, with such bowing, would have been able to sustain the loading at the time of the collapse with an appropriate factor of safety. This modeling also indicated that the amount of initial distortion (i.e. distortion that existed before the plates were loaded) needed to create the observed bowing would only have reduced the strength of the affected plate, relative to that of an undistorted plate, by a few percent at most.

Failure of the I-35W Bridge began with the failure of the improperly designed gusset plates at a U10 node, in the vicinity of the L9-U10 compression diagonal. Failure at this node was followed very quickly by a similar failure at the other U10 node, which then led to the complete collapse of the deck truss system. The ability of the structure to carry the collapse-level construction loads and associated traffic loads for a few hours was most likely due to one or both of the following factors:

- The ductility of the plate failure mode, which required development of substantial plastic strains
- Changes in the loading at critical regions of the plates associated with changes in structure temperatures and/or roller bearing restraint conditions

TABLE OF CONTENTS

LIST OF TABLES

LIST OF FIGURES

I-35W BRIDGE OVER THE MISSISSIPPI RIVER
Collapse Investigation

Minneapolis, Minnesota

1 INTRODUCTION

A catastrophic failure of the 1,907-foot long I-35W Bridge over the Mississippi River in Minneapolis, Minnesota occurred on August 1, 2007 at approximately 6:05 pm CDT when all three deck truss spans and several approach spans suddenly collapsed. Bridge deck overlay work was underway at the time of the collapse with four of the eight traffic lanes closed to traffic. Approximately 110 vehicles including construction equipment and materials were on the structure at the time of the collapse. Thirteen people were killed and 145 people were injured.

This report describes and presents the results of WJE's investigation into the failure of the I-35W Bridge. An aerial view of the collapse is shown in Figure 1.1. It was evident early-on in the investigation, from observations presented in Chapter 4, that the collapse initiated in the main span at the south end of the bridge, at a location referred to in the report as Node U10. The report describes the region in the vicinity of Nodes U10 in substantial detail.

1.1 Background

Interstate 35 is a major north-south route through Minnesota. It is divided into parallel arterials I-35E and I-35W through the Minneapolis-St. Paul metropolitan area. Interstate 35W crosses the Mississippi River at the I-35W Bridge located between Washington Avenue on the south bank and University Avenue on the north bank. Figure 1.2 is an overall aerial view showing the location of the bridge near downtown Minneapolis. The bridge is located down river of the Lower St. Anthony Falls Lock and Dam operated by the Corps of Engineers and upstream of the 10th Avenue Bridge owned by the City of Minneapolis.

The I-35W Bridge, also known as Minnesota Department of Transportation (MnDOT) Bridge No. 9340, was designed by Sverdrup & Parcel and Associates, Inc. in 1965, and opened to local traffic in 1967 [1]. It consisted of a three-span continuous deck truss and 11 multi-girder and concrete voided slab approach spans for a total bridge length of 1,907 feet. Figure 1.3 shows a view of the west side of the deck truss. As of 2004, the bridge was carrying an average daily traffic count of 141,000 vehicles with heavy commercial truck traffic daily counts of 5,640 trucks across the four traffic lanes in each direction.

MnDOT was responsible for inspection and maintenance of the I-35W Bridge. The structure was routinely inspected since it was opened to interstate traffic in 1971 and has undergone in-depth inspections annually since 1994. The predominant inspection findings over these years have included riding surface deterioration, deck joint failures, bearing corrosion, concrete pier deterioration, and approach span fatigue cracking. The last National Bridge Inventory Inspection (NBIS) inspection was completed in June 2006. A Special Inspection was carried out in May 2007 to inspect selected members of the deck truss.

Several construction projects have been carried out to address maintenance and operational concerns. A 2-inch thick low slump concrete overlay was added to the bridge deck in 1977. In 1986 and 1998, locations of distortion-induced fatigue cracking in the multi-girder approach spans were repaired. In 1998,

the concrete median and barrier rails were replaced or modified to improve safety and limit water infiltration at the longitudinal joint in the bridge deck. A de-icing system was also installed at that time to reduce the potential for black ice caused by the combination of cold weather and moisture produced by heavy vehicle congestion, and nearby waterfalls, power plants and industrial facilities.

A deck patching and overlay project was implemented in June 2007 and involved milling 2 inches from the existing bridge deck, repairing full-depth and partial-depth portions of the deck at isolated locations, and replacing the entire deck surface with a new concrete overlay. At the time of the collapse, the two outside northbound lanes and two inside southbound lanes were closed to traffic. The contractor was preparing to install the new overlay on the river crossing portion of the two inside southbound lanes. Materials and equipment were stockpiled on the bridge near the south end of the overlay work.

Concerns over the potential for fatigue cracking in the non-redundant deck truss led to an initiation of a research study by the University of Minnesota that was completed in 2001 [2]. This detailed assessment found "that fatigue cracking of the deck truss [was] not likely." A subsequent study by URS Corporation re-examined the susceptibility of the bridge to fatigue cracking, the internal redundancy behavior of the structure, and possible fatigue and redundancy retrofit options. Reports summarizing their findings were submitted in 2006 [3] and 2007 [4]. Recommendations by URS included non-destructive examination of all fatigue sensitive details in tension members and removal of measurable defects, reinforcing selected truss members with steel plates to provide internal member redundancy should a fracture occur, or a combination of both options. MnDOT elected to pursue the non-destructive examination option.

After the collapse of the I-35W Bridge, rescue efforts by state, county and local agencies began immediately. One-hundred forty-five people were injured and 13 people killed. Wiss, Janney, Elstner Associates, Inc. (WJE) began its investigation on Thursday, August 2, 2007 after responding to a request from MnDOT for assistance.

1.2 Overview of Investigation

WJE was retained by MnDOT to lead an investigation into the cause of the I-35W Bridge collapse. Due to the national significance of this bridge collapse, the National Transportation Safety Board (NTSB) assumed the role of lead investigator. As a participating party in the investigation, MnDOT requested that WJE coordinate all of its on-site investigative work with the NTSB to facilitate information sharing and to avoid duplication of efforts. WJE was assisted in its investigation by subconsultants TranSystems Corporation, John W. Fisher and Associates, Inc., and Robert J. Connor and Associates, LLC.

WJE's investigation was divided into the following five broadly defined tasks briefly described in the following sections.

1.2.1 Document Review

All documents relevant to design, construction, inspection, maintenance, and the condition of the I-35W Bridge were assembled by MnDOT after the collapse and placed on their website for public access. WJE used these documents as the source of background information for its investigation.

1.2.2 Field Documentation

Major structural members were labeled post-collapse for accurate identification. Information was collected about each member including verification of design and shop drawing information, post-

collapse description of damage, final orientation, indications of fatigue cracking, and corrosion conditions. Existing loads on the bridge were evaluated, including in-place deck weight and construction loads. Members or components of interest were marked for removal, as were locations for possible testing. Structural components removed and placed in the lay-down yard were re-examined to document previously obscured conditions.

1.2.3 Removal and Storage Operations

WJE assisted MnDOT in interviewing contractors and developing a recommended list of demolition equipment. WJE worked with Carl Bolander and Sons Company, St. Paul, Minnesota, the selected contractor, in planning and overseeing removal and demolition of the bridge components in order to ensure proper documentation, adequate preservation of selected components, and appropriate opportunities for investigators to examine and record conditions both at the site and at the lay-down areas. Reasonable measures were taken to preserve the condition of critical members as they were moved with the understanding that some damage (e.g. cutting and local deformation) was unavoidable. All work was coordinated with the NTSB who maintained authority over the site.

1.2.4 Materials Testing

Selected components of the bridge were sampled and subjected to testing in accordance with appropriate standards to determine physical, chemical, and other properties of interest. The testing work was performed by WJE and the Federal Highway Administration (FHWA). The information was used to supplement analytical work. Selected member fractures were subjected to fractographic examination to characterize initial defects and other relevant features by the NTSB and Dr. John W. Fisher.

1.2.5 Structural Analysis

Various structural engineering calculations were carried out to aid in the determination of the cause of the bridge collapse. Related efforts included finite element modeling of the deck truss spans to provide information regarding member and connection demands; three-dimensional finite element analysis of various failure scenarios; detailed, non-linear finite element modeling to evaluate actual performance characteristics of gusset plates, and simple hand analyses to determine whether or not certain elements warranted more in-depth evaluation.

1.3 Organization of Report

This report is organized into seven chapters. Chapters 2 and 3 contain background and general site condition information and are entitled *Description and History of Bridge* and *Site Conditions*. Chapters 4 through 6 describe the work carried out during this investigation. These consist of *Observations and Work at Bridge and Lay-down Sites, Materials and Special Testing*, and *Structural Analysis*. Chapter 7 entitled *Discussion and Assessment* presents the cause of the bridge collapse and contributing factors. This chapter is followed by *Acknowledgments* and *References*.

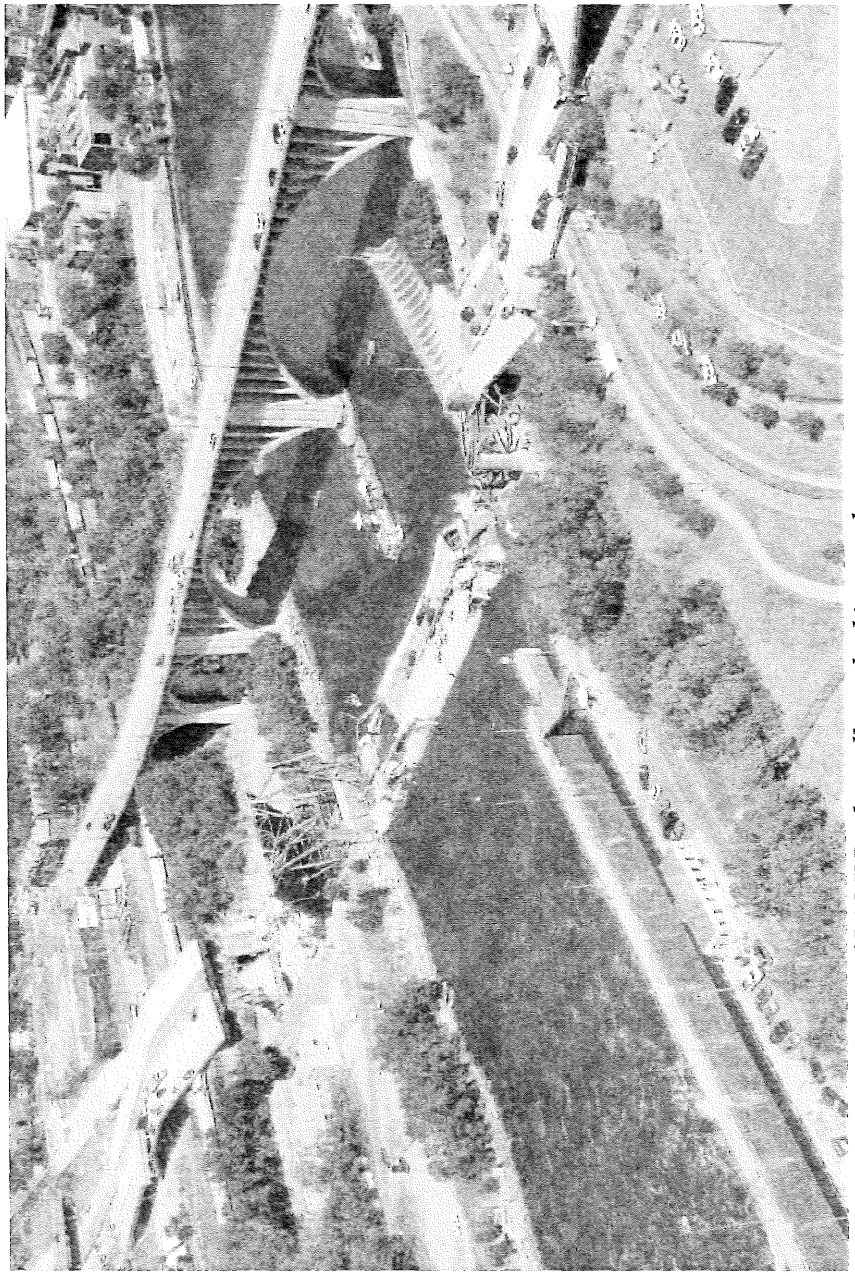

Figure 1.1. Overall view of I-35W Bridge collapse looking northeast.

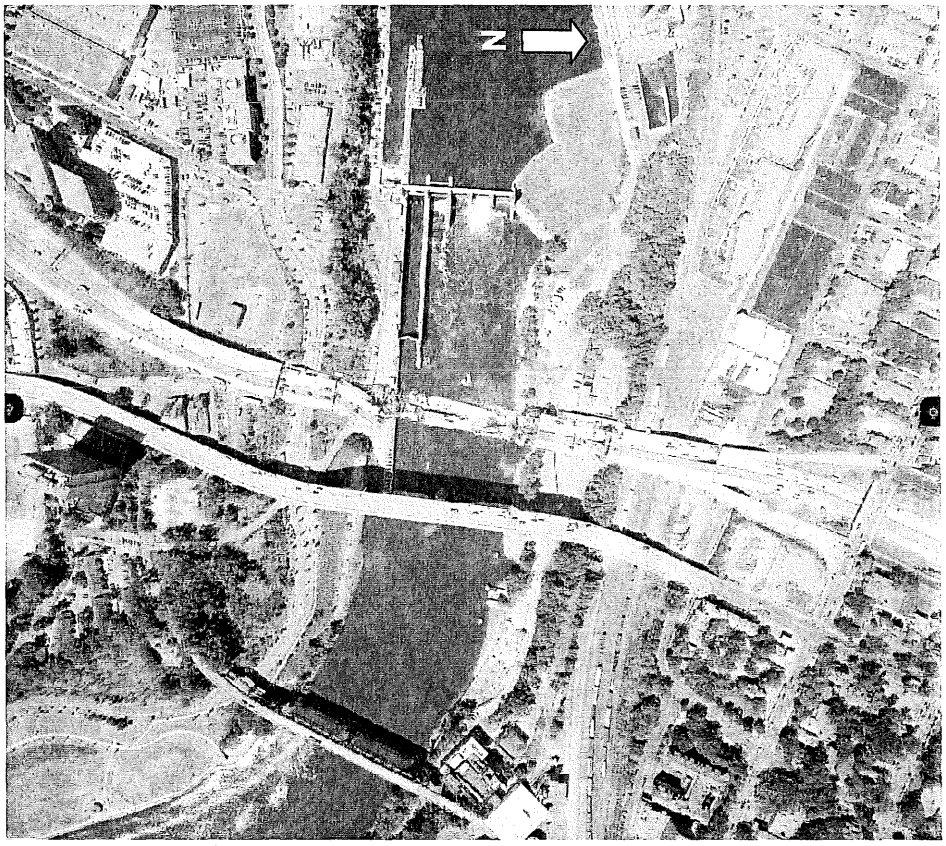

Figure 1.2. Aerial view of region around the I-35W Bridge (Bridge No. 9340).

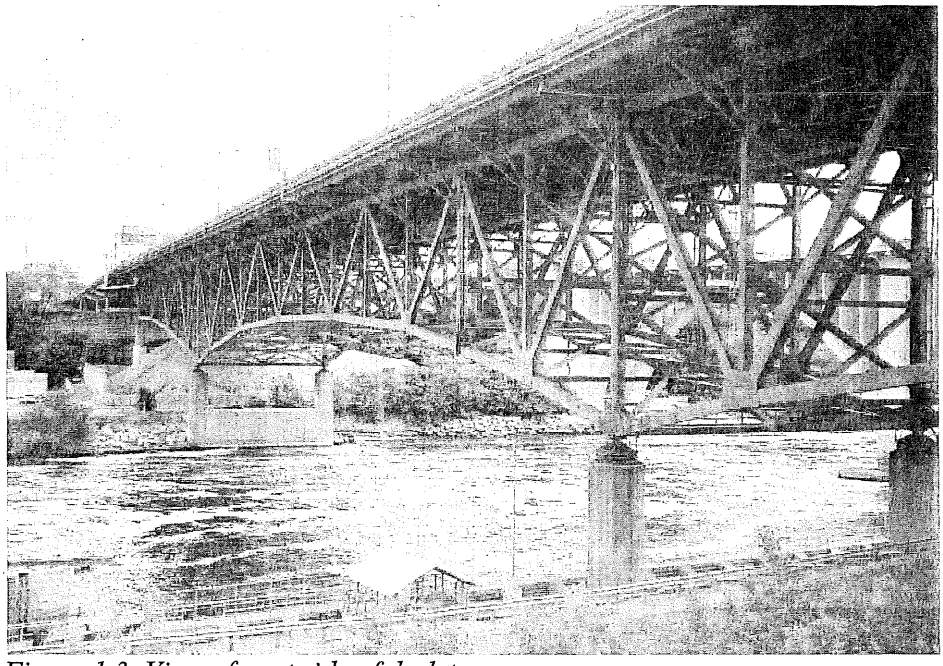

Figure 1.3. View of west side of deck truss.

2 DESCRIPTION AND HISTORY OF BRIDGE

The information presented in this chapter was obtained from MnDOT records assembled after the bridge collapse or by information released by the NTSB. These records are available to the public via the NTSB website www.ntsb.gov/dockets/Highway/HWY07MH024 and MnDOT website www.dot.state.mn.us/i35wbridge.

2.1 Description of Bridge

The I-35W Bridge, also known as Bridge 9340, consisted of a three-span continuous deck truss with a cantilever overhang at each end, and 11 multi-girder and voided concrete-slab approach spans, for a total bridge length of 1,907 feet. A plan and elevation drawing of the bridge is shown in Figure 2.1. Spans 1 to 5 were multi-steel girder spans forming the south approach spans between the South Abutment and deck truss. The deck truss made up a portion of Span 5, Spans 6 to 8, and a portion of Span 9. Spans 9 to 11 were multi-steel girder approach spans between the deck truss and Pier 11. Spans 12 to 14 were continuous concrete voided slab spans between Pier 11 and the North Abutment.

The structure carried three 12-ft traffic lanes and one 12-ft acceleration/deceleration lane in each direction over the Mississippi River. The bridge deck was wider at the north end of the north approach to accommodate on and off ramps, and curved slightly in the south approach. A typical cross section through the deck truss at Pier 7 is shown in Figure 2.2. The original reinforced concrete bridge deck thickness was 6 1/2 inches. The deck was subsequently overlayed. A 4-foot wide center median consisting of Type F concrete railing with a precast concrete median cap separated the northbound and southbound traffic and covered a longitudinal deck joint. The outside barrier rails included 10-inch tall safety curb with concrete barrier and iron rail posts. A 2 ft-8 in. tall concrete face was subsequently added in front of the rail posts.

The bridge was supported on reinforced concrete piers consisting of a footing, two circular columns (three columns for Piers 12 and 13) and a pier cap. Piers 6 and 7 also had an ice breaker wall above the footing. Piers 1 to 4 and Piers 9 to 13 were founded on steel piles while Piers 5, 7, and 8 were founded on rock. Pier 6 was supported on 48-inch diameter caissons socketed into rock. The north and south abutments were stemwall-type abutments founded on piles. Table 2.1 lists pier information.

Table 2.1 - Summary of Piers

Pier No.	Foundation	Column Diam.	Max. Height*
1	Steel piles	3′	30′-7”
2	Steel piles	3′-6”	31′-9 1/2”
3	Steel piles	3′-6”	30′-8 1/8”
4	Steel piles	3′-6”	30′
5	Spread footing	8′	38′-7 3/4”
6	Caissons	10′-6”	43′-4”
7	Spread footing	10′-6”	49′-6 3/4”
8	Spread footing	8′	62′-2 1/2”
9	Steel piles	3′-6”	28′-4 1/2”
10	Steel piles	3′-6”	22′-10 1/8”
11	Steel piles	3′	22′-3 5/8”
12	Steel piles	2′-6”	18′-7”
13	Steel piles	2′-6”	16′-3 7/8”

* Measured from top of footing to top of pier cap.

2.1.1 Deck Truss

The three-span continuous deck truss had a total centerline length of 1,064 feet with a 456-foot long river span and two 304-foot long side spans that included two approximately 38-foot long cantilever overhangs. The two trusses consisted of 28 panels, 7 in each side span between piers with one in each cantilever overhang and 12 in the river span. Each truss panel measured 38 feet with the exception of the south panel in the cantilever overhang which had chord lengths for the east and west trusses of 40 ft-4 in. and 35 ft-8 in., respectively. The trusses varied in depth from 30 feet at each end support to 60 feet over Piers 6 and 7. Midspan truss depth was 36 feet.

Nodes between panels were designated 0 (south end) through 14 (midspan) and 13′ through 0′ (north end). Top chord nodes were identified with the prefix 'U' and bottom chord nodes with the prefix 'L'. Figure 2.3 shows the structural framing and member identification for the deck truss.

The steel trusses consisted of welded box-shaped top and bottom chords, welded box-shaped vertical and diagonal compression members, and welded H-shaped vertical and diagonal tension members. Except for the top plates on the top chord, the top and bottom cover plates on the box-shaped members were fabricated with 10 inch by 20 inch perforations (access holes) spaced at 3 ft-6 in. centers. There were no perforated top cover plates used in the top chord. Some of the box-shaped members contained center web plates to stiffen the side plates while others had welded intermediate interior diaphragms spaced approximately every 15 feet. The nominal width of the truss members was 1 ft-9 in. Truss chord members were nominally 2 ft-4 in. deep, while the depth of the verticals and diagonals varied from 15 inches to 28 inches. Upper chord members were continuous through odd-numbered nodes while lower chord members were continuous through even-numbered nodes. Truss members were connected at nodes with 1/2-inch, 5/8-inch, 3/4-inch, or 1-inch thick gusset plates. Connections were made using 7/8 inch diameter rivets.

Floor trusses spanned 72 ft-4 in. between centerline of deck trusses at each node and extended beyond the trusses on each side by 16 ft-4 in. The floor trusses were composed of various rolled, wide flange shapes welded to gusset plates at node points. For identification purposes the nodes were numbered as shown in Figure 2.4. Floor truss members were identified by their beginning and end nodes, e.g. FTU5-FTL6.

The floor trusses supported fourteen 27WF94 stringers. The stringers were continuous between deck expansion joints and were composite with the deck approximately 30 feet on each side of the expansion joints. Based on previous inspection notes, stringers were numbered from west to east as S1, S2, etc.

Vertical sway frames in a chevron configuration were connected at each node with the exception of Nodes 0 and 0′. These frames consisted of a welded box-shaped 14-inch deep by 12-inch wide bottom strut and two 12-inch square diagonals. At Nodes L6 to L10 and L6′ to L10′, a second level of sway framing was added. The intermediate or middle strut framed into the truss vertical member at each end. Refer to the cross section shown in Figure 2.2 for member location and identification.

Two levels of lateral bracing were used in the bridge framing. The bracing was oriented with the chevrons pointing to the center of the bridge. The lower laterals were welded box-shaped sections measuring 14-inches tall by 12-inches wide. The upper lateral framing was 12-inch square welded box sections. Figure 2.3 shows the upper and lower lateral bracing locations and identification of truss nodes.

The deck truss spans were supported on a combination of fixed and expansion steel bearings. Expansion bearing assemblies at Piers 5, 6, and 8 enabled longitudinal movement of the bridge through a series of

rack-mounted rollers. The bearing at Pier 7 was fixed. Finger joint expansion devices were used at each end of the deck truss. Transverse strip seal deck expansion joints were located at U4, U8, U14, U8′, and U4′.

2.1.2 South Approach Spans

The 416-foot long south approach spans crossed a local street as well as an access road for the navigation locks. These five spans consisted of 14 rolled shape and/or welded plate girders that supported and acted compositely with the reinforced concrete deck. Span lengths varied from approximately 51 feet at Span 1 adjacent to the south abutment to 110 feet at interior Spans 3 and 4. Girders were spaced at 8 ft-2 in. centers and consisted of 33WF118 for Spans 1 and 2 and 48-inch deep welded plate girders for Spans 3 to 5. The girders were curved to accommodate the roadway alignment. Each girder was laterally braced by steel diaphragms spaced approximately 22 feet on center. The plate girders all framed into an end cross girder at the north end of the approach portion of Span 5. This portion of the span was supported by the cantilevered deck truss framing at U0. Girders were labeled from east to west, G1, G2, etc.

Four concrete piers (Piers 1 through 4) supported the steel girders and their bearings. At the south end, the superstructure terminated at the South Abutment. A hinge joint was located just south of Pier 2. Rocker bearings supported by the end truss floor beam were used at U0. Longitudinal expansion was accommodated by a finger joint in the deck located south of Pier 2 and at the north end of Span 5 at U0. A strip seal was used at the South Abutment.

2.1.3 North Approach Spans

The north approach spans consisted of a three-span continuous welded steel multi-girder section and a three-span continuous concrete voided slab section for a total length of 427 feet. The north approaches spanned a large stone retaining wall and four lines of railroad tracks. In the steel framing section, the fifteen, 48-inch deep plate girders ended at the south cross girder of Span 9 (U0′) and flared out to eighteen, 36-inch deep plate girders (33-inch deep for G1) in Spans 10 and 11 to accommodate the northbound exit ramp. Intermediate diaphragms were regularly spaced between girders. Shear studs were provided to compositely attach the reinforced concrete deck to the girders. Spans 12 to 14 consisted of 2-foot thick, continuous voided concrete slabs which flared to the north and included a separate northbound exit ramp structure.

Five reinforced concrete piers supported the north approaches. Piers 9 to 11 supported the superstructure on fixed and expansion bearings while Piers 12 and 13 were integral with the voided slab. The cantilevered end of the trusses at U0′ supported the cross girder on rocker bearings at the south end of Span 9 while the north approach spans ended at the North Abutment. Longitudinal expansion was accommodated by a finger joint located at the south end of Span 9 at U0′ and by a strip seal joint at Pier 11 and the North Abutment.

2.2 Design

Design of the I-35W Bridge was based on the *1961 AASHO Design Specifications* and *1961, 1962 Interim Specifications* [5], and *Minnesota Highway Department (M.H.D.) Standard Specifications for Highway Construction, 1964* [6]. All welding was in accordance with the *Specifications for Welded Highway and Railroad Bridges* published by the American Welding Society [7]. These specifications are based on allowable stress design procedures and use unfactored loads. The American Association of State High

way Officials (AASHO) was eventually replaced by the American Association of State Highway and Transportation Officials (AASHTO) as the official body governing highway and bridge design in the US.

2.2.1 Design History

Various river crossing alternates were considered prior to the construction of the I-35W Bridge, including a plate girder structure and a deck truss having four longitudinal trusses. The two truss, three-span continuous deck truss structure eventually selected reduced the width and weight of the superstructure and eliminated a river pier [8]. The selected span lengths were able to accommodate the width of the river crossing, variable ground topography, and existing roadway geometrics. The multi-girder steel approach spans were selected for economics due to the constraints placed by existing railroad tracks passing under the bridge on both sides of the river. The voided concrete slab used in Spans 12 to 14 allowed for the variable roadway width at the north end of the bridge and improved vertical clearance over 2nd Street, S.E.

Welded truss members were approved over riveted members to save an estimated 20 percent of the steel weight. The original design concept for the truss members and connections included extensive use of M.H.D. 3318 (A514) high strength (yield equal to 100 ksi), low alloy steel, commonly referred to as T-1 steel or "QT" on the drawings, to minimize weight through the use of thinner plates [9]. Figure 2.5 shows truss locations using T-1 steel as they were originally proposed [10]. The project file indicates that calculations to size the plates in each member were originally performed in October 1963 [11].

In December 1963, Sverdrup & Parcel submitted a proposed connection design at U12 as shown in Figure 2.6 [12]. The drawing calls for 1/2-inch thick QT gusset plates. Calculations received through the NTSB indicate that chord splice designs were ongoing through January 1964 [13]. These calculations include tension checks for gusset plate thickness and rivet capacities. Calculations for the U10 tension chord splice indicate 1/2-inch thick gusset plates using M.H.D. 3310 (A441) steel identified as "AS" on the drawings. Node U12 calculations match the drawing submitted in December and indicate the use of 1/2-inch thick QT steel.

Subsequent documentation in the project file indicated a desire by MnDOT in early 1964 to reduce the use of 3318 (A514) material and eliminate it from truss members due to concerns over welding T-1 steel and access concerns over fabricating and inspecting internal diaphragms required to stiffen the thinner T-1 cover plates [14][15]. The handwritten note in the margin of Figure 2.5 indicates that the members were re-proportioned to eliminate T-1 from the truss members. In the final design, only the upper and lower Node 8 gusset and splice plates used 3318 material. Figure 2.7 is a reproduction of the Sverdrup & Parcel design drawing for Nodes U10 and U12; note that the U12 gusset plate thicknesses were changed to 1 inch and material grade to AS.

Approximately 4,800 tons of steel were used in the construction of the I-35W Bridge. The bridge was constructed for a cost of $5.8 million.

2.2.2 Materials

The steel deck truss members and approach framing were fabricated using M.H.D. materials as specified in Table 2.2.

Table 2.2 - Summary of Bridge 9340 Steel Materials Specifications

Location	Description	M.H.D. No.	ASTM Number	Yield Strength, (ksi)	Tensile Strength, (ksi)
Truss/Approaches	Plates ≤ 3/4 inch	3310	A441-60T	50	70
Truss/Approaches	Plates > 3/4 inch	3309	A242	50/46*	70/67*
Truss/Approaches	Other	3306	A36-62T	36	60 - 80
Truss	Quenched Tempered	3318	A514-64	100	110 - 130
Truss/Approaches	7/8 inch Rivets	3316 Type I	A141-58	28	52 - 62
Truss/Approaches	1 inch Rivets	3316 Type IV	A406-59T	50	68 - 82
Truss/Approaches	High Strength Bolts	3391B Style II	A325-61T		115

*M.H.D. 3309 spec. value/ASTM A242 spec. value

The concrete design strength was specified at 4,000 psi. Intermediate grade reinforcing steel with an allowable stress of 20,000 psi was specified.

2.2.3 Design Loads

Truss members were designed to resist a combination of dead load (DL), live load (LL), impact (I), transverse wind load (W), wind load on live load (WL) and centrifugal forces (CF). The forces were combined as follows:

Group I = DL + LL + I
Group II = DL + 75 pounds W
Group III = Group I + 30%W + WL +CF

The bridge was designed for eight lanes of traffic in each direction. An H20-S16-44 truck with alternate military interstate loading was used for the live load design. A 26,000 pound concentrated load was also used in combination with lane live load. Code-prescribed lane loading reductions were used.

Impact percentages varied from 13 percent for the back spans to 9 percent for the main span truss members. The cantilever overhangs at U0 and U0′ had impact forces of 21 percent and 17 percent, respectively. Floor trusses, verticals (except U8-L8), and stringers received an impact of 30 percent. Table 2.3 lists the member forces for the Group I design. Table 2.4 provides a summary of the truss reactions for the Group I loadings.

The design was based on a maximum wind velocity of 100 miles per hour in accordance with the specifications. A temperature range from -30°F to 120°F was considered with the design temperature equal to 45°F.

Table 2.3 - Truss Member Group I Design Forces, kips†

Member	Dead Load	Live Load	Impact	Total
U0-U2	439T	244T	51T	734T
U0′-U2′	796T	309T	53T	1158T
U2-U4	226C	513C/437T	67C/39T	870C/307T*
U2′-U4′	31C	513C/473T	67C/43T	855C/732T*
U4-U6	516T	536T/443C	48T/58C	1119T/56C*
U6-U8	1762T	607T	67T	2436T
U8-U10	1551T	537T	59T	2147T
U10-U12	486C	402C	36C	924C
U12-U14	1899C	817C	74C	2790C
L1-L3	80T	333T/345C	43T/31C	608T/456C*
L1′-L3′	190C	394C/333T	35C/43T	722C/308T*
L3-L5	18C	572T/490C	74T/44C	906T/828C*
L3′-L5′	137C	510C/572T	46C/74T	955C/785T*
L5-L7	1087C	539C	70C	1696C
L7-L8	2533C	787C	87C	3407C
L8-L9	2543C	790C	87C	3420C
L9-L11	559C	324C	36C	919C
L11-L13	1311T	642T	58T	2011T
L13-L13′	2036T	861T	78T	2975T
U0-L1	560C	811C	65C	936C
U0′-L1′	1014C	393C	67C	1474C
L1-U2	662C	462C	60C	1184C
L1′-U2′	771C	481C	63C	1315C
U2-L3	192T	325T/217C	43T/24C	594T/102C*
U2′-L3′	291T	343T	45T	679T
L3-U4	321T	259T	29T	609T
L3′-U4′	220T	258T/200C	29T/26C	521T/42C*
U4-L5	640C	331C	36C	1007C
L5-U6	883T	344T	38T	1265T
U6-L7	1174C	415C	46C	1635C
L7-U8	1216T	388T	43T	1647T
U8-L9	1560T	476T	52T	2088T
L9-U10	1689C	548C	60C	2288C
U10-L11	1432T	489T	54T	1975T
L11-U12	1215C	459C	51C	1725C
U12-L13	834T	380T	42T	1256T
L13-U14	214C	285C/213T	31C/24T	552C/66T*
U1-L1	323C	207C	62C	592C
U2-L2	266T	207T	62T	535T
U3-L3	320C	207C	62C	589C
U4-L4	234T	207T	62T	503T
U5-L5	318C	207C	62C	587C
U6-L6	275T	207T	62T	544T
U7-L7	333C	207C	62C	544C
U8-L8	2527C	714C	79C	3320C
U9-L9	331C	207C	62C	600C
U10-L10	271T	207T	62T	540T
U11-L11	269C	207C	62C	538C

Member	Dead Load	Live Load	Impact	Total
U12-L12	270T	207T	62T	539T
U13-L13	330C	207C	62C	599C
U14-L14	244T	207T	62T	513T

† Unless noted otherwise, forces apply to opposite member as well.
C = compression force T = tension force

* Includes reversal due to live load when 90% of dead load is considered.

Table 2.4 - Group I Reactions, Kips

Pier/Node	Dead Load	Live Load	Impact	Total
5/L1	1098	497	65	1660
6/L8	3660	1001	110	4771
7/L8′	3589	999	110	4698
8/L1′	1446	557	72	2075

2.3 Construction

The bridge was constructed between 1965 and 1968 by Industrial Construction Division, Minneapolis, Minnesota, according to Minnesota Department of Highways Bridge Construction and Engineering weekly and monthly reports. The foundations, footings, and pier columns and caps were constructed between November 1965 and August 1967. Erection of the approach spans began in November 1966. Erection of the main steel truss spans started May 9, 1967 and was completed August 11, 1967. By November 1967, except for the electrical system and painting, the bridge construction was complete.

A review of the construction file indicates the following issues and resulting changes occurred during construction:

- An auger became stuck at the plan location of Caisson No. 15 at Pier 6. Therefore, Caisson No. 15 was not installed at the plan location, but offset from Caisson No. 21, with a rock socket approximately 8 foot lower than Caisson No. 21. The pier footing was redesigned to accommodate this new location.
- Additional borings were taken at Pier 4 due to the presence of fill. No changes were determined to be necessary.
- Welded shop splices of the top and bottom chords of the floor trusses were eliminated.
- Rivets designed to anchor the casting to the truss at the expansion bearings at U0 and U0′ could not be installed. Therefore, turned bolts were approved and installed instead.
- The erection sequence of Span 6 was modified to avoid a falsework bent positioned in the roadway and over a storm sewer.
- The anchor bolts at Piers 6 and 7 were drilled and grouted prior to the erection of the steel for the bearings.
- Riveting was originally specified to occur after erecting the truss spans. To expedite commencement of erection of the adjacent approach spans, riveting followed erection of individual truss sections as closely as possible. This change in sequence assumed that holes in joints were milled for the rivets to act in bearing.

During erection, the end bearings of the deck truss were temporarily supported approximately 10 inches low to facilitate closure of the main truss at U14, and then jacked up and placed on the final bearings at

Piers 5 and 8 followed by final detailing. The truss reactions at Piers 5 and 8 were measured using the hydraulic jacking system during closure of the main steel trusses to determine the actual loads. No overstresses to the truss members and no reactions beyond tolerable limits were recorded during the erection procedure. At the time of the closure, most stringers in Span 7 were not in place.

2.4 Inspections

The NBIS were enacted by Congress in 1968 in response to the 1967 Silver Bridge collapse in West Virginia. The NBIS required Federal Aid Highway bridge owners to inventory their bridges and inspect them every 2 years. However, MnDOT has carried out routine bridge inspections for the I-35W Bridge annually since the bridge was opened to interstate traffic in 1971.

Revisions to the NBIS in 1988 after another bridge failure resulted in special inspection requirements for bridges with fracture critical members. MnDOT followed these special inspection requirements as part of subsequent annual inspections. Beginning in 1994, in-depth fracture critical inspections, in addition to routine bridge inspections, were performed by MnDOT annually. Conditions noted in routine inspection reports between 1994 and 2006 were also noted in the fracture critical inspection reports.

The I-35W Bridge was a non-redundant truss structure and thus was potentially susceptible to catastrophic failure as a result of a truss member not being able to carry its required forces. MnDOT inspected the structure in accordance with fracture critical bridge inspection standards set forth in the NBIS. A fracture critical inspection of steel members in tension consists of an arms-length inspection using visual and other non-destructive evaluation techniques. Because one of the primary causes of failure in fracture critical members is fatigue, tension members with fatigue-sensitive details are of particular concern. Fatigue-sensitive details in truss tension members, if subjected to cyclical live load stress have the potential for crack initiation, growth, and fracture.

The deck truss contained several fatigue-sensitive details including welded diaphragms and intermittent fillet welds in truss tension members and longitudinal stiffener terminations and plug welds in floor trusses. Laboratory testing has classified certain welded details based on their performance under in-plane fatigue loading. The details have been assigned categories, with a Category A detail performing at the highest level with respect to stress range versus cycles and a Category E or E′ detail performing at the lowest level.

In the I-35W Bridge, the welded tabs attaching the internal diaphragms to the truss tension members are classified as Category D details while the floor trusses contain Category E details. The constant amplitude fatigue limit for Category D and E details is 7.0 ksi and 4.5 ksi, respectively. Cyclic tensile stress ranges below these values are assumed to produce no fatigue growth in a member.

2.4.1 Summary of Routine Inspection Findings

The structural deficiencies noted during the annual routine inspections between 1971 and 1994 (time prior to fracture critical bridge inspection standards) included the following items. The first year in parenthesis indicates when the condition was first noted; the year following in italics is when the condition was no longer noted in the inspection reports. Subsequent years indicate that the condition was observed again or was in a different location.

- Substructure
  - Approach spans:
    - Minor scrapes and spalls on Pier 9 east column due to a 1969 train derailment (1973).
    - Cracks and spalls on Pier 11 (1977/*1985*).
    - Moderately deteriorated pier caps at north end of bridge (1983/*1985)*.
    - Spalling on pier (3rd pier from North Abutment) (1980/*1982*).
    - Some concrete areas require patching (1987).
    - Cracking and spalling on the south abutment bridge seat (1978).
  - Main truss spans:
    - A vertical crack in the west column of Pier 7 (1974).
- Superstructure
  - Approach spans:
    - Isolated corrosion of girder bottom flanges below center median and deck expansion joints, and pack rust on stringer in Span 4 (1988).
    - Cracked stiffeners on south cross girder (1986/*1987*)
  - Main truss spans:
    - Loose or broken bolts at stringer-to-floor truss connections (1991-1993).
    - Light corrosion of members below open finger joints (1972).
    - Corrosion and/or section loss of floor trusses (1979), truss members (1982) and connections (1987) below median and deck expansion joints. Specific locations of corrosion were noted as follows:
      - Corrosion on top flanges of Span 7 (1988).
      - Section loss of the L11E gusset plate and of the L13 sway brace (1993).
      - Severe corrosion of L7-L8E (1979, *as of 1985 still present*)
      - Missing cotter pin at a floor truss diagonal strut connection (1993).
      - Nicks and weld flaws in some members; no cracking noted (1992).
      - Cracks at welds in Floor Truss 5 (1993).
      - Cracks at welds at stringer bearing block (1993).
      - Loose pin connection at diagonal strut between floor truss and stringer (1985).
      - Section loss and cracks at stiffener welds in the north floor beam (1992, *1992*).
- Bearings
  - Approach spans:
    - Corroded bearing plates at South Abutment (1988).
    - Possible "frozen" Pier 4 expansion bearings (1993).
  - Main truss spans:
    - Dirt/debris under roller bearings (1982, *still present as of 1986*)
- Deck
    - Cracking, spalling and/or delamination of the concrete overlay (1971/*1972 cracks sealed*, 1973/*1978,* 1979/*1992 NB east two lanes*).
    - Limited movement capability at some expansion joints (1974).
    - Deteriorated slab soffit concrete under median (1983/*1985*, 1987).

2.4.2 Summary of Fracture Critical Inspection Findings

Fracture critical inspections of the bridge performed after 1999 generally did not include inspection of the interiors of the truss members as screens had been installed over the perforations to prevent access for

pigeons. During inspections in 2004 and every year after, the covers were removed from the tension and reversal members to visually inspect and test any questionable welds with magnetic particle test equipment. The last inspection of the bridge was performed by MnDOT in May 2007.

The structural deficiencies noted during the fracture critical and routine inspections between 1994 and 2007 included the following items:

- Substructure
  - Approach spans:
    - Pier 1 tilted north due to extensive corrosion at the Span 2 hinge (1996).
    - Cracking of Pier 2 was observed (2003).
    - Delaminations were observed on Pier 10 (2003).
    - Spalling of Pier 11 in areas not previously repaired (1994).
    - Cracking and spalling on the south abutment bridge seat (1994).
  - Main truss spans:
    - Minor cracking/staining of both Piers 5 and 8 from leaking deck joints (1994).
    - A vertical crack in the west column of Pier 7 (1995).
- Superstructure
  - Approach spans:
    - Fatigue cracks in the girder webs at the top of diaphragm connections in negative moment regions of the spans (1998, *1998-1999*, 2000).
    - Paint flaking, surface rust, section loss and/or moderate surface pitting of girder ends under expansion joints (1994).
    - Corroded south cross girder and rocker bearings (1994, *1998-1999*), cracked stiffeners along south cross girder (1997, *1997*)
    - Crack in stiffener of north cross girder (1992/*1992,* 1998/*1998)*,
    - Section loss of girder and east hinge rocker corroded (1996/*1998-1999*)
  - Main truss spans:
    - Loose or broken bolts and rotated bearing blocks at stringer-to-floor truss connections (1994).
    - Corrosion and/or section loss of floor trusses, truss members and connections below medians and deck expansion joints (1994). Specific locations of corrosion were noted as follows:
      - L8′E-L9′E (2003)
      - L11E (1995)
      - L13E (1995)
      - U11 gusset (1994)
      - U13 gusset (1994)
    - The end floor trusses and middle portions of the floor trusses, sway bracing, and stringers were painted in 1999.
    - Surface rust at the ends of stringer near expansion joints (1994).
    - Cracks in tack welds at internal diaphragms in members:
      - L12-L13, east and west (1996)
      - L13-L14, east and west (1996)
      - L13-U14, east (2004)
      - L14-L13′, east and west (1999)
      - L13′-L12′, east (1997) and west (2004)

    - L12′-L11′, east (1999).
  - Gouge along a connection weld of floor truss web member (2000)
  - Bent diagonal between the top and bottom chord of a floor truss, reportedly due to original construction.
  - Cracked welds between floor truss and stringer bearing (1994).
  - Surface corrosion and pitting on interior of box members (1995).
  - Missing cotter pin at a floor truss connection (1994).
  - Corroded areas ground out on U9W-U10W and on U8W-L9W (*1994*).
  - Flanges show out-of-plane bending at L6′W-U6′W (2006).
  - Fascia stringers exhibit minor section loss (2006).
- Bearings
  - Approach spans:
    - Corroded rocker assemblies (1994).
    - Corroded hinge at Span 2, located below an open finger joint, expanded beyond movement capabilities and "frozen" (1994/*1999*). The bearing surface moved off the plate (2002).
  - Main truss spans:
    - Corroded truss end rocker bearings and main truss bearings (1994). The bearings at Piers 5 and 8 were functioning properly. However, the bearings at Pier 6 did not show signs of movement (1997).
- Deck
  - Approach spans:
    - Spalling on the underside of the median and exterior deck soffits, along with some transverse leaching cracks; full depth deck repair patches (1994/*1998*, 1999).
  - Main truss spans:
    - Spalling on the underside of the median and exterior deck soffits, along with some transverse leaching cracks; full depth deck repair patches (2001).
    - Spalling, patch repairs, and extensive delamination in the overlay (1994/*1998,* 1999/*2001,* 2002).

An underwater inspection in 2000 by Collins Engineers, Inc. found Pier 7 to be in good condition with no defects of structural significance. An underwater inspection in 2004 by Ayres Associates found no evidence of scour or changes to structure condition.

2.4.3 Load Rating

First appearing in the Federal Register April 27, 1971, the NBIS regulations required bridge authorities to rate bridges to determine their safe load carrying capacity in accordance with the AASHO *Manual for Maintenance Inspection of Bridges 1970.* Later NBIS regulations required load rating in accordance with the AASHTO *Manual of Condition Evaluation of Bridges* [16] or AASHTO *Guide Specifications for the Strength Evaluation of Existing Steel and Concrete Bridges* [17]. Load rating was required in the interest of public safety, due to state and federal requirements, and as a basis for prioritizing replacement. Bridges should be load rated when they are new, after reconstruction, when deficiencies are noted by inspectors, and for permit load applications.

Each bridge should be load rated for both an Inventory Rating and Operating Rating level. Inventory loading represents the typical load crossing the bridge (HS20). The rating considers the condition of the existing bridge and any associated deterioration and is used for comparison to new bridge construction

ratings. The Operating Rating is the maximum permissible live load on the bridge. As with the Inventory Rating, the Operating Rating also considers the existing condition of the bridge. Bridges which have Operating Ratings below acceptable limits may require posting to limit the type of traffic permitted on the bridge.

MnDOT completed a load rating of the I-35W Bridge in 1979 possibly associated with the 1977 overlay work; however, there are no calculations indicating the rating method or members rated. The bridge was given an Inventory Rating of HS15.9 and an Operating Rating of HS30.6.

In 1995, the approach spans for the I-35W Bridge were load rated in accordance with the load factor design approach. The load rating indicated an Inventory Rating of HS20 and an Operating Rating of HS33. The rating was controlled by flexure at midspan of the steel girders in Span 4 of the south approach spans. Load rating of the deck truss spans were not performed. A follow-up load rating was carried out in 1997 to account for the additional weight from the modified barrier rails. The load rating also included the deck truss stringers. The results from this load rating indicated that the same members as in 1995 controlled the bridge rating; however, the Inventory and Operating Ratings rating were reduced to HS19 and HS31.5, respectively. According to MnDOT, the 1997 bridge rating was never entered into the bridge management database.

In addition to load ratings, inspection ratings also influence the administrative ranking of a bridge with regard to rehabilitation or replacement funding. Bridges with a National Bridge Inventory (NBI) condition rating of "4" or less for the deck, superstructure, or substructure or an appraisal rating of "2" or less for structural condition are considered "Structurally Deficient". Those with an appraisal rating of "3" or less for deck geometry, underclearances, approach roadway alignment, or structural condition are considered "Functionally Obsolete". Any bridge classified as structurally deficient is excluded from the functionally obsolete category. An un-posted bridge classified as structurally deficient can still safely carry its rated load.

As of the June 2006 inspection, the following ratings were assigned to the I-35W Bridge: Deck = 5, Superstructure = 4, and Substructure = 6. Due to the poor condition rating of a "4" for the superstructure, the bridge was classified as "Structurally Deficient".

The condition and appraisal ratings are used in part to calculate a sufficiency rating for a bridge. The sufficiency rating is then used to establish funding eligibility and priority for bridge replacement. Other factors affecting the sufficiency rating include the load rating, average daily traffic, and the detour length.

2.5 Repair and Overlay Work

Several construction projects to address maintenance and operational concerns have occurred since the I-35W Bridge was completed in 1967. The following sections outline the primary work completed prior to August 2007.

2.5.1 1977 Overlay Work

A bridge deck restoration and overlay placement project was completed in 1977 [18]. Research in the 1970's led MnDOT to increase the concrete cover over the top mat of reinforcing steel to 3 inches using a high-density overlay. The restoration work included joint reconstruction at all 11 expansion joints, Type 1 bridge deck removal in the southbound lanes of Spans 4, 5, and 10, Type 3 bridge deck removal as required, reconstruction of the traffic barriers, hinge repairs, and structural steel painting near joints. Type

1 involves removing concrete down to the level of the top reinforcing steel while Type 3 is full depth. For the overlay, 1/4 inch of concrete was scarified and replaced with a two-inch thick wearing course of low slump concrete. For this project, the overlay concrete constituent materials were stockpiled below the bridge and batched using a mobile concrete mixer on the bridge deck.

2.5.2 1985 Pier 11 Repairs

Repairs were undertaken in 1985 to reconstruct the Pier 11 pier cap [19]. The work included removing unsound concrete and anchoring shotcrete to the existing pier cap. Also during this time period, a 1-foot thick reinforced concrete shell was cast against Pier 8 to help strengthen the pier from lateral loads of dredging material stored by the Corps of Engineers under the bridge. Figure 2.8 shows the reinforced pier. The fill material was provided to contractors wanting clean fill. The fill was subsequently removed after 2001 due to security concerns because of the fill height providing unrestricted access to the truss members [20].

2.5.3 1998 Roadway and Structural Steel Repairs

Numerous repair procedures were instituted in 1998 to address various operational and maintenance issues. The work included replacement of the concrete median and steel plate beam barrier with a new concrete slab and Type F concrete barrier with precast concrete caps in order to limit water infiltration through the longitudinal deck joint [21]. Other work involved facing the existing outside barrier with a 10-inch thick by 2 ft-8 in. high segment of concrete to create a new barrier profile. Figure 2.9 shows the new facing. New expansion joint strip seal glands were installed at both abutments and Pier 11.

Retrofits were made to arrest cracks adjacent to the cross girder bearing at the third girder connection of the north approach span and to install new bracing at the same location. The rocker bearings were cleaned at both cross girders.

In October 1998, a routine inspection by MnDOT identified a long crack in the Girder G2 diaphragm connection in Span 9, as shown in Figure 2.10. The retrofit included drilling out the crack tips with a 6-inch diameter hole saw and bolting 3/8-inch thick plates to the girder web.

A new de-icing system was also installed to reduce the potential for black ice caused by the combination of cold weather and moisture from heavy vehicle congestion, nearby waterfalls, power plants and industrial facilities.

2.5.4 1999 - Painting and Approach Span Steel Modifications

In 1999 the approach span interior diaphragms were modified to address out-of-plane, distortion-induced cracking at 33 identified locations [22]. The modifications involved removing nine lines of diaphragms in negative moment regions of the approach spans, lowering their elevation to the girder bottom flange, and drilling new bolt holes as shown in Figure 2.11. Under-size diameter bolts were snug tightened in the holes to permit slight diaphragm end rotations. Arrest holes were drilled in the girder webs to remove crack tips at all 33 of these connections.

The modification was part of a contract which consisted of painting approximately 20 percent of the steel members, removing bird droppings and nesting material, and installing plastic covers over perforations in deck truss members to prevent entry from birds. The painting limits were generally below the longitudinal deck joint, each side of the deck truss and Pier 2 joints.

2.5.5 2000 to 2007 Miscellaneous Maintenance

In 2001, an overlay repair project was undertaken to improve the bridge riding surface. Fifteen-thousand square feet of the 219,000 square foot of deck was repaired.

Repairs to the Pier 2 hinges were undertaken to correct over extension of the sliding plate bearings. The bearings were re-set and the hinge painted.

2.5.6 2007 Overlay Work

A bridge patching and overlay project began in the summer of 2007 as part of a larger corridor reconstruction program [23]. The work on the I-35W Bridge included removal of 2 inches of the 1977 overlay, patching of unsound bridge deck concrete, placement of a new 2-inch concrete overlay, rehabilitation of the deck expansion joints, and reconstruction of the anti-icing system. Concrete patching included both Type 1 and Type 3 repairs. Refer to Section 2.7 for specific details of the overlay work.

2.6 Previous Studies

To address cracking issues in the approach spans and potential fatigue concerns associated with the non-redundant deck truss portion of the I-35W Bridge, MnDOT retained the services of several outside consultants to independently evaluate elements of the bridge. Each of the consultants produced a report detailing their work. The following sections summarize the scope and findings of these reports.

2.6.1 Bridge Support Strain Monitoring of Bridge 9340 - TH35W over Mississippi

In 1997, a small instrumentation study was carried out to determine the stress near the Girder G3-to-cross girder connection in the north approach spans [24]. Earlier inspections had found cracking at this location just above the cross girder bearing. The distortion-induced cracking was thought to be a result of a restrained rocker bearing or G3 end rotations under live load. Eight strain gages were installed and monitored by Maxim Technologies/Twin City Testing, St. Paul Minnesota. Information from the study was used to develop a retrofit at the cross girders

2.6.2 Bridge 9340 - Load Test Results

Routine bridge inspections had identified cracking at 33 approach span diaphragm-to-girder connections, as discussed earlier. The University of Minnesota (U of M) was engaged in 1998 to evaluate whether lowering the diaphragms and reducing the rigidity of the connections would improve their performance [25]. Instrumentation was placed on Girders G2 and G6 north of Pier 3 and strains were measured as three 50,000 pound control trucks in different configurations travelled over the bridge. The results found a reduction in girder stress as a result of repositioning the diaphragms and reducing the connection rigidity; subsequently, all approach span diaphragms in negative moment regions were repositioned.

2.6.3 Fatigue Evaluation of the Deck Truss of Bridge 9340

A research report evaluating the fatigue performance was submitted by the U of M in 2001. The purpose of the research was threefold

1) *characterize the actual statistical distribution of the stress ranges;*
2) *evaluate the potential for fatigue cracking in the deck truss and, if there is the potential for cracking, to estimate the remaining life;*
3) *recommend increased inspection or retrofitting, if necessary.*

The U of M work included a literature review, field testing, and analysis of the deck truss. The impetus behind the testing was that the bridge was designed using specifications later determined to be unconservative with respect to fatigue. Using design live load stress ranges, the Category D and E details found in the deck truss were thought to have limited remaining fatigue life. An instrumentation and field testing program was instituted to determine the actual stress range in critical members. This information was then used to estimate the fatigue life and calibrate a finite element model of the bridge.

Node 10 was selected for instrumentation due to catwalk access to both trusses. Six strain gauges were installed in each truss on members U8-U10, L9-U10, and L9-L11. Gauges were also installed in FT10 on Top Chord U5-U6, Diagonal U5-L6, and Bottom Chord L4-L6. To measure the effects of load reversal on a member, U4-U6 was also selected on the west truss as was L3-U4, a highly stressed tension member.

Nine MnDOT tandem-axle trucks, each weighing about 51,000 pounds, were used in four test configurations. These configurations included 1) three trucks single-file simultaneously in each left lane travelling at a crawl, 2) nine trucks in a 3 by 3 configuration travelling at highway speeds, 3) nine trucks single-file positioned in the traffic lane over the truss travelling at highway speeds, and 4) three trucks side-by-side travelling at highway speeds. By comparison to the test loading, the design lane loading previously used to analyze the truss for fatigue was approximately equal to 80,000-pound trucks spaced at 125 foot intervals.

Test 1 produced a stress range of 4.1 ksi in the floor truss bottom chord and was the largest stress range recorded in any member in all four tests. Test 2 yielded the highest stress range in the main truss, with stress ranges in the lower chord, diagonal, and upper chord members framing into Node 10 of 1.9 ksi, 1.5 ksi, and 1.2 ksi, respectively. Tests 3 and 4 did not yield higher stress ranges.

Extended monitoring of normal traffic passage was also done between March and August 2000 to prepare stress range histograms to assess fatigue life. Data indicated that the peak stress ranges were comparable to the load test stress ranges. The measured data also revealed that no values exceeded the constant amplitude fatigue limit of 4.5 ksi for Category E details.

Various two-dimensional and three-dimensional finite element models were created to analyze the deck truss. Strain gauge data was used to calibrate the model to better reflect actual bridge behavior. Results found the stress range in the deck truss members below the fatigue limit for a Category D detail. Similar results were found for the Category E details in the floor trusses. The U of M report concluded that fatigue cracking in the deck truss was not expected.

2.6.4 *Initial Inspection Report for: Fatigue Evaluation of Bridge 9340 35W Over Mississippi River*

In 1998, due to the observed cracking in the approach spans, MnDOT prepared an in-house action plan to address possible performance issues associated with the I-35W Bridge [26]. The minutes of a meeting held on November 23, 1998 called for the creation of an action plan in the event the truss members develop major cracks. After numerous conversations with other consultants and a subsequent request for proposals, MnDOT awarded a contract to URS Incorporated to provide a comprehensive study of the I-35W Bridge.

The first component of the contract was a limited field inspection of the bridge. In June 2003, URS and MnDOT inspectors examined the truss members, floor beams, truss bearings, truss connections, miscellaneous connections and bracing members. An arms-length inspection requiring removal of the access hole covers was carried out at critical truss members. URS also marked bearing positions to assess their movement. The overall condition of the truss was identified as being good with regard to corrosion. Localized corrosion was noted below deck joints and inside some of the truss members. The bearings did not appear to be moving freely. No fatigue cracks were noted. Figure 2.12 shows a photo of Node U10W taken during the inspection. Node U10E is shown in Figure 2.13. As will be established later, these were the critical nodes involved in the collapse of the bridge. Figures 2.14 and 2.15 show Nodes U10'W and U10'E, respectively. These photos were part of a large catalog of photos taken by URS during the inspection that documented all connections [27]. The photo descriptions indicate the gusset plates were in good condition and noted the sensors installed by the U of M. There was no mention of the gusset plate distortion observed at all four locations shown in the photos.

2.6.5 Second Inspection Report for: Fatigue Evaluation of Bridge 9340 35W Over Mississippi River

A second inspection was carried out by URS with MnDOT in November 2003. The focus of this inspection was the assessment of the bearings. URS field measurements found inconsistent measurements between trusses. Figures 2.16 to 2.18 are photos of bearings at Pier 5, Pier 6, and Pier 8, respectively, taken during this inspection [28].

2.6.6 Fatigue Evaluation and Redundancy Analysis: Bridge 9340 I35W- Over Mississippi River

In 2007, URS completed its comprehensive study of the I-35W Bridge and submitted a draft report. The primary objectives of this report were

1) *identify critical superstructure members that are most susceptible to cracking,*
2) *evaluate structural consequences if one of the critical members should sever, in terms of load redistribution and load carrying capacities of remaining members,*
3) *develop contingency repairs to selected fracture critical members, and*
4) *establish measures for improving structural redundancy and minimizing tensile stresses in the trusses, and develop a preferred deck replacement staging plan.*

A strength evaluation of the truss members carried out by URS determined that the truss members were appropriately designed in accordance with the 1961 design specifications if considered as axial members pinned at the connections. However, if subjected to the higher design loads specified in the 2004 AASHTO LRFD Bridge Design Specifications and if considered fixed at each end and thus subjected to both in-plane and out-of-plane bending forces, URS determined that certain truss members in the U0-U1 cantilever overhang of the truss were found to be overstressed with regard to their ultimate capacities.

A fatigue evaluation of the truss by URS confirmed the U of M findings that there were no fatigue concerns. In spite of these findings, URS and MnDOT were still concerned about the non-redundant nature of the deck truss and cited 1) limited access to possible fatigue cracks should they occur, 2) the 3.5-inch length of the welded tabs which approaches the 4-inch lower limit established for a Category E fatigue detail, and 3) the potential to underestimate the number of fatigue cycles using the design fatigue truck due to heavier than average traffic as reasons to further evaluate the bridge. In subsequent work, URS identified 26 tension members in each truss most sensitive to fatigue. Six members within each truss

did not meet the performance requirements of a Category E detail; however, the members did meet the Category D detail fatigue threshold limit.

Eight tension members (L1-L2, U0-U1, L3-U4, U4-U5, U3′-U4′, L4-L5, L12-L13, and L13-L14 and symmetric members) were further evaluated for structural redundancy and retrofit options. Under a series of live load conditions, each of the critical members was removed from the model and the subsequent members and connections capacities checked. URS based these checks on the AASHTO provision requiring connection strengths to be 75 percent to 100 percent of the member strengths. The results of the redundancy evaluation found that in the event of the loss of one of the eight studied members, 20 truss members would subsequently fail leading to catastrophic failure of the bridge.

URS proposed three possible retrofit options: 1) retrofitting the 52 critical tension members with a bolted plate option to provide internal redundancy to the members. Figure 2.19 shows the proposed redundancy plate locations. 2) Non-destructive examination of all 52 members with removal of any preexisting defects exceeding one quarter of the web plate thickness. 3) A combination of retrofitting 24 of the most fatigue sensitive members and non-destructively testing the remaining 28 fracture sensitive members.

2.7 Current Overlay Work

As described in previous sections, a bridge patching and overlay project began in June 2007. Progressive Contractors Incorporated (PCI) was the general contractor for the project. Work on the I-35W Bridge began by rotomilling the two outside northbound lanes followed by the two southbound outside lanes. After completing the work in the outside southbound lanes, southbound traffic was moved to these lanes and the two inside southbound lanes were subsequently milled as shown in Figure 2.20.

The deck was profiled at the expansion joints during milling to remove the minimum specified 2 inches of existing deck. A 9-inch wide gutter on the outside lanes remained to allow the new overlay to match the existing surface. Type 1 (partial depth) and Type 3 (full depth) concrete patches were then installed after milling, as was new expansion joint concrete.

Beginning at the end of June, PCI began placement of the new concrete overlay. The overlay material was a low-slump, cement-rich concrete which required site batching instead of being supplied by conventional ready mix trucks. PCI elected to stage the mixing equipment and materials just beyond the end of each scheduled concrete placement. Typical equipment staged during concrete placements included a concrete mixing truck, 3000 gallon water truck, bulk cement truck(s), skidsteer, and concrete buggies. Stock piles of coarse aggregate and sand were staged near the mixing equipment. A Bidwell vibratory screed, initially positioned at the opposite end of each placement, was used to place the new concrete overlay.

In total, seven placements were completed before August 1. Preparation for the eighth placement was underway on the day the bridge collapsed. Table 2.5 summarizes the various placement dates, reported quantity of concrete placed, and a description of where equipment and materials were stockpiled. Refer to Figure 2.21 for an illustration of the various concrete placements.

In five placements, the concrete staging area was located off the bridge. During the July 6 placement, two crews were used to place the overlay on the southbound outside lanes of the south approach and deck truss spans. Starting in the middle, each crew worked towards the end of the bridge. Equipment and materials for the southbound crew were staged off the bridge while the equipment and materials for the northbound crew were staged on the north approach spans.

During the June 23 pour, equipment and materials were staged on a portion of the northbound outside lanes of Spans 8 and 9. At this location, three 24-ton loads of coarse aggregate and three 24-ton loads of sand were stockpiled. An additional load of coarse aggregate and sand were stockpiled on the ramp.

On August 1, PCI was preparing to place the overlay for the two southbound lanes from Node 0′ at the end of the deck truss south to Node 14, the deck truss centerline. At the time, concrete patch repairs south of Pier 6 had not achieved their design strength so loads were not placed on the deck in this area. Equipment and materials were subsequently staged between Pier 6 (Node 8) to Node 14. Figure 2.22 is a photograph of the bridge taken from a commercial airline passenger showing the material stockpiles. The photo was taken at approximately 3:30 pm.

In the period between the photo and the bridge collapse at 6:05 pm, the contractor delivered the bulk cement truck and consolidated the aggregate and sand stockpiles with the skidsteer. According to the contractor, all equipment/materials were in place by 5:00 pm. The contractor was loading the mobile mixer in preparation to batch concrete when the bridge collapsed. Placement was to start at 7:00 pm.

Based on interviews, photos, and weight tickets, the NTSB compiled the best estimate of construction loads and their respective positions on the bridge at the time of the collapse. Figure 2.23 shows the position of equipment and materials staged between Node 8 and Node 14. An estimated 577,235 pounds of construction loads were present in this region, including 383,200 pounds of aggregate.

A review of post-accident interview transcripts and project documents reveal no mention of concerns for staging equipment and materials on the bridge. PCI indicated that they asked MnDOT about storing materials on the bridge prior to July 6 to avoid having to move the material and were told by MnDOT that it was fine [29]. MnDOT does not recall any request by PCI for permission to stage materials on the bridge [30].

Table 2.5 - Summary of Overlay Placements

Date 2007	Location	Concrete Quantity	Description
June 28	SB - outside lane, onramp wedge	10.4 CY	Equipment/materials staged on ramp
July 2	SB - outside lanes, north abutment to Node 0′	90 CY	Equipment/materials staged on ramp
July 6	SB - outside lanes, south abutment to Node 0′	288 CY	Two crews worked from middle of pour each way to end of bridge. Equipment/materials staged off bridge on south and on north approach spans.
July 19	NB - outside lanes, south abutment to Pier 6	150 CY	Equipment/materials staged off bridge
July 23	NB - outside lanes, Pier 6 to Node 4′	115.5 CY	Equipment/materials staged from Node 4′ to just past Node 0′
July 25	NB - outside lane, Node 4′ to off ramp	98 CY	Equipment/materials staged on ramp
July 27	NB - outside lane, Node 4′ to north abutment	124 CY	Equipment/materials staged on ramp
August 1	SB - inside lanes, Node 14 to Node 0′	±95 CY	Equipment/materials staged between Pier 6 and Node 14

2.8 Traffic Loading

MnDOT maintains loop detectors to record traffic volumes and speeds over the I-35W Bridge. As of 2004, the Average Daily Traffic (ADT) count for the I-35W Bridge was 141,000 vehicles with an Average Daily Truck Traffic (ADTT) equal to 5,640 or 4 percent trucks. Values were for traffic in both directions over 24 hours.

URS examined the traffic data during a week in September 2004 as part of its comprehensive study of the bridge and determined the average weekday traffic for northbound and southbound vehicles was 78,500 and 80,310, respectively. The heaviest peak hour demand was found to be 4:00 pm to 5:00 pm with a northbound volume of 6,330 vehicles and a southbound volume of 4,980 vehicles. The average weekday truck traffic was 350 trucks per hour in each direction.

Trucks with single axle weights exceeding 20,000 pounds, tandem axle weights over 34,000 pounds, or a gross vehicle weight over 80,000 pounds are required to obtain an overweight permit prior to travelling across interstate bridges in Minnesota. MnDOT issued over 3,200 overweight permits during the 12 months preceding the collapse. Fifty of those permit loads crossed the I-35W Bridge [31]. Those permits included 31 trips by mobile cranes with total gross weight up to 144,500 pounds and 19 other permit loads with a total gross weight up to 145,000 pounds. The City of Minneapolis Fire Department indicated that 19 fire engines crossed the bridge within the previous 12 months [32]. The heaviest fire engine had a rear axle weight of 47,740 pounds and a gross vehicle weight of 66,400 pounds. At the time of the collapse there were no overweight vehicles on the bridge. The heaviest vehicle crossing the bridge at the time of the collapse was a semi tractor trailer weighing approximately 50,900 pounds.

Section 1513 of the *2005 MnDOT Standard Specifications for Construction* specifies that contractors shall comply with the same load restrictions as normal legal traffic [33]. The restriction applies to bridges open to traffic as well as those under construction and has been in effect since 1968. Should a contractor elect to move an overweight vehicle such as a mobile crane on to a bridge, approval from the MnDOT Construction Project Engineer is required. The MnDOT Construction Project Engineer would commonly consult with the Regional Construction Engineer in the Bridge Office when a contractor requests approval for an overweight load. The Load Rating Unit or Design Unit would subsequently evaluate the bridge to determine the acceptability of the overweight load and any conditions such as restricting traffic loading for the load crossing. A review of the records by WJE found no request for MnDOT to evaluate construction loading. No calculations were found which evaluated the truss capacity against the expected construction loads on the bridge.

2.9 Anti-Icing System

An anti-icing system was installed to reduce winter vehicular accidents on the bridge. The nearby Lower St. Anthony Falls on the Mississippi River, power plants and industrial facilities created a moisture-rich environment causing ice formation on the bridge deck during the winter months. Vehicular exhaust from traffic congestion on the bridge also provided a source of moisture for ice formation. The system was the first of its kind installed in the US.

Boschung Company Incorporated designed, furnished and installed the anti-icing system. It included sensors, a Road Weather Information System (RWIS), a computerized control system, 38 valve units, and 76 spray nozzles which dispensed potassium acetate. An adjacent pumphouse contained a 3,100 gallon liquid anti-icing chemical storage tank. Sensors monitored the bridge deck temperatures and, with the RWIS, relayed real-time conditions to a computer control site at a MnDOT maintenance yard. The

computer control system used the sensor and RWIS information to control the application of potassium acetate. When directed to spray, the valve units located in the center median would release potassium acetate to the spray nozzles. Eight nozzles were located in the barrier walls at the north end of the bridge while 68 flush-mounted spray disks were spaced 55 feet on center in each direction of travel. Figure 2.24 shows a typical deck-mounted spray disk. When activated, each nozzle would release a charge of potassium acetate in approximately 2 seconds with the whole system operation cycle requiring 10 to 12 minutes to complete.

Potassium acetate was selected over other liquid anti-icing chemicals because it is non-reactive with structural steel and reinforcing steel in concrete, biodegradable, and available in bulk quantities. The Cryotech's CF7® potassium acetate used in the system contains no chlorides and has a freezing point of minus 76 °F. During the summer months, the potassium acetate was replaced with water to allow the system to be maintained and tested.

An in-house study by MnDOT to evaluate the performance of the anti-icing system found that the system correctly detected hazardous conditions, applied the anti-icing chemical and prevented formation of ice build-up. This reduced accidents by 68 percent during the study period. It was noted during the study, that the Cryotech CF7® reacted with galvanized metals [34]. MnDOT did a follow-up inspection and found no evidence of loss of galvanizing on elements routinely exposed to the anti-icing chemical [35].

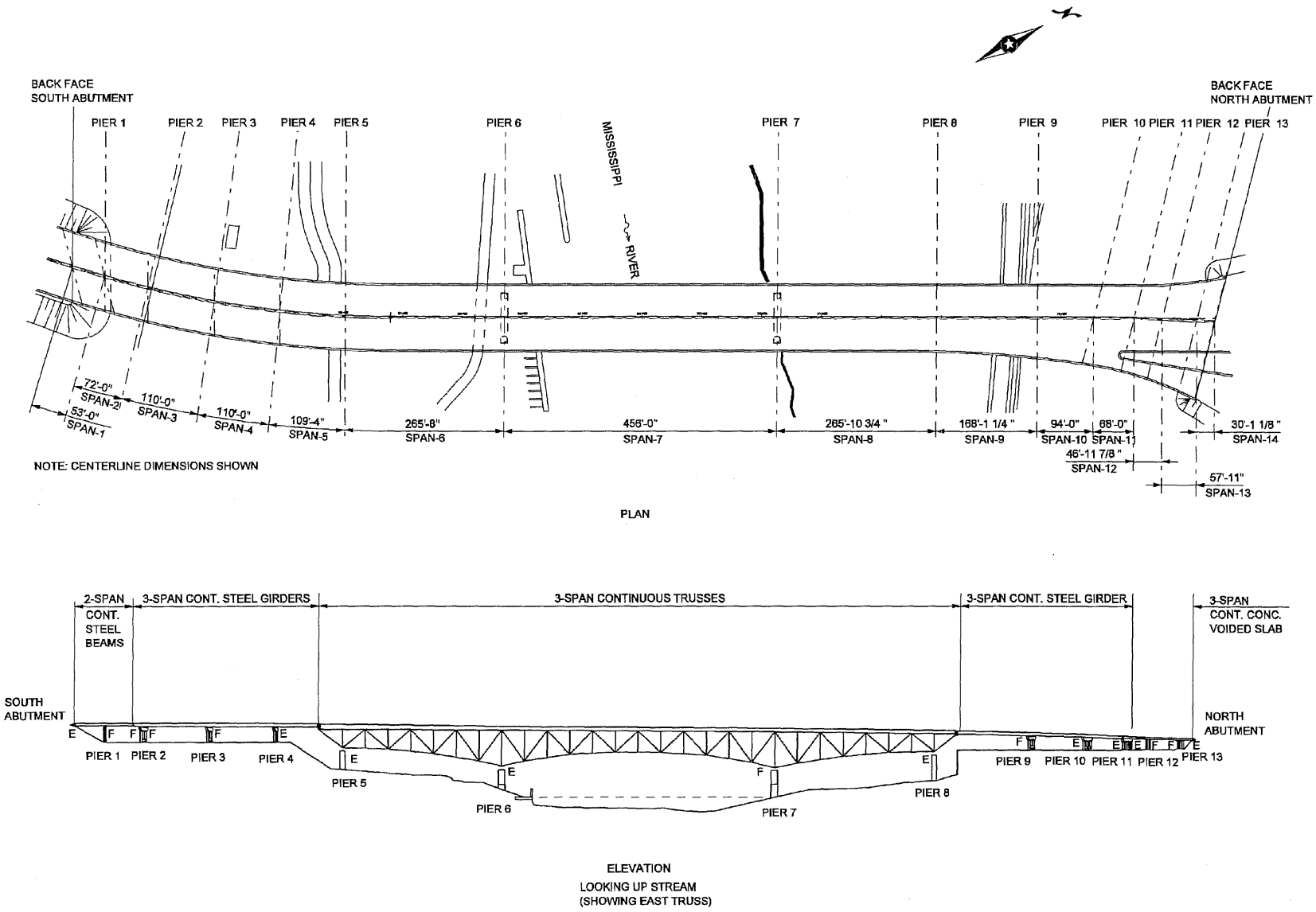

Figure 2.1. Plan and elevation of bridge.

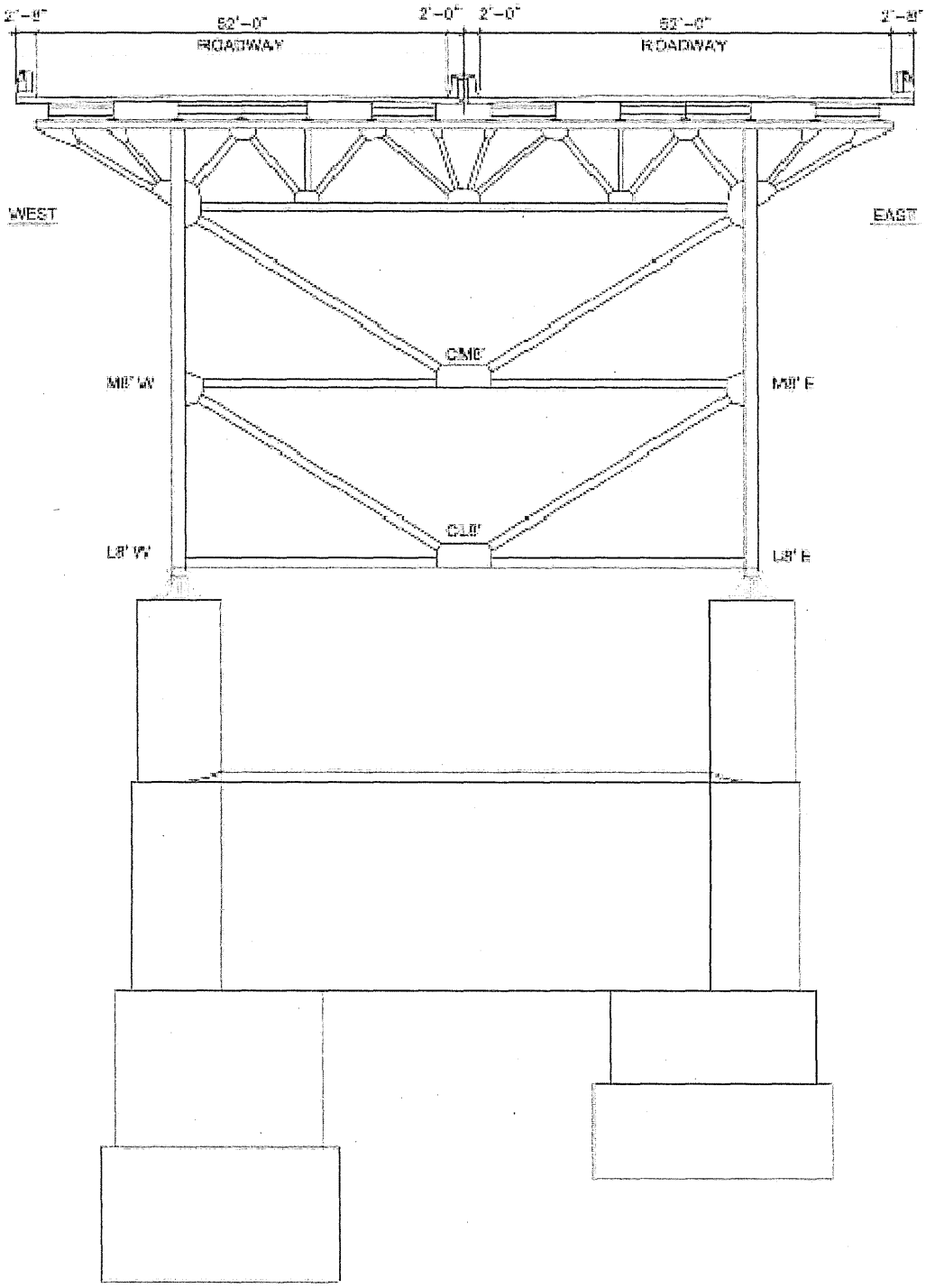

Figure 2.2. Deck cross section at Pier 7.

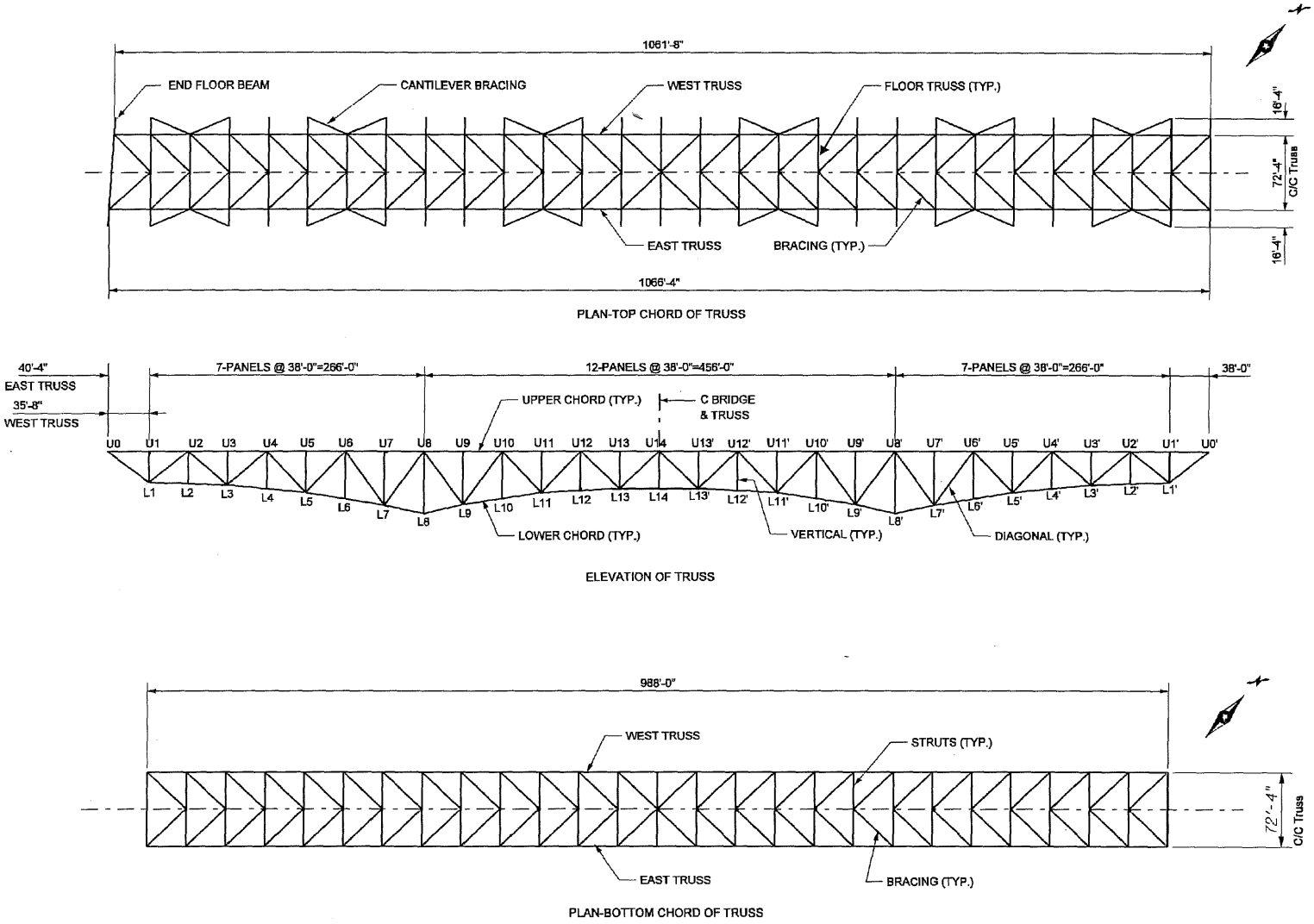

Figure 2.3. Deck truss structural framing.

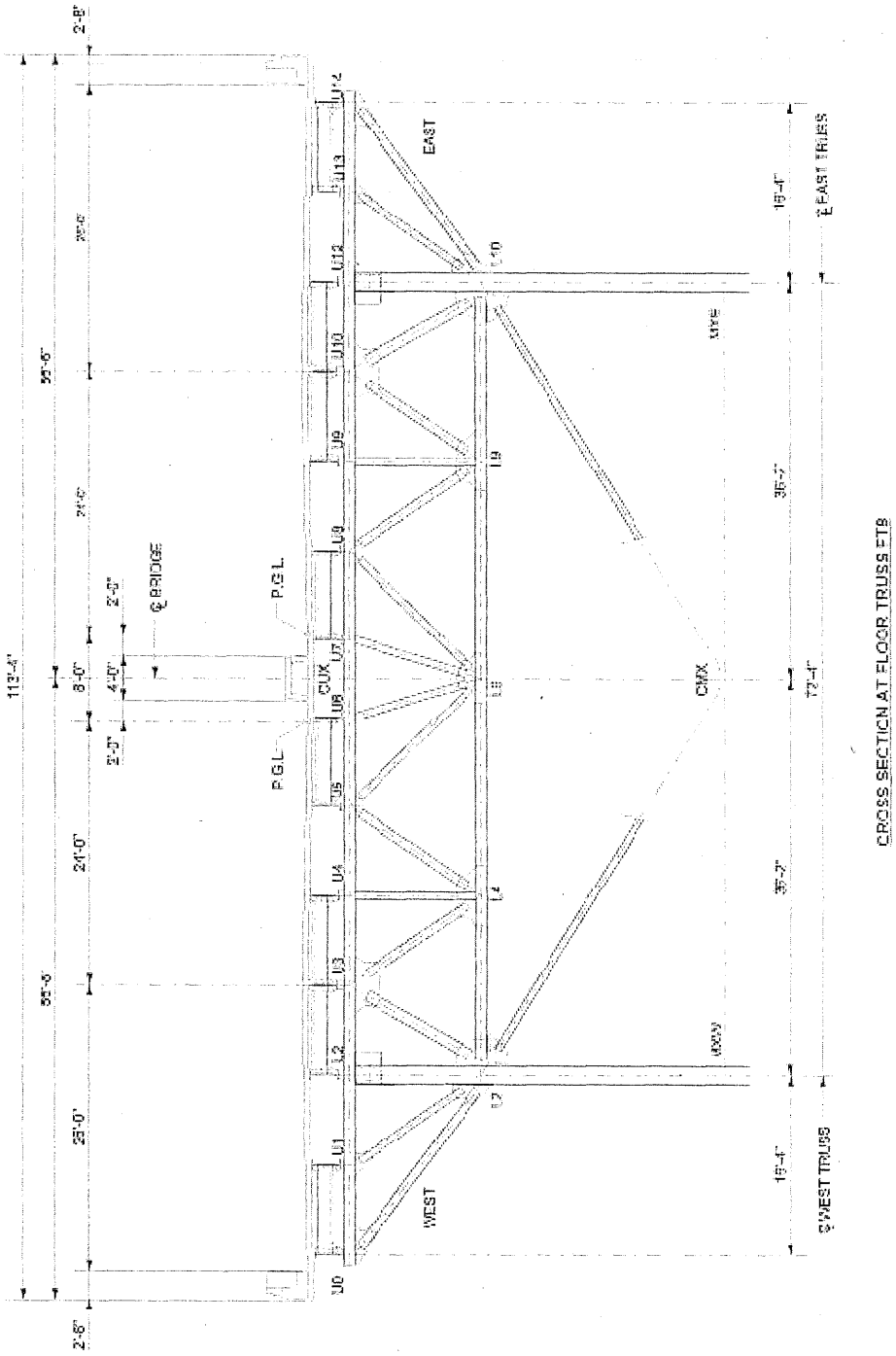

Figure 2.4. Floor truss framing and member identification.

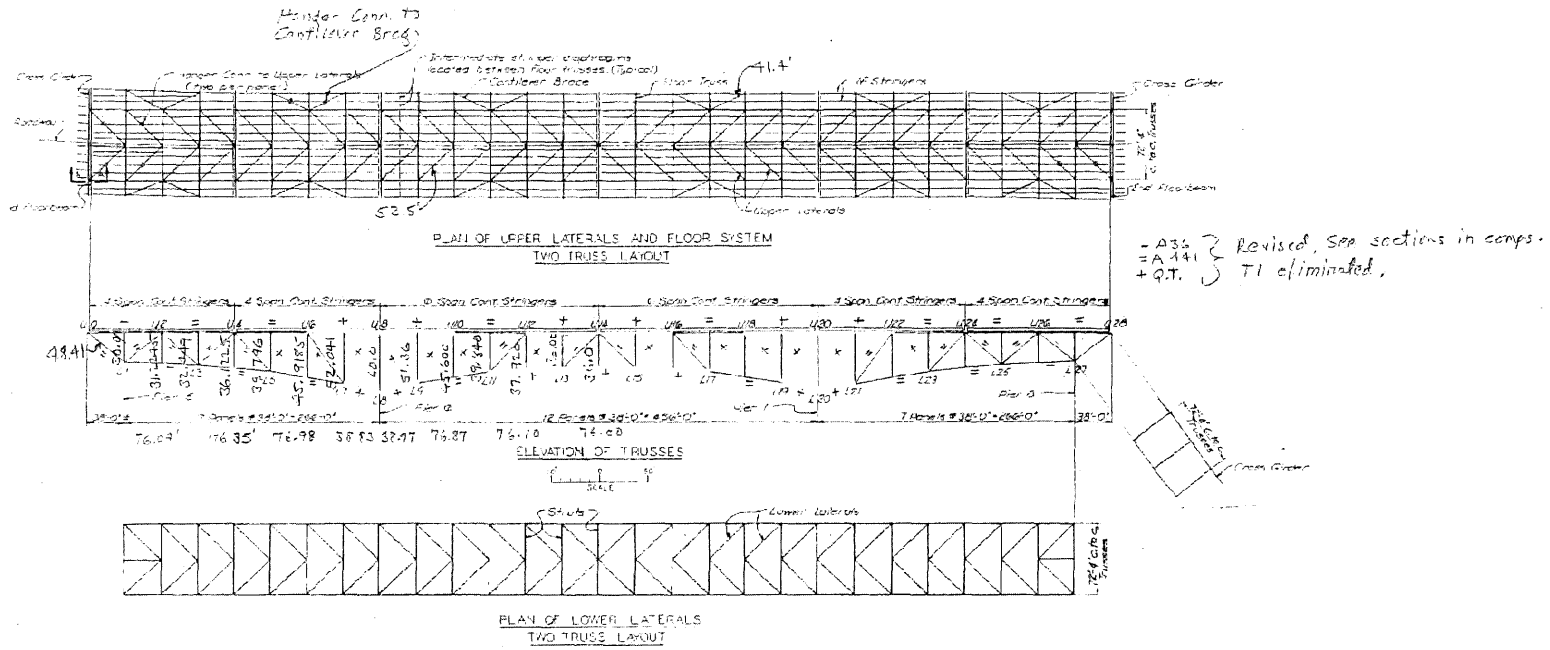

Figure 2.5. Proposed steel grades for truss members from 1963, later modified in 1964.

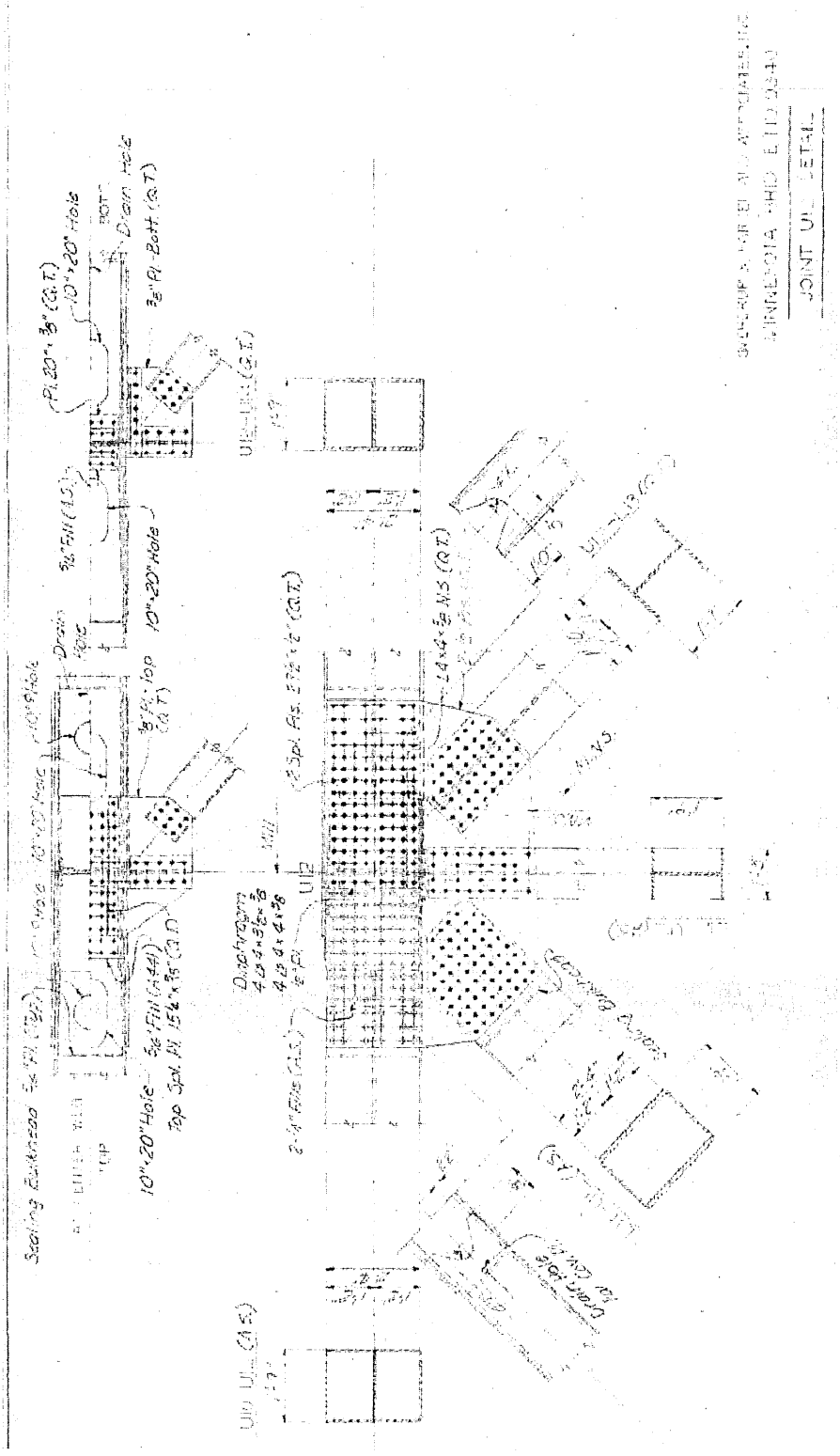

Figure 2.6. Sample gusset plate design presented to MnDOT in 1963.

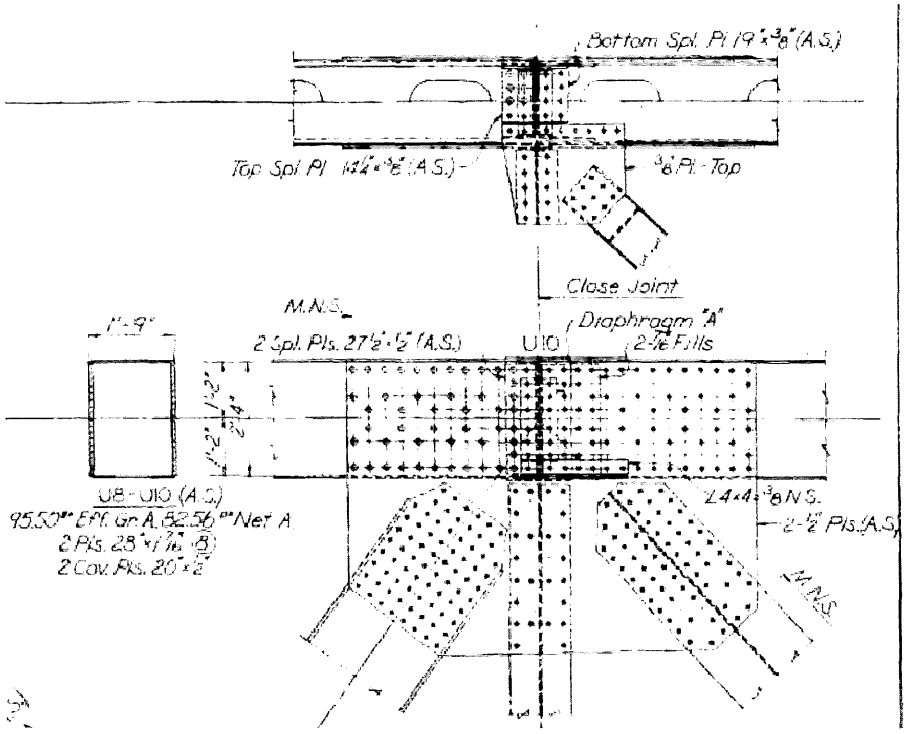

a) Node U10

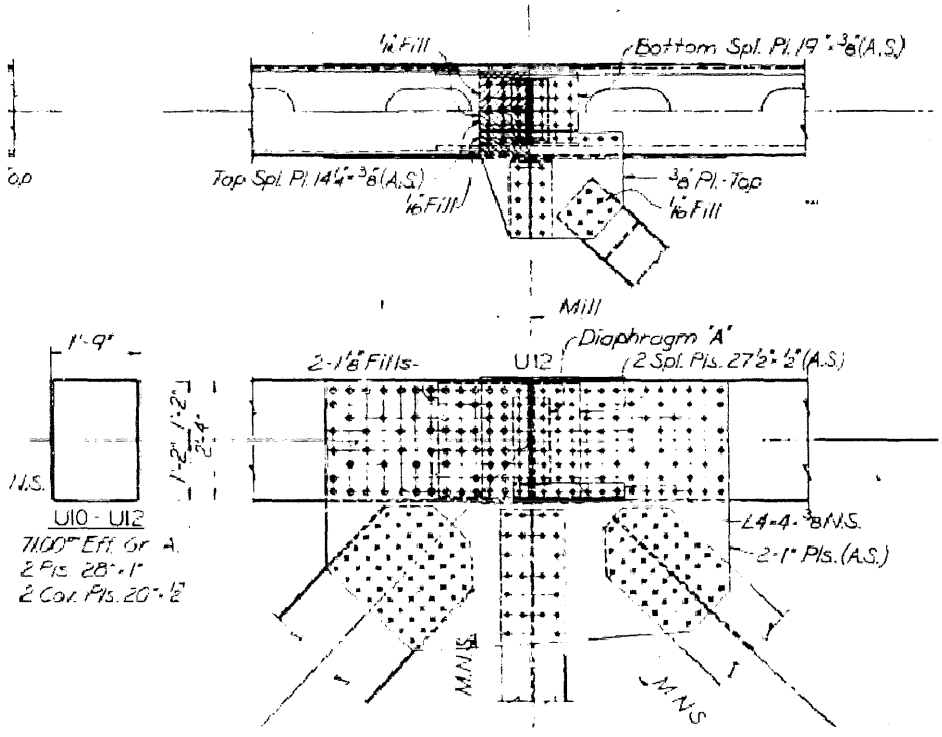

b). Node U12

Figure 2.7. Reproduction of design drawings for Nodes U10 and U12.

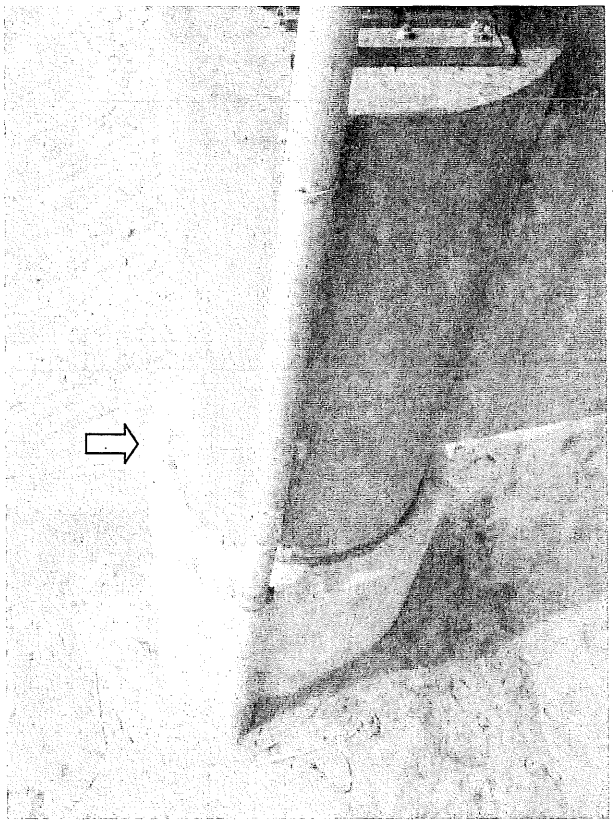

Figure 2.8. Pier 8 modifications to accommodate lateral loads from dredge material.

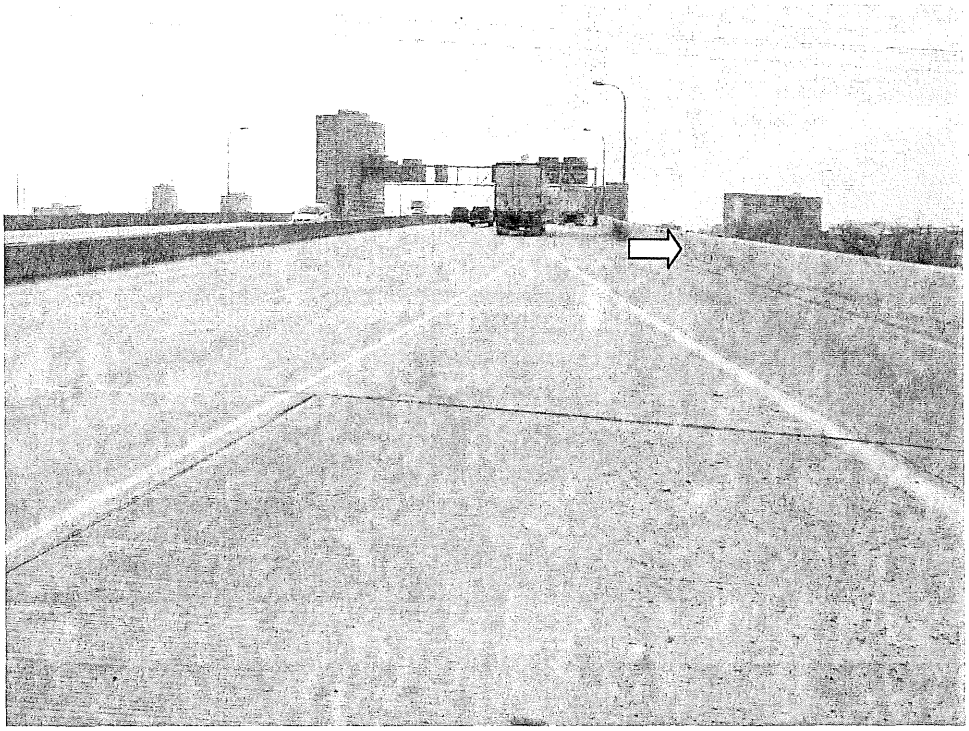

Figure 2.9. Modified barrier rail with new concrete facing shown on right.

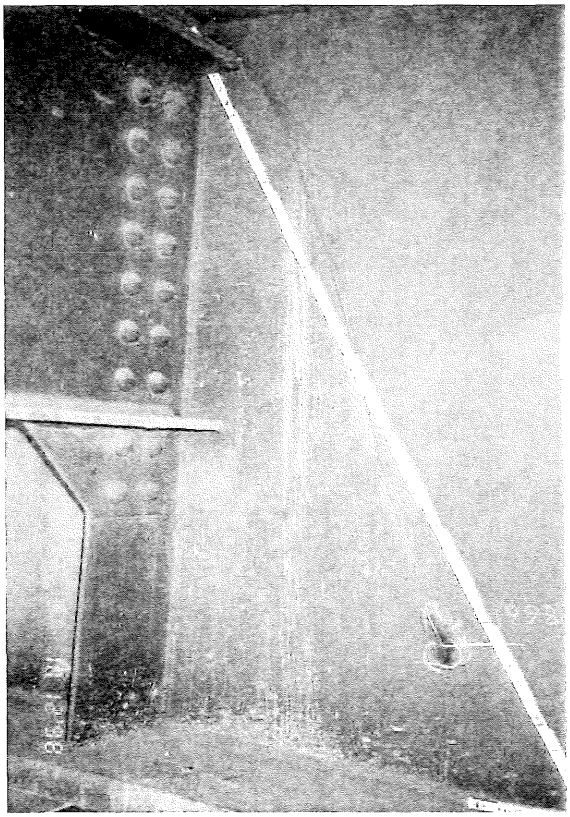

Figure 2.10. Crack observed in 1998 at Span 9 Girder G2 diaphragm connection extending into web plate.

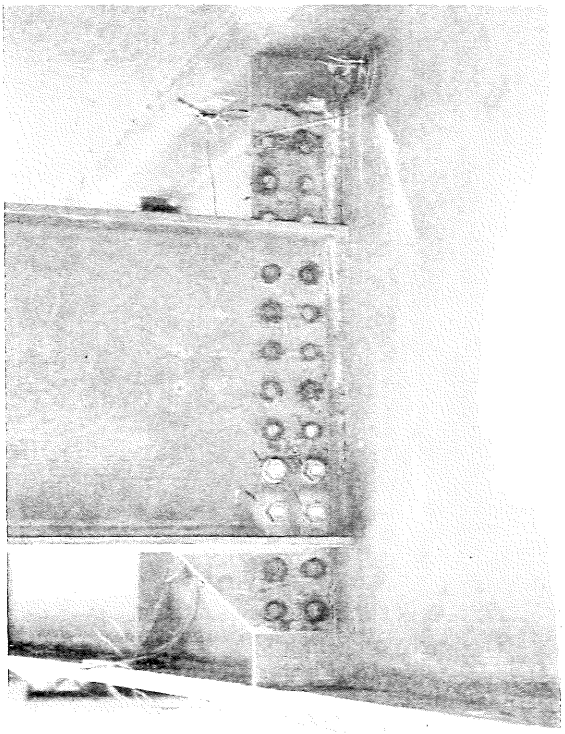

Figure 2.11. View of diaphragm connection lowered to reduce cracking in 1999.

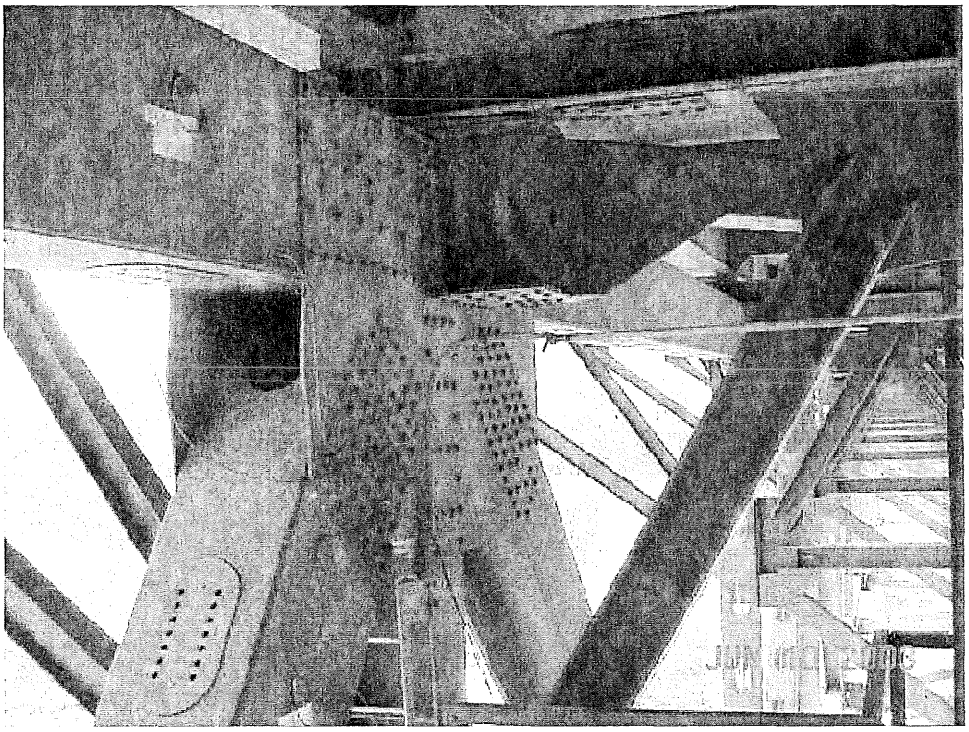

Figure 2.12. URS photo of Node U10W.

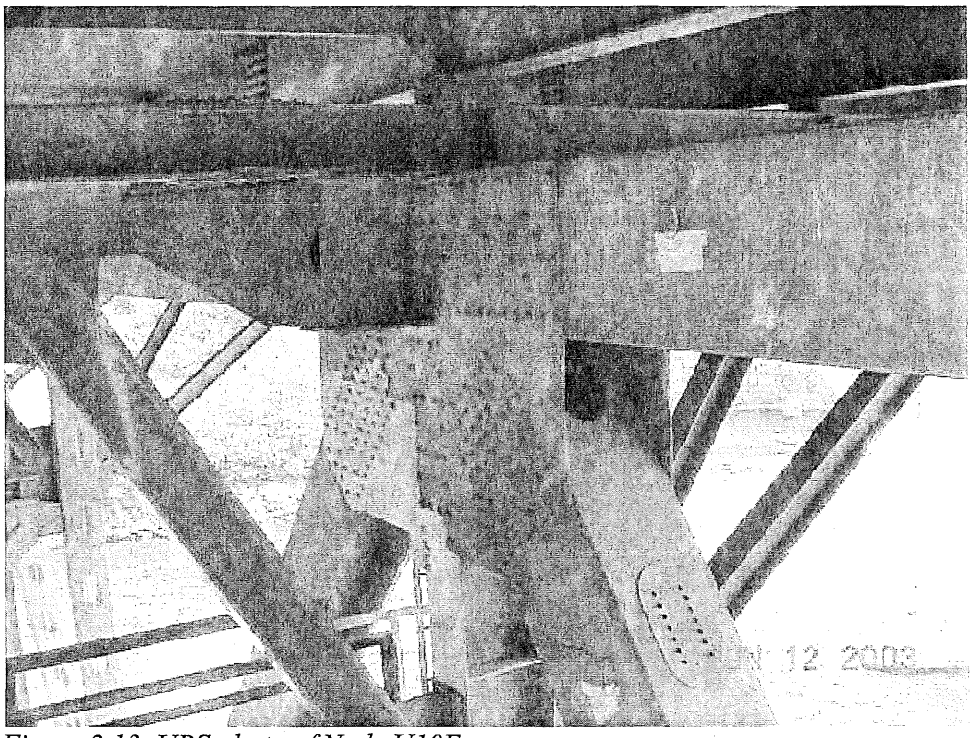

Figure 2.13. URS photo of Node U10E.

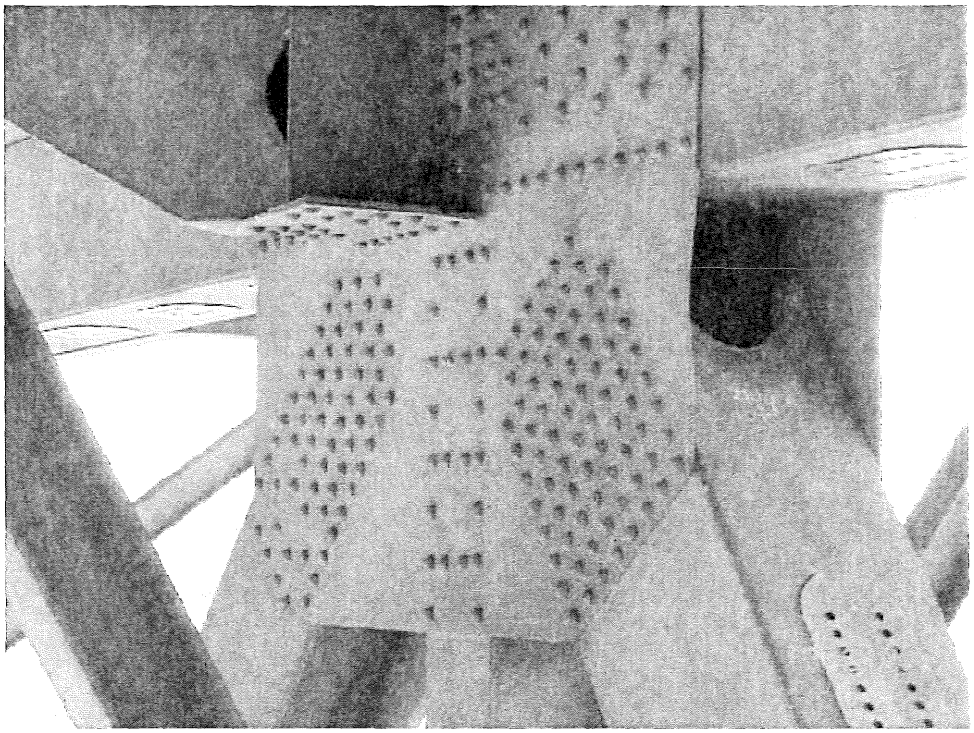

Figure 2.14. URS photo of Node U10'W.

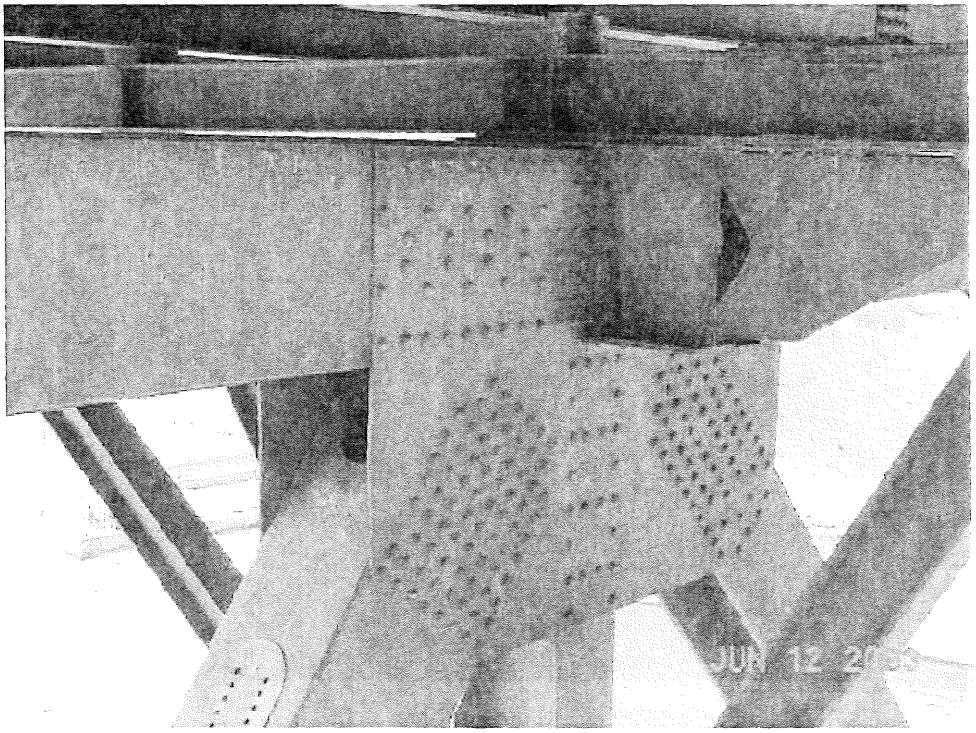

Figure 2.15. URS photo of Node U10'E.

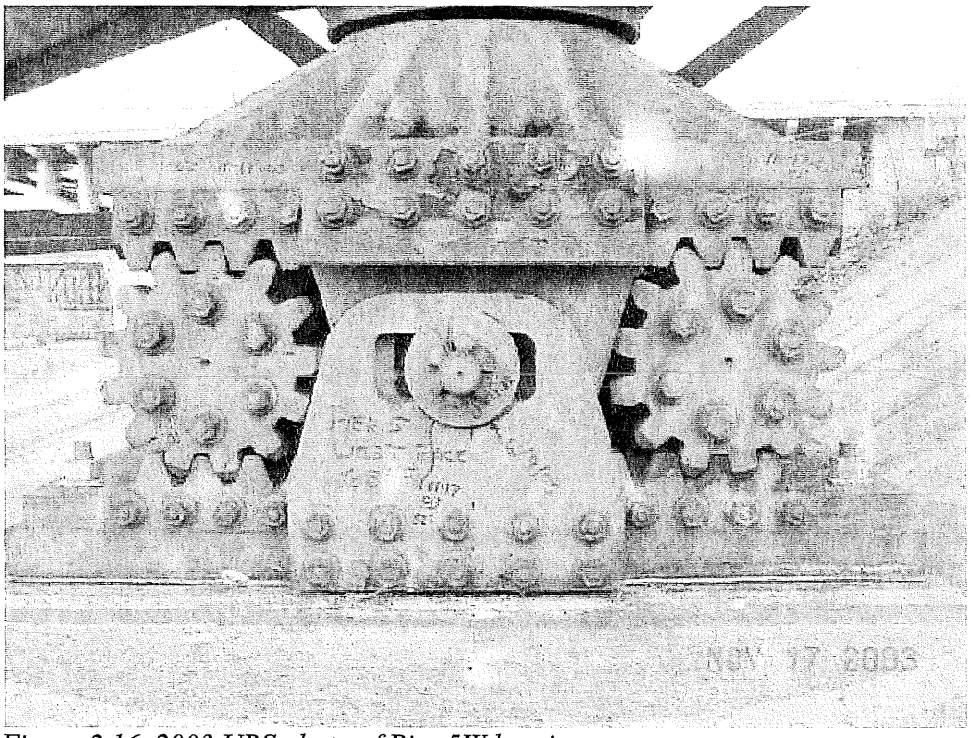

Figure 2.16. 2003 URS photo of Pier 5W bearing.

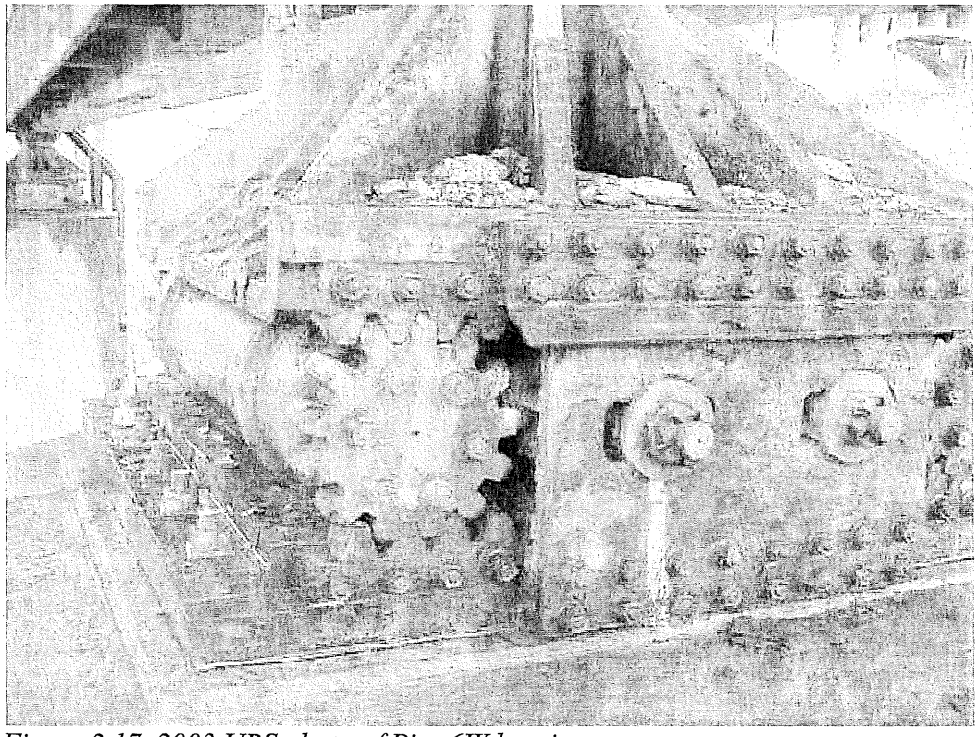

Figure 2.17. 2003 URS photo of Pier 6W bearing.

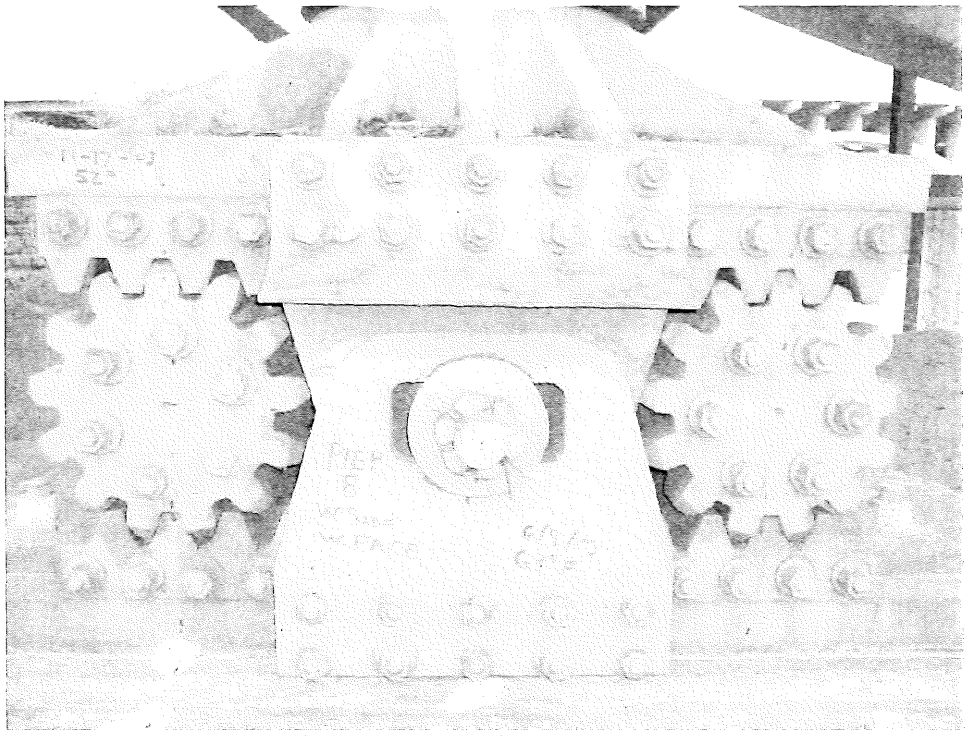

Figure 2.18. 2003 URS photo of Pier 8W bearing.

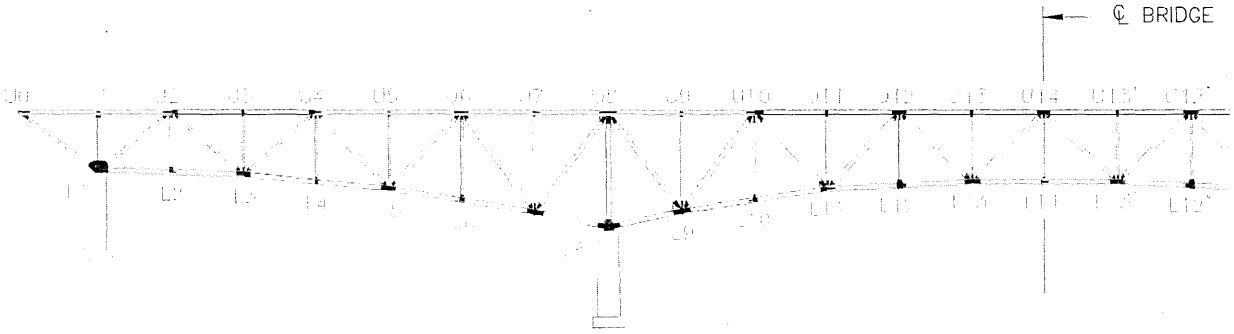

Figure 2.19. Reinforcement plate retrofit locations proposed by URS (retrofits symmetric).

Figure 2.20. Ongoing overlay work by PCI during July 2007. Note milling operations in southbound inside lanes (view looking south).

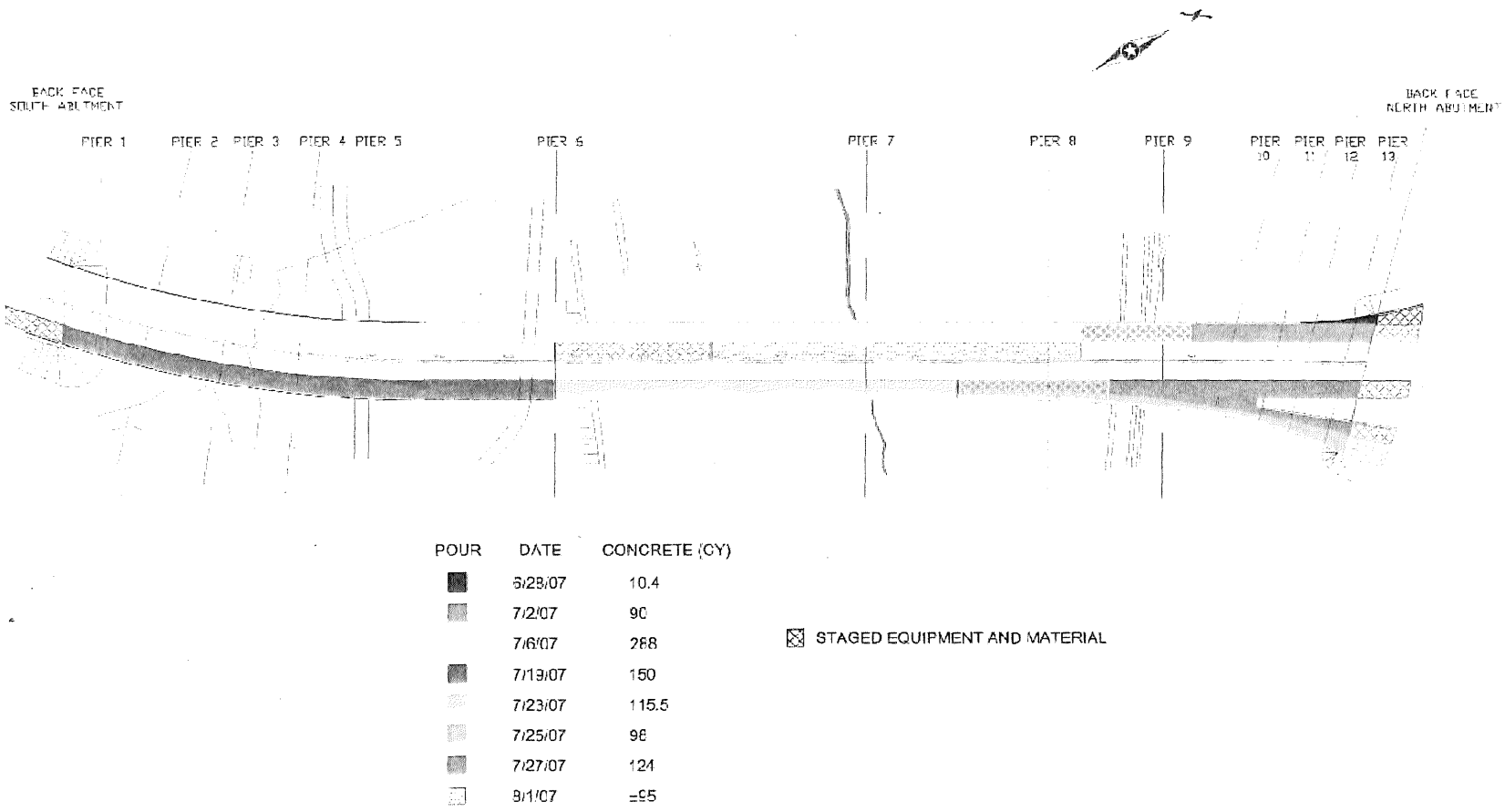

Figure 2.21. Bridge deck pour sequences used by PCI. Note material staging locations on bridge.

Figure 2.22. Photo showing equipment and material placement on deck at approximately 3:30 pm on August 1, 2008.

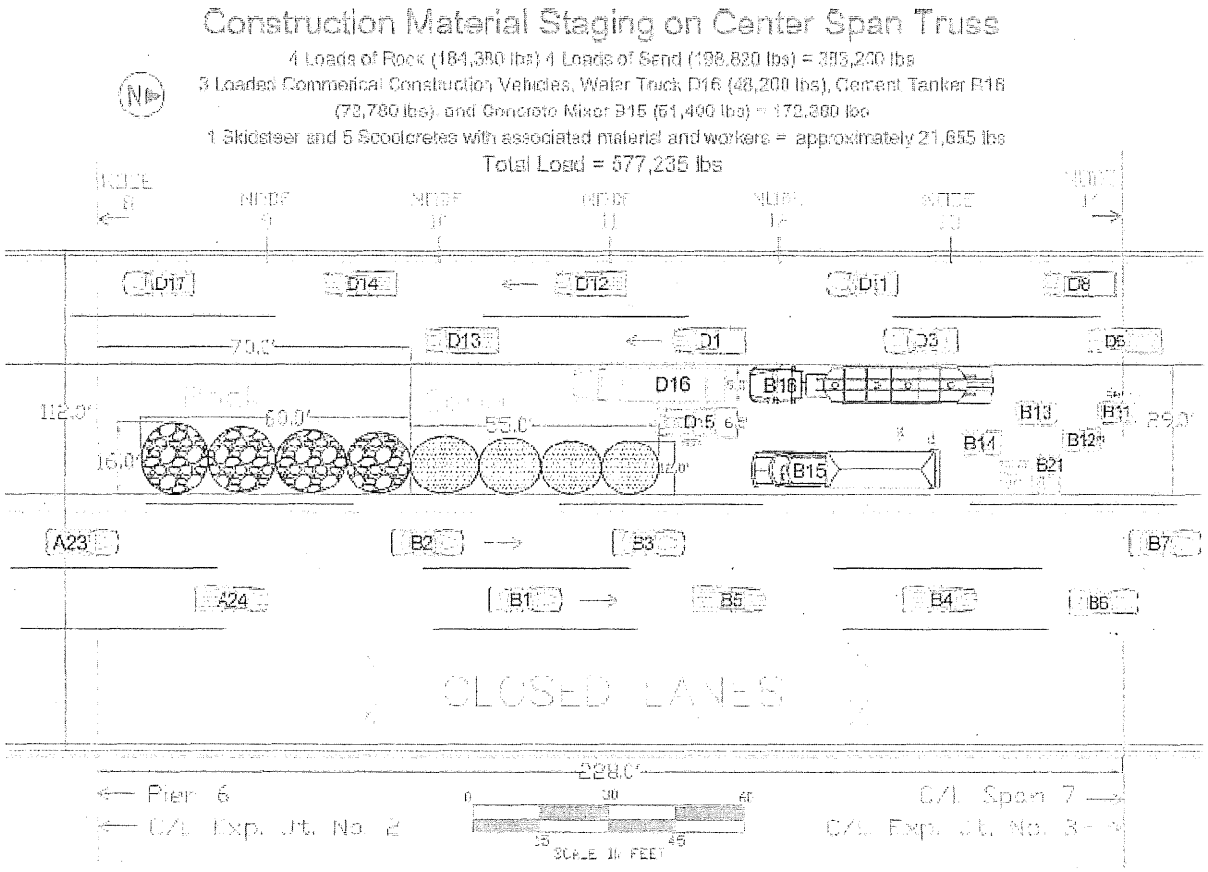

Figure 2.23. NTSB best estimate of construction loads and their respective positions on the bridge at the time of the collapse.

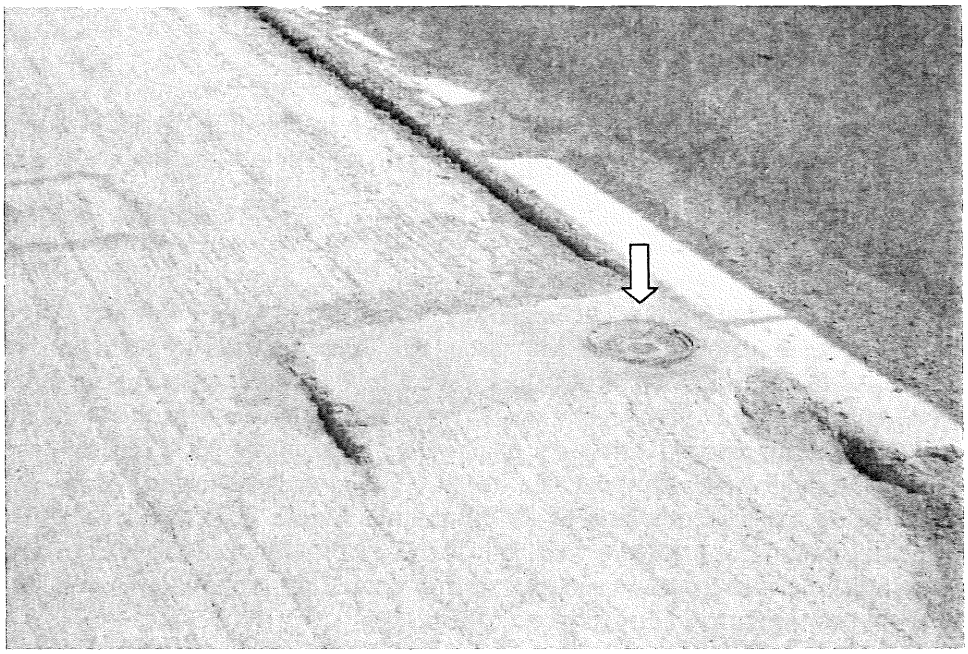

Figure 2.24. Anti-icing spray head installed in deck. Note ongoing 2007 overlay work.

3 SITE CONDITIONS AND INFORMATION

This chapter summarizes the conditions at the I-35W Bridge in the time period leading up to and including the day of the collapse. Conditions examined include site geology, seismicity, the adjacent falls, scour, sewer outlets, weather, and terrorism.

3.1 Geologic Setting

The site is positioned over a stable crust encompassing much of the upper Midwest. It is underlain by Paleozoic shallow marine sandstones, shales and carbonates deposited as seas periodically covered the land. The bowl-shaped Twin Cities Basin has thick layers of Paleozoic sediments with older bedrock exposed at the edges of the basin. Subsequent glacial advances and retreats deposited till across the basin as recently as 14,000 years ago. Overlapping moraines produced an irregular series of hills and depressions which eventually filled to become lakes. Glacial runoff formed rivers including the Minnesota and Mississippi Rivers. Erosion at the Minnesota River's confluence with the Mississippi River near Ft. Snelling eventually created a waterfall on the upper portion of the Mississippi River. This waterfall slowly eroded the river bedrock and moved upstream at a rate of about 4 feet per year to the present day location of St. Anthony Falls just west of the bridge.

The Mississippi River has continued to erode the glacial till and expose the underlying bedrock. The predominant formations observed are from the Ordovician age and include in vertical succession: St. Peter Sandstone, Glenwood Shale, and Platteville Limestone. Figure 3.1 shows a cross section through the Mississippi River valley near the bridge site [36].

At the bridge site, bedrock can be found at the surface to 50 feet below the surface. The Platteville Limestone is the upper rock formation observed on both the north and south river banks. Where it has not eroded, the formation is typically 32 feet thick. The material requires drilling and blasting to excavate; however, it is tends to weather irregularly and spall. Underneath the Platteville Limestone is a 2 foot to 3 foot layer identified as the Glenwood Shale. The shale, when exposed tends to disintegrate. Together with the Platteville Limestone, the Glenwood Shale forms a hard top over the sandstone formations below.

At over 150-foot thick, the St. Peter Sandstone is the lowest formation in the series and forms the base of the Mississippi River. The St. Peter Sandstone is highly friable and has led to the development of cave formations under the overlain Glenwood Shale and Platteville Limestone. It has good confined compressive strength and low-to-moderate compressibility. Tunneling operations are common in this stratum, particularly due to the solid Platteville formations above.

The deck truss foundations were supported within the St. Peter Sandstone. The bedrock has a compressive strength ranging from 670 psi to 2800 psi within the harder formations, 100 psi to 300 psi in softer zones. The approach spans were founded on piles embedded in the Platteville Limestone which has compressive strengths of between 8,500 psi and 26,800 psi. The design drawings allow a maximum foundation pressure of 10 tons per square foot or 139 psi for the truss piers. As part of the original subsurface investigation, 34 borings were taken at each abutment and pier. Five of the borings were taken in the river. No evidence of underground caverns were noted during the subsurface investigation or encountered during construction.

3.2 Seismicity

The Twin Cities Basin is considered one of the most seismically stable regions within the US. The craton underlying the bridge is the interior portion of a continental plate. There are no active faults within the bridge region. Only about 19 small-to-moderate earthquakes have been recorded in Minnesota since 1860; the largest was estimated to have a magnitude of 5.0 [37]. These earthquakes are attributable to movements along ancient fault lines. None of the earthquakes were centered near the Twin Cities.

There was no recorded seismic activity in and around the bridge site on August 1, 2008. The only seismic activity in the U.S. recently predating the collapse occurred at approximately 6:00 am on July 31, 2007 when a magnitude 3.2 earthquake was recorded outside Los Angles, California [38].

3.3 Lower St. Anthony Falls Lock and Dam

The Upper and Lower St. Anthony Fall locks make possible commercial and recreational navigation along the Mississippi River above and below the falls. The St. Paul District of the U.S. Army Corps of Engineers operates and maintains the locks. Various dams and cut-off walls have been constructed since 1870 to preserve the falls and the navigation above the falls from the constant erosion of the limestone layer. The lower lock and dam were completed in 1956 as part of the Minneapolis Upper Harbor Project. There were no on-going construction or operational issues associated with the lock or dam on the day of the collapse.

The lock and dam facility includes several security cameras. One of these cameras, positioned below the falls at the end of the lock, has a view of the deck truss from approximately Node 11W to the north end of the bridge. This camera footage captured the collapse on August 1 shortly after initiation. As can be seen in the series of video frames in Figure 3.2, initiation of the collapse appears to occur off camera to the right or south followed by failure of the river crossing span in the vicinity of Node 10'W. The bridge structure appears to remain nearly horizontal as it falls into the river.

3.4 Sewer Outlets

Two subterranean storm sewers cross the bridge site and empty into the Mississippi River. A 14-foot semi-elliptical, concrete-lined storm sewer with an outlet located at the south end of the bridge was constructed in 1963. It flows north along the west side of the bridge, turns and crosses under the bridge between Piers 5 and 6, and outlets to the river. The storm sewer at the north end flows south under Piers 13 to 9. It continues south and passes to the west of Pier 8 and ends at the river on the east side of Pier 7. This tunnel consists of a 12-foot diameter, concrete-lined section and a 12 foot by 12 foot box section constructed using cut-and-cover techniques. The north tunnel was constructed in 1965. Both tunnels are located in the St. Peter Sandstone and pass below the approach span bridge piers by at least 40 feet [39].

Following the collapse, the City of Minneapolis Department of Public Works carried out an inspection of the tunnels to assess their condition. They found both tunnels to be structurally sound without signs of distress associated with the collapse. There were no indications of significant movement. Large debris was noted in the box structure portion of the north tunnel [40].

3.5 Scour

Scour is a phenomenon in which material within the streambed is removed or scoured from around bridge substructure elements. It can occur as part of a storm event in which high stream flow rates are produced, from increased water velocity due to the constriction of the natural waterway by the bridge structure, or

from the natural movement of sediments downstream. Scour can cause loss of support for substructure elements resulting in settlement or instability.

The I-35W Bridge did not have a pier within the Mississippi River. Pier 7 was constructed adjacent the north side river bank and could have been exposed to scour. As noted in Chapter 2, underwater inspections in 2000 and 2004 found no signs of scour or effects on the structure at Pier 7. There were no large storm events causing high flow rates immediately prior to the collapse.

3.6 Weather Conditions

Weather at the time of the bridge collapse was clear and hot. Records from the University of Minnesota for the 24-hour period of August 1, 2008 show an air temperature at the 6:05 pm time of the collapse of 92.1 degrees F after a peak temperature reading of 92.9 degrees F at 4:30 pm [41]. Figure 3.3 is a temperature plot for August 1, 2007. Weather records at the nearby Lower St. Anthony Falls weather station indicated a peak temperature of 93 degrees F [42].

Weather records for this time period also indicated light-to-moderate winds out of the southwest between 10 to 18 mph. Figure 3.4 shows the wind and gust data for August 1, 2007. No precipitation was recorded within 24 hours of the collapse.

3.7 Terrorism

In 2003, MnDOT requested assistance from the Federal Highway Administration Engineering Assessment team to evaluate the structural vulnerability of critical highway structures in Minnesota. The team identified specific structural vulnerabilities, recommended mitigation and countermeasure options, and highlighted issues requiring further study [43].

The study revealed that the approach spans were more vulnerable due to ease of access from the underside. The deck truss was less susceptible to a terrorist act because of the increased time necessary to substantially weaken any of the primary members. Recommendations for the I-35W Bridge included both temporary measures to be instituted during high alert levels and permanent structural mitigation items. MnDOT implemented two of the recommendations which included the installation of gates on catwalks to limit access to the underside of the trusses and removal of the dredge material below Span 8.

After the collapse, state and federal authorities examined the collapse site for evidence of nefarious acts. No evidence of explosives or purposeful damage of structural members was found.

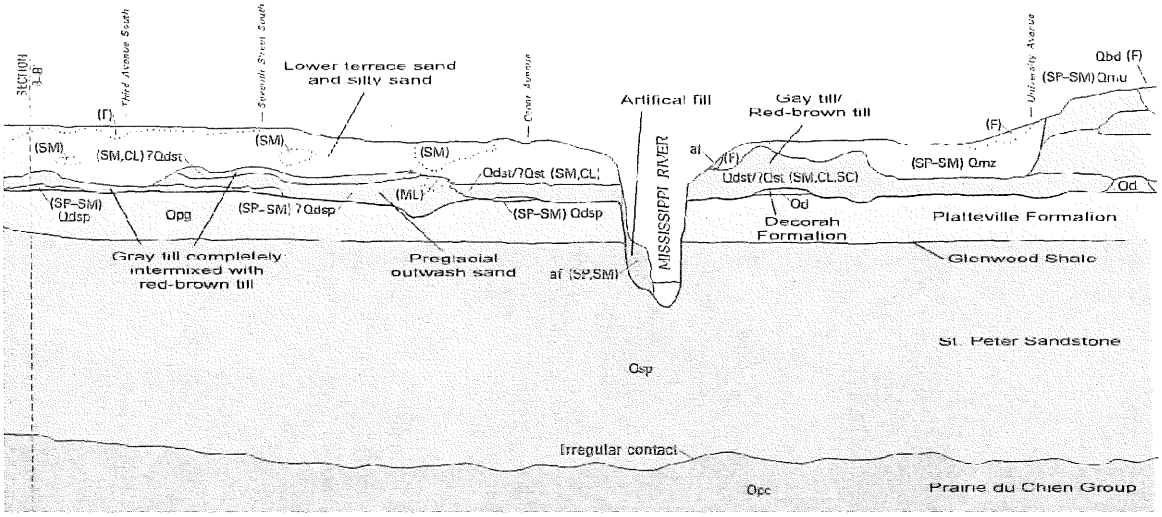

Figure 3.1. Geological section through Mississippi River valley near bridge site [36]. Vertical scale exaggerated 20 times.

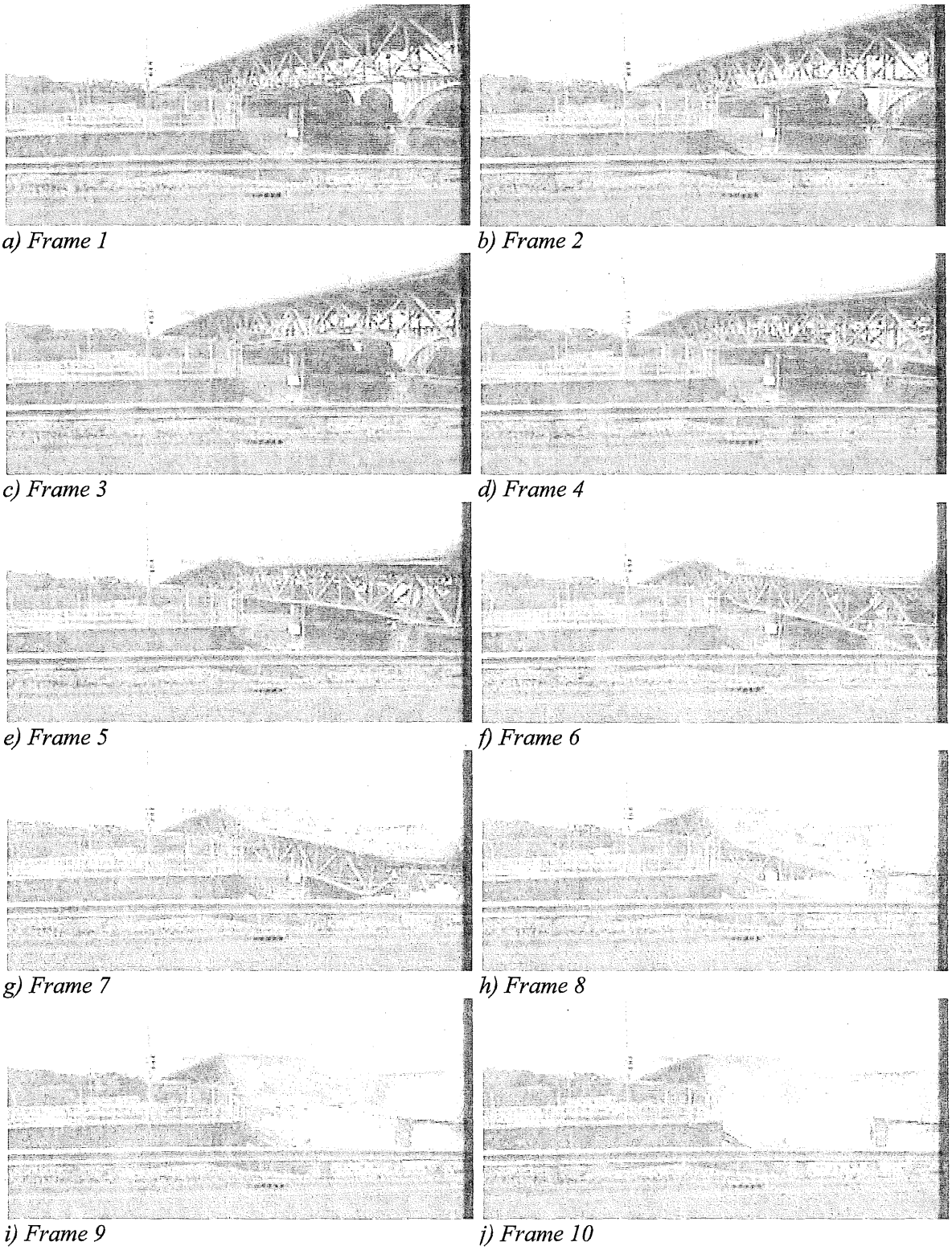

a) Frame 1 *b) Frame 2*

c) Frame 3 *d) Frame 4*

e) Frame 5 *f) Frame 6*

g) Frame 7 *h) Frame 8*

i) Frame 9 *j) Frame 10*

Figure 3.2. Video images capturing collapse from a U.S. Corps of Engineers security camera. Note first node on right edge of Frames 1through 6 is Node L11W.

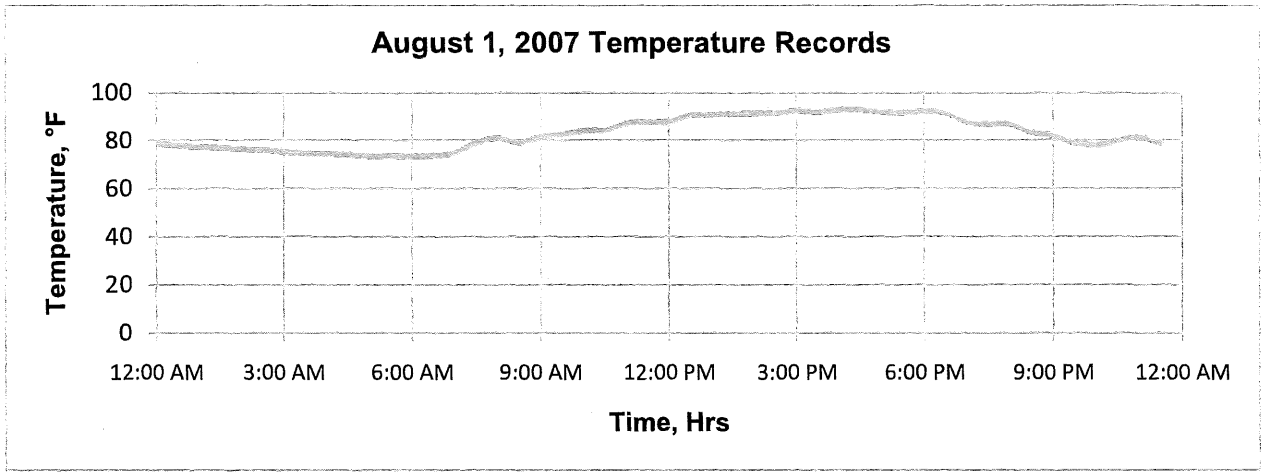

Figure 3.3. Temperature data for August 1, 2007 from U of M.

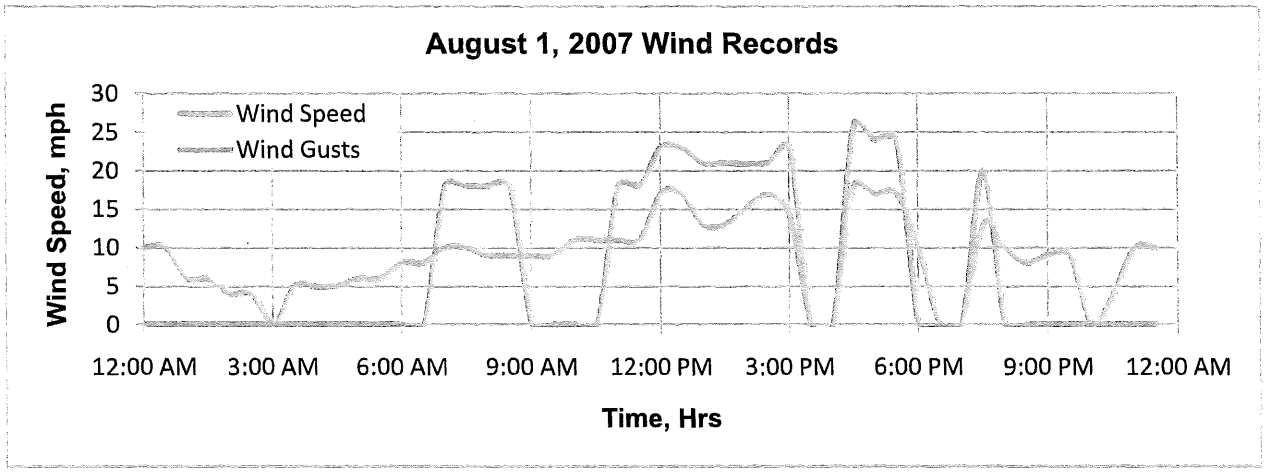

Figure 3.4. Wind data for August 1, 2007from U of M.

4 OBSERVATIONS AND WORK AT BRIDGE SITE

WJE was retained by MnDOT at the request of Minnesota Governor Tim Pawlenty. This chapter provides an overview of the work carried out by WJE at the bridge site and presents observations relevant to the investigation.

4.1 Investigation Parties and Roles

Due to the loss of life and the possible implications for similar bridge structures, under the as-amended Federal Aviation Act of 1958 and the Independent Safety Board Act of 1974, the NTSB was authorized to act as the lead federal agency. The NTSB investigation process utilizes the party system in which designated interests are asked to participate in the investigation under the guidance of the NTSB. Parties are limited *to persons, government agencies, companies, and associations whose employees, functions, activities, or products were involved in the accident or incident and who can provide suitable qualified technical personnel actively to assist the investigation.* Representatives of claimants or insurers are not permitted as parties. No entity is afforded the right to participate in NTSB investigations. The NTSB identified the following parties for the I-35W Bridge investigation:

- Federal Highway Administration (FHWA)
- Hennepin County Sheriff's Office
- Jacobs Engineering (Sverdrup & Parcel)
- Minneapolis Police Department
- Minnesota Department of Transportation (MnDOT)
- Progressive Contractors Inc. (PCI)

The party process requires each participant to coordinate investigation activities with the NTSB and to share all collected information among parties. As part of the investigative process, all party members are restricted in their release of information to non-party members. Parties can be removed from the investigation if they do not comply with NTSB instructions or if they conduct themselves in a manner prejudicial to the investigation.

WJE's investigation team included TranSystems Corporation, John W. Fisher and Associates, Inc., and Robert J. Connor Associates, LLC. As agents of MnDOT, WJE's team participated as a party representative in the NTSB investigation.

The WJE team assisted MnDOT and the NTSB with numerous field activities. A list of the major activities is included below.

- Post-collapse structural documentation
- NTSB Structural Investigation Group participation
- Structural stability assessment and recommendations
- Concrete core sample removal from piers and bridge deck
- Demolition contractor selection, coordination and technical assistance
- 24-hour recovery operations documentation
- Site safety plan development
- Survey monitoring and laser scanning coordination and assessment
- Pier movement monitoring system installation
- Member nomenclature/identification system implementation

- Salvage number assignment and member tracking
- Removal operations monitoring and documentation
- Lay-down site layout and piece positioning
- Steel sample marking, removal, and shipping
- Pier footing exploration
- Inspection of truss tension members and approach spans for fatigue cracking
- Nodes U10 and L11 and FT10 shipping preparation
- Fractographic examination of samples

4.2 Chronology of Field Activities

Figure 4.1 is an aerial image taken shortly after the collapse. MnDOT contacted WJE on August 2 and requested assistance with the field investigation into the cause of the bridge collapse. WJE arrived on site later that day and completed a preliminary review of the drawings and brief walk-through of the collapse site. On August 3, WJE received verbal notice-to-proceed from MnDOT to serve as a participant in the collapse investigation in close coordination with the NTSB.

Early inspection observations by WJE, NTSB, and FHWA which included member failure characteristics, debris orientation, and video images, suggested that the failure initiated in the vicinity of the U10 nodes. By August 7, investigators were aware of a design error of the U10 gusset plates. Subsequent field documentation was used to verify this finding.

During this period, the field investigation was restricted due to the ongoing operations to recover collapse victims. The recovery operations intensified as they continued around-the-clock under the direction of the Hennepin County Sheriff beginning August 15 and concluding August 20 after recovery of the last victim.

Removal operations under the direction of MnDOT/WJE began immediately after the conclusion of the recovery operations. Three crews working 12-hour days, 6 days a week were utilized. The initial work focused on clearing the river channel, which was opened to limited commercial barge traffic on September 6. Removal of structural steel from the site was substantially complete by October 12.

Truss members from Node 0 to Node 7 and Node 0′ to Node 7′, in addition to selected samples from the approach spans, were relocated to Afton, Minnesota. The remainder of the trusses (Node 8 to Node 8′) and the Pier 5, 6, 7, and 8 bearings were arranged in the lay-down site at the Bohemian Flats located immediate down river of the collapse site. Nodes U10E and U10W were shipped to the NTSB Training Academy in Ashburn, Virginia. On-site activities related to removal and storage of bridge components was essentially complete as of November 9. In February 2008, the Node L11 members and gusset plates were also shipped to Virginia. Floor Truss 10 was subsequently shipped to Virginia in August 2008.

4.3 Removal Process

Removal of the bridge was carried out by Carl Bolander and Sons Company, St. Paul, Minnesota. Throughout the entire process, care was taken to maintain the integrity of the members for further documentation and examination. Immediately after the collapse, the post-collapse positions of the truss structural elements that were not submerged were thoroughly documented via detailed ground-based photographs, aerial photogrammetry, and ground-based laser surveys as well as via survey measurements and photographs.

Victim recovery efforts took precedence over all aspects of the structural investigation. Most portions of the structure between Nodes 9 and 11 located in the river channel were removed in the effort to recover victims. Two barge-mounted excavators with hydraulic shears, in combination with a barge-mounted lattice boom crane, were used to remove debris. US Navy and commercial demolition divers assisted the heavy equipment operators during this process. The NTSB and WJE were limited in their ability to direct the demolition contractor during these operations. However, relevant pre- and post-collapse information was subsequently confirmed for members removed during this period. Figure 4.2 shows the site during this initial removal process.

Next, the south approach spans were demolished, followed several weeks later by the north approach spans. To knock down the multi-girder spans, the concrete deck was broken apart using a hydraulic hoe ram positioned on the deck. Hydraulic shears and cutting torches were then used to cut the steel girders into transportable pieces. The concrete piers were then broken apart. All concrete, reinforcing steel and structural steel was subsequently released by the NTSB and MnDOT and was disposed. Figure 4.3 shows the beginning of the south approach span demolition.

Later work involved the removal of the concrete deck from the deck truss spans to expose the underlying structural steel. To obtain access to the river span, a stone causeway was constructed into the river from the north side of the river. Three demolition crews were established on the bridge site. Crew A was located on the south side, Crew B on a barge and causeway in the river, and Crew C on the north side of the bridge. To facilitate the removal of steel in the river, a 550-ton hydraulic crane was mobilized on site and positioned on the causeway. Other heavy equipment used during the removal included three 110 ton lattice boom crawler cranes and hydraulic excavators outfitted with shears. The demolition contractor used oxy-acetylene torches for most cutting operations along with some oxygen-fed cutting lances. Figures 4.4 to 4.7 show various stages of the removal operations.

Once the structural steel was exposed and investigators documented the condition of each member that was not submerged, the structural steel was then cut, removed and transported to either the Afton or Bohemian Flats site for storage and further documentation. Steel from Nodes 0 to 7 and Nodes 0′ to 7′ was transported by truck to Afton. Steel from the river span between Nodes 8 and 8′ was loaded onto barges and transported downriver to Bohemian Flats.

Procedures were established to track all structural steel pieces removed from the site. Each portion of the structure was labeled with a unique salvage mark to indicate the type of member (Truss -T, Floor Truss-FT, Bracing-B, or Stringer-S) and consecutive piece number (1,2,3, etc.) as well as the removal crew (A, B, or C). Thus, a truss piece removed from the river by Crew B would be labeled T5-B if it were the fifth piece removed by Crew B. Similarly, the bracing member removed by Crew A would be labeled B33-A if it were the 33rd piece removed by Crew A. Some members were cut for handling purposes once they arrived at the storage sites. When this occurred, the separated piece(s) were labeled with an "L" for the crew location at the lay-down yard (e.g. T24-L). Samples removed for material testing were not assigned salvage numbers. Table 4.1 provides a piece count summary for each removal crew and lay-down site.

Table 4.1 - Piece count summary

Location	Number of Pieces
A	518
B	315
C	529
Lay-down L	229
Total	1591

Data collected with each salvaged piece included information on individual members constituting the piece, the date the piece was removed and/or cut, match-marks to identify cut lines between members, and associated photo numbers.

To facilitate further evaluation of the critical members involved with the collapse, a lay-down yard was developed at Bohemian Flats (Flats) downriver from the bridge site. The site is a city park reclaimed from a former coal storage yard. Figure 4.8 shows an overall view of the Flats. All structural steel from Nodes 8 to 8′ as well as the bearings from Piers 5, 6, 7, and 8 is stored in the Flats. A rigging crew supplied by Armstrong Crane & Rigging, Corp, New Brighton, Minnesota, used a 175-ton hydraulic crane to lift the pieces from the barge and position them in the lay-down area to represent their original positions in the bridge. This steel has not been released by the NTSB and is under 24-hour surveillance.

This work also included staging members at the Afton storage site as shown in Figure 4.9. Steel at the Afton site was released by the NTSB but remains under the control of MnDOT.

4.4 Truss Reconfiguration at Lay-down Site

Both trusses from Nodes 8 to 12 and Nodes 8′ to 12′, as well as the floor trusses from FT8 to FT12 and FT8′ to FT12′, were reconfigured to represent the original position of the members relative to one another. As shown in Figure 4.10, each truss is positioned with the inside face of the truss exposed. The truss members were supported on blocking to allow for some limited access below the member, if necessary. The constricted site often required multiple staging of members to enable the crane to set them in their final location. Some members were cut due to lifting limitations of the crane and concerns about the stability of the pieces.

The salvaged floor trusses were positioned with the side facing the river centerline facing down. Figure 4.11 shows the ten floor trusses laid out at the Flats. All floor trusses were subsequently relocated to the parking lot and near the reconfigured main trusses to provide access for the contractor for the new bridge.

The bearings from Piers 5, 6, 7, and 8 were also reconfigured at the site. The remaining structural steel at the Flats was positioned as noted in Figure 4.8.

4.5 Location of Major Components

The following narrative describes the locations of the major bridge components. An overall post-collapse photo taken August 3 is shown in Figure 4.12.

Most of the main deck truss, Span 7, collapsed into the river, including the concrete deck and stringers between the expansion joints at Nodes 8 and 8′, both main trusses, all floor trusses, and lateral bracing and sway bracing members between Nodes U10 and L9 and Nodes U10′ and L9′. Most of these framing

members were covered by the fallen bridge deck, as shown in Figure 4.13. The primary failure regions in the main trusses on the north and south ends of this submerged section were essentially symmetric.

At the south end on both the east and west trusses, Upper Chords U8-U10 and Diagonals L9-U10 fractured from Nodes U10 and Lower Chords L9-L11 pulled out of Nodes L9 as shown in Figure 4.14. Vertical L9E-U9E was completely detached from the main truss nodes. Vertical L9W-U9W was still partially attached to both upper and lower nodes.

At the north end, similar to the south end, Upper Chords U8′-U10′ and Diagonals L9′-U10′ fractured from Nodes U10′ and Lower Chords L9′-L11′ pulled out of Nodes L9′ on both the east and west trusses as shown in Figure 4.15. Diagonal L9′W-U10′W had also fractured just above L9′W and was buried under the collapsed portion of the span in the river. Vertical L9′E-U9′E was detached at U9′E but still partially attached at L9′E. Vertical L9′W-U9′W was detached from the main truss nodes and was resting on top of the collapsed bridge deck in the river.

Floor trusses FT10 through FT10′ were located under the collapsed portion of the span in the river. Floor Truss FT9 was completely detached from the main trusses and sprawled over the guidewall at the south bank of the river. Floor truss FT9′ was still partially attached to the main truss verticals and was suspended in air just south of Pier 7 with the east end hanging below Node L9′E by the east truss vertical and the west end resting on top of the collapsed portion of the bridge in the river.

The deck truss framing south of Node 9 collapsed onto the sloped grade extending from the south river bank to Pier 5. The position of the lower nodes relative to the piers indicated that the south end span moved north approximately 10 feet towards the river as it collapsed. From the deck expansion joint at Node 4 to Node 8, the tops of both the east and west trusses collapsed towards the east such that in the vicinity of Node 8 both trusses were positioned with their east sides facing downward (see Figure 4.14). Lower Chord L7E-L8E had completely detached from both L7E and L8E and was lying on the ground on the north side of Pier 6. Node L7E was positioned on the ground directly south of Pier 6E and the lower chord of the east truss from Node L7E to L1E was generally aligned with its original position between Pier 5E and Pier 6E. Node L8E, however, had shifted both north and west off its bearing and rested on the ground north of Pier 6 under the collapsed west truss. Node L8W was suspended in air north of Pier 6. The Pier 6 bearing rollers were dispersed on the ground north of Pier 6. The upper casting hold-down pin fractured from the L8 Nodes and the casting was found on the ground near the rollers on the north side of Pier 6. The deck and stringers between Nodes 4 and 8 collapsed to the east with the upper chords of the trusses.

From Node 0 to Node 4, the upper chords of both trusses collapsed almost directly over the lower chords. Several of the lower nodes were partially buried in the sloped grade approximately 10 feet north of their original position. The upper nodes were general positioned south of their respective lower nodes and very near their original position. The deck and stringers were still in place relative to the upper nodes. Nodes L1 of both trusses moved north off of Pier 5 and rested on the ground approximately 10 feet from the pier. Diagonals U0-L1 of both trusses were resting on top of Pier 5 with significant bending damage due to impact on the pier. All bearing rollers and the upper castings were found on the ground north of Pier 5 with the exception of the southernmost roller at each bearing, which was found on the south side of Pier 5E and on top of Pier 5W. The upper castings had separated at the spherical surface from the L1 nodes. The north end of the adjacent approach span, Span 5, had also collapsed, as it relied on the end floor beam of the deck truss at U0 for support. Spans 1 through 4 did not collapse, as shown in Figure 4.16.

The deck truss framing north of Node 9′ remained on the north bank of the river. Span 8 collapsed onto the ground below as shown in Figure 4.17. Pier 7, which supported the trusses with fixed bearings, was tilted south toward the main truss span that had collapsed into the river. Nodes U8′ to U6′ rotated north about the previously fixed bearing of Nodes L8′ on Pier 7. The shear pins at the top of the bearings fractured and Nodes L8′ rested against the north side of the Pier 7 columns. Node L1′ of both trusses moved south off of Pier 8 and rested on the ground approximately equal distance from the pier.

From Node 2' to Node 5', the collapsed bridge deck obscured most of the structure, with the exception of FT4 which had punched through the bridge deck at the Node 4 expansion joint. The bearing rollers and upper castings were dispersed on the ground south of Pier 8, with the exception of the northernmost roller on the west bearing which was found on the north side of the pier. The U0′-U2′ sections of both trusses were draped over the top of Pier 8. Similar to the condition at U0, the south end of the adjacent approach span, Span 9, had also collapsed, as it relied on the end floor beam of the truss at U0′ for support. The Span 9 superstructure was still supported on Pier 9 at its north end. Spans 10 through 14 remained erect with the exception of Span 11 of the southbound roadway which collapsed to the ground after the superstructure was pulled south off the bearings at Pier 11. An overview of the north approach spans is shown in Figure 4.18.

4.6 Examination of East and West Deck Trusses

The condition of each member and connections was documented in its post-collapse state. Observations were made primarily from the ground and from climbing onto and under portions of the collapsed structure. A crane and manbasket were used to access the U10′ end of Upper Chord U9′W-U10′W for documentation prior to removal. Because several members were not visible in the post-collapse state of the structure, observations were also made at various stages of the removal process and in the lay-down yards at Bohemian Flats and Afton. Due to restricted access during the recovery operations, documentation of the framing members in the water at the south bank of the river was limited. Much of the steel between Nodes 9 and 11 was removed as part of victim recovery operations.

4.6.1 Nodes 10 to 10'

As stated previously, much of the structure between Nodes 10 and 10′ had collapsed into the river. Most of these truss members were submerged and/or covered by the concrete bridge deck. Portions of the trusses around U10W, U10E, U10′W, and U10′E were protruding out of the water and exposed for examination (see Figure 4.13). Documentation at the U10 and U10′ nodes will be discussed in more detail below. Nodes U11′ of both trusses were also visible. At both of these nodes, the gussets were largely intact, with some deformation due to displacement and rotation of the vertical members relative to the upper chords.

After removal of the deck and stringers, the upper chords of both trusses were at least partially visible above the surface of the water, as shown in Figure 4.19. The upper chords and gussets from Nodes 12 to 11′ were primarily intact. The relative position of the nodes in the river was consistent with the structure dropping straight down. The upper chords of the trusses had rotated slightly inward toward each other, particularly north of U14. Truss members between Nodes 10 and 11 were removed as part of recovery operations and therefore were not thoroughly documented until after they were removed.

The lower nodes of the structure from L10 to L10′, as well as most of the lower chord, diagonal, and vertical truss members in this region were submerged and were therefore examined after being removed to the lay-down area. As such, it was sometimes difficult to determine whether local member

deformations occurred during the collapse or during the removal process. Much of the damage appeared to be generally symmetrical and consistent with large impact forces on the lower chords that occurred when they struck the river bottom. The locations of plastic hinges (large inelastic deformations from bending of members) and fractures in the east and west deck truss members are identified in Figures 4.20 and 4.21. Much of this documentation for Nodes 10 to 10′ was performed in the lay-down yard. At lower nodes with a single vertical framing into the lower chord, the vertical members were typically detached as a result of fractures through the gussets, or fractures through the member, or a combination thereof. In addition, there was often impact damage to the lower chord at these nodes ranging from scrapings and dents in the top cover plate to punching through the top and bottom cover plates, as observed at L12′W and L12′E, as shown in Figure 4.22. Nodes L13 and L13′ were largely intact but severely deformed with many members detached due to failure of the rivets. Nodes L11 and L11′ of both trusses were some of the most severely deformed and fractured nodes. The L11 and L11′ nodes are discussed in more detail below.

Pitting corrosion was noted at some gusset locations, primarily in the lower nodes. Corrosion measurements were recorded at Nodes L12E, L14E, and L10′W, as well as the L11 and L11′ nodes discussed below. Even the most severe pitting was highly concentrated, covering relatively small areas of the affected plates; typically along a narrow band parallel to and just above the top of the lower chord.

4.6.1.1 Nodes U10 and U10′

Post-collapse photos of the U10E, U10W, U10′E, and U10′W nodes are shown in Figures 4.23 through 4.26, respectively. The failure modes at these four nodes were very similar. At each location, both gussets fractured around the ends of Upper Chords U8-U10 and U8′-U10′ and the ends of compression Diagonals L9-U10 and L9′-U10′. Upper Chords U10-U12 and U10′-U12′ and Diagonals U10-L11 and U10′-L11′ were still attached at the nodes. The flanges of the vertical truss members were typically still riveted to the gussets; however, at all locations except for U10′W, the vertical member flanges had fractured just below the node and the webs had separated from the flanges within the node.

The fracture locations in the east and west gussets of Nodes U10E and U10W are illustrated in Figures 4.27 and 4.28. The conditions at the U10′ nodes were similar. Portions of the gusset plates still attached to Diagonals L9-U10 showed that the members translated west relative to the node at both U10E and U10W as shown in Figure 4.29. In addition, the L9-U10 diagonals exhibited severe splitting of the cover plates near the U10 node as shown in Figure 4.30, which was caused by the top chord being pulled downward through the diagonal member. The splitting at U10W was more extensive than U10E, extending approximately 12 ft-6 in. from the node. The bottom cover plate of Upper Chord U9-U10 had partially fractured and was pushed upward into the member as shown in Figure 4.31. The top cover plate of Upper Chord U10-U11 had separated from the side plates and was peeled back from the upper chord splice at U10 toward node U11 as shown in Figure 4.32. At U10E this portion of the cover plate had fractured from the upper chord.

Field measurements verified the thickness of the U10 and U10′ gusset plates (i.e. 0.5 inch) was consistent with the both the design and shop drawings. No significant corrosion or other form of damage was noted on the any of the U10 gusset plates.

4.6.1.2 Nodes L11 and L11′

As with the U10 nodes, the failure modes at the L11E, L11W, L11′E and L11′W nodes were very similar. The fracture locations in the east and west gussets of Nodes L11E and L11W are illustrated in Figures 4.33 and 4.34. The conditions at the L11′ nodes were similar. Typically, both gussets were completely fractured along the top of the lower chord, with partial and sometimes complete fractures in the gussets

around the ends of the diagonals at many locations. The cover plates of the diagonal members were typically splayed apart as shown in Figure 4.35, and the vertical members were severely distorted with extensive separations between the cover and side plates. Scrapings on the members as well as the orientation of the fractured and bent edges of the gussets showed that the upper half of the gusset plates, with the diagonal and vertical members attached, punched through the lower chords, as shown in Figure 4.36. This damage is consistent with large upward impact forces on the lower nodes as the truss hit the river bottom. It is also consistent with the fact that the collapse video shows the L11W and L11'W nodes intact as the center section of the main span is falling (see Figure 3.2, Frames 3 and 4).

Field measurements verified the thickness of the L11 and L11′ gusset plates (i.e. 0.5 inch) was consistent with the both the design and shop drawings. Some corrosion was noted on both gussets of the L11 and L11′ nodes in the area above the lower chords. The corrosion was typically worse on the inside gusset plates with some localized pitting and associated section loss. Corrosion-related section loss of the L11 gusset plates was evaluated by WJE at accessible locations. Measurements were collected just above the top surface of the lower chord where the localized pitting corrosion was present on the inside surface of the plates. The fractures in the plates typically occurred directly below this line of pitting, as seen in Figure 4.37. Measurements were collected at discrete points spaced at one or two inch intervals along a predominantly linear plane across the plate. Measurements were intentionally collected at points slightly away from the fracture surfaces to minimize the effects of necking associated with ductile yielding on plate thickness. Readings could not be made with the micrometer at locations where the plate did not fracture near the line of pitting or where the plate was folded over providing a free edge for measurement.

Subsequent to the WJE field measurements, the NTSB performed extensive laboratory measurements on the areas of corrosion of the four gusset plates from nodes L11E and L11W. The NTSB conducted both electronic point micrometer measurements and laser scan measurements to determine the average net section loss for each gusset plate. Table 4.2 summarizes the mean plate thickness measurements and the estimated section loss taken from the NTSB test report [44]. The net section loss for the four L11 gusset plates varied from 5 to 20 percent. The inside gusset plates at the L11 nodes exhibited the worst corrosion.

Table 4.2 - Summary of NTSB Corrosion Measurements of Nodes L11E and L11W Gusset Plates

Location	Micrometer Measurements			Laser Scan Measurements		
	No. of Readings	Mean (in.)	Section Loss (%)	No. of Readings	Mean (in.)	Section Loss (%)
L11E, east plate	59	0.455	8.9	125	0.471	5.9
L11E, west plate	99	0.409	18.2	197	0.413	17.3
L11W, east plate	63	0.397	20.6	133	0.417	16.7
L11W, west plate	65	0.441	11.8	129	0.447	10.6

4.6.2 Nodes 0 to 9

From Nodes 0 to 9, several of the truss members exhibited plastic deformation as a result of impact with the ground or relative movement between truss members, particularly between Nodes 1 and 5 where the upper chord collapsed onto the lower chord. The locations of plastic hinging and complete fractures in the deck truss members are identified in Figures 4.20 and 4.21. The hinges typically developed near the nodes in the chord and diagonal members, and between the lower node and the connection to the floor truss lower chord in the vertical members. The more severe deformations were accompanied by separation of the welds between the side and cover plates of the box sections and sometimes partial fractures, as shown

in Figure 4.38. The majority of the truss members remained intact with complete fractures at Upper Chords U0-U1 and Diagonals U0-L1 of both trusses, Lower Chord L1E-L2E, and Verticals L1E-U1E, L2E-U2E, and L9E-U9E. Lower Chord L7E-L8E was also completely detached at the nodes.

Upper Chords U0-U1 and Diagonals U0-L1 on both the east and west trusses were fractured near Nodes U1 and L1, respectively. As stated previously, the trusses were pulled north during the collapse and as a result, Nodes U1 and L1 fell to the ground north of Pier 5, while U0-U1 and U0-L1 remained on top of Pier 5 with significant crushing from the impact.

Lower Chord L7E-L8E was completely separated and largely displaced from Nodes L7E and L8E. The rivets were fractured on both side plates at L7E, and on the west side plate at L8E. The east side plate of the member fractured through the rivet holes. There was a partial fracture in L7E-L8E approximately 20 feet south of L7E, extending across the top cover plate and partially down the side plates as shown in Figure 4.39. The fracture in L7E-L8E and detachment from its nodes resulted from the large upward force on the lower chord member as the east truss impacted the top of the east column of Pier 6.

Lower Chord L1E-L2E fractured from L1E along the first line of rivets. The final position of L1-L2E was such that its L1 end was approximately 20 feet north of Node L1E. Verticals L1E-U1E and L2E-U2E fractured near L1E and L2E, respectively, as a result of being compressed between the upper chord and diagonal members and the lower chords. At the L9E node, the west side plate of Vertical L9E-U9E had fractured through the rivet holes. The rivets attaching the east side plate had failed, and the member was completely detached from L9E.

While the majority of the gusset plates from Nodes 0 to 9 remained intact with varying levels of distortion, many of the gussets connecting a single vertical member to the upper or lower chord had fractured. This occurred at Nodes U1E, L2W, U3E, L4E, L4W, U5E, and U9E, as indicated in Figures 4.20 and 4.21. Between Nodes 0 to 5, the vertical members were subjected to large compressive forces as the bridge impacted the ground and the upper chord collapsed onto the lower chord, resulting in severe deformations and buckling of these members. At locations where the gussets were still intact, there was typically compression buckling of the gussets between the vertical and the chord members.

At Nodes L3E and L3W, both gussets had fractured along the top of the lower chords in a manner comparable to Node L11, as shown in Figure 4.40. The failure mode was gross section at the top of the lower chord at some locations and net section through the top row of rivets in the lower chord at other locations. Nodes L5E and L5W also exhibited similar to, but not as severe, behavior as Node L11. At L5E and L5W, the top portion of both gusset plates, with the vertical and two diagonal members attached were bent at close to a 90 degree angle west, as shown in Figure 4.41. The gussets were largely intact with only a few partial fractures. Nodes L3E, L3W, L5E, and L5W, as well as L1W, were at least partially impounded and buried into the sloped ground below as a result of the significant impact forces associated with the bridge hitting the ground and the upper chord collapsing onto the lower chord.

At Nodes U2E, U2W, U4E, and U4W, the gusset plates developed partial fractures around Diagonals L1E-U2E, L1W-U2W, U4E-L5E, and U4W-L5W, respectively, as shown in Figure 4.42. The gussets were typically buckled in the region between the aforementioned diagonal and the upper chord member. The distress exhibited in the gussets was comparable to the early stages of failure at Nodes U10, and resulted from large compressive forces in the diagonal members when the bridge impacted the ground.

All gusset plate thicknesses were verified with the design and shop drawings and no discrepancies were noted. Light surface corrosion was observed on some main truss elements in the areas of the expansion joints at Nodes 0, 4, and 8. However, no significant section loss was noted on the gussets or primary truss members.

4.6.3 Nodes 0′ to 9′

Most of the east and west trusses between Nodes 2′ to 5′ were inaccessible immediately after the collapse because they were lying on the ground and were covered by the deck. After removal of the deck, most of the truss members from Nodes 2′ to 5′ were still obscured by the concrete debris and were not thoroughly inspected until they were removed from the site. A similar situation occurred with Upper Chords U0′-U2′ of both trusses which were draped over the top of Pier 8.

There was very minimal damage between Nodes 8′ and 7′. In this area, the trusses had simply rotated to the north about Nodes 8′ and displaced off the fixed bearings at Pier 7. As a result of this rotation and impact with the ground, lower chords L6′-L7′ of both trusses developed hinges just north of L7′, and Nodes U6′ were positioned north of Nodes L6′, essentially on top of lower chord L5′-L6′. The upper nodes from U5′ to U2′ all collapsed to the north of their respective lower nodes, with the upper chords landing on top of the lower chords. Several of the vertical and diagonal members experienced plastic deformations as a result of the combined compressive forces and translation of the upper nodes relative to the lower nodes. The plastic hinging and complete fracture locations are identified in Figures 4.20 and 4.21. Fractures were observed in Diagonal U0′E-L1′E, Verticals L1′E-U1′E and L1′W-U1′W, and the gusset plates at L1′E, L1′W, U2′E, and U2′W, all in the area where Upper Chord U0′-U2′ of both trusses remained draped over Pier 8 and the remaining portions of Span 8 had collapsed to the ground. Similar to Span 6, the distress at Nodes U4′E and U4′W showed deformations indicative of high compression forces in the diagonals causing deformation in the gusset plates. Upper chord hinges were also observed adjacent to these nodes.

Light surface corrosion was observed on some main truss elements in the areas of the expansion joints at Nodes 0′, 4′, and 8′. The most extreme case was at U4′E where the outer surface of the east gusset plate and the rivets exhibited moderate corrosion and isolated areas of pack rust, as shown in Figure 4.43. However, the noted corrosion did not lead to a significant reduction in section of the gusset plates at Node U4′E, or at any other gusset plates or primary truss members.

4.7 Examination of Floor Trusses

The floor trusses exhibited distortion and distress resulting from the collapse of the main trusses. However, most of the floor truss sections between the vertical members of the main trusses remained at least partially attached to the main truss verticals. The distortion occurred at FT11 and FT11′ which were buried by the bridge deck during the collapse. Removal and recovery efforts contributed to some of this distortion, particularly at FT11. FT5 through FT8 also exhibited more complex overall distortion between the east and west trusses as a result of the collapse and the eastward rotation of the main trusses. In addition, FT1′ sustained considerable impact damage as it was draped across Pier 8 underneath the main truss upper chords and portions of the deck. FT9 and FT9′ were not significantly distorted between the east and west trusses. They were, however, significantly displaced, with FT9 completely detached from the main truss vertical members and sprawled vertically over the guidewall on the south side of the river; and FT9′ partially attached to L9′-U9′E and hanging on the south side of Pier 7.

The cantilevered portion of the majority of floor trusses were typically bent downward due to a combination of displacement of the supporting vertical truss members and buckling of the two outer floor truss diagonals. In some cases, the floor truss upper chord was fractured near the main truss upper chord support due to the extreme downward bending of the cantilever section.

The most typical condition observed in the floor trusses was tearing in the gusset plates around the flange tips of the diagonal and vertical members resulting from distortion of the members and gusset plates, as a result of the collapse as shown in Figure 4.44. In the most severe cases, the gusset plates completely fractured around the end of the diagonal and vertical members, as shown in Figure 4.45. Separation of the gusset plate or web member base metal from the weld on the chord member, as shown in Figure 4.46, also occurred at several locations. Another typical condition observed at several of the floor trusses was partial or complete fractures at the connection of the upper lateral braces to the spreader beam between the two center diagonals of the floor trusses, as shown in Figure 4.47.

The floor trusses in the vicinity of the concentrated construction loading – FT9, FT10, and FT11 – did not exhibit any non-typical conditions with the exception of FT10 which developed a fracture in the upper chord between Nodes FT10U10 and FT10U12. This fracture occurred subsequent to the initiating bridge collapse event and is described in more detail in Section 4.14.

4.8 Examination of Laterals and Sway Frames

The observed damage to the lateral and sway frame bracing members was related to the collapse of the main trusses. Failure at the connections of the bracing members was observed at several locations, as shown in Figures 4.48 and 4.49. Observed failure modes included gross and net section fractures through the connection angles and plates, fractured rivets, and net section fractures through the bracing member at the connection. The bracing members were generally intact along their length; however, several members were hinged at one or two locations as a result of the collapse.

Moderate-to-severe corrosion was observed at some connections of the bracing members to the main truss nodes, particularly at the expansion joint locations. Corrosion measurements were recorded for the bracing connection plates at U4E, U4W, L8E, L8W, L13E, L13W, L9′W, L8′E, and L8′W. Observations at these locations noted pitting in the top and bottom connection plates and pack rust. At L8′E and L8′W, portions of the bottom cover plate of the lower horizontal sway brace had corroded through as shown in Figure 4.50, but there were no fractures through the member at the location of reduced section. Knife edging was observed along a portion of the fracture surface at five locations – the bottom connection plate to the lower lateral at L8W, L8′E, and L8′W, the bottom connection plate to the lower horizontal sway brace at L9′W, and the top connection plate to the upper lateral at U4′E. This condition was most severe at U4′E, as shown in Figure 4.51.

4.9 Examination of Stringers

The observed distress in the deck and stringers was related to the collapse of the main trusses. The deck on the main truss spans separated into distinct sections between the expansion joints at Nodes 0, 4, 8, 14, 8′, 4′, and 0′. There was also a relatively clean transverse break in the deck at Node 12. Transverse cracking or breaks in the deck were present along the upper chords of the floor trusses at several locations. Longitudinal cracking or breaks in the deck were present along the upper chords of the main trusses. These cracks reflected over the main and floor truss upper chords and resulted from the significant upward impact forces as the trusses hit the ground or river bed. The only exception was Nodes 6′ to 8′, where the deck remained intact. There was also a longitudinal separation between the southbound

and northbound lanes from Node 8 to 8′. The deck sections between Nodes 8 and 11 folded on top of each other in a z-shaped pattern as the continuous stringers in this portion of the deck tried to span the Node U10 truss fractures, eventually pulling the deck from the Node 8 expansion joint over Pier 6 and into the water.

The stringers exhibited in-plane and out-of-plane distortions as a result of the collapse as shown in Figure 4.52. There were also several instances of localized damage as a result of impact during the collapse. The bearing area of each stringer was documented to determine whether there was any localized failure due to concentrated loading. Typical conditions observed at the bearing locations consisted of localized distortions of the stringer webs and flanges, distortion of the diaphragms, and tears at the diaphragm stiffener welds as a result of the distortion of the diaphragms. These conditions were all due to the distortion of the stringers as a result of the collapse.

4.10 Examination of Bearings

Documentation of the bearings included the post-collapse location and condition of the various components of the bearing assemblies. In addition, the bearing assemblies were reassembled in the lay-down yard to determine their pre-collapse position and to look for indications of how they had been functioning before the collapse.

4.10.1 Pier 5

The upper castings of both bearing assemblies were found on the ground approximately 20 feet north of Pier 5, in line with their respective bottom chords. The hold-down pins connecting the upper castings to the flange castings on Nodes L1E and L1W had fractured. The upper casting for the east bearing assembly was positioned top side up as shown in Figure 4.53, while the upper casting for the west bearing was positioned top side down. On the east bearing, the north roller and the center roller were located on the ground near the Node L1E approximately 10 feet north of Pier 5, and the south roller was positioned on the concrete embankment on the south side of Pier 5. On the west bearing, the center and north rollers were located on the ground near Node L1W while the south roller remained on top of Pier 5. The lower bearing plate of both bearing assemblies remained on top of Pier 5. The anchor bolts along the north edge of the bearing plate were worn due to contact from the rollers.

The bearing assemblies were not heavily corroded. After reassembly of the bearing components in the lay-down yard, wear marks consistent with normal bearing operation, as seen in Figure 4.54, indicated that the bearings had been functioning at some time. However, it was impossible to determine to what extent the bearings were operational at the time of the collapse.

4.10.2 Pier 6

At Pier 6, the upper castings of both bearing assemblies were found on the ground approximately 20 feet north of Pier 6, positioned top side up. The hold-down pins connecting the upper castings to the flange castings on Nodes L8E and L8W had fractured. The four rollers of each bearing assembly were also found on the ground north of Pier 6, near their respective upper castings. The two center rollers of each bearing were still attached to the hold down plate at one end, as shown in Figure 4.55. The lower bearing plate of both bearing assemblies remained on top of Pier 6 with damage to the north anchor bolts from contact with the rollers.

Light-to-moderate corrosion was noted on the rollers of both bearing assemblies. The corrosion on the rollers of the west bearing was slightly more advanced with some pack rust observed on the bottom surface of the roller and in between the gear teeth at the roller ends, as shown in Figure 4.56. Pack rust was also observed in the teeth of the lower rack. Wear marks on some of the rollers indicated that the bearings had been functioning at some point in time. However, it was impossible to determine to what extent corrosion had affected bearing operation at the time of the collapse.

The northernmost roller and the next adjacent roller of both bearing assemblies had impact markings at approximately 11 inch centers as shown in Figure 4.57. During the reassembly of the bearing components, these markings were found to be consistent with contact from the anchor bolts on the north edge of the bearing plate. In addition, the second roller from the north in the east bearing and the all rollers except the northernmost roller of the west bearing had some degree of impact damage on the ribs of the rollers caused by impact with the front edge of the lower bearing plate. The two southernmost rollers of both bearings had scrapings about 20 inches apart that appeared to be caused by contact with the main truss lower chords.

4.10.3 Pier 7

The bearings at Pier 7 were fixed bearings. The bearing assemblies remained anchored on the top of Pier 7 after the collapse with no notable damage or distress other than some indentations at the top of both castings along the north edges. At the west bearing, the vertical dome pin had fractured off due to the rotation of the trusses to the north and the bottom portion of the pin remained with the bearing assembly as shown in Figure 4.58.

4.10.4 Pier 8

At Pier 8, the upper casting of the east bearing assembly was positioned on the ground approximately 14 feet south of Pier 8E underneath Lower Chord L1′E-L2′E. The upper casting of the west bearing assembly was positioned on the ground south of Pier 8W, on the west side of Node L1W, top side down. The brass dome casting had broken off the upper casting and was lying on the ground approximately 12 feet west of Pier 8W. The hold-down pins connecting the upper castings to the flange casting on Node L1′E and L1′W had fractured. At the east bearing, the south and center rollers were positioned on the ground south of Pier 8E near the upper casting and the north roller was positioned on the ground approximately 10 feet west of Pier 8E in line with the north face of that pier. At the west bearing, the south and center rollers were positioned on the ground south and east of Pier 8W, and the north roller was standing on its end at the base of Pier 8W on its north face. The lower bearing plate of both bearing assemblies remained on top of Pier 8 with flattening of the anchor bolts along the south edge of the bearing plate due to contact from the rollers.

Light surface corrosion was noted on the rollers of the bearing assemblies. After reassembly of the bearing components in the lay-down yard, wear marks consistent with normal bearing operation indicated that the bearings had been functioning at some time. However, it was impossible to determine to what extent the bearings were operational at the time of the collapse.

4.11 Examination of Piers

No notable distress was observed at Pier 5 except for minor impact damage from the main truss bearings and lower chords. Similar damage was noted for Pier 6. Both piers remained plumb.

Pier 7 with the fixed bearings had rotated about its base and was tilted 9.4 degrees south towards the river, as shown in Figure 4.59. There were some scrapings and impact damage on the north face of Pier 7 caused by Nodes L8'E and L8'W. An exploratory excavation adjacent the Pier 7 footing was made to determine where the rotation in the pier had occurred. The investigation found a separation between the foundation seal and footing.

The pier columns at Pier 8 were also tilted south towards the river. The outer shell around the pier columns exhibited significant cracking and joint separation associated with this rotation, as shown in Figure 4.60. Exploratory excavations at both Pier Columns 8E and 8W revealed fractured concrete at the ends of the footing dowel bars.

4.12 Examination of South Approach Spans

4.12.1 Concrete Bridge Deck and Parapets

The top surface of the concrete bridge deck and parapets exhibited many large transverse cracks over Pier 4 consistent with the collapse of the approach portion of Span 5. No other areas of significant structural distress (cracking, distortion, displacement, etc.) were evident in the bridge deck or overlays.

4.12.2 Steel Girders and Diaphragms

The steel superstructure south of Pier 3 was intact and had not been significantly affected by the collapse. South of Pier 3, girders generally appeared to be plumb, connections appeared undamaged, and all diaphragms were in place.

Plastic hinging was evident in the steel girders in the vicinity of Pier 4 as shown in Figure 4.61, where the bottom flange of the girders had buckled laterally north and south of Pier 4. The diaphragms at Pier 4 stabilized the girders directly over the pier, forcing the deformation to occur between the pier and the first line of diaphragms immediately north and south of Pier 4. Beyond these north and south diaphragms, the bottom flanges of the girders remained relatively straight. The girders in Span 4 just south of Pier 4 were lifted slightly by the collapsed portion of Span 5 causing them to slope slightly towards the south. No significant lateral movement of the steel superstructure was evident at any of the piers. Some localized distress in the diaphragm connections was visible in the vicinity of Pier 4.

4.12.3 Bearings

Bearings at the south abutment, and Piers 1 through 3 were intact, with generally light-to-moderate surface corrosion. Bearings at the south abutment, Pier 2, and Pier 4 were expansion bearings while the bearings at Piers 1 and 3 were fixed. Previous MnDOT inspection reports had raised concerns about the bearings at the hinged expansion joint south of Pier 2 locking up. However, these conditions were not evident. The upper bearing and rocker plates of the Pier 4 bearings translated relative to the lower bearing plates due to the collapse of Span 5, as visible in Figure 4.62. The steel girders came to rest on the north side of Pier 4.

4.12.4 Piers and Abutments

In general, the concrete piers and abutments were in good condition, with little visible distress. Isolated areas of shrinkage cracking and delaminated concrete (typically 5 square feet or less) were apparent on some of the piers, but these areas did not appear to be structurally significant. Some localized spalling was apparent at the north face of Pier 4 where the steel girders came to rest directly atop the pier.

Previous MnDOT reports indicated that Pier 1 has tilted slightly northward, but this tilting was not readily evident.

4.13 Examination of North Approach Spans

4.13.1 Concrete Bridge Deck and Parapets

The top surface of the concrete bridge deck in Spans 9 and 10 exhibited transverse cracking up to 7/8 inches wide and negative curvature consistent with the pattern of the collapse. The parapets also exhibited cracking and rotation. The deck and parapet were lifted in Span 10 due to the collapse of Span 9. The deck joint at Pier 11 widened as a result of the collapse of Span 9 and associated upward displacement in Span 10. No significant visible distress was evident in the voided slabs and parapets of Spans 12, 13, and 14.

4.13.2 Steel Girders and Diaphragms

The steel girders remained relatively straight in Span 9, but sloped downward to the south from the top of Pier 9 towards the crossbeam at Node U0′. The steel girders landed atop two railcars near the middle of Span 9 and overhung the stone wall north of Pier 8.

The steel superstructure for both the northbound and southbound roadways remained erect in Span 10 but experienced significant plastic hinging and widespread local deformation. The steel girders underwent lateral-torsional buckling consistent with excessive negative moment developing about 25 feet north of Pier 9 following the collapse of the main truss as shown in Figure 4.63. The girder bottom flanges buckled laterally between the diaphragm lines north of Pier 9 on both the northbound and southbound roadways and also at the second diaphragm line north of Pier 9 on the southbound roadway, with plastic hinges present at approximately 15 and 30 feet north of Pier 9, respectively. The extent and magnitude of the plastic hinging was greater in the southbound lanes where both Spans 9 and 11 collapsed to the ground. Many diaphragm connections distorted or failed their bolted connections due to the collapse and the buckling of the girders. None of the girders for either roadway exhibited significant plastic deformation in the northern half of Span 10. Both roadways lifted upward significantly in Span 10 due to deformation of the underlying girders and the collapse of Span 9 (as well as Span 11 for the southbound roadway). Girders G2 through G7 (numbered from east to west) supporting the northbound lanes lifted off of the bearings at Pier 10 and were suspended above the top of the pier cap.

The steel superstructure for the northbound lanes remained erect in Span 11, but the southbound lanes collapsed at Pier 11 as shown in Figure 4.64. The steel girders in both structures translated at least 5 to 7 inches southward as a result of the plastic hinging of girder bottom flanges and significant upward displacement which occurred north of Pier 9. The girders supporting the southbound lanes pulled off Pier 11. The girders supporting the northbound lanes moved south 5 to 7 inches but were generally straight and did not show obvious signs of deformation or distortion and were still bearing on the south edge of Pier 11. The bottom flanges for the southbound lane girders, Girders G8 through G14 exhibited plastic hinging just north of the Pier 10 bearings with the hinges resting directly over top of the Pier 10 bearings and on the north edge of the pier cap. These girders were relatively straight north of Pier 10 and sloped downward towards Pier 11 where the bearings rested on the ground.

4.13.3 Bearings

Bearings at Pier 9 were designed as fixed bearings for longitudinal movement, while the bearings at Piers 10, 11, and the north abutment were designed as expansion bearings. The voided slabs were integral with

the concrete piers at Piers 12 and 13. Bearings at the north abutment were intact and nested and no distress or evidence of movement was present at the slab/pier interfaces at Piers 12 and 13. The curved plates of some voided slab bearings at Pier 11 were offset several inches either north or south of center. The fixed bearings of the southbound lane girders at Pier 9 dislodged and translated west due to the collapse. Southward movement of the superstructure also dislodged the expansion (sliding) bearings at Piers 10 and 11. The girders supporting both the southbound and northbound roadways lifted and shifted off of the expansion bearings at Pier 10 following plastic hinging in the girder bottom flanges north of Piers 10 and/or 9. The upper bearing plates of the Pier 10 bearings remained connected to the girder sole plates but these components translated approximately one to two feet south and up to one foot west of the lower bearing plates and were either suspended above, or minimally supported on, the south edge of the pier as shown in Figure 4.65. The northbound lane girders remained suspended above the pier following the collapse such that they effectively spanned between Piers 9 and 11. The southward movement of the southbound roadway was significant enough to pull the upper bearing assemblies off of Pier 11, leading to the partial collapse of this span. Southward movement of the northbound roadway occurred, but the Pier 11 bearings still partially rested on the pier as shown in Figure 4.66.

4.13.4 Piers and Abutments

The concrete piers and abutments were in good condition, with little visible distress. Isolated areas of shrinkage cracking and delaminated concrete (typically 5 square feet or less) were observed on some of the piers, but these areas were not structurally significant. Some localized spalling was exhibited where the steel girders or bearing assemblies impacted or came to rest directly on top of Piers 10 and 11 at the southbound roadway due to the collapse of Spans 9 and 11. No spalling was present in the vicinity of the bearing locations of the northbound roadway and off-ramp.

4.14 Fracture Critical Inspection

Throughout the collapse investigation, members and structural components were carefully examined for signs of distortion, buckling, fractures, pre-existing conditions and other features. As part of the investigation, details classified as fatigue sensitive (Category D and E Details) in tension members were inspected for any signs of crack initiation or extension at the weld terminations. Note that during the design period for this bridge, *AASHO Standard Specifications for Highway Bridges* did not include the current fatigue detail categories. The first fatigue guideline that included detail categories, as used currently, was the *1974 AASHTO Interim Specifications* [42].

For the I-35W Bridge, the worst category detail used in fabrication of deck truss primary members was a condition classified as Category D. This condition is associated with the intermediate diaphragms used in box members subjected to tension forces. Intermediate diaphragms used in the compression members were connected using intermittent fillet welds to the box resulting in a Category C detail. However, AASHO did not allow transverse welding on tension members. Therefore, tension numbers had the intermediate diaphragms connected with eight small tab plates oriented longitudinal to the member to eliminate the transverse weld issue. Floor truss fabrication included several weld terminations classified as Category E details. These included the slotting of WF member ends to complete node connections, short longitudinal stiffeners to strengthen the WF member web terminations at the node gusset plate, and welded reinforcement plates with tapered ends for top and bottom chord members. These tapered reinforcement plates occurred at four locations and were connected using three types of welds: fillet welds at the tapered ends, plug welds along the centerline of the plate, and slot welds along the plate edge.

4.14.1 Primary Truss Box Members

For all box shaped members subjected to tension and reversal stresses, the 3 1/2 inch long diaphragm tab connector weld terminations were inspected. In total, 76 truss box members in the primary truss were subjected to tensile stress ranges. Figure 4.67 illustrates the tension and reversal members. In general, each box member includes two intermediate diaphragms consisting of a 3/8 inch thick plate connected with eight 3 1/2 inch x 3 1/2 inch x 3/8 inch welded tabs. Many of the diaphragm plates were held in position for fabrication using tack welds. During previous bridge inspections, a few cracked tack welds were found and documented. Figure 4.68 shows the intermediate diaphragm details taken from both the Sverdrup & Parcel design drawings and the Allied Structural Steel Company shop drawings. Two 3 1/2 inch tabs are connected on each side of the box member using a single-sided 1/4 inch fillet weld. Figure 4.69 shows a typical intermediate diaphragm connection and tab connections used in a tension box member. Since the 1974 adoption of current *AASHTO Bridge Fatigue Design Specifications*, this type attachment results in a Category D detail and the weld terminations could be susceptible to crack growth if a small percentage of the variable live load stress ranges exceed the 7.0 ksi constant amplitude fatigue threshold.

In total, approximately 150 intermediate diaphragm plates and over 1,000 tab connections were subjected to in-depth inspection at the two lay down storage sites. In-depth inspection included internal member access, cleaning, good lighting and magnetic particle test methods (MT), as needed. None of the tab weld terminations beyond those previously noted from the inspections were found to exhibit any signs of initial cracking or crack extension. At diaphragms that were distorted or displaced from their original location, due to the collapse, the box member plate material was carefully inspected at the weld termination sites for any sign of crack extension into the base material. Figure 4.70 shows a box member side plate with the intermediate diaphragm displaced from its welded connection and the remaining welds are clearly visible on the plate. No indications of crack extension were found in the base material at any of these locations. In addition, none of the cracked tack welds found during previous inspections exhibited any extension that resulted in unstable crack growth. Figure 4.71 is a view of a typical cracked tack weld at an intermediate diaphragm connection. Note during this period, tack welds were used to hold plates in position to complete the final connection. Cracked tack welds are rather common in bridge structures and have typically resulted from shrinkage, thermal contraction or fit-up problems during fabrication or erection. Tack welds have fatigue cracked through their throat when they have transferred stress between an attachment to a member and the tack weld is perpendicular to the direction of stress in the member. Experience has shown that in almost every case, such cracks are benign.

4.14.2 Floor Truss Members

For all floor truss members, several of the welded details used to complete node connections are classified as fatigue sensitive. These conditions include many Category E details. Figure 4.72 includes a drawing of a typical floor truss taken from the design drawings and member modifications and weld details from the shop drawings to complete fabrication. Figure 4.73 shows the tapered reinforcement plate taken from the shop drawings, used at two top chord and two bottom chord nodes with high member forces located adjacent to truss supports. These taper reinforcement plates are shown connected with three weld types: fillet welds, slot weld and either 12 or 16 plug welds (fillet welds in holes) to strengthen the chord web plates. In addition, the nodes shown in Figure 4.72 show the reinforcement stiffeners used along the centerline of each WF member at the web-to-gusset plate connection.

All of these type connection details in tension areas are classified as fatigue sensitive. Since the collapse of the bridge could have initiated from a floor truss member failure, all floor trusses were examined for

fractures, distortion and areas of concern with particular attention given to floor trusses FT8 through FT12 located below the area of construction loading on the date of the collapse. Throughout the examination of the floor trusses, no member fractures, indications of pre-existing cracks or defects were noted from any of the fatigue sensitive details that could have initiated member failure. At many locations, large deformations from the collapse caused the initiation of cracking at the ends of the flange and reinforcement plates as shown in Figure 4.74.

One fracture of interest was found in the top chord member of FT 10, the most severely loaded floor truss, approximately 5 1/2 feet west of the center line of main truss Node U10E (i.e. adjacent to FT10U10) as shown in Figure 4.75. The fracture was mainly flat through the lower half of the chord and exhibited a chevron pattern indicating initiation was from a weld between the bottom flange of the top chord member and the gusset plate of FT10U10. Figure 4.76 shows a close-up view of the origin region. The origin was small without any sign of pre-existing stable crack extension. Through the upper chord portion of the top flange, the fracture was on a slant plane, consistent with ductile fracture. The top flange of the upper chord, in areas adjacent to the fracture, were deformed upward indicating that bending forces were present in the top chord member as the facture progressed. Examination of the underside of the top chord bottom flange in the area between the fracture and Node U10E revealed deformation and impact marks associated with the west side plate of truss diagonal L9E/U10E. Hence it has been concluded that the fracture in the top chord member of FT10 was a result of the force applied during the impact of the L9E/U10E diagonal into the floor truss. This floor truss fracture occurred subsequent to the initial bridge collapse event.

4.14.3 Bridge Approaches

An examination of the fatigue cracks and associated retrofit repairs was carried out on the North and South Approach spans. Post-collapse conditions were compared with the conditions reported in the MnDOT June 2006 *Fracture Critical Bridge Inspection In-Depth Report for the I-35W Bridge* [43].

South Approach Inspection. Several cracks noted in the 2006 MnDOT report at the first diaphragm line south of Pier 3, the first diaphragm line north of Pier 3, and the first diaphragm line north of Pier 4 were unchanged from the conditions noted in that report. Retrofits were also observed at these diaphragm lines. The retrofits usually consisted of 2-inch diameter core holes in the girder webs and/or diaphragm stiffeners near their intersection with the top girder flange. At all locations, the existing crack was contained by the retrofit. No cracks or repairs were found at any other South Approach spans locations.

North Approach Inspection. The diaphragms for Span 9 were intact; however, some short length cracks were observed at all five diaphragm lines. These short cracks resulted from extreme deformations caused by the collapse and were located at ends of stiffener welds used for diaphragm connections to girder webs. All cracks previously noted at the first diaphragm line south of Pier 9 in the 2006 MnDOT Report were unchanged from the conditions noted in that report. In Span 10, cracks were found at the first diaphragm line north of Pier 9. These conditions were unchanged from conditions noted in that 2006 MnDOT report with the one exception of Girder G6 where a pre-existing crack near the top flange appeared to have extended due to the collapse. Several additional short cracks caused by collapse-induced deformation were documented at the first and second diaphragm lines north of Pier 9.

No instances of pre-existing cracks were noted for Span 11 in the 2006 MnDOT report, and no new cracks were identified during the post-collapse examination. Diaphragms and their connections to the girders generally were intact with isolated distortion at some locations due to the collapse.

4.15 Survey Information

Shortly after the collapse, MnDOT mobilized its survey crews to assist with monitoring the stability of the debris pile, measuring pier positions, and documenting the existing position of the debris pile. WJE worked closely with MnDOT to monitor and collect this information.

4.15.1 Debris Monitoring

Survey targets were positioned on key structural components on both sides of the river to measure potential movement of the debris pile. These measurements were taken twice a day until the member showed no signs of movement or was disturbed during removal operations. The survey measurements showed the debris pile to be stable with measured movements attributed to thermal expansion/contraction of the steel. MnDOT surveyors also monitored the structural steel in Span 9 during operations to remove the contents from the rail cars crushed under the bridge. Measurements were taken to determine whether the supported span was settling as the contents were removed. No movement was measured. Figure 4.77 shows the crushed rail cars supporting Span 9.

During the recovery operations, WJE was also asked to install sensors on Piers 6 and 7 to trigger an alarm in the event the structural debris on the piers shifted. Figure 4.78 shows this sensor mounted adjacent Pier 6. No events were triggered.

4.15.2 Pier Measurements

After the collapse, the top of Pier 7 was inclined 9.4 degrees to the south. Survey measurements indicated an increase in rotation by approximately 0.2 degrees during construction of the causeway. No further movement was observed.

A location and elevation survey was completed for all of the deck truss piers. With the exception of Piers 8E, 8W and 6E, survey measurements were taken without interference from debris atop the pier. Elevations were taken at the top of the bearing plate or dome casting while distances were measured from the center of each bearing. Figures 4.79 to 4.82 show the survey measurement locations for each pier. Additional measurements were taken at Pier 6E as structural debris was removed.

A comparison of calculated top of pier elevations with design drawing and erection elevations is shown in Table 4.2. The values were calculated by subtracting the bearing plate thickness from the survey measurement. With the exception of Piers 7 and 8 which had rotated, the calculated values were within 0.36 inches of the plan elevations.

Table 4.3 - Comparison of Pier Elevations

Pier	Plan Elevation (ft)	Measured Elevation (ft)	Difference (in.)
5E	802.65	802.62	0.36
5W		802.63	0.24
6E	771.33	771.30	0.36
6W		771.31	0.24
7E	769.56	769.79	2.76
7W		769.79	2.76
8E	796.21	796.18	0.36
8W		796.29	0.96

A comparison of plan center-to-center dimensions with measured span dimensions for Span 6 indicates a length of 1.4 inches less than plan. The center-to-center measurements of Span 7 are 8 ft-4 in. less than plan due to the rotation of Pier 7. The measured length of Span 8 is about 5 ft-9 in. longer than plan as a result of both Piers 7 and 8 rotating.

4.15.3 Post Collapse Laser Mapping

Detailed electronic laser mapping was undertaken by MnDOT survey crews to document the post-collapse position of all bridge members above the water. Two laser stations manufactured by Leica Geosystems, Inc. were used for this purpose. For the measurements, the laser took a series of individual readings spaced 0.10 feet apart in a 360-degree by 270-degree panoramic view. Often times, the scanning field was electronically fenced or focused to include only the debris pile to reduce the amount of data collected. From each set-up, a collection of point clouds was created that were registered together to create a three-dimensional map of the debris pile accurate to approximately 0.15 inches (4 mm) at 164 feet (50 m). In total, 62 set-ups were required to map the bridge. This map would have enabled investigators to determine individual member geometries and locations relative to one another in the event that access to members was restricted or extensive damage to members occurred during removal. Figure 4.83 is an illustration of the debris pile using the software.

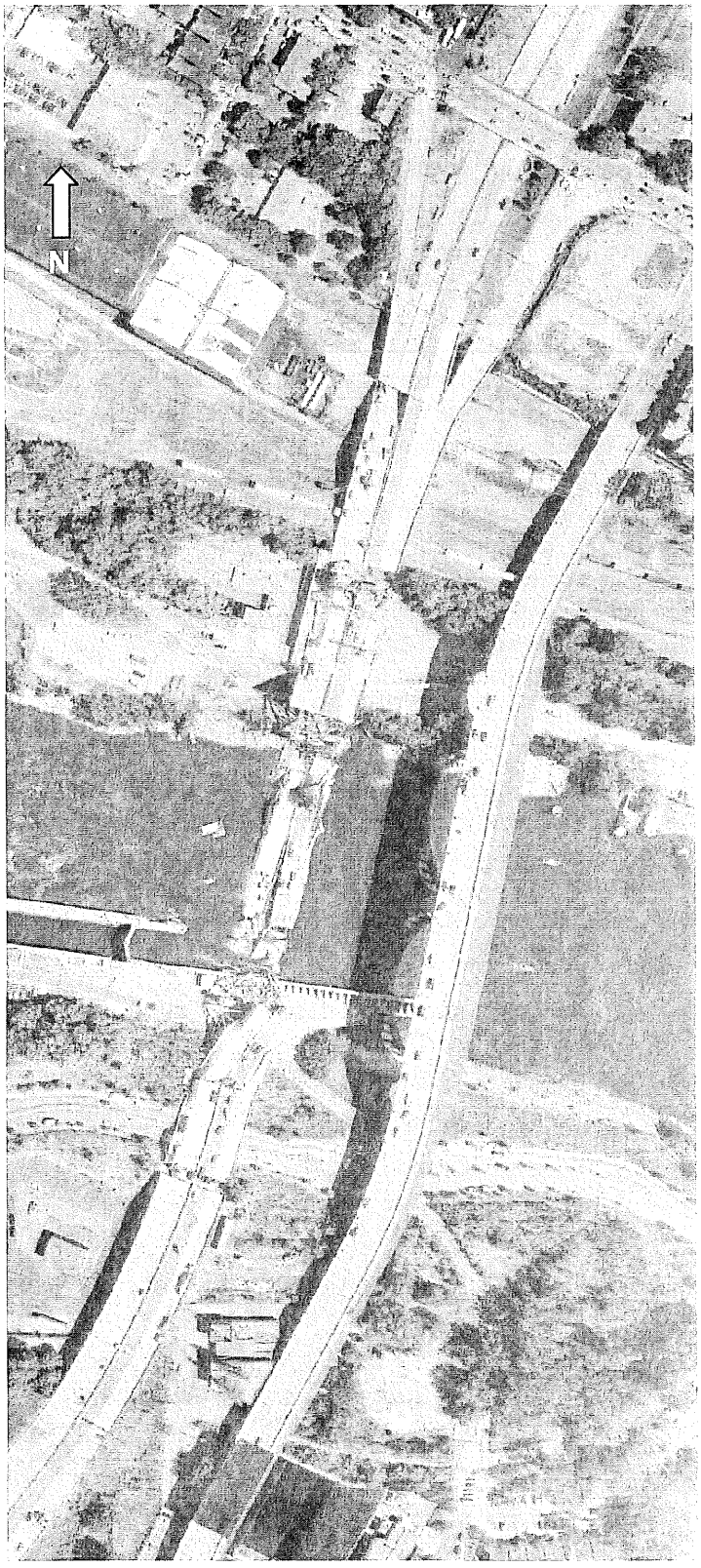

Figure 4.1. Aerial view of collapse site.

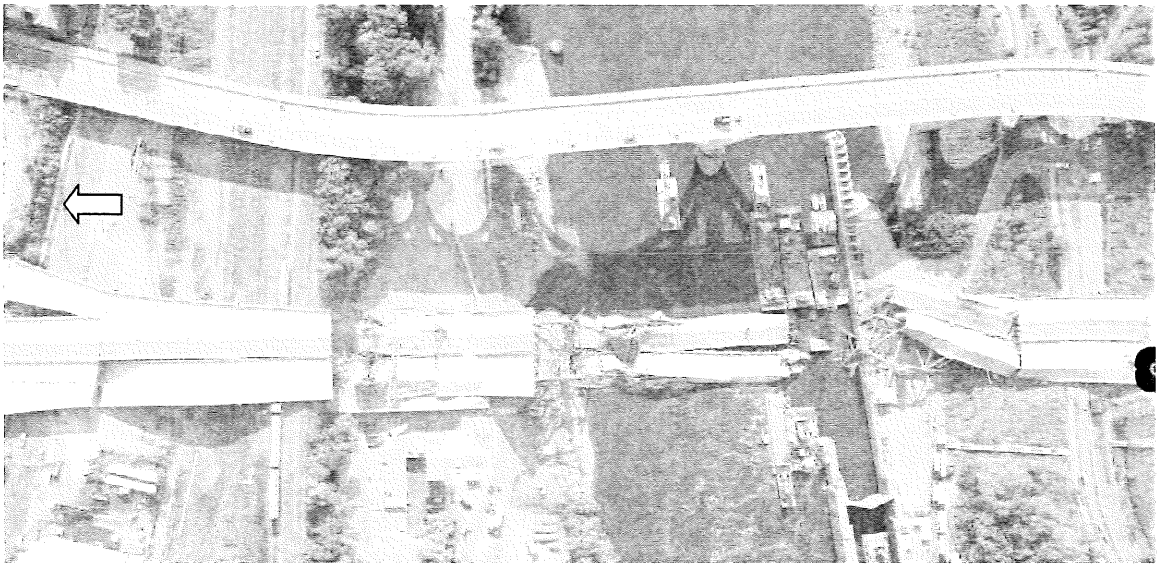

Figure 4.2. Recovery phase of the removal process (Aug. 17).

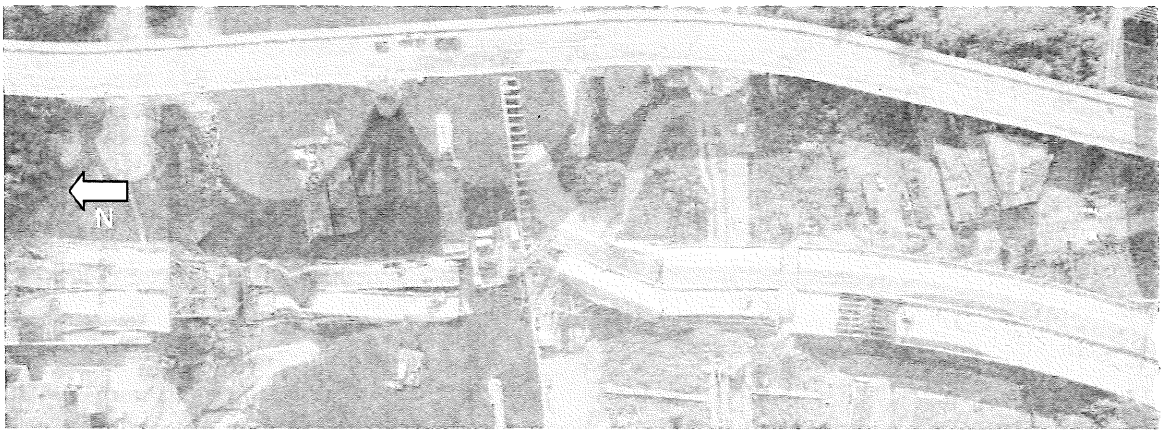

Figure 4.3. Second phase of the removal process involving demolition of the south approach spans (Aug. 24).

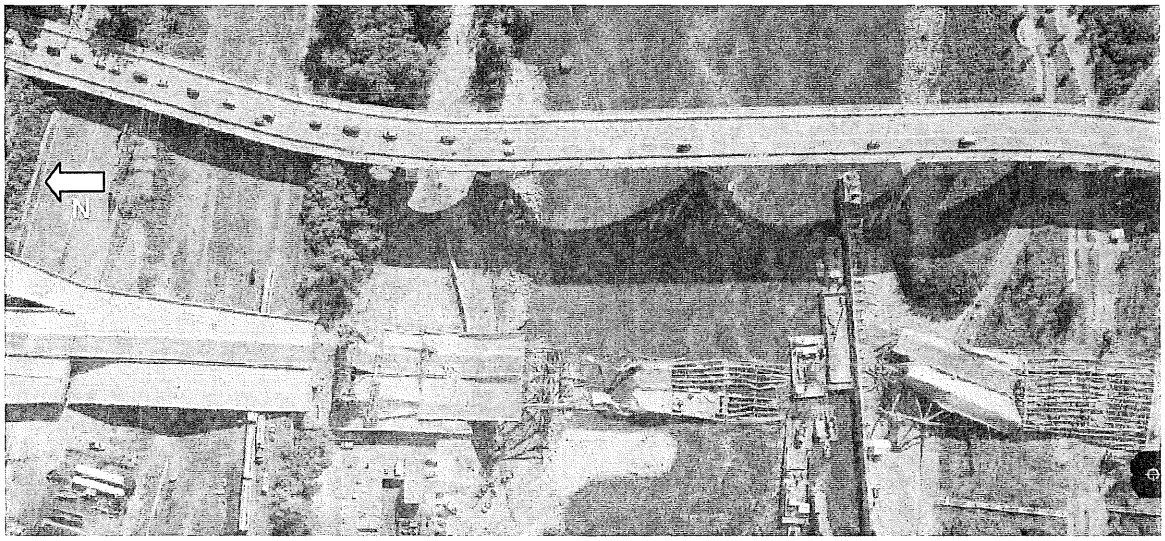

Figure 4.4. Third removal phase showing exposed truss steel after removal of deck (Aug. 31).

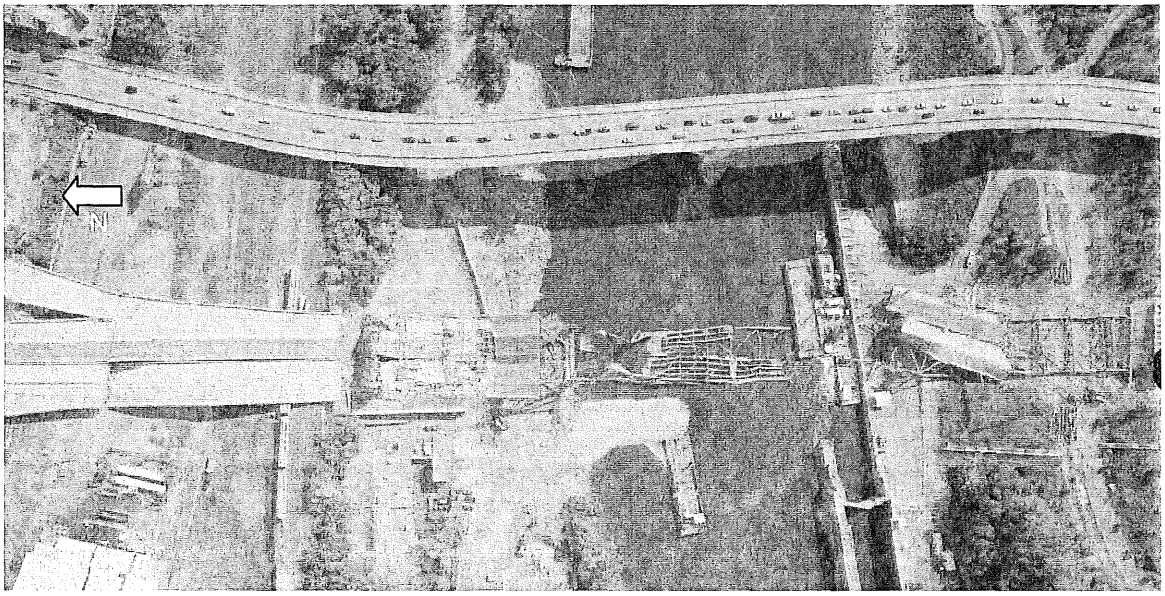

Figure 4.5. Opening of navigation channel (Sept. 10).

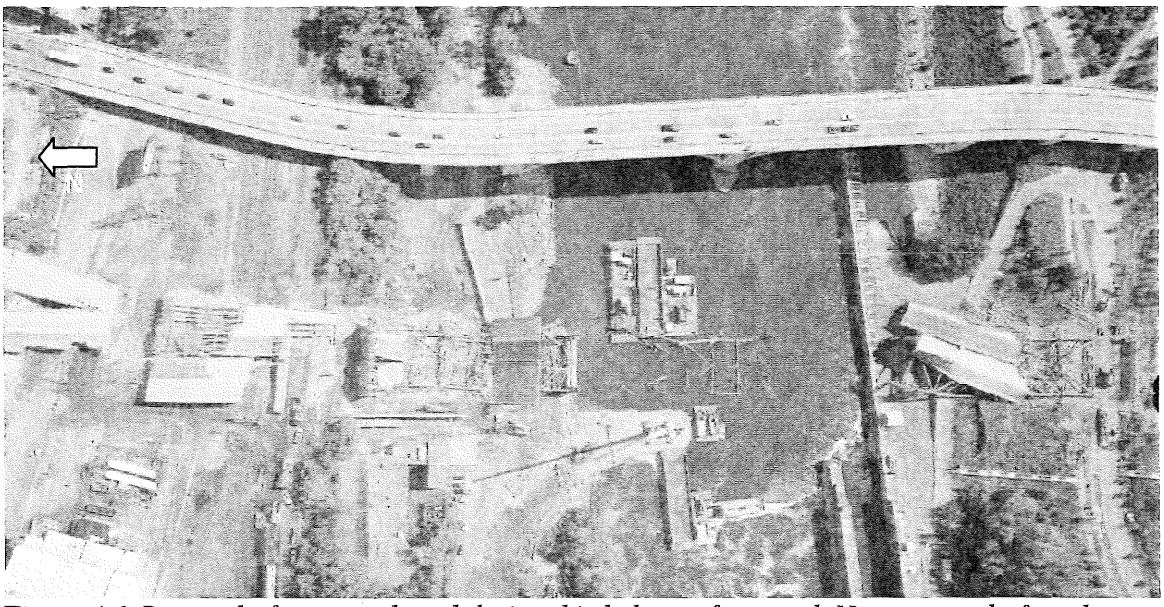

Figure 4.6. Removal of structural steel during third phase of removal. Note removal of north approach spans (Sept.19).

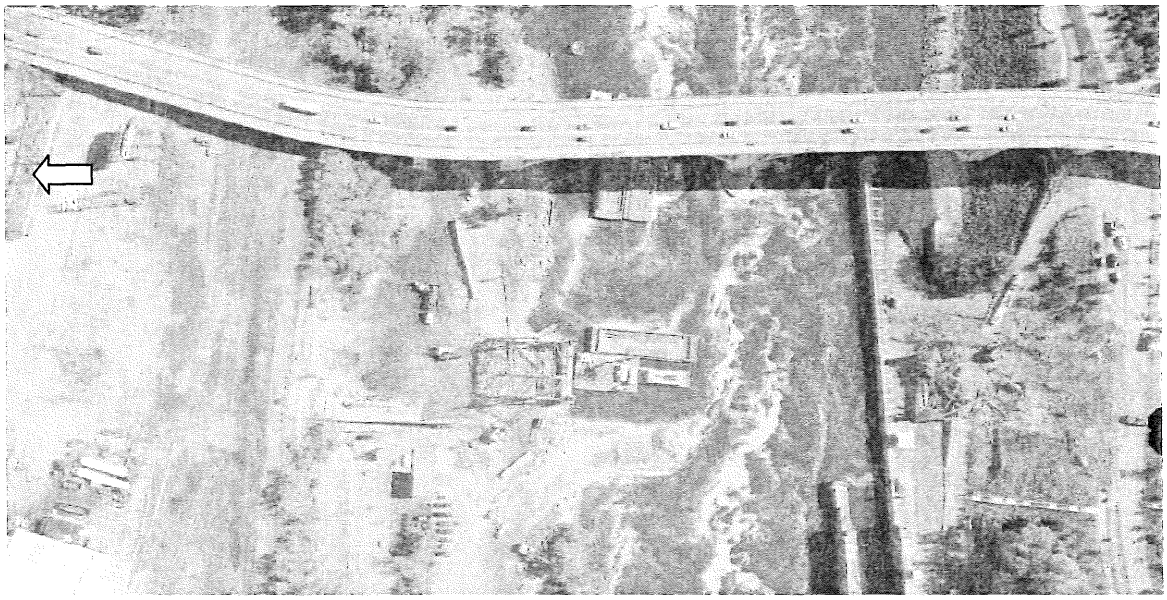

Figure 4.7. Final removal operations (Oct. 4).

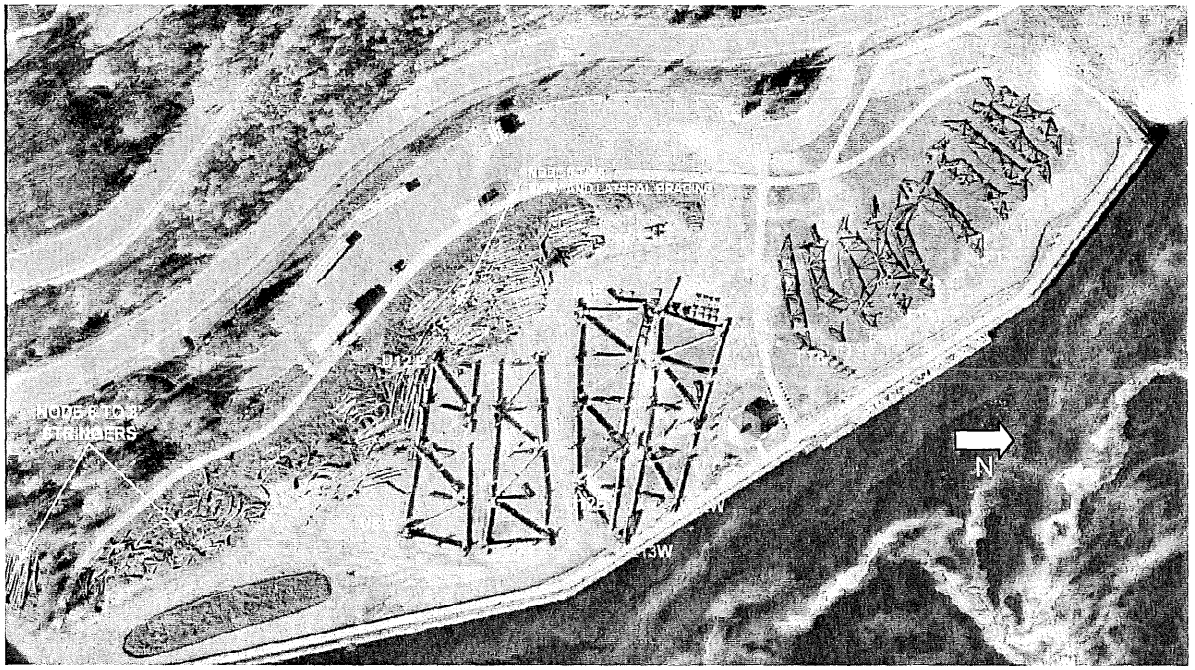

Figure 4.8. Bohemian Flats lay-down site.

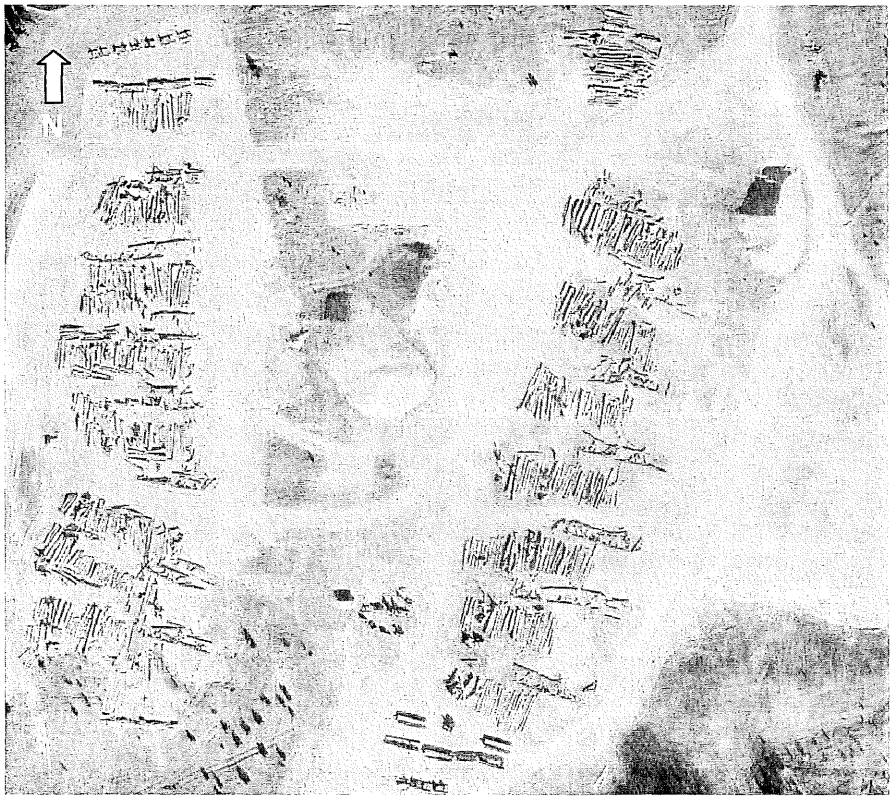

Figure 4.9. Afton storage site.

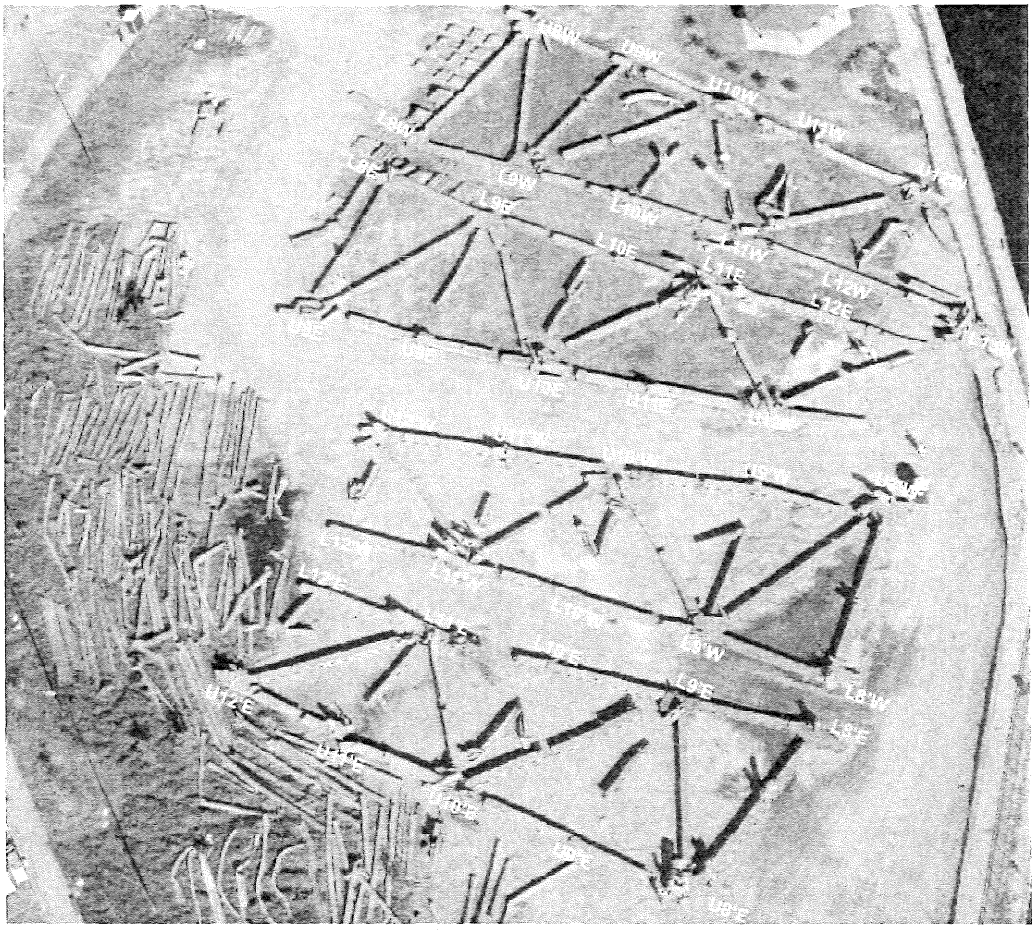

Figure 4.10. Truss lay-down for Nodes 8 to 12 and Nodes 8'to 12'.

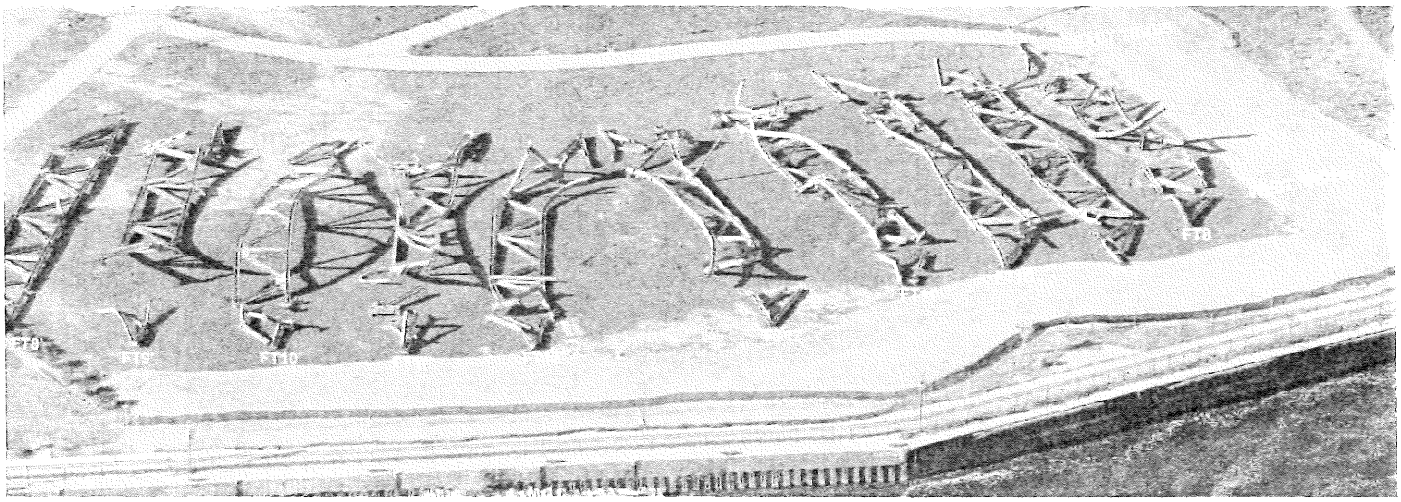

Figure 4.11. Floor truss lay-down.

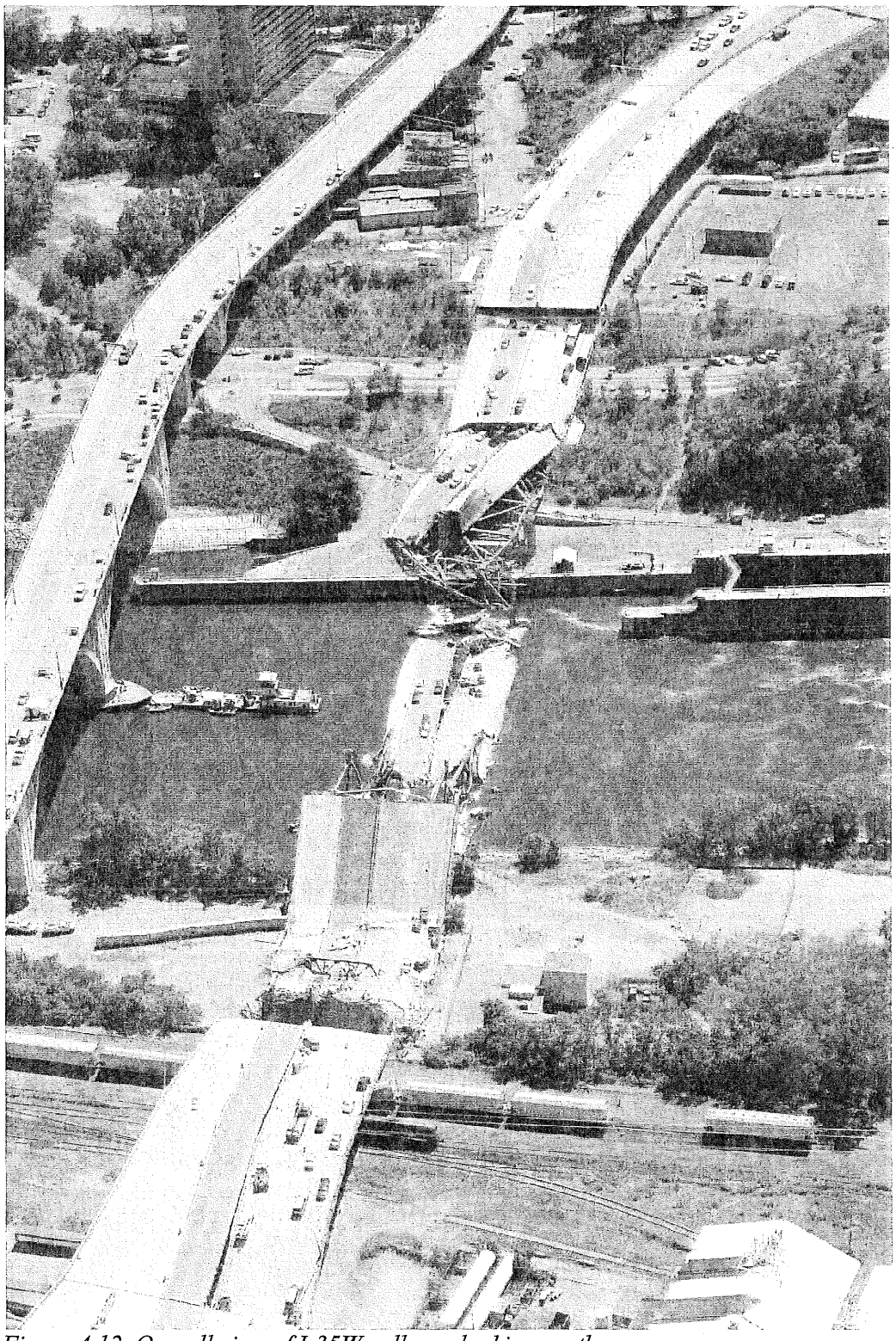

Figure 4.12. Overall view of I-35W collapse looking south.

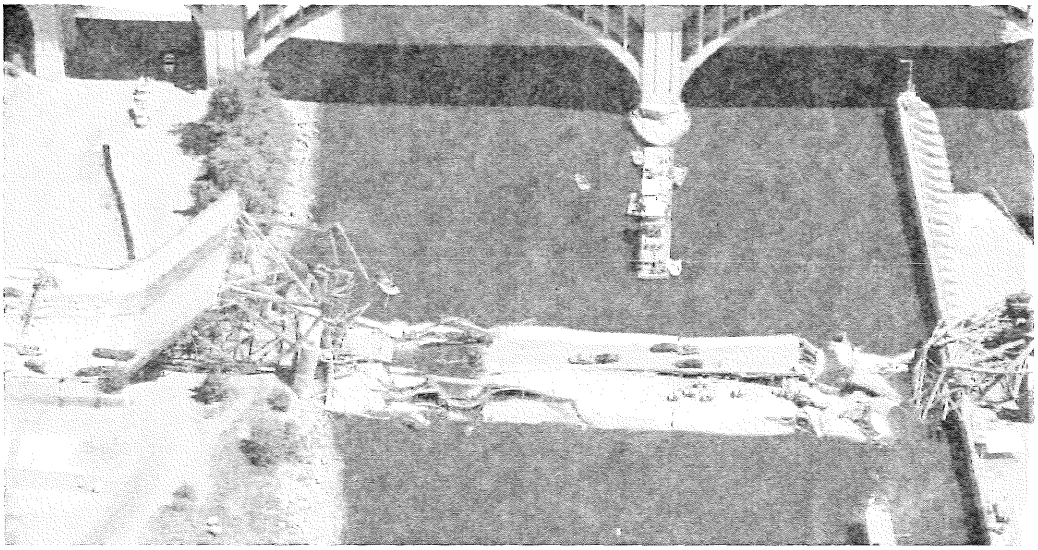

Figure 4.13. Post-collapse view of Span 7 looking east.

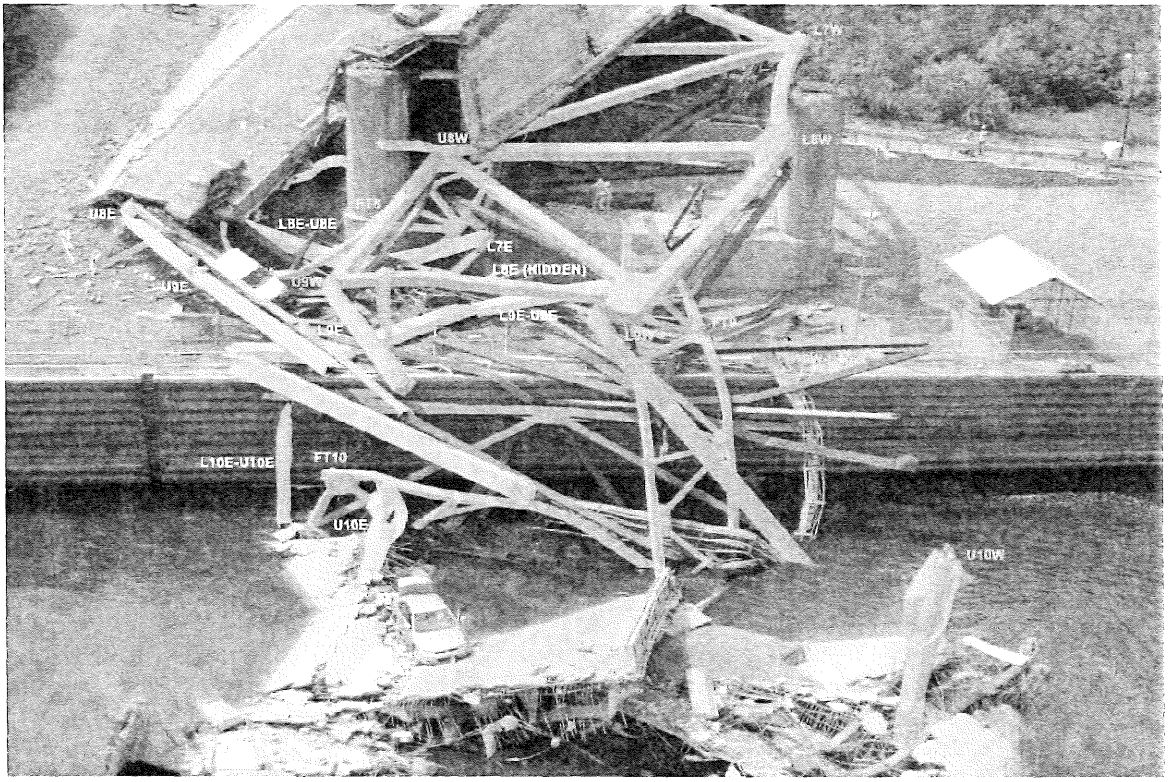

Figure 4.14. Post-collapse view of south bank of river at Pier 6.

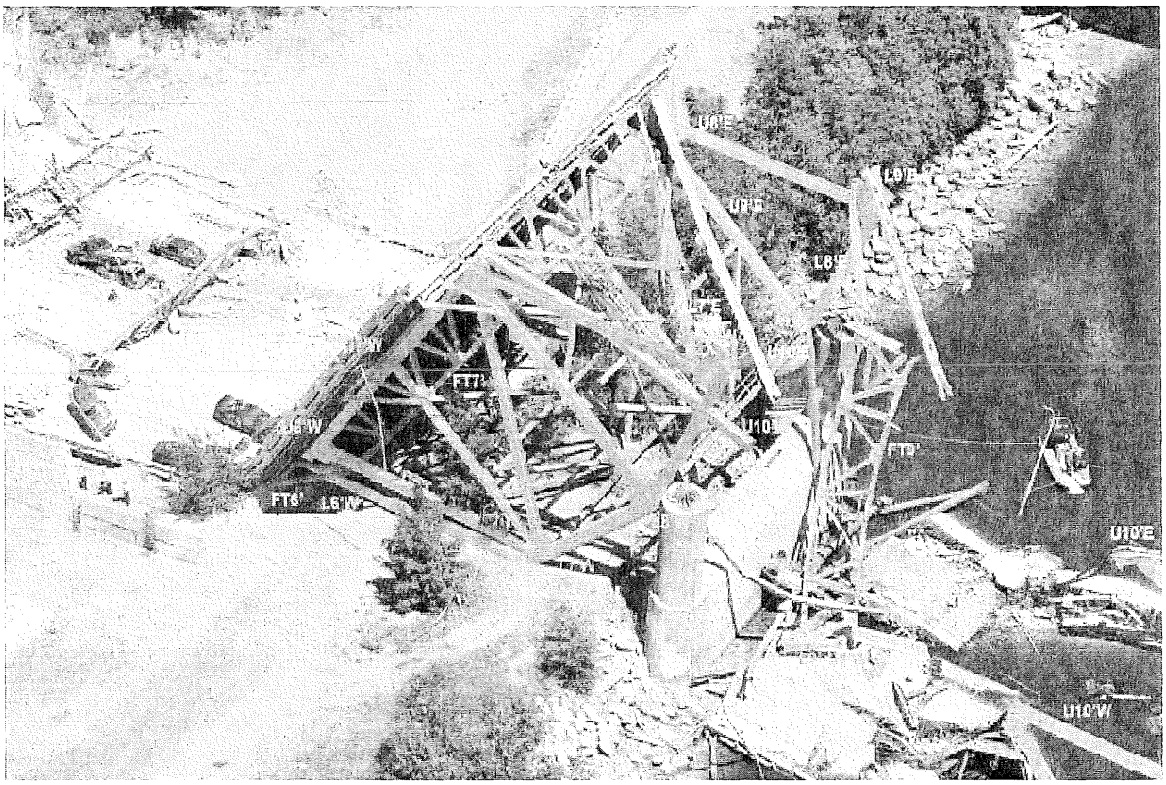

Figure 4.15. Post-collapse view of north bank of river at Pier 7.

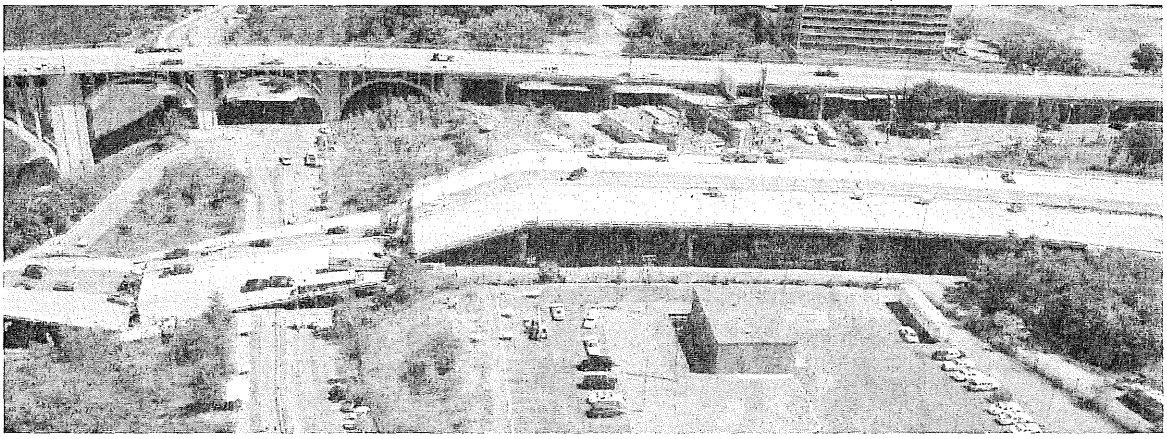

Figure 4.16. Post-collapse view of south approach spans looking southeast.

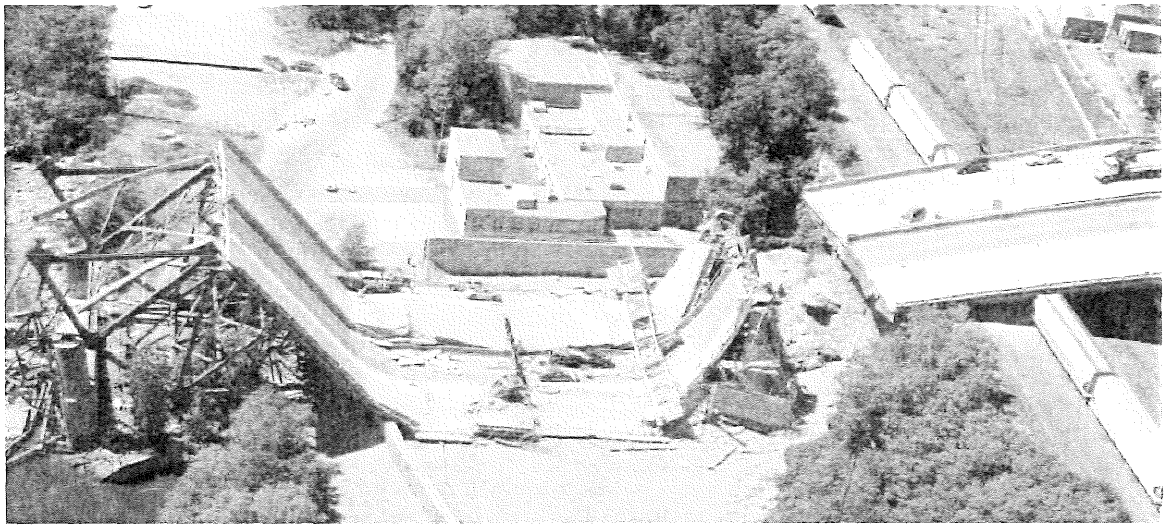

Figure 4.17. Post-collapse view of Span 8 looking west.

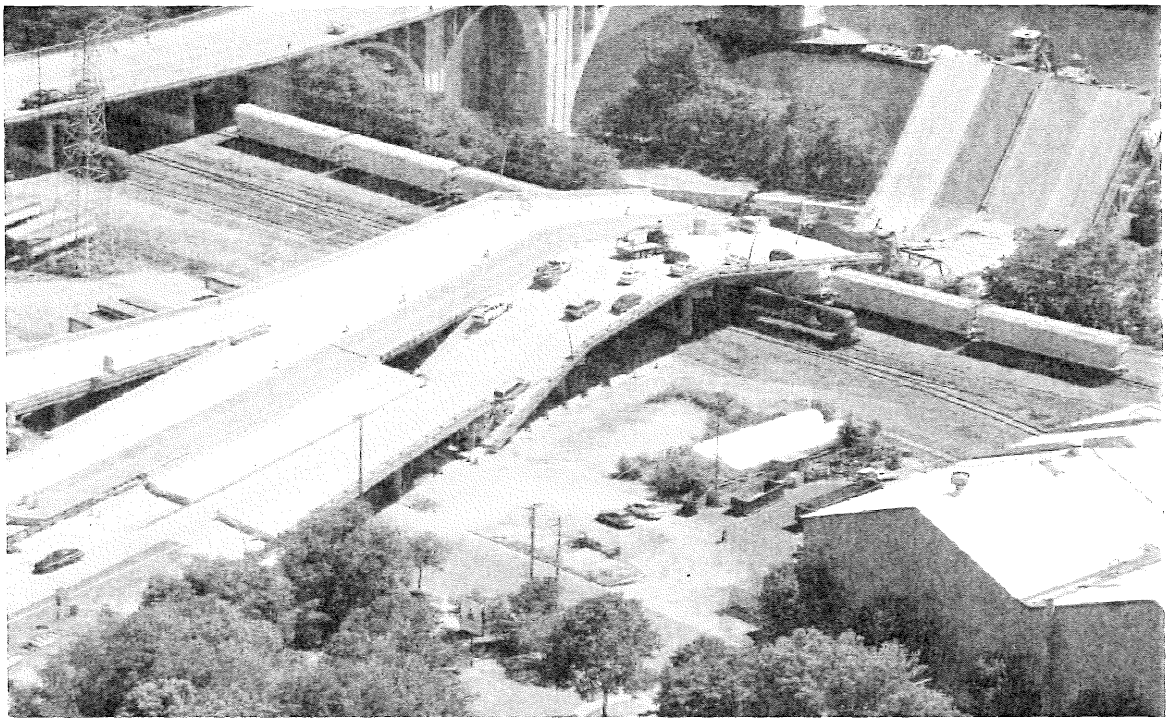

Figure 4.18. Post-collapse view of north approach spans looking southeast.

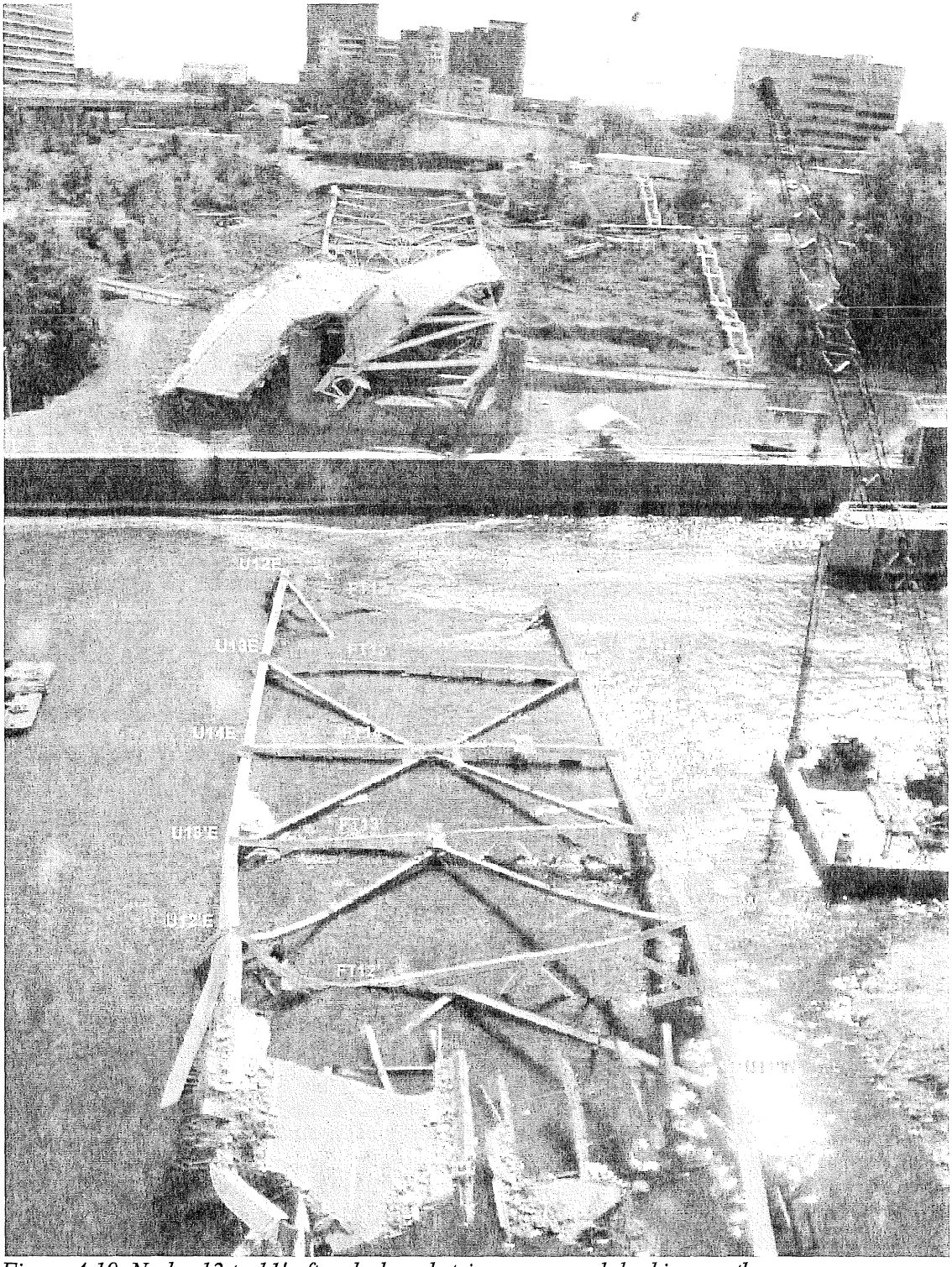

Figure 4.19. Nodes 12 to 11' after deck and stringer removal, looking south.

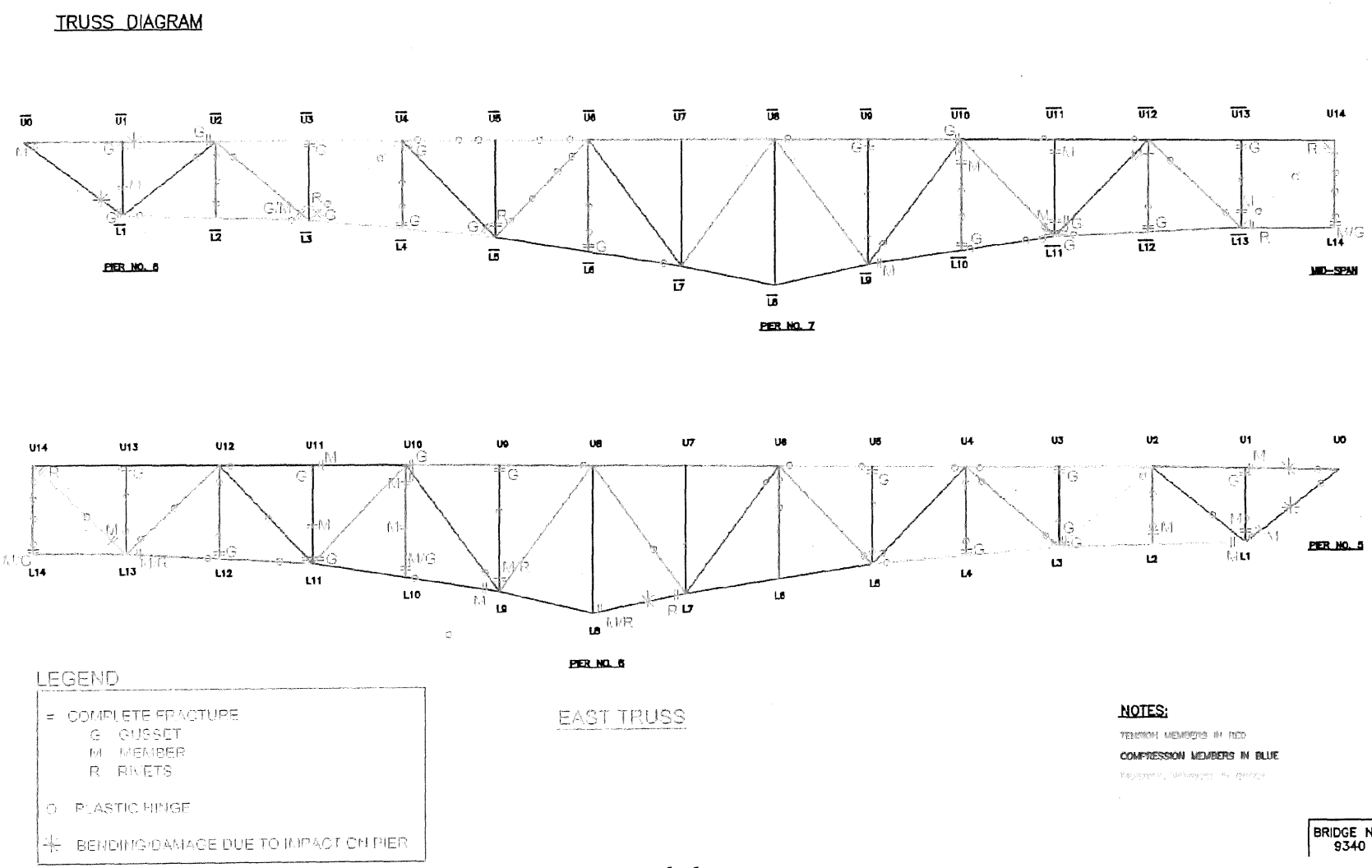

Figure 4.20. Diagram of plastic hinging and fracture locations in east deck truss.

TRUSS DIAGRAM

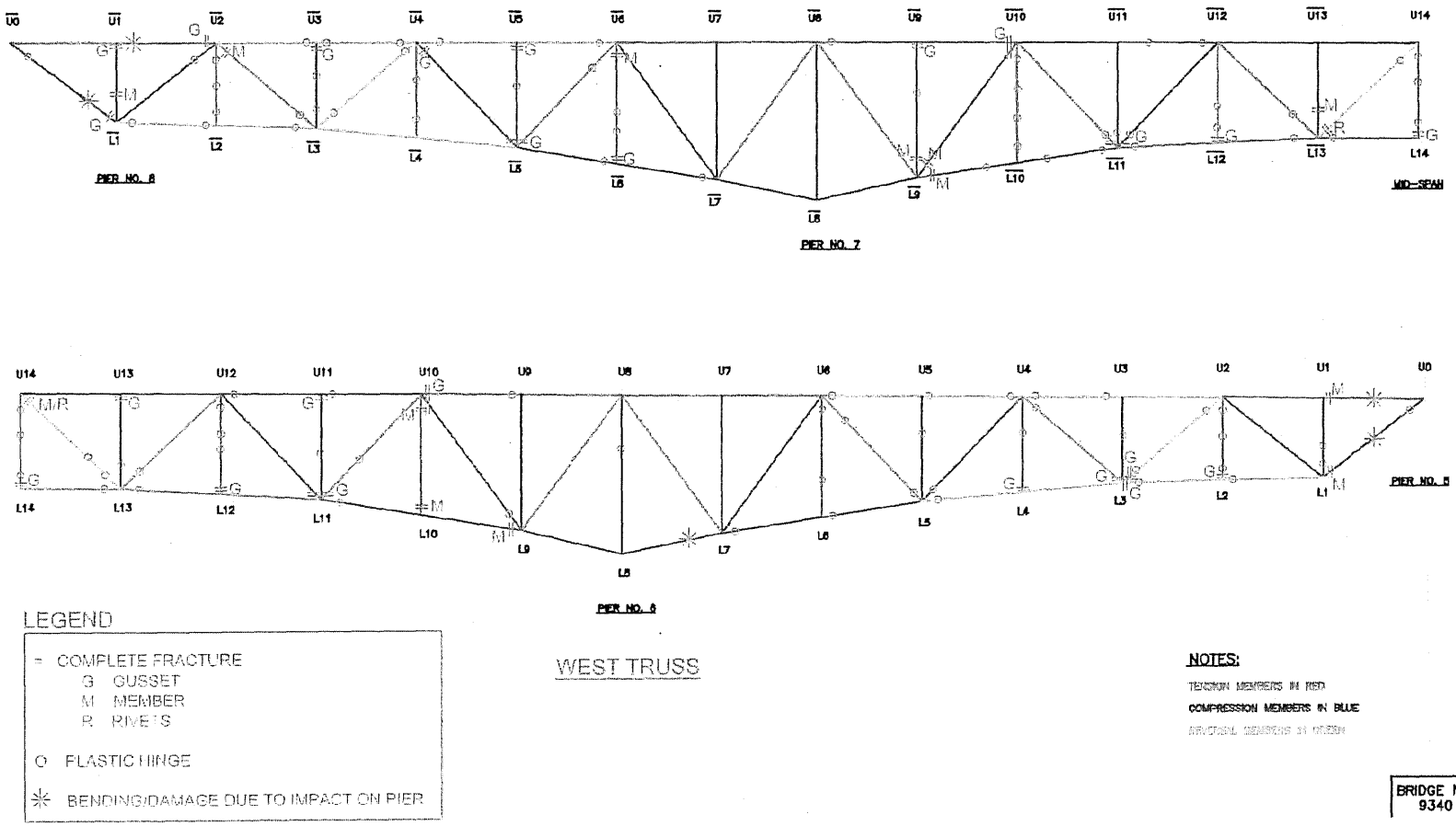

Figure 4.21. Diagram of plastic hinging and fracture locations in west deck truss.

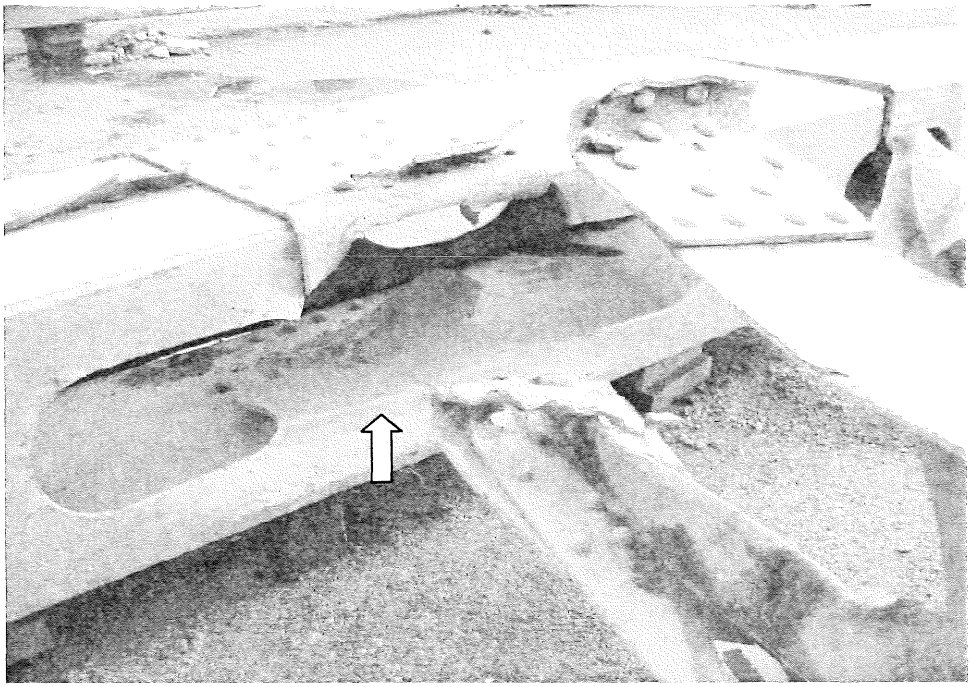

Figure 4.22. Impact damage on top cover plate of lower chord at L12'E.

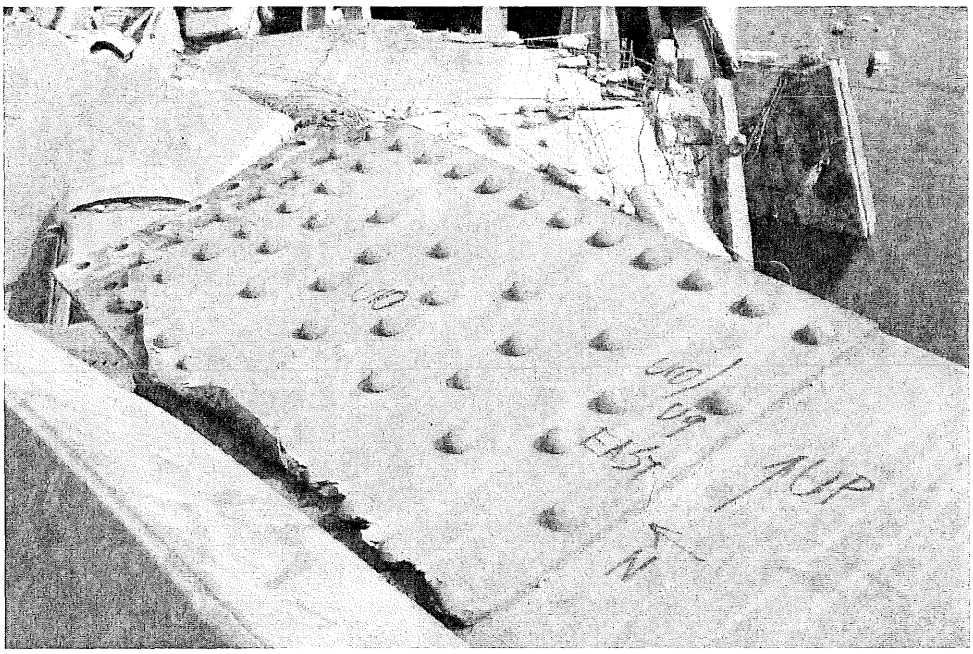

a) West side gusset at U10 end of Upper Chord U9E-U10E

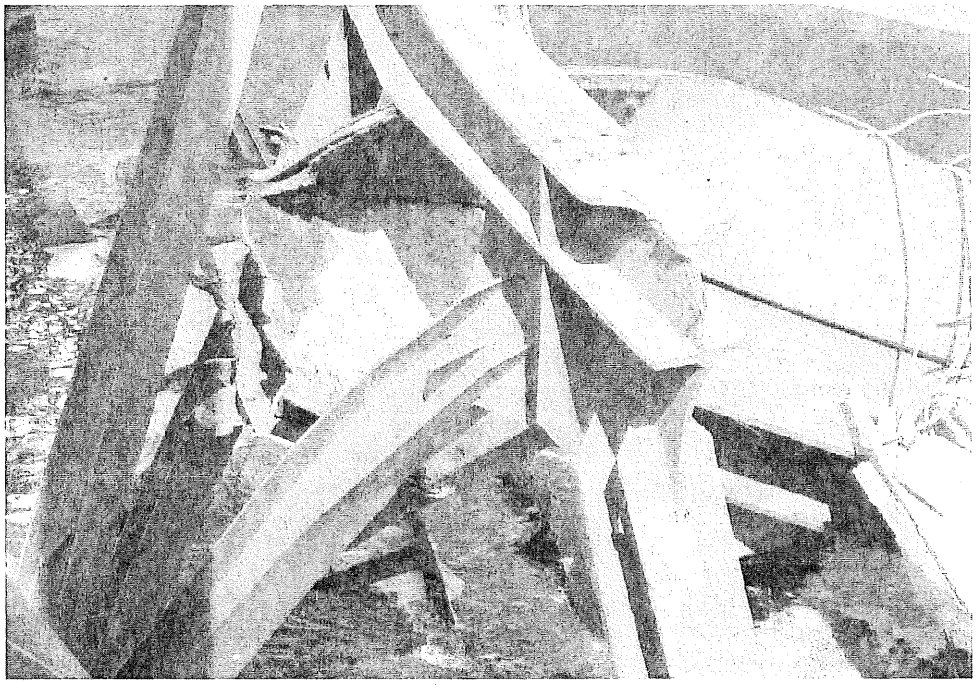

b) Node U10E, east elevation

Figure 4.23. Node U10E post-collapse condition.

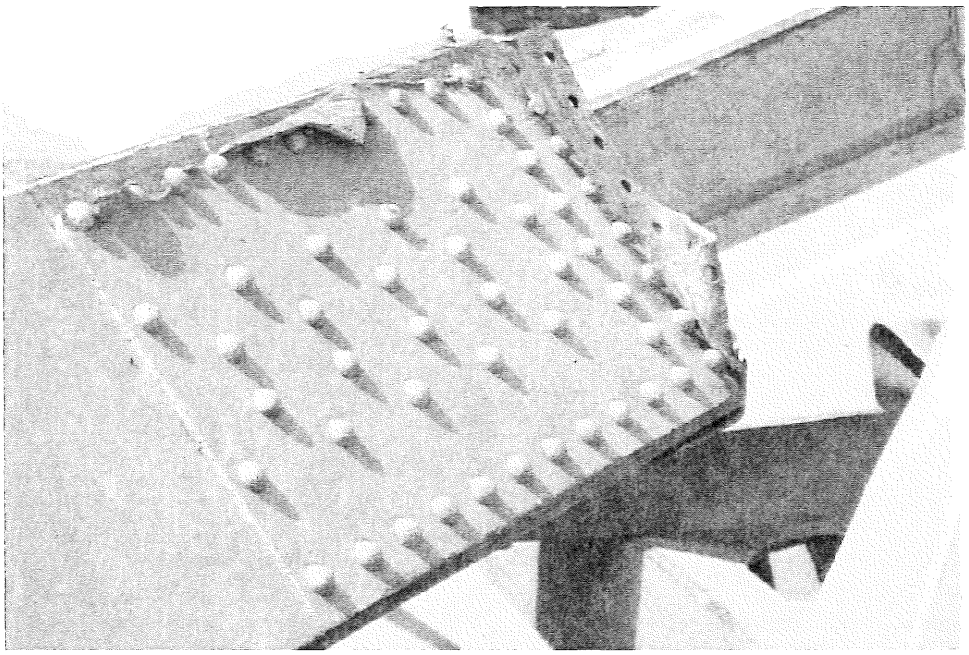

a) U10 end of Upper Chord U9-U10W, west gusset (top cover plate of U9-U10W facing down)

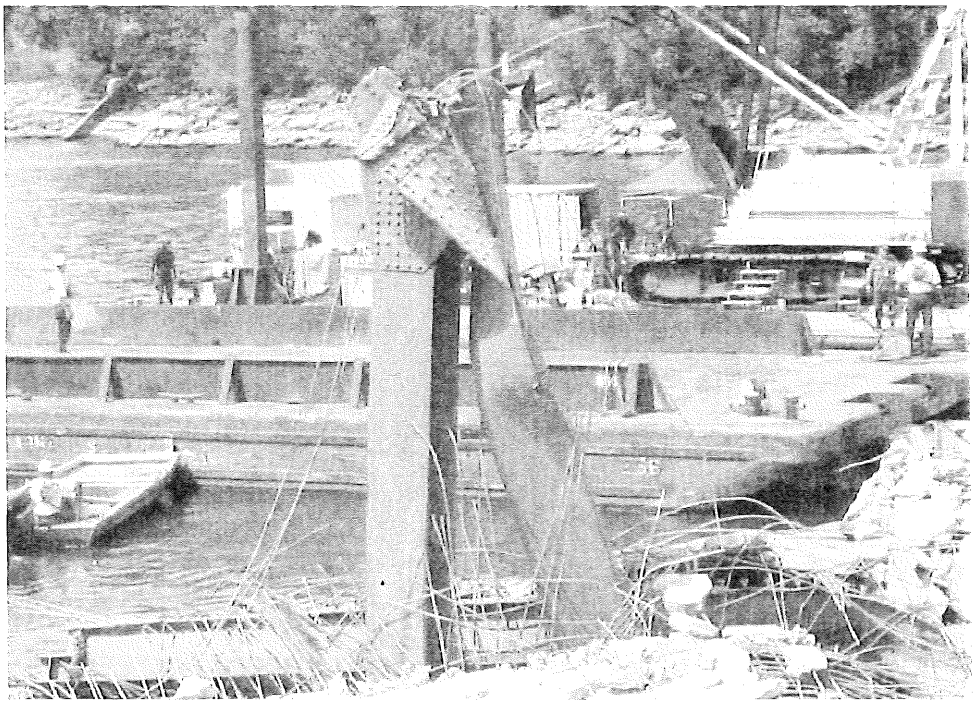

b) Node U10W, east elevation.

Figure 4.24. Node U10W post-collapse condition.

a) U10' end of Upper Chord U9'-U10'E (top cover plate, and east gusset shown)

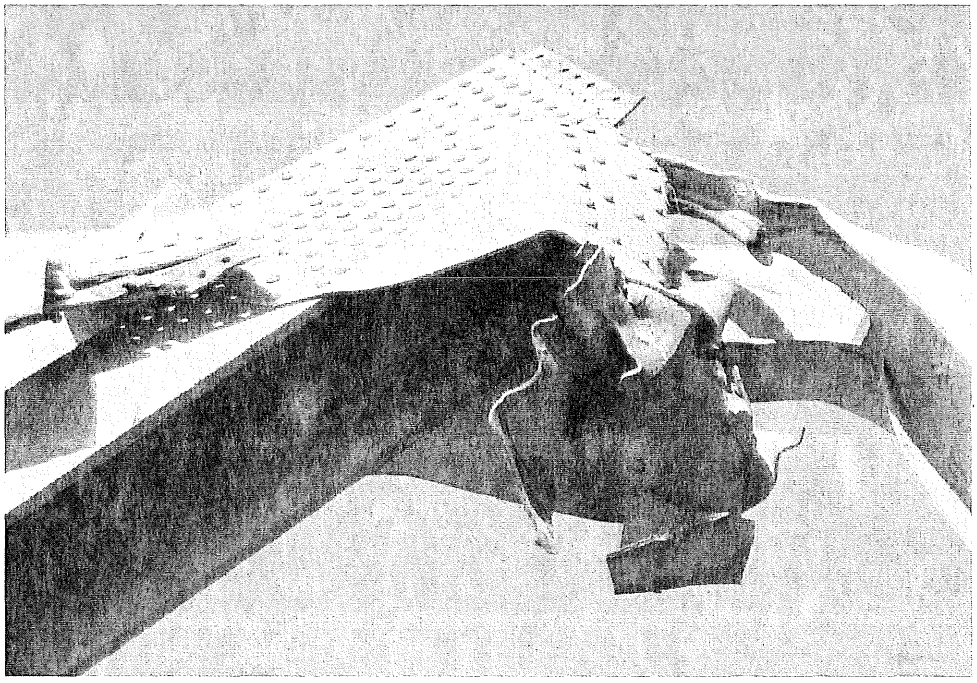

b) Node U10'E, east elevation.

Figure 4.25. Node U10'E post-collapse condition.

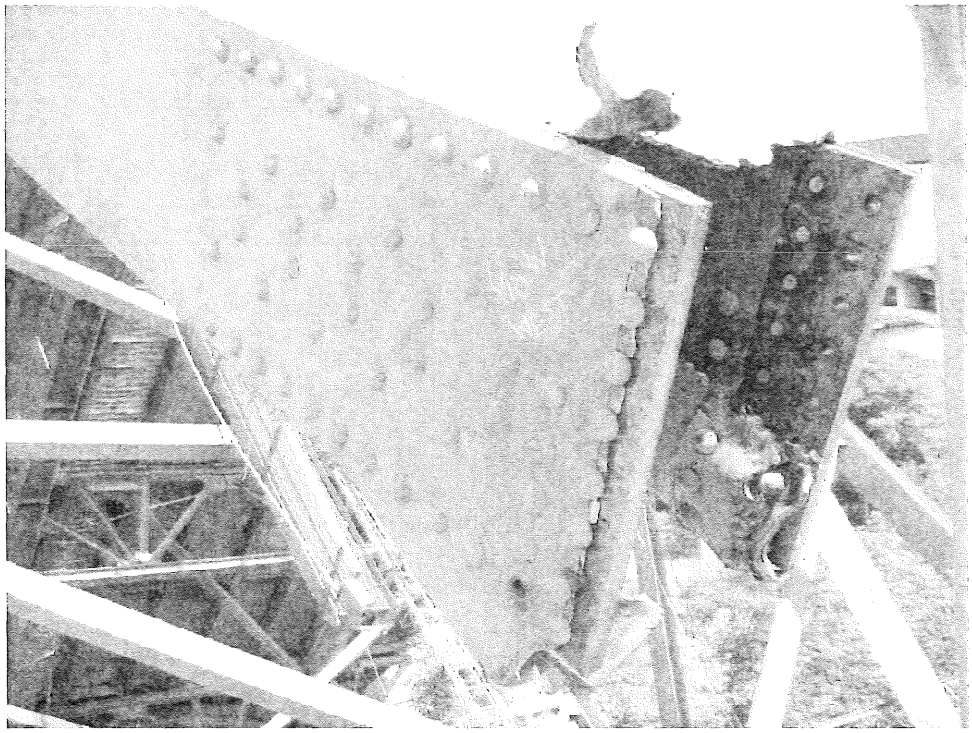

a) U10'end of Upper Chord U9'-U10'W, west gusset

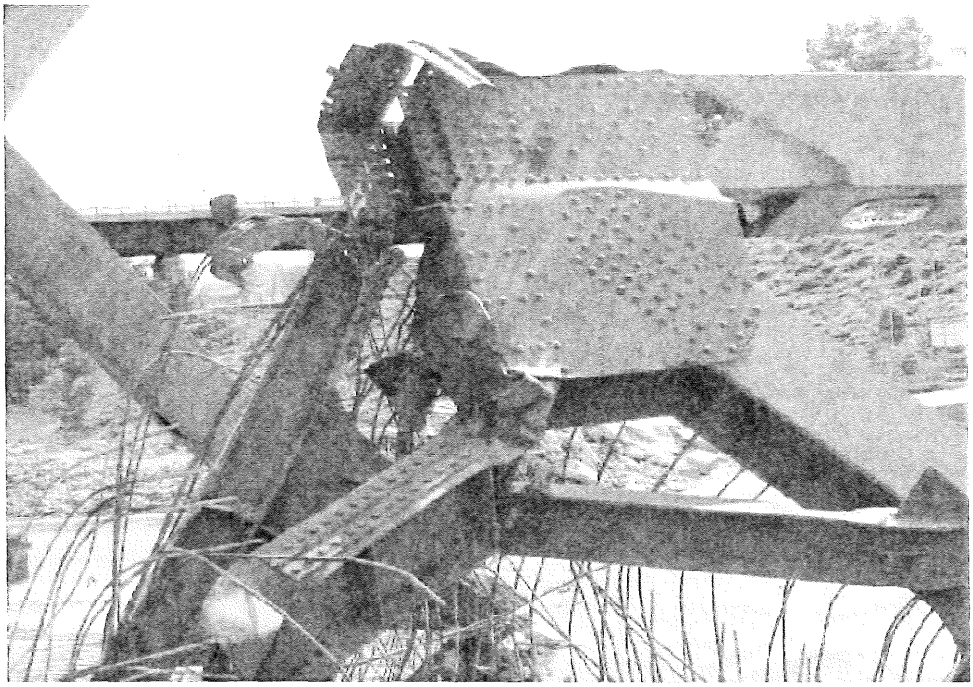

b) Node U10'W, west elevation.

Figure 4.26. Node U10'W post-collapse condition.

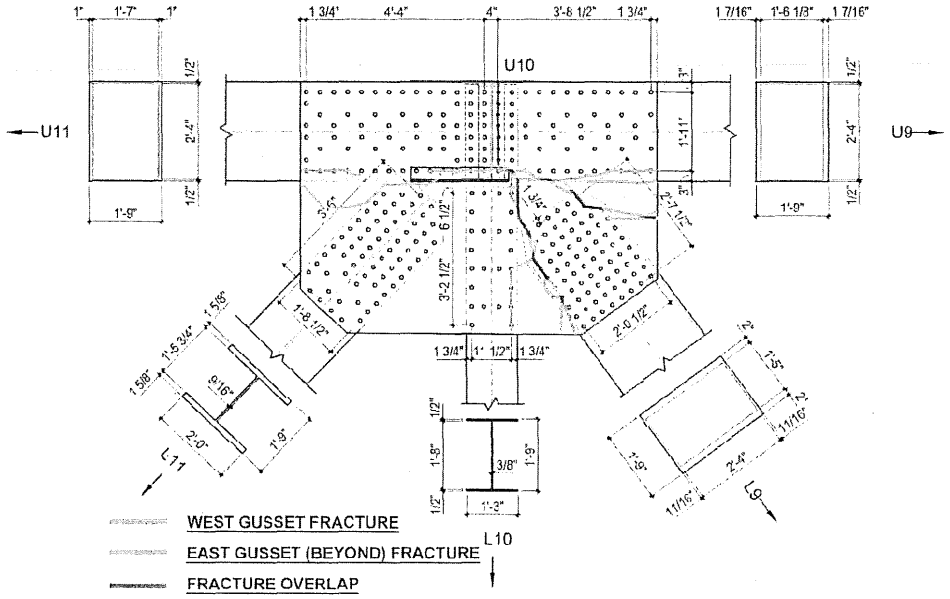

a) Schematic of fractures in U10E gusset plates (base drawing by FHWA).

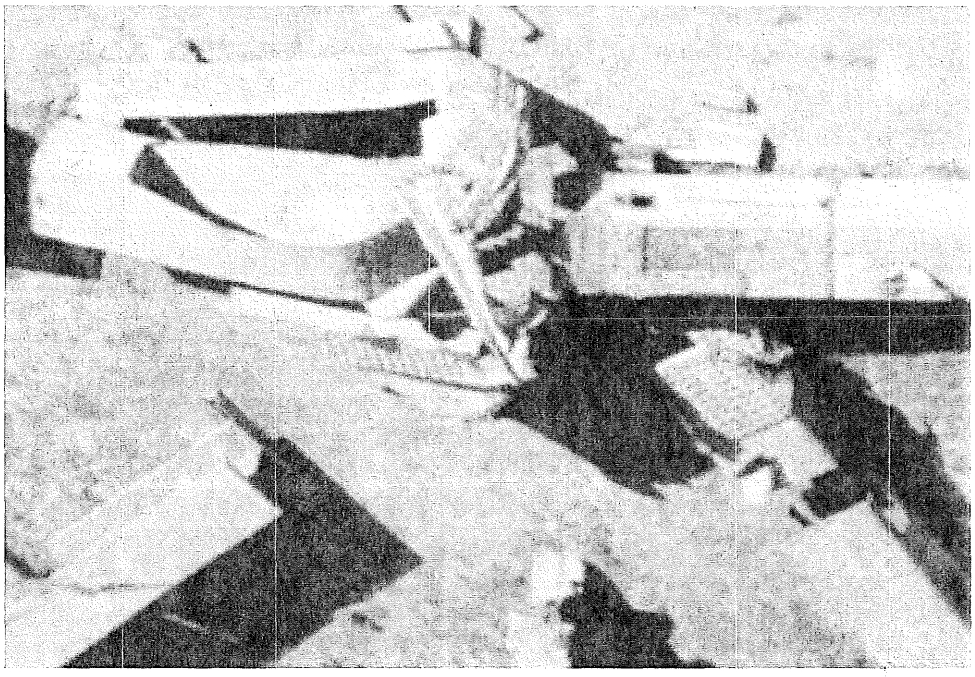

b. Node U10E in lay-down yard, west elevation facing up.

Figure 4.27. Node U10E gusset plate fractures locations.

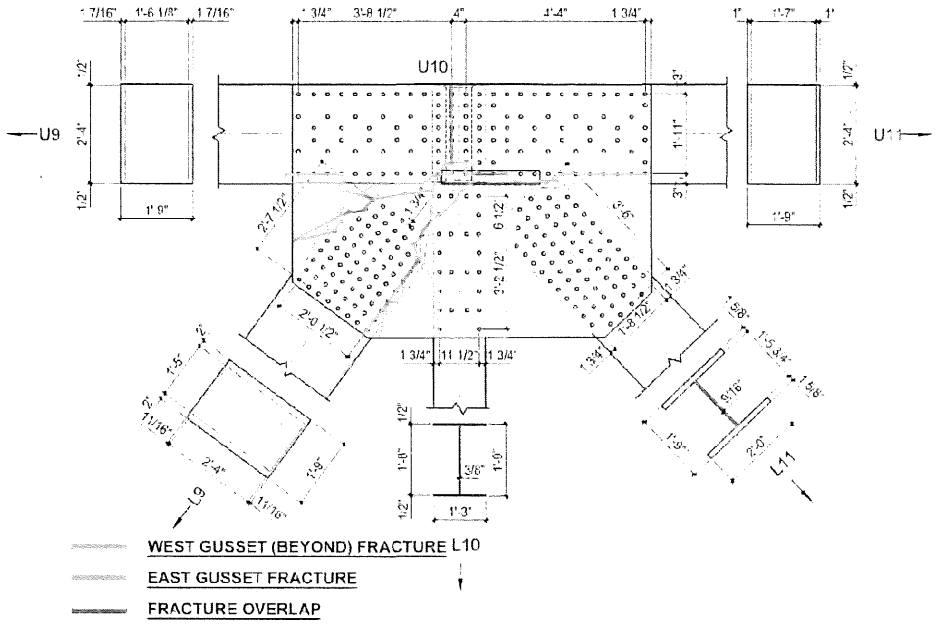

a) Schematic of fractures in U10W gusset plates (base drawing by FHWA).

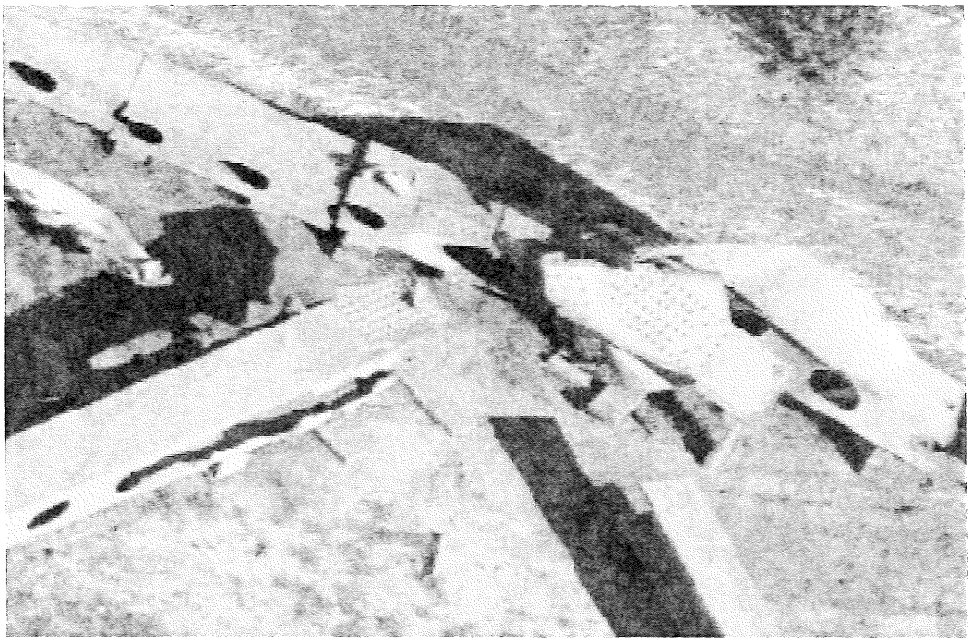

b) Node U10W in lay-down yard, east elevation facing up.

Figure 4.28. Node U10W gusset plate fracture locations.

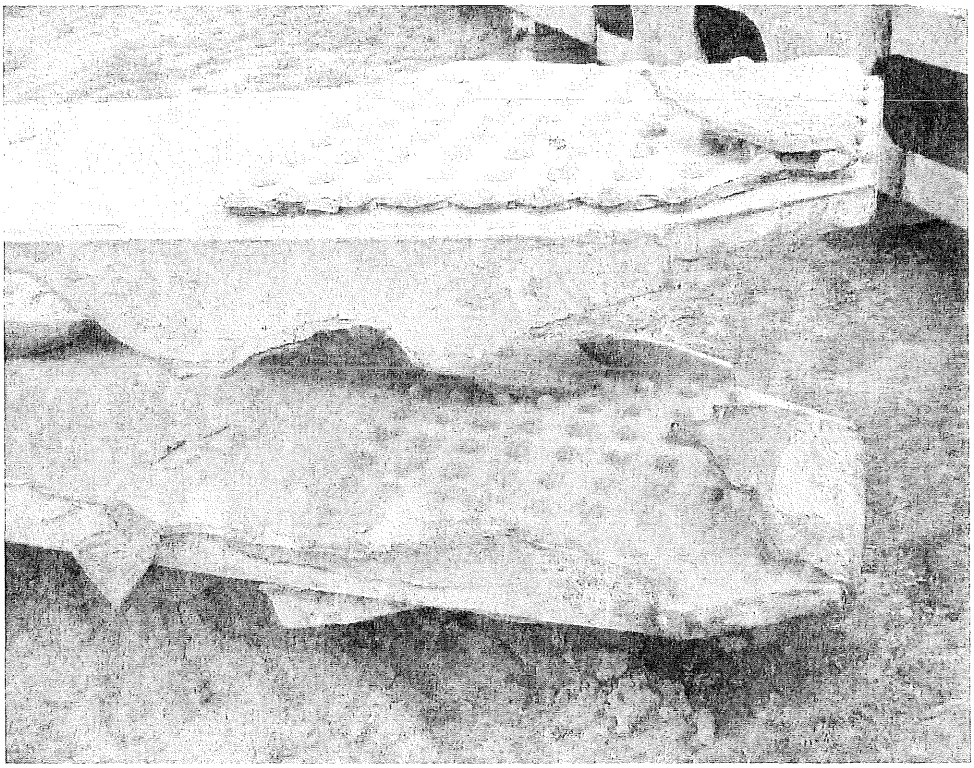

Figure 4.29. L9-U10W, U10W end, east elevation facing up.

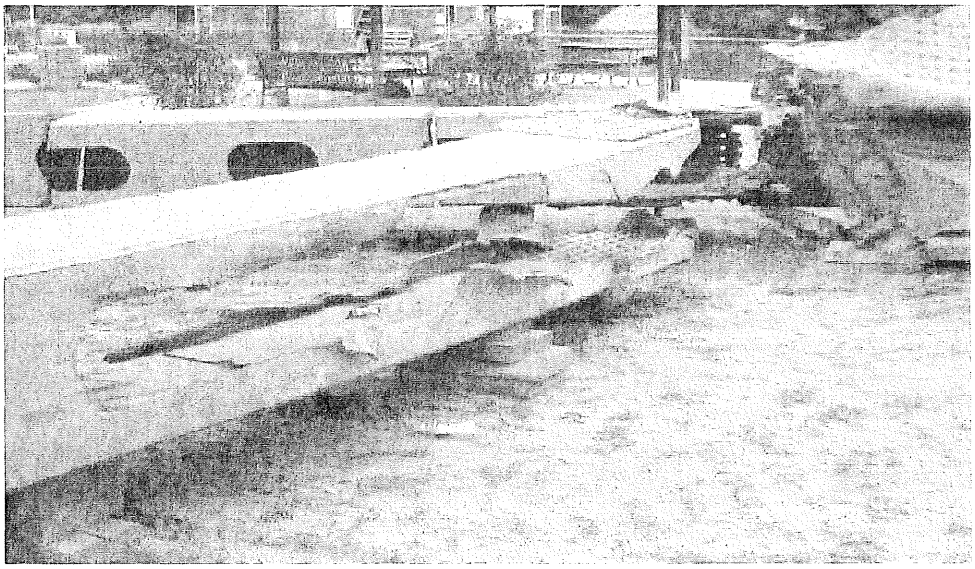

Figure 4.30. Splitting of cover plates at U10 end of Diagonal L9-U10W, east elevation facing up.

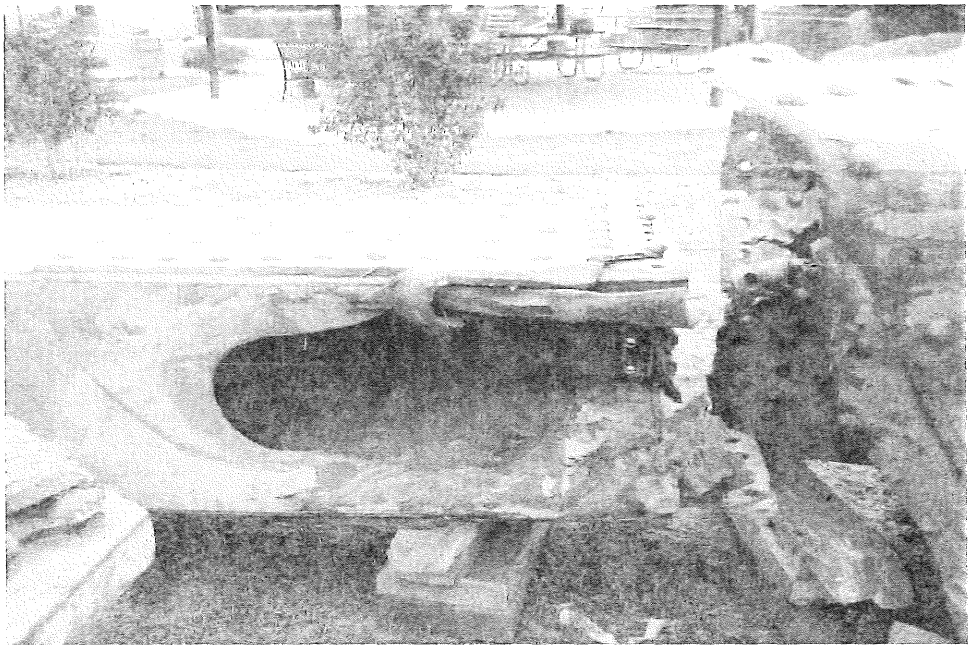

Figure 4.31. Bottom cover plate pushed into Lower Chord U9-U10W at U10.

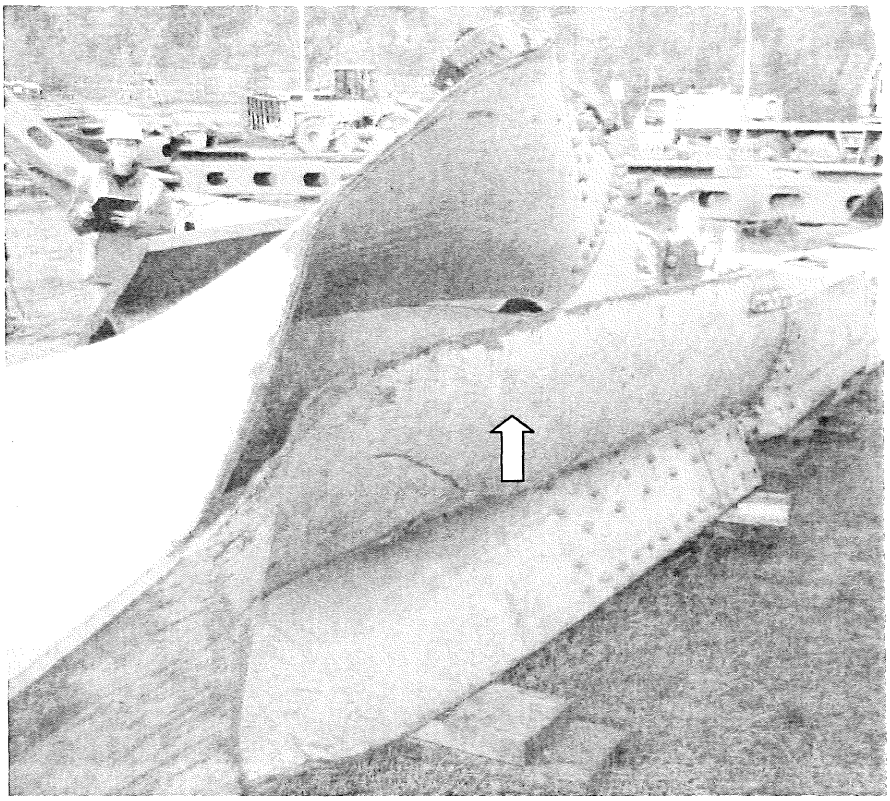

Figure 4.32. Top cover plate of Upper Chord U10W-U11W separated from side plates at U10.

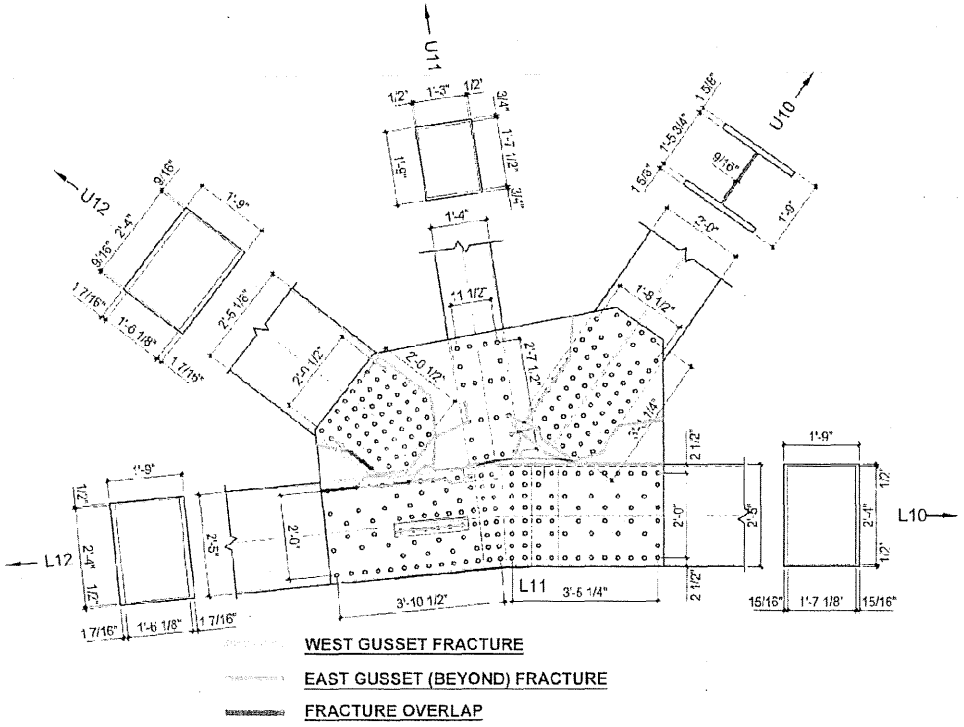

a) Schematic of fractures in L11E gusset plates (base drawing by FHWA).

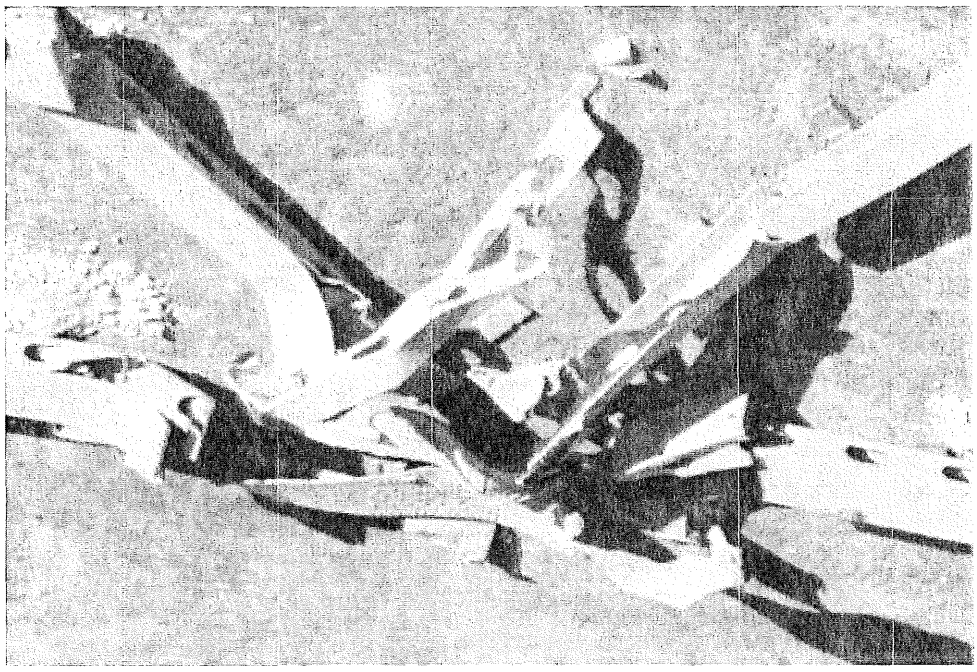

b) Node L11E in lay-down yard, west elevation facing up.

Figure 4.33. Node L11E gusset plate fracture locations.

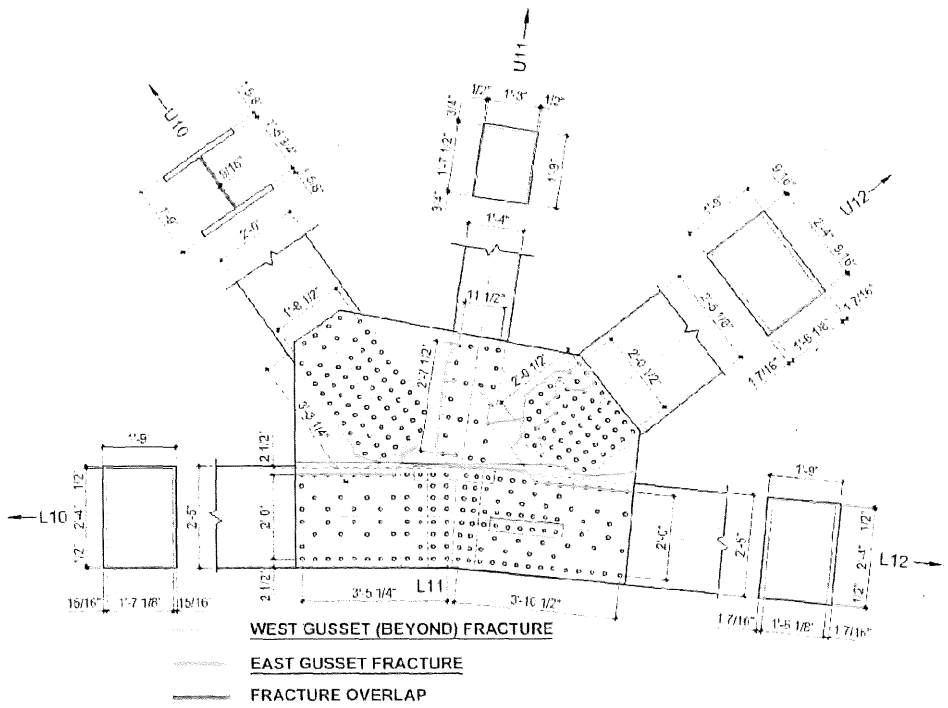

a) Schematic of fractures in L11W gusset plates (base drawing by FHWA).

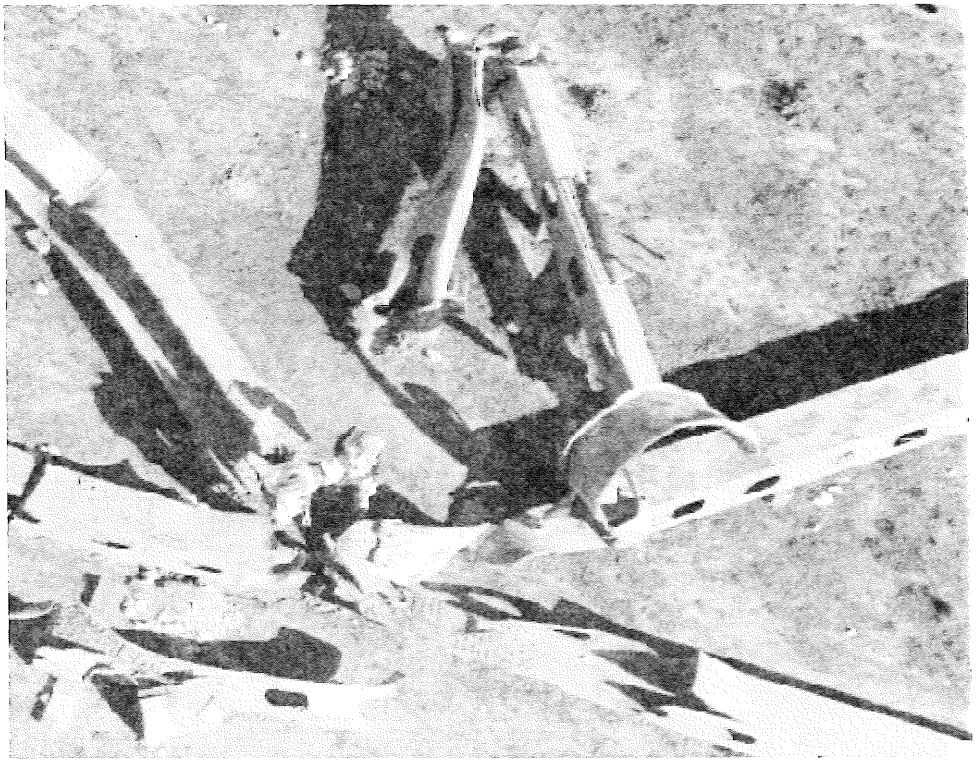

b) Node L11W in lay-down yard, east elevation facing up.

Figure 4.34. Node L11W gusset plate fracture locations.

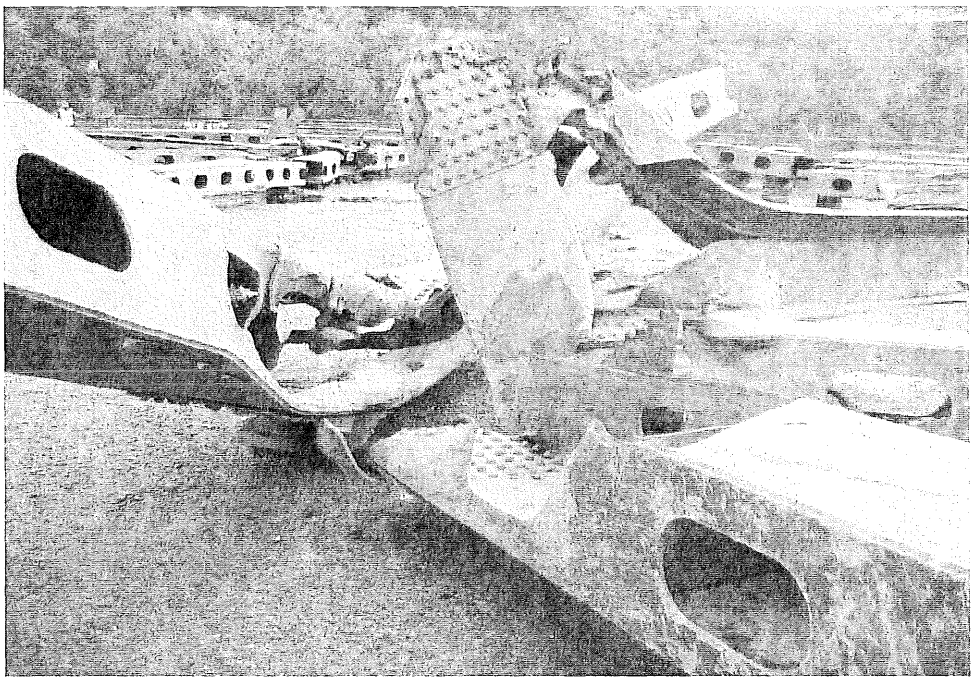

Figure 4.35. L11'E, west elevation facing up.

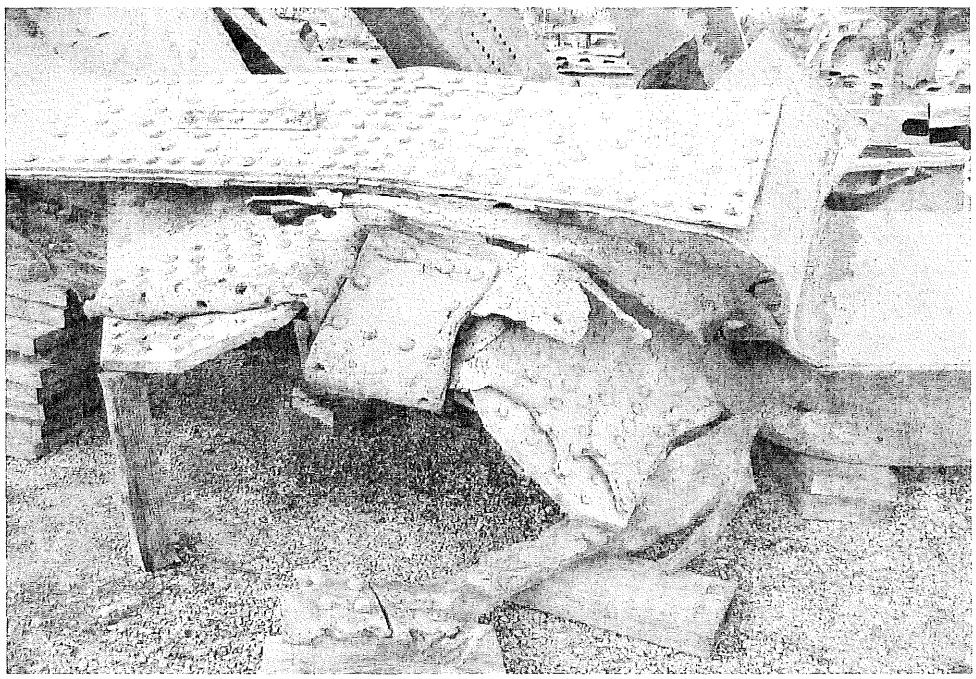

Figure 4.36. L11'W, east elevation facing up.

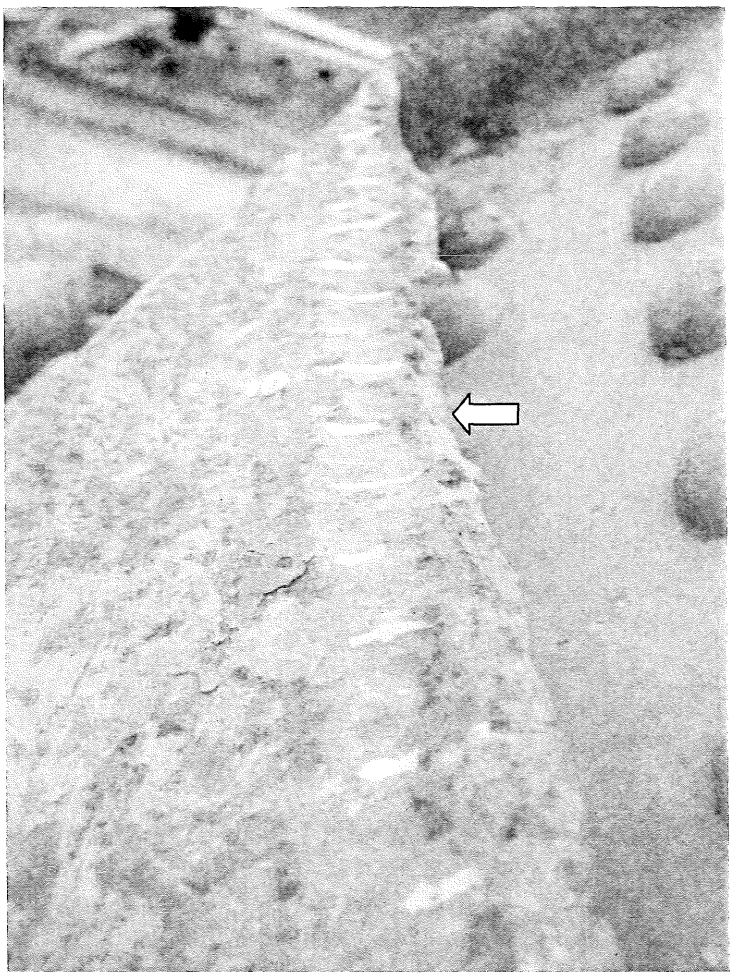

Figure 4.37. Pitting resulting from corrosion near the fracture surface of L11W. Note fractured edge adjacent to plate section loss.

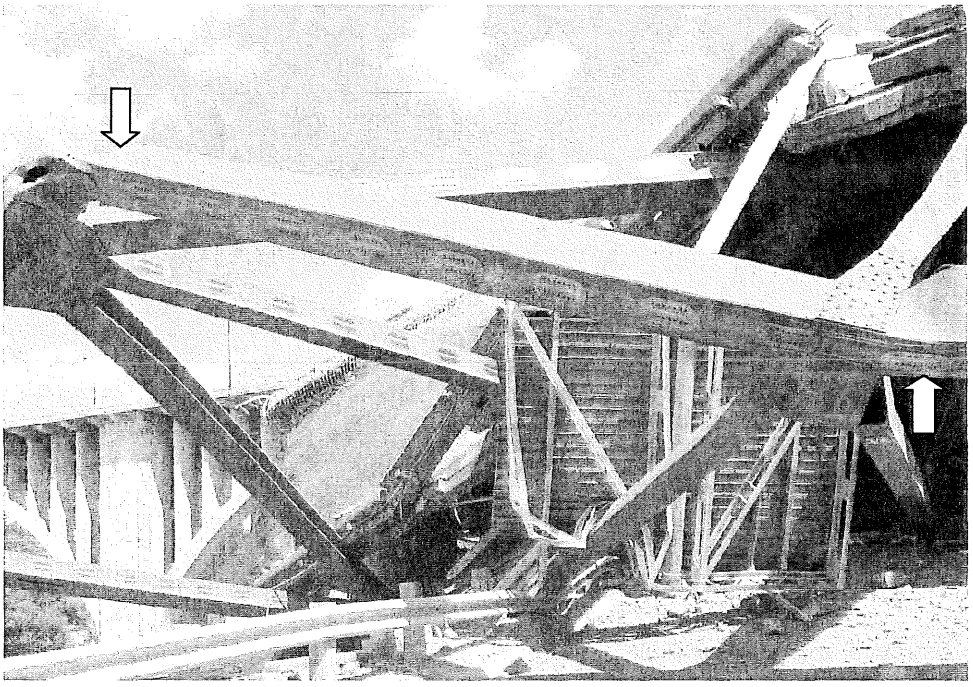

Figure 4.38. Lower chord L6W-L7W looking east. Note plastic hinging south of Node L7W and south of Node L6W.

Figure 4.39. Partial fracture in Lower Chord L7E-L8E.

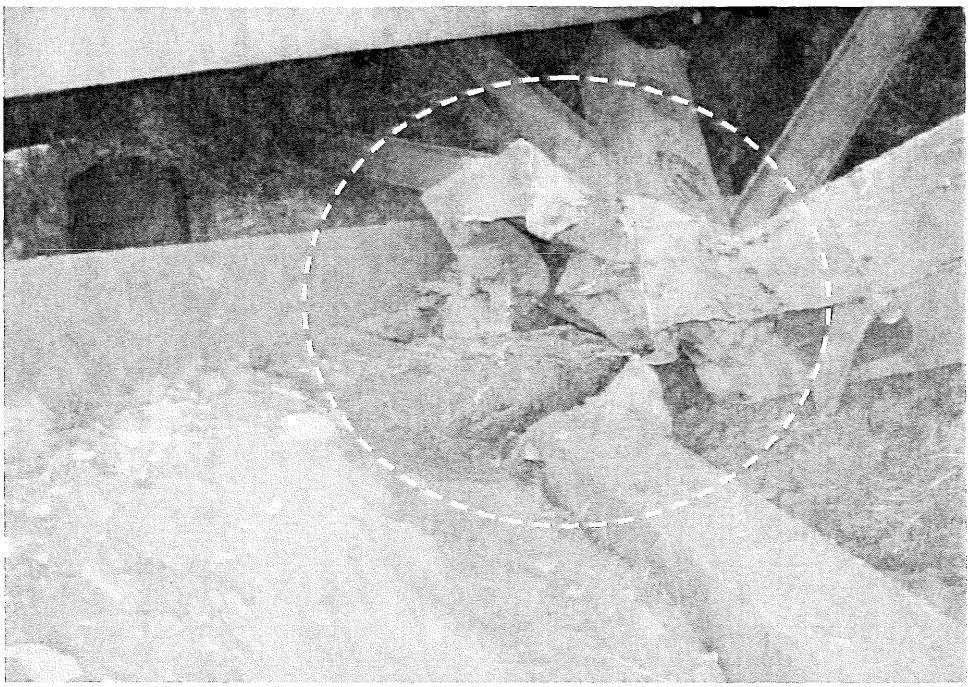

Figure 4.40. Node L3E, west elevation.

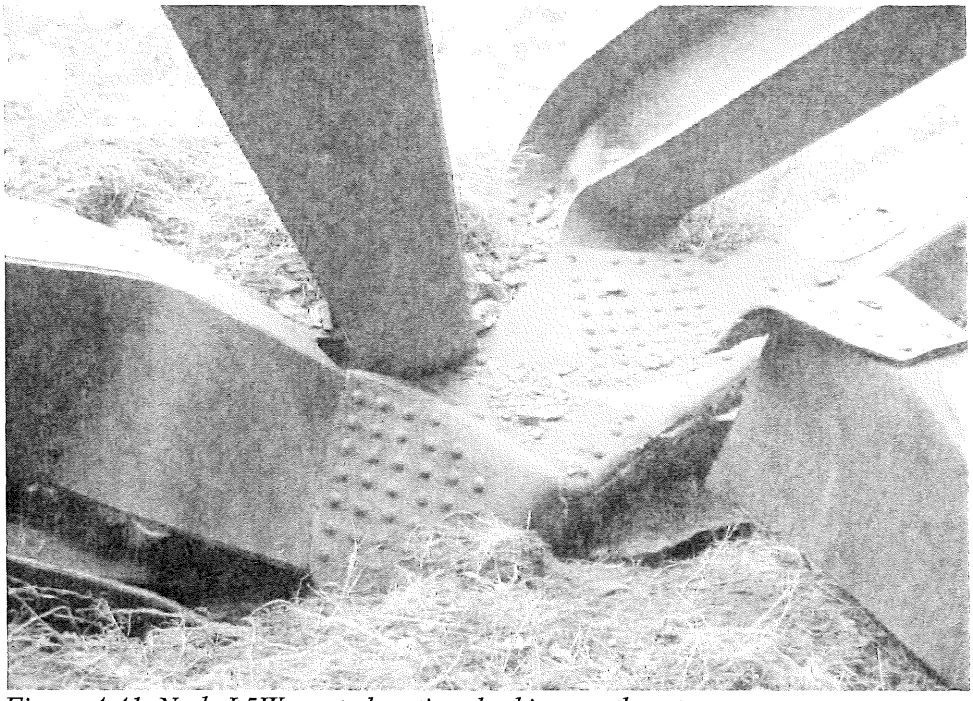

Figure 4.41. Node L5W, east elevation, looking northeast.

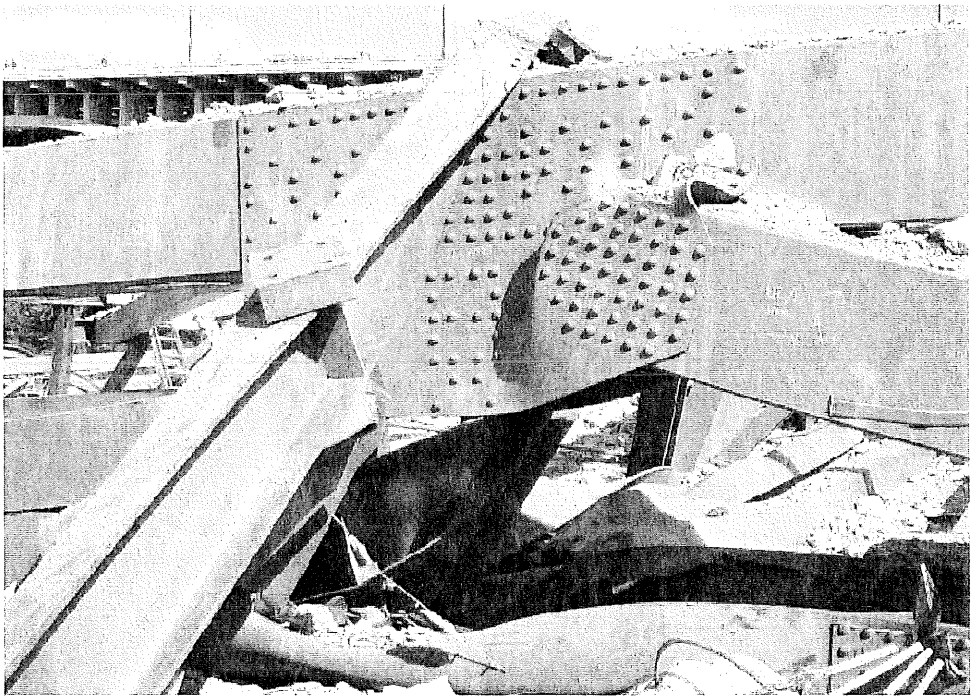

Figure 4.42. Node U2W, west elevation.

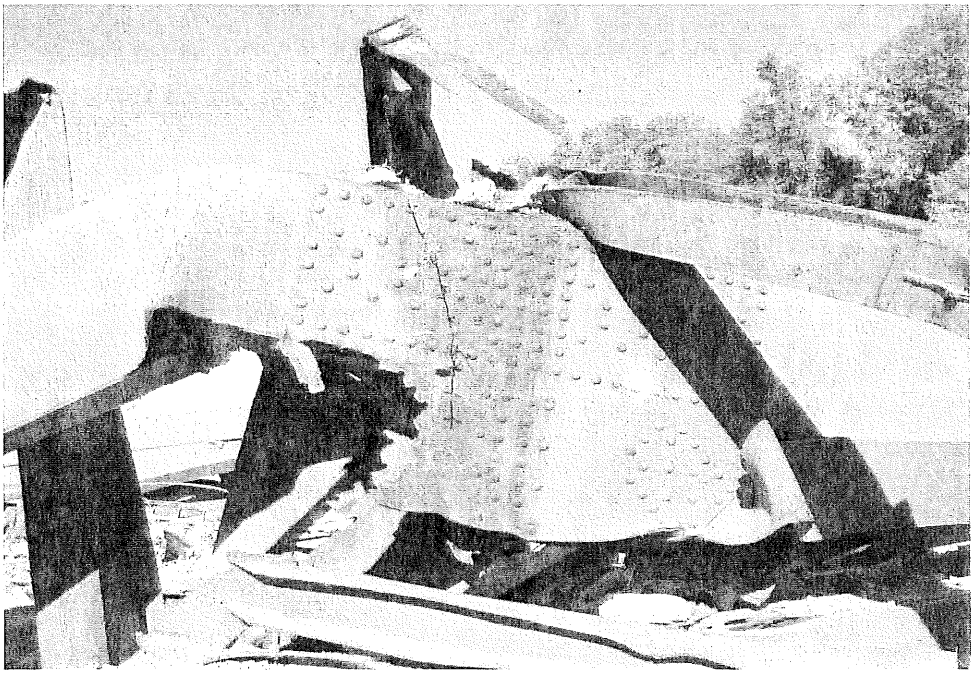

Figure 4.43. Corrosion on east gusset at U4'E.

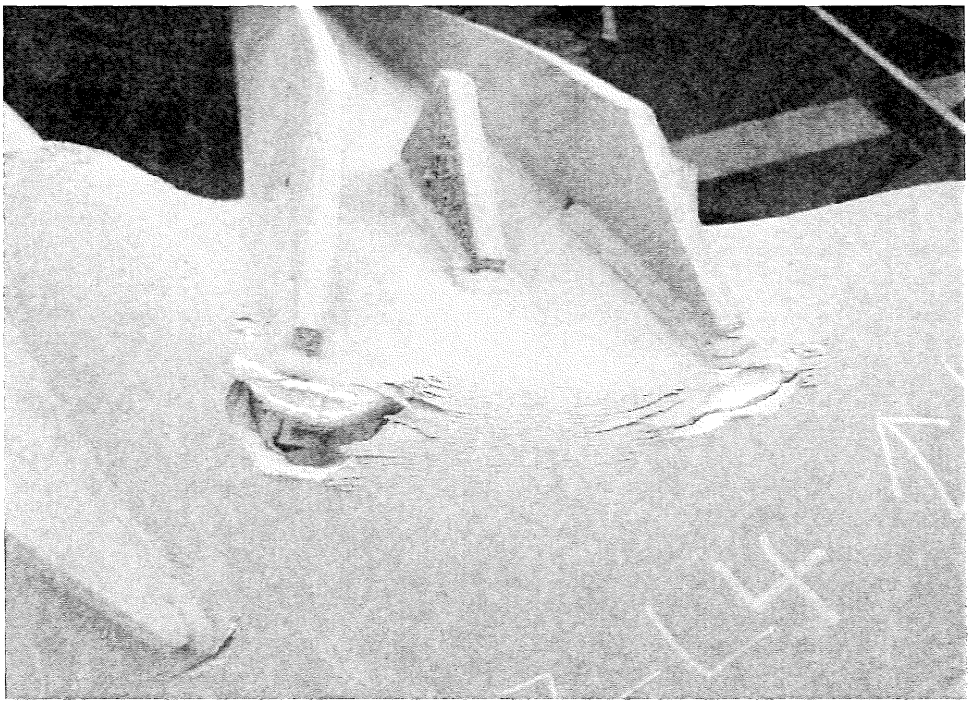

Figure 4.44. Tearing in gusset plate at flange tips of floor truss diagonals (FT7L4).

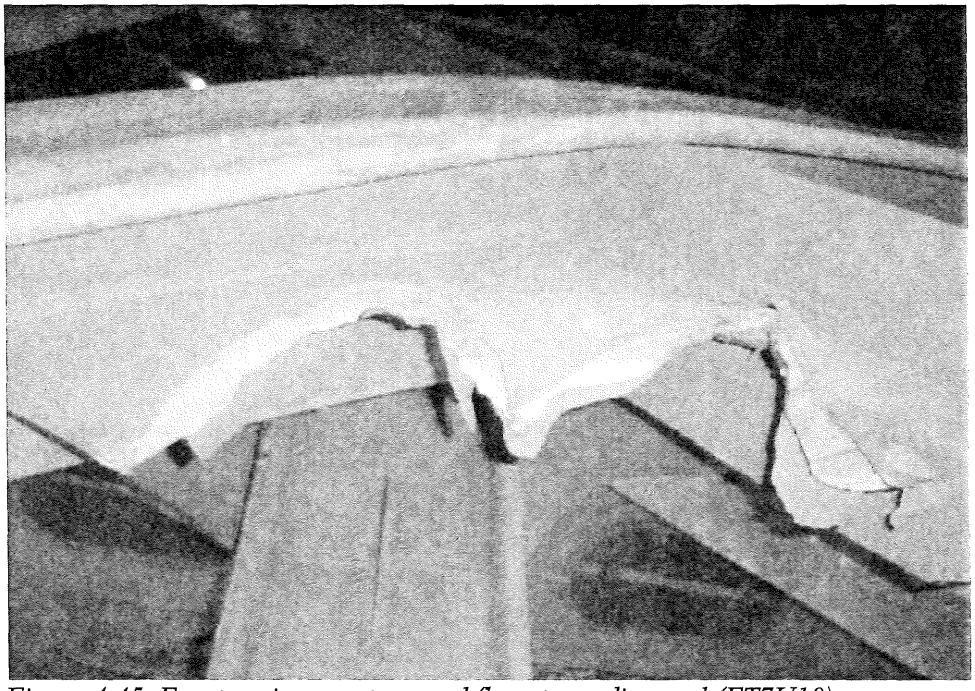

Figure 4.45. Fracture in gusset around floor truss diagonal (FT7U10).

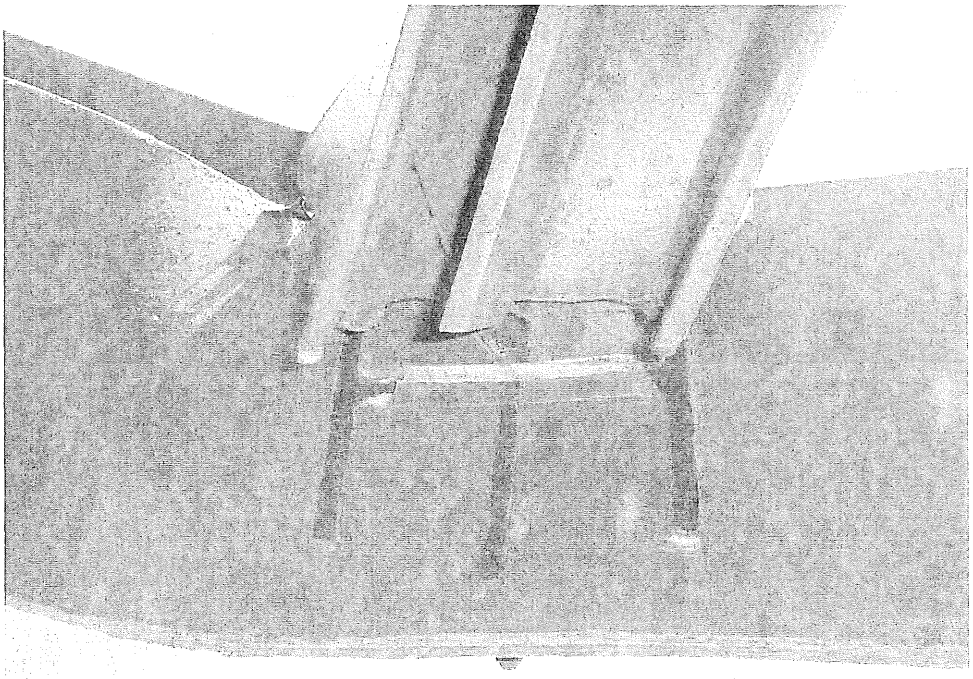

Figure 4.46. Separation of web diagonal from weld to upper chord (FT8U6).

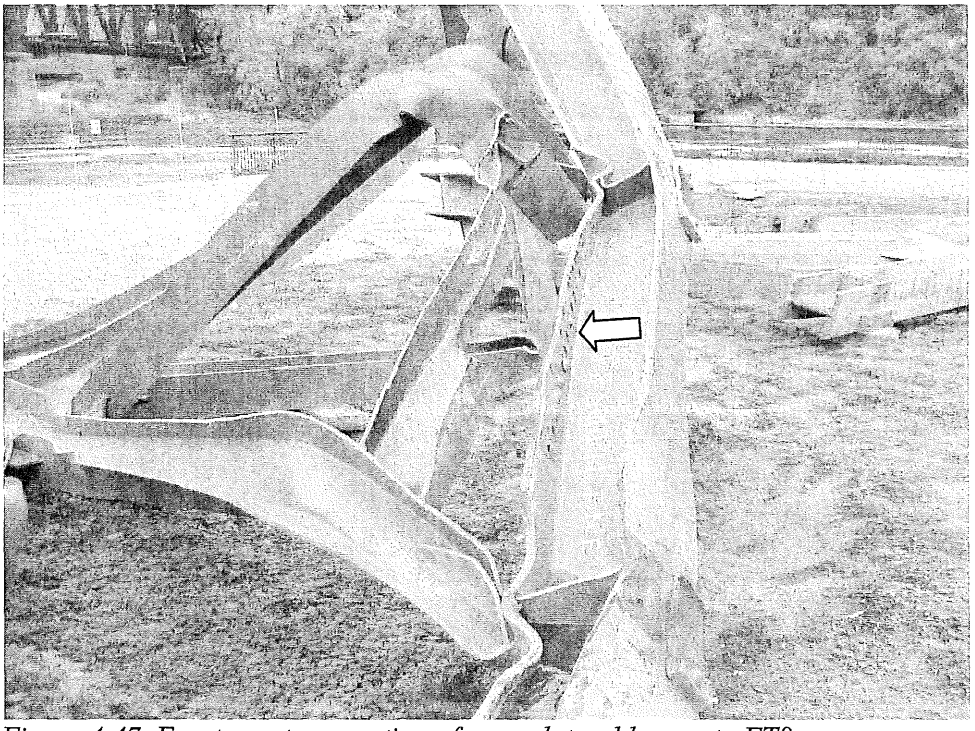

Figure 4.47. Fracture at connection of upper lateral braces to FT8.

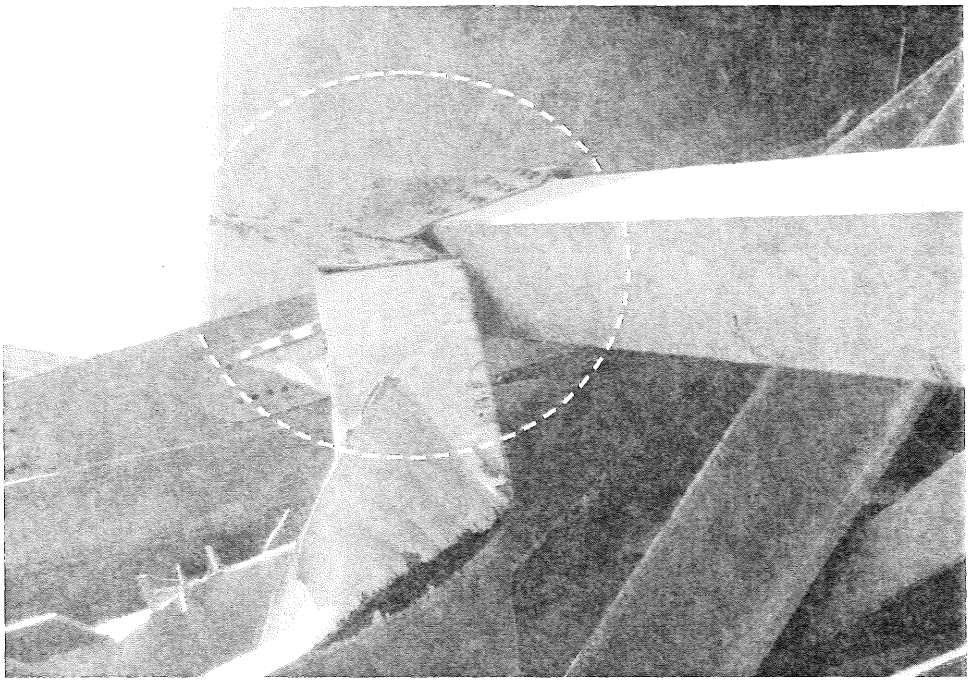

Figure 4.48. Detached end of mid-horizontal sway CM8-M8W and lower sway diagonal CL8-M8W.

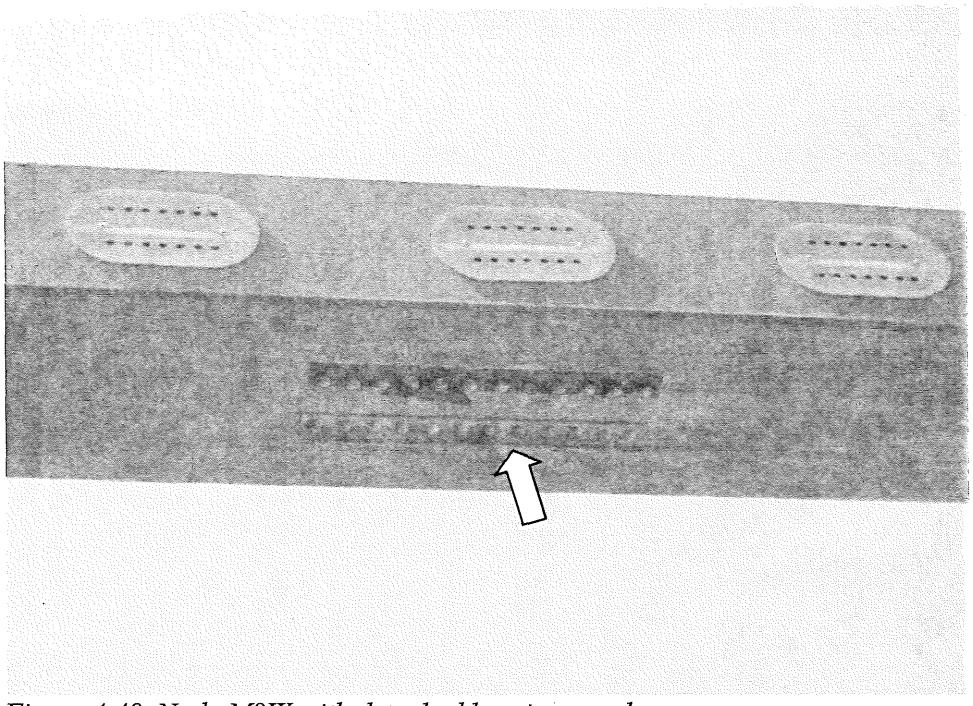

Figure 4.49. Node M8W with detached bracing members.

Figure 4.50. Corrosion on bottom of lower sway horizontal CL8'-L8'E at L8'E.

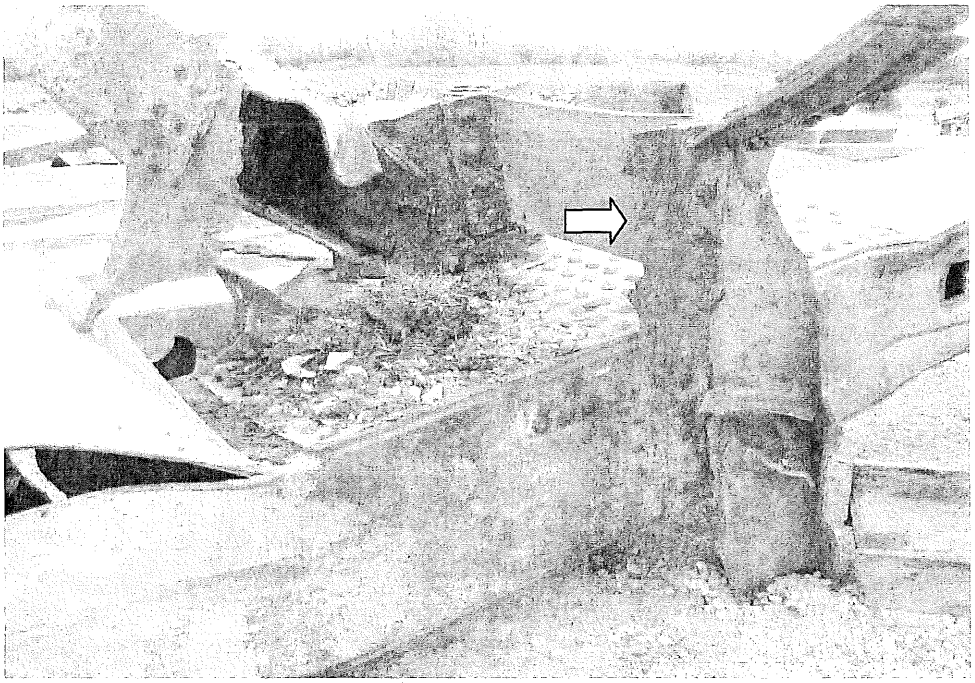

Figure 4.51. Corrosion on top connection plate to upper lateral at U4'E.

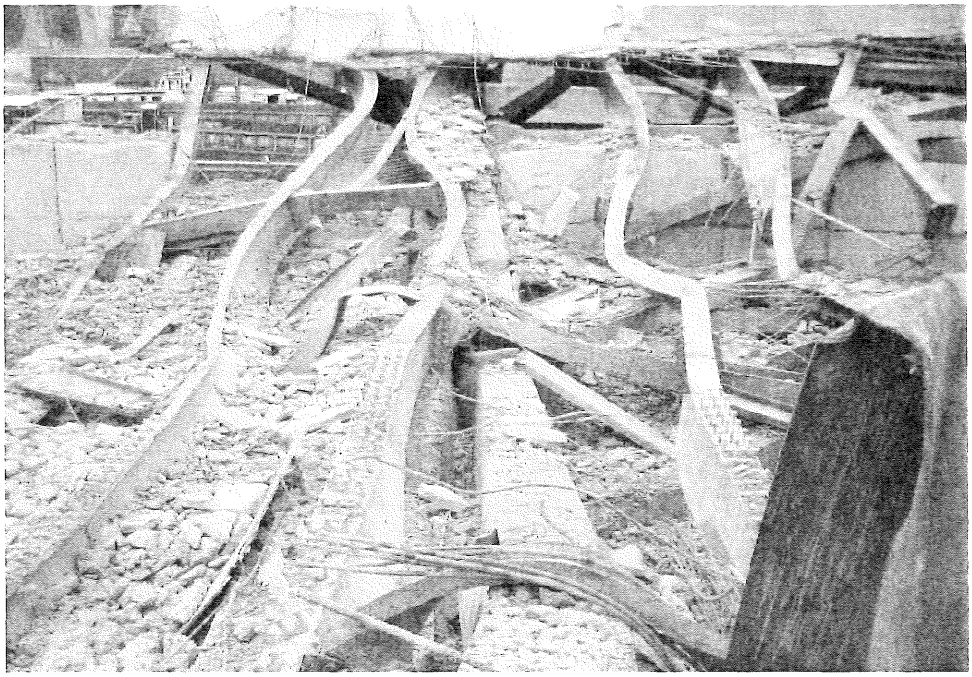

Figure 4.52. Typical distortion of stringers (Nodes 2' to 4', southbound lanes).

Figure 4.53. Post-collapse location of L1E, upper casting and north and center rollers.

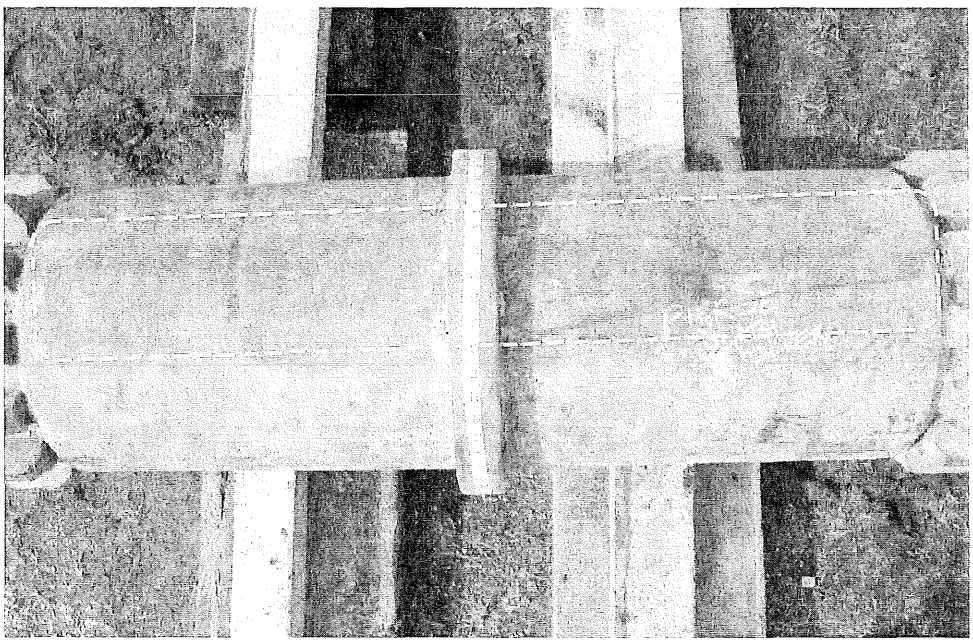

Figure 4.54. Wear marks on north roller of Pier 5 east bearing.

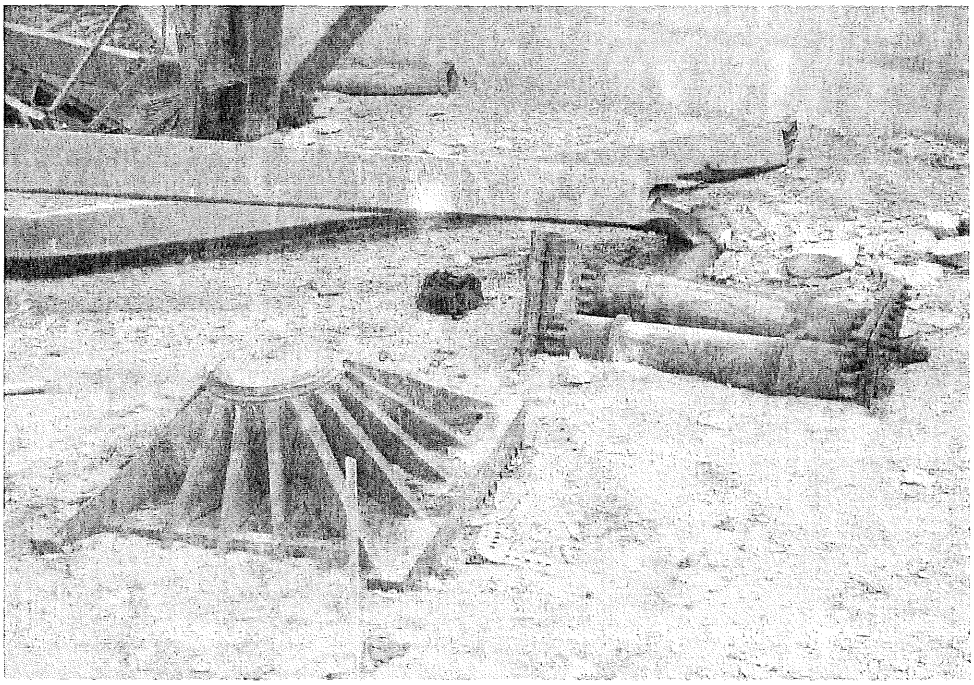

Figure 4.55. Post-collapse location of Pier 6 west bearing upper casting and rollers.

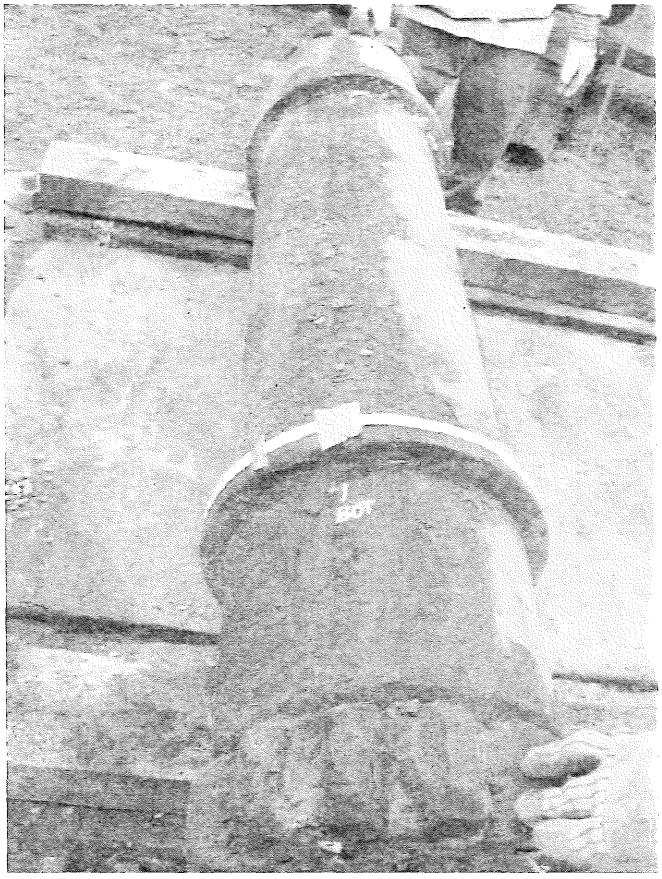

Figure 4.56. Corrosion on bottom of roller of west bearing at Pier 6.

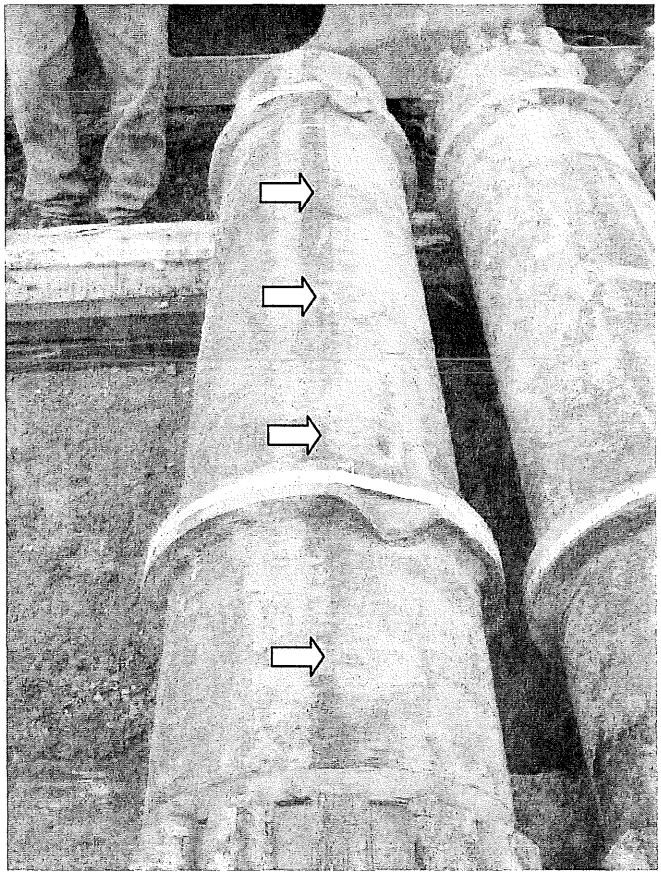

Figure 4.57. Impact markings from base plate anchor bolts on second roller from north in Pier 6E bearing.

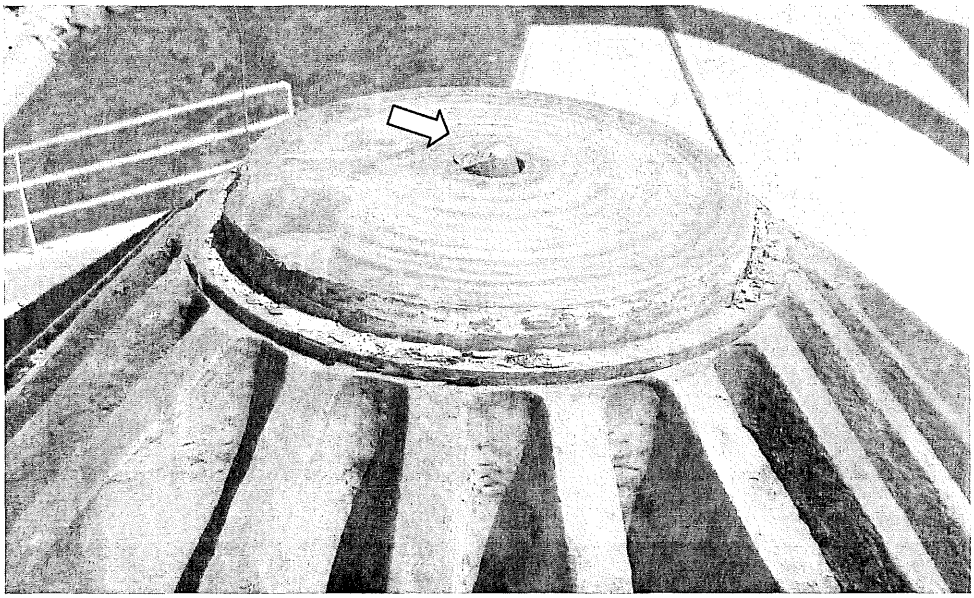

Figure 4.58. West bearing on Pier 7.

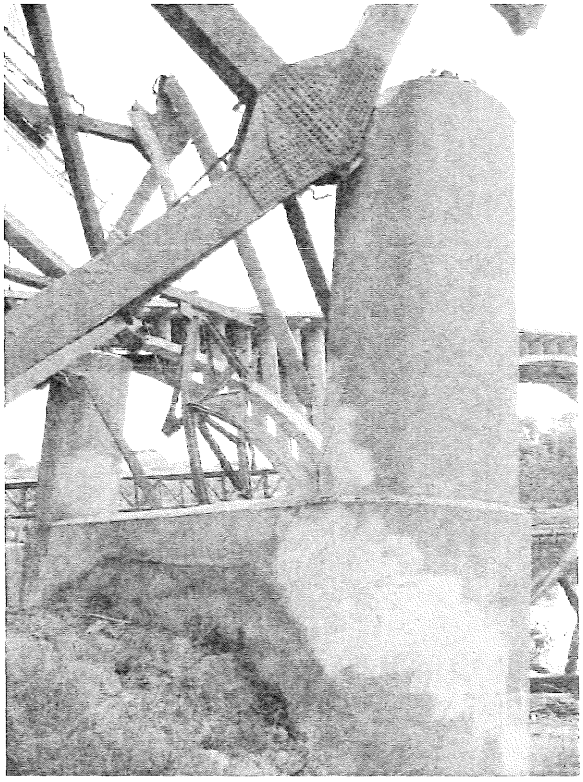

Figure 4.59. Pier 7 rotated towards river.

Figure 4.60. Pier 8 fractured at base.

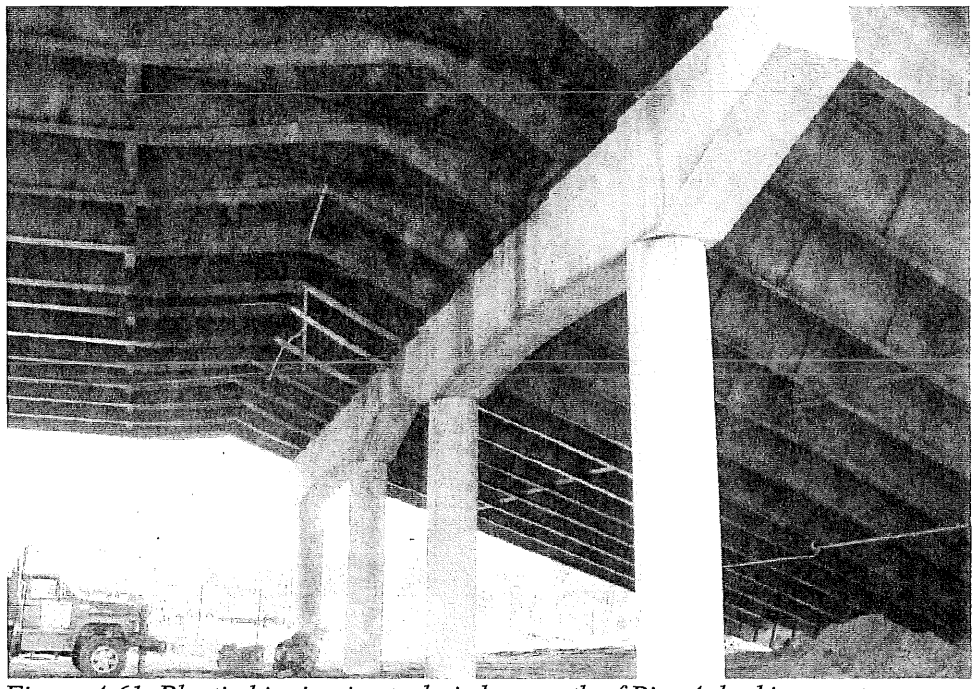

Figure 4.61. Plastic hinging in steel girders south of Pier 4, looking west.

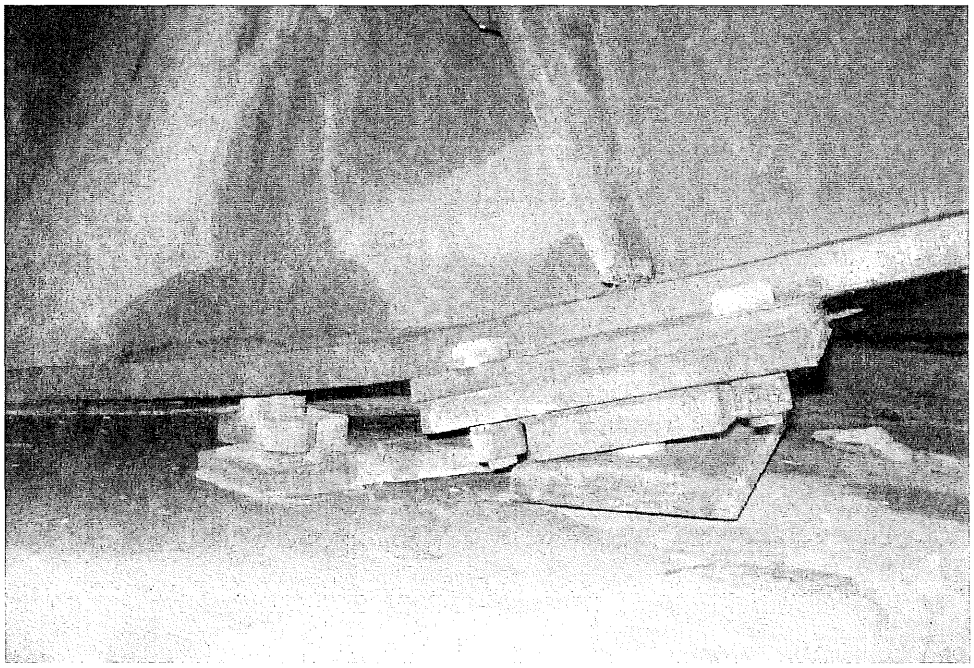

Figure 4.62. Displacement of rocker plate relative to lower bearing plate at Pier 4

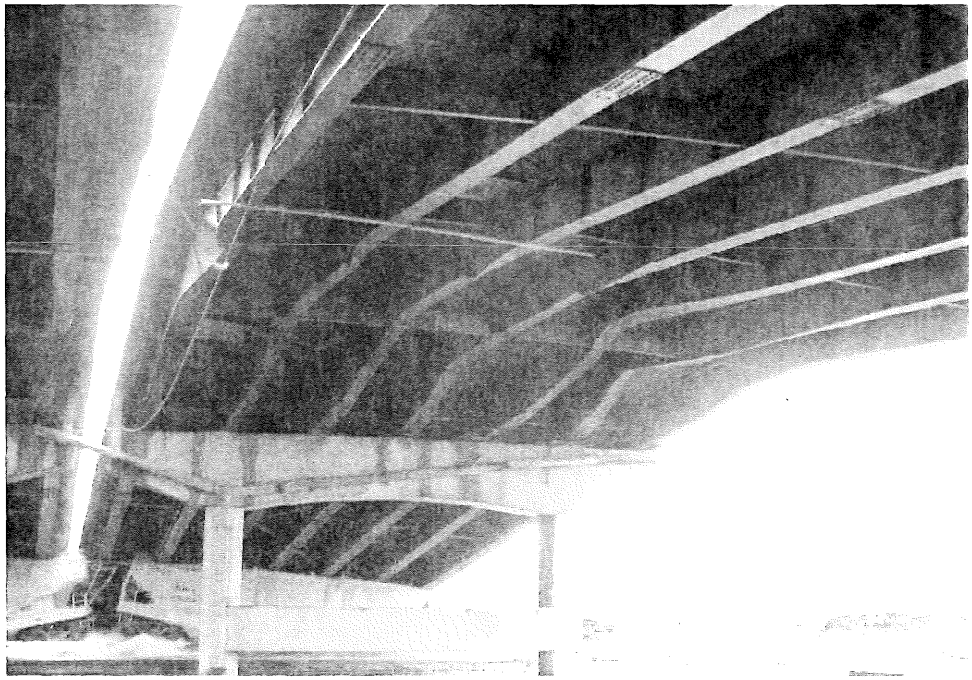

Figure 4.63. Plastic hinging in the steel girders north of Pier 9, looking south.

Figure 4.64. Collapse of the southbound lanes of Span 11 at Pier 11.

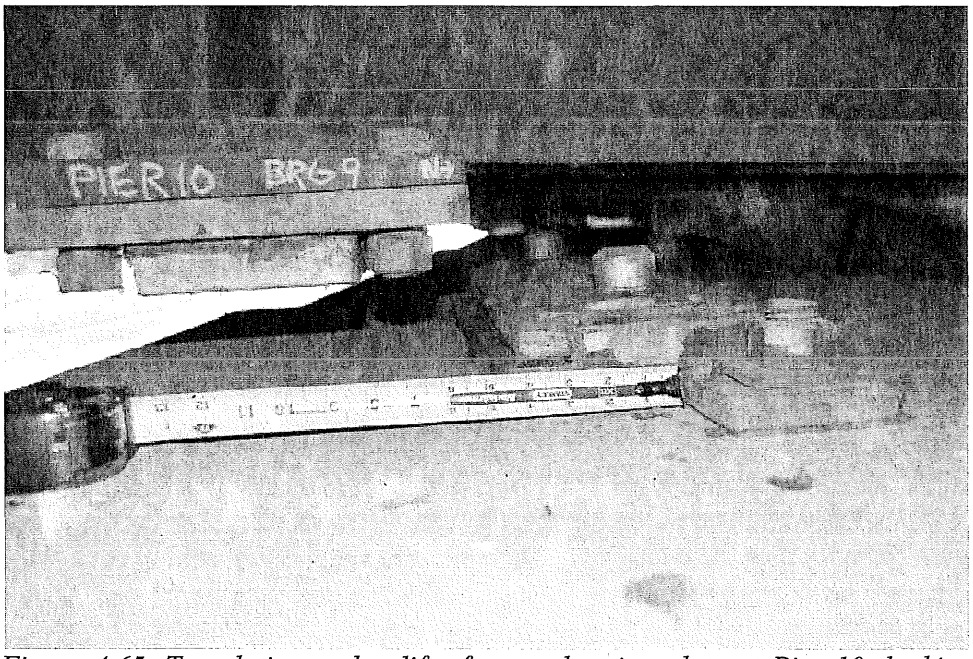

Figure 4.65. Translation and uplift of upper bearing plate at Pier 10, looking west.

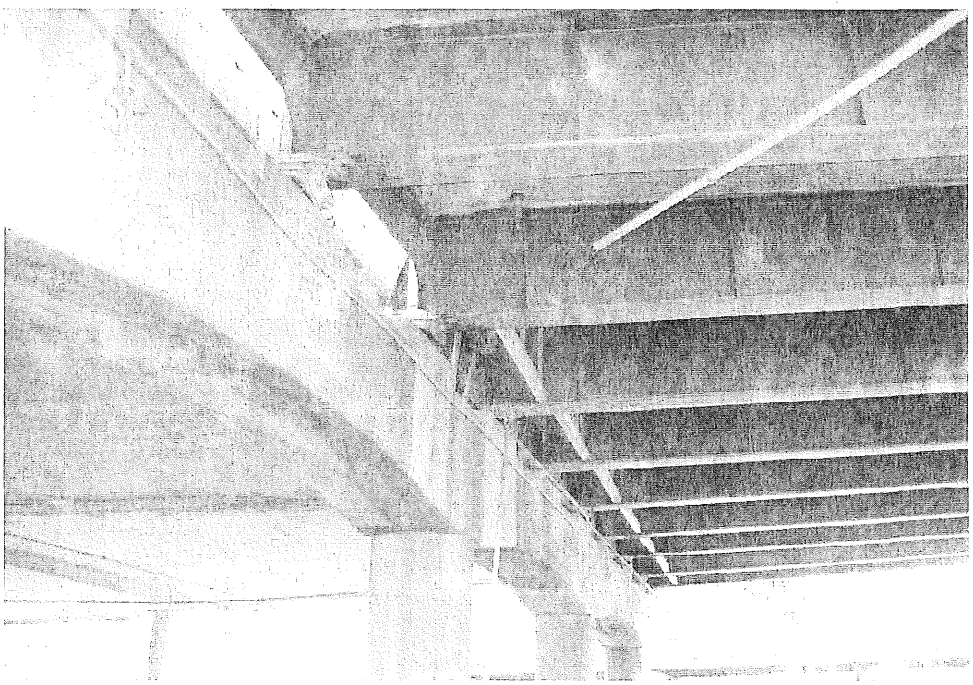

Figure 4.66. Southward displacement of bearings of the northbound lanes at Pier 11.

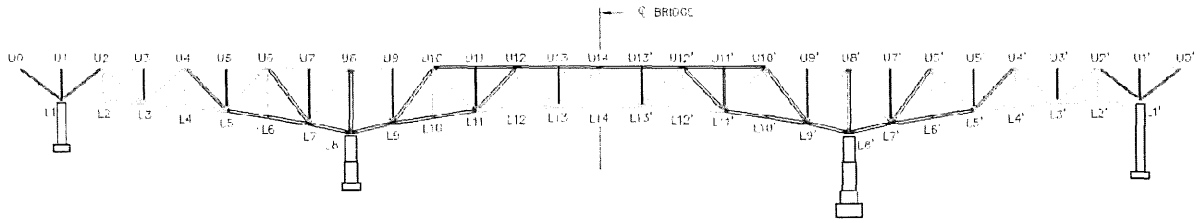

Figure 4.67. Truss elevation showing tension and stress reversal members highlighted in yellow.

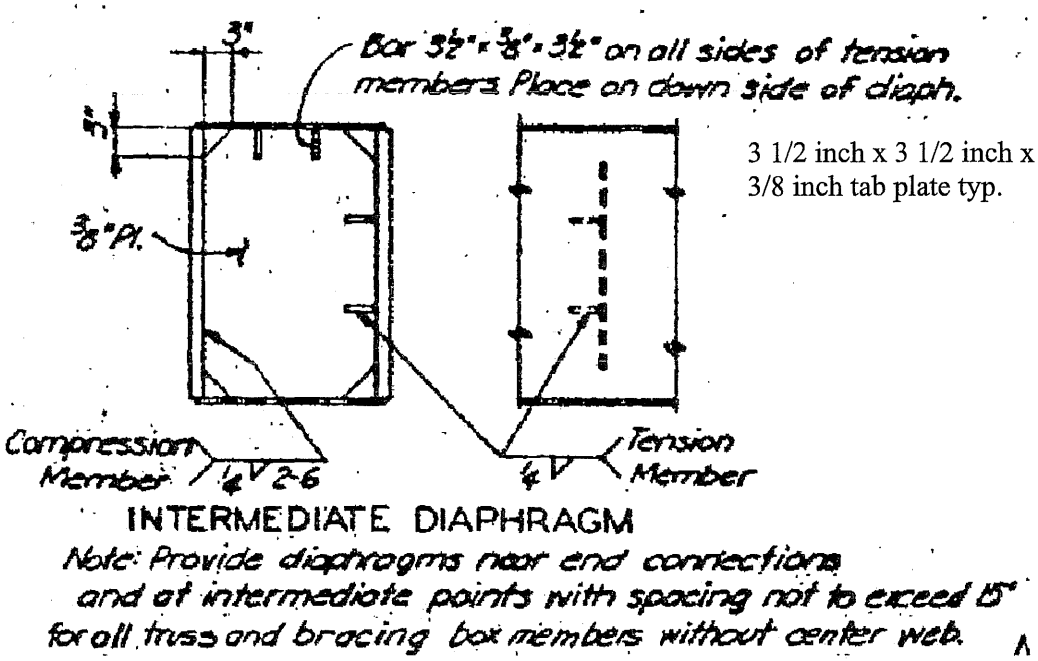

a) Detail from Sheet 21 Sverdrup & Parcel contract drawings.

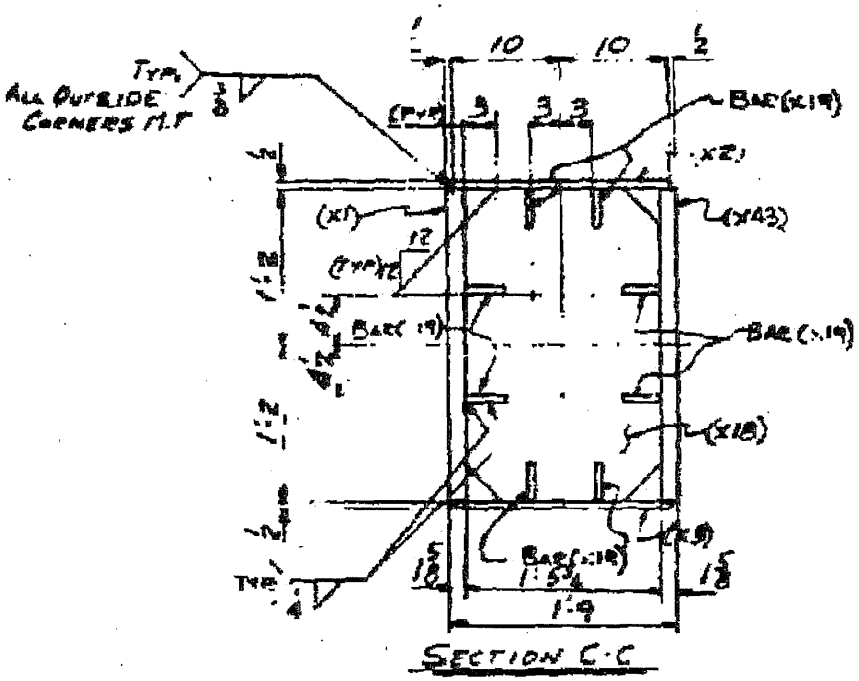

b) Detail from Allied Structural Steel Company shop drawings

Figure 4.68. Intermediate diaphragm details for truss box members.

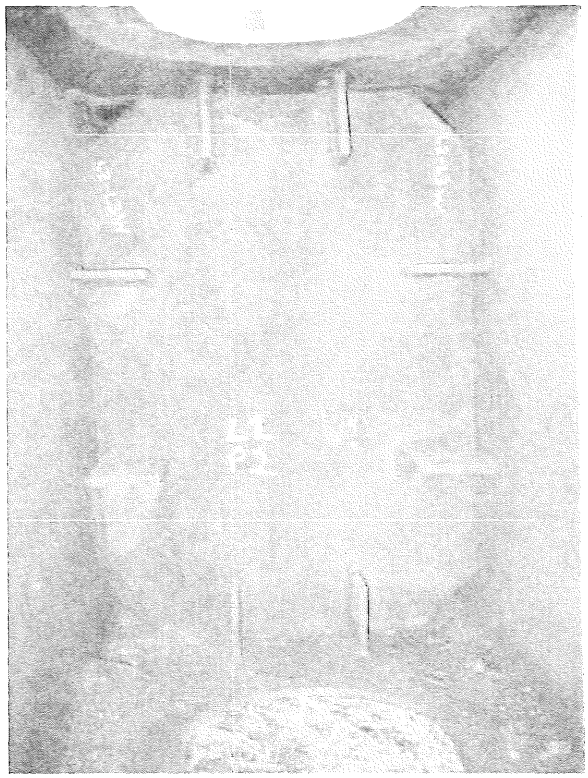

a) Truss box member L2-L3 west. Note eight connection tabs.

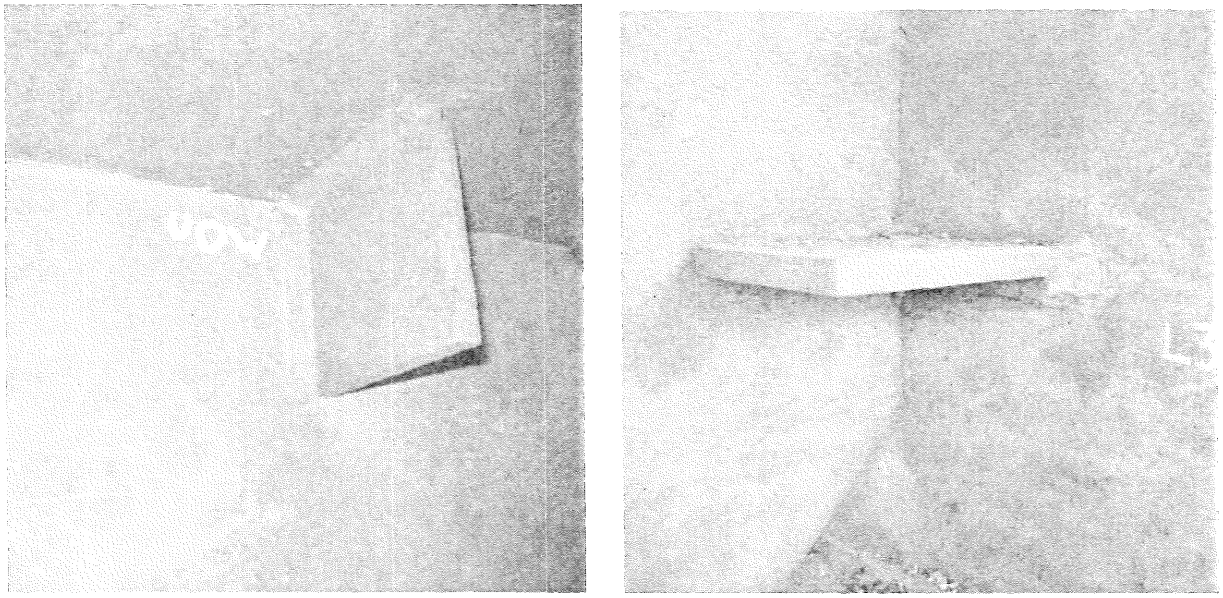

b) Views of 3 1/2 in. x 3 1/2 in. x 3/8 in. bar connectors showing 1/4 in. fillet weld (single side).

Figure 4.69. Typical intermediate diaphragm connection.

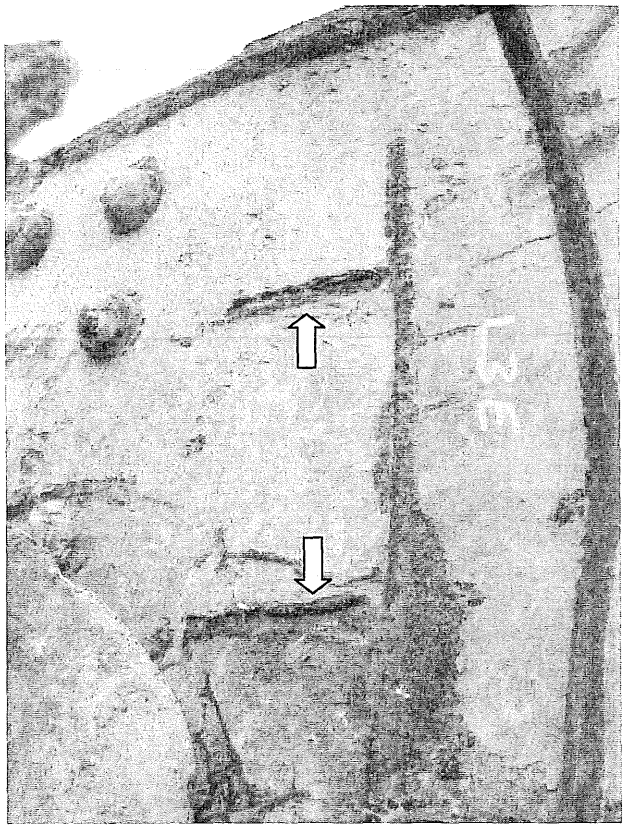

Figure 4.70. View of box member side plate showing connection locations of displaced diaphragm. Note weld terminations were carefully inspected for cracking. Arrows indicate tab welds.

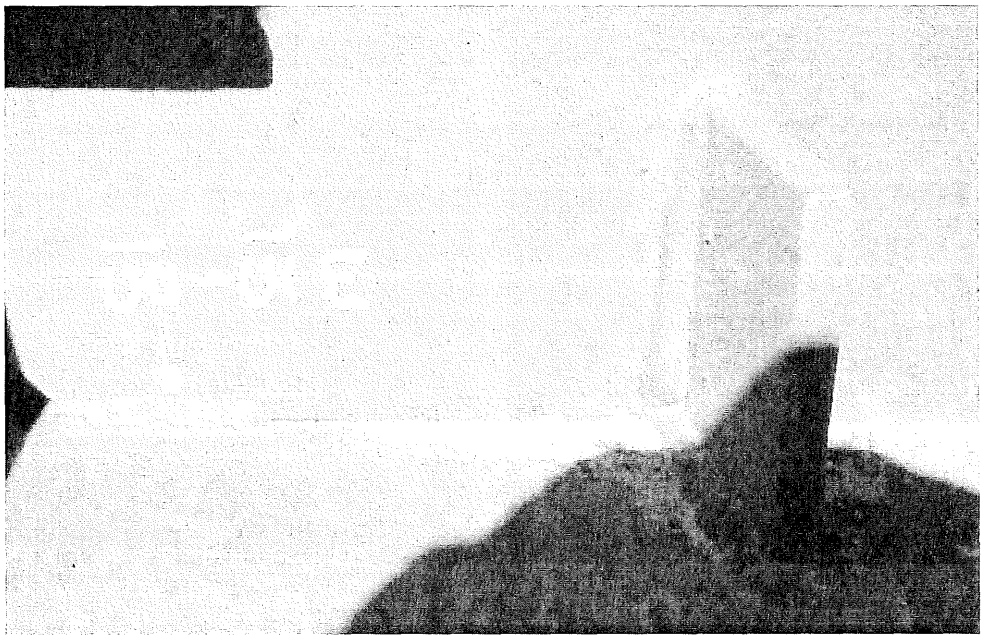

Figure 4.71. Typical cracked tack weld at an intermediate diaphragm.

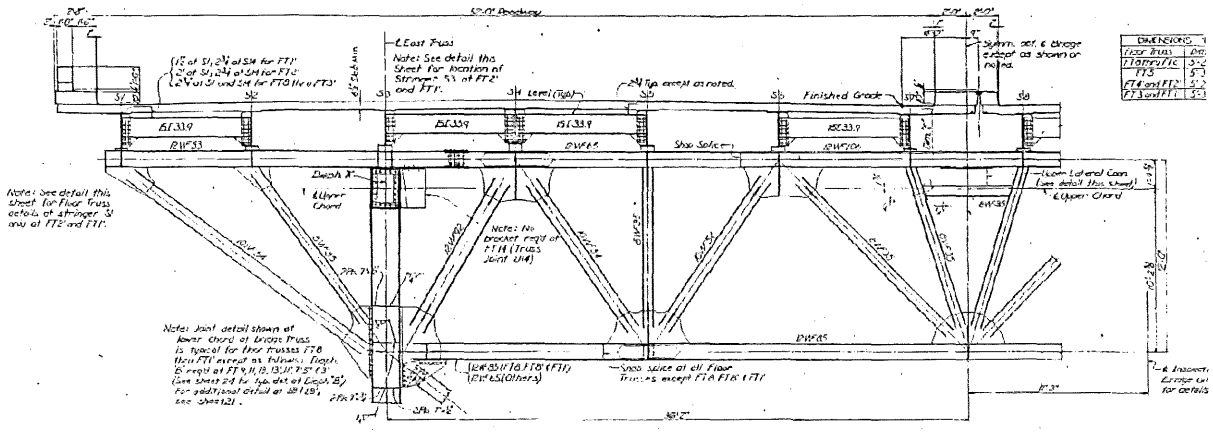

a) Floor truss details reproduced from Sverdrup & Parcel Drawing No. _25.

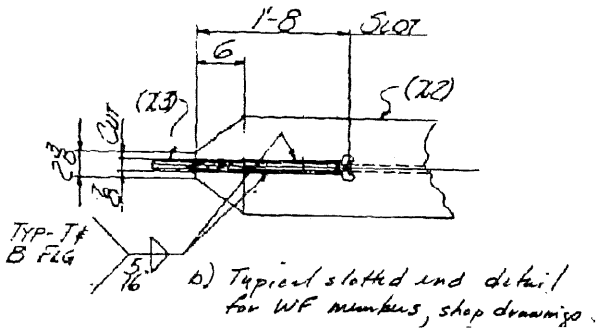

b) Typical slotted end detail for WF members, shop drawings

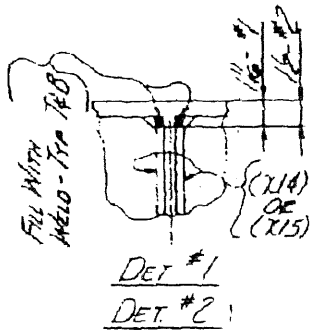

c) Tapered plate slot weld detail along length

Figure 4.72. Floor truss framing details.

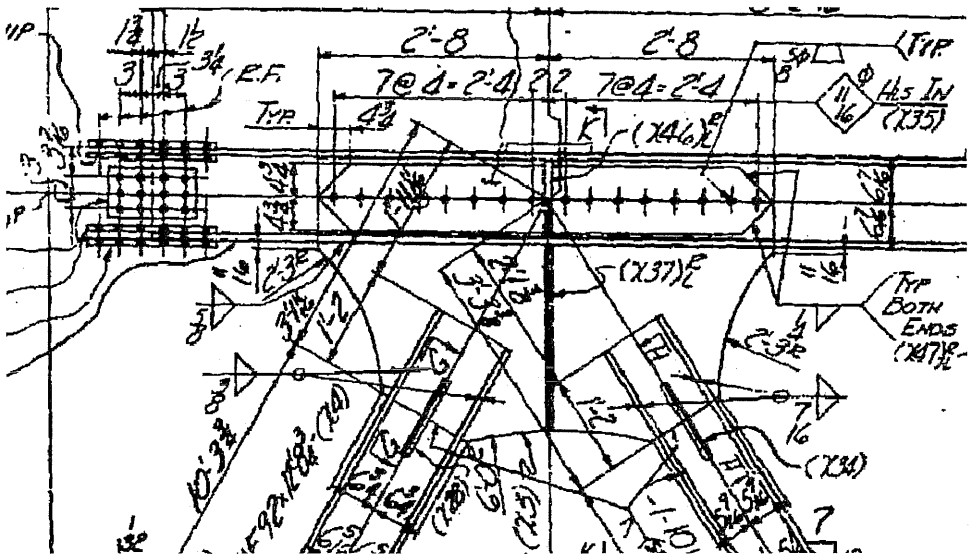

a) Top chord node detail

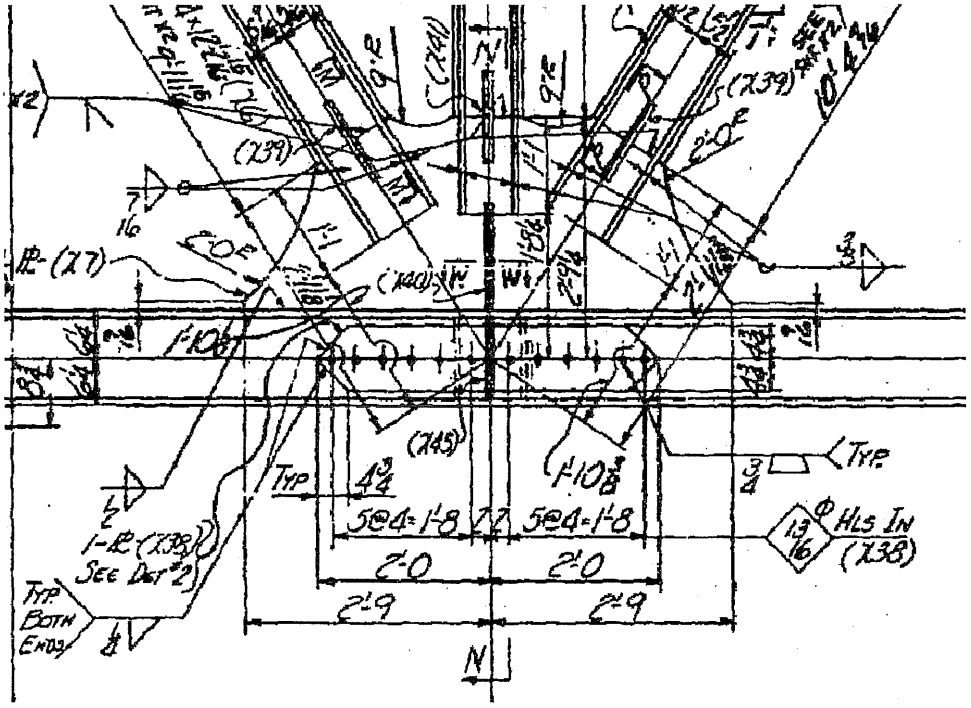

b) Bottom chord node detail

Figure 4.73. Floor truss welded details at node connections with tapper reinforcement plate.

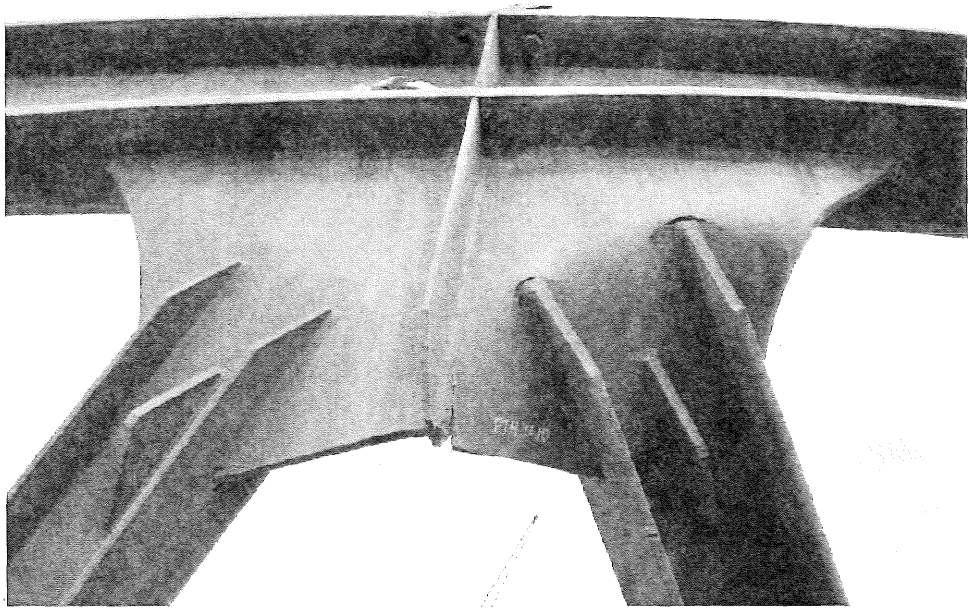

Figure 4.74. Typical cracking at floor truss weld terminations due to collapse.

Figure 4.75. Fracture in the top chord of FT10 near Node U10 East. View looking west.

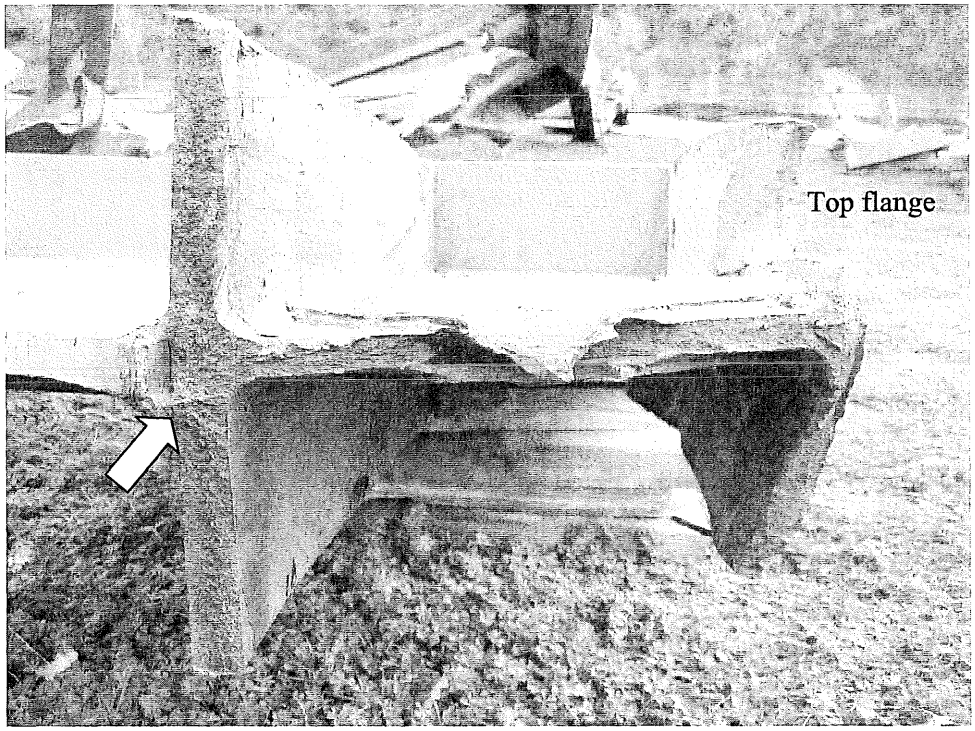

Figure 4.76. Close-up of fracture. Arrow indicates the origin location.

Figure 4.77. Railcar crushed under north approach.

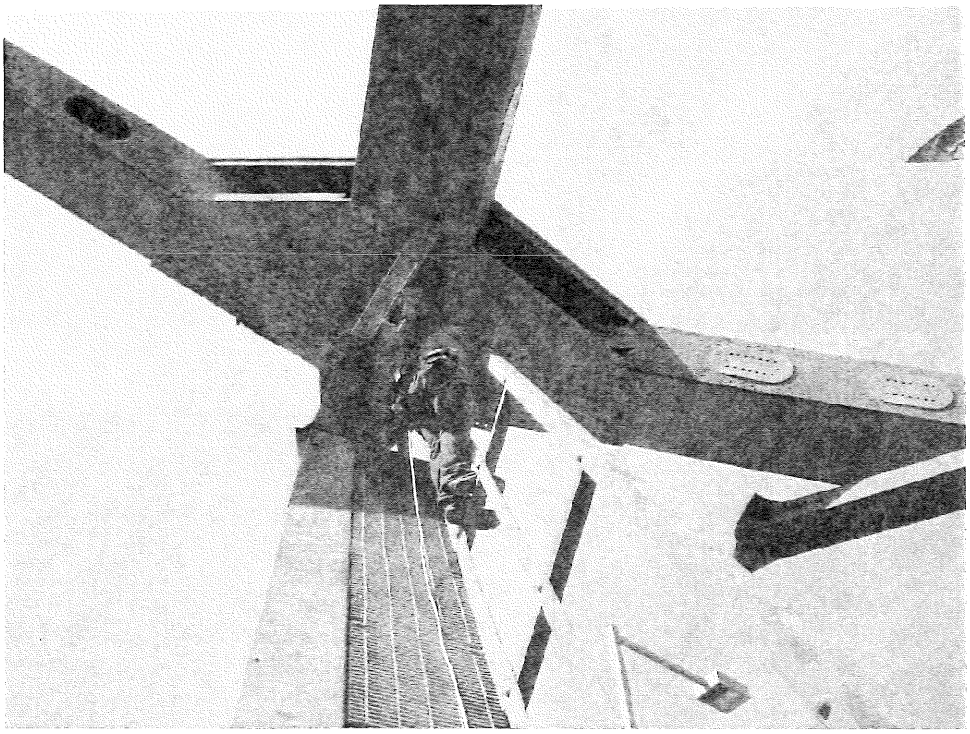

Figure 4.78. Sensor being installed on Node L8W to monitor movement of debris pile.

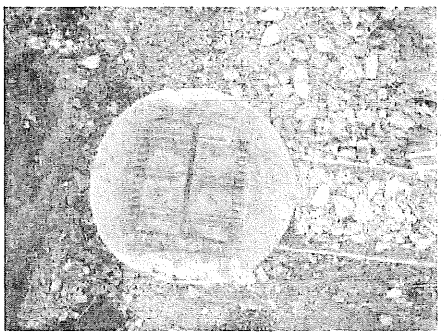

a) Pier 5E

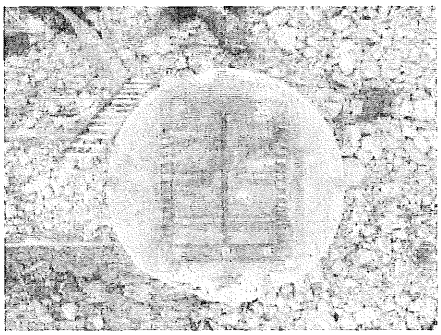

b) Pier 5W

Figure 4.79. Survey points on Pier 5

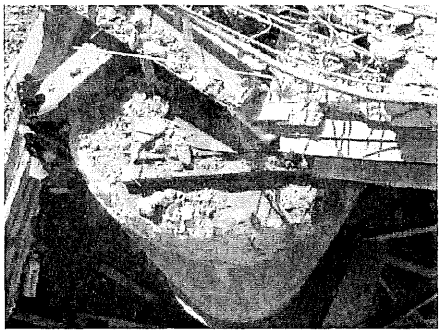

a) Pier 6E

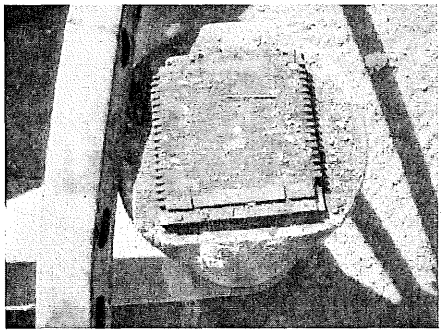

b) Pier 6W

Figure 4.80. Survey points on Pier 6

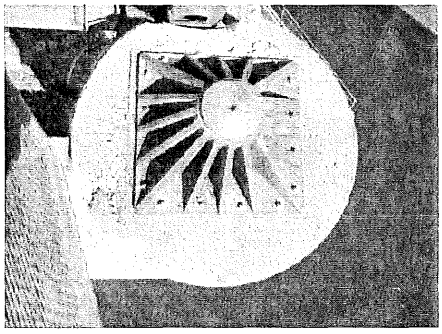

a) Pier 7E

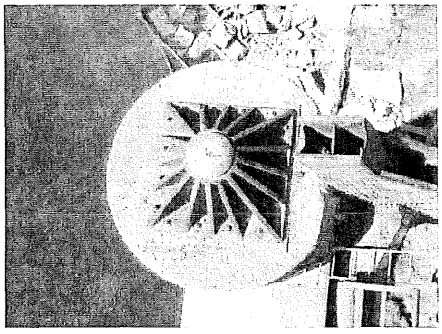

b) Pier 7W

Figure 4.81. Survey points on Pier 7

a) Pier 8E

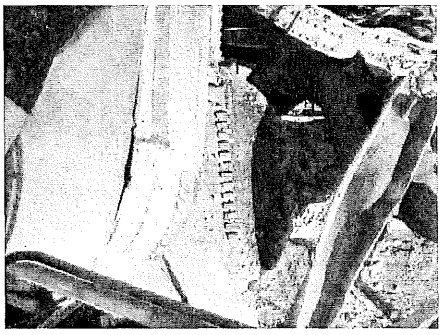

b) Pier 8W

Figure 4.82. Survey points on Pier 8.

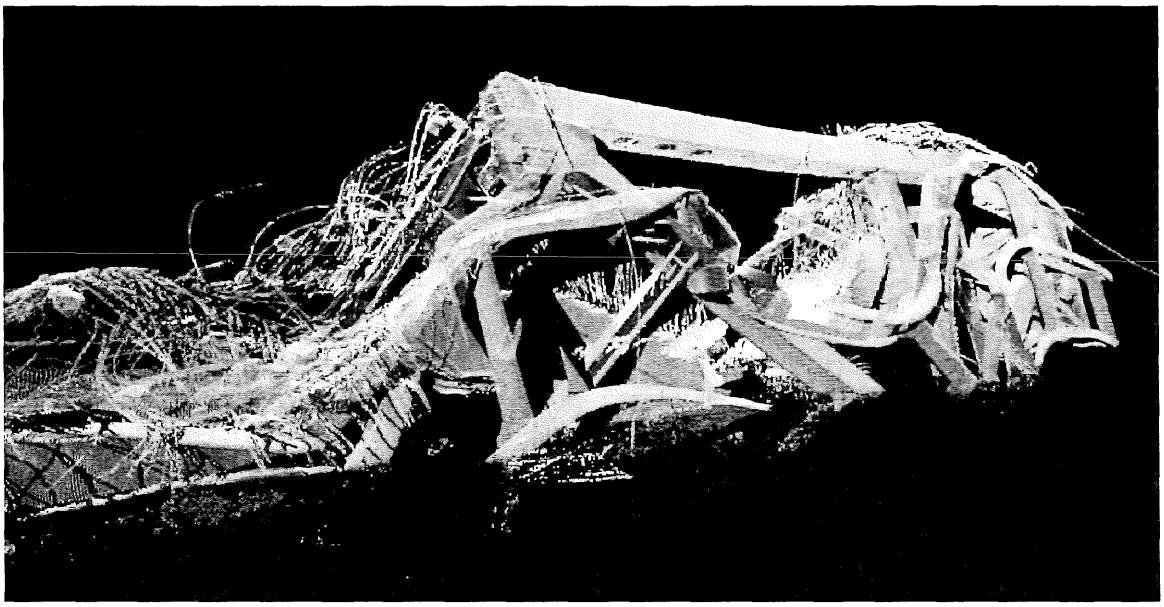

Figure 4.83. Laser scan image of structural steel.

5 MATERIALS AND SPECIAL TESTING

Samples were obtained from the concrete bridge deck and piers and from the main truss U10 gusset plates in order to verify the properties of the materials used in construction. Evaluation and testing of the concrete cores were performed at WJE's Northbrook, Illinois laboratory and at FHWA Turner-Fairbank Highway Research Center laboratory (FHWA-TFHRC), McLean, Virginia. Laboratory tests included determination of density, compressive strength, modulus of elasticity, and coefficient of thermal expansion. The core samples from the bridge deck were also used to measure the deck thickness at various locations in order to accurately determine the self-weight of the structure. Testing of steel samples from the U10 gusset plates, truss members, and FT10 members was performed by FHWA-TFHRC to determine tensile strength, Charpy V-notch impact toughness, and fracture resistance [44]. In addition, fractographic examination of the L10W-L11W west side plate using scanning electron microscope (SEM) was performed by NTSB in Washington D.C. and by John W. Fisher and Associates, Inc. (Fisher) at ATLSS Center at Lehigh University, Bethlehem, Pennsylvania.

5.1 Deck Thickness Measurements

Cores were extracted from the concrete deck by WJE and Advanced Concrete Sawing Inc. (ACS) to establish as-built properties of the deck and overlay at various locations. Sixty cores were removed from the truss span deck and eight cores were taken from the deck of the north and south approach spans. An electric coring machine was used to remove samples over land while a hydraulic-powered coring machine was used to extract and retrieve cores over water. Figure 5.1 shows the concrete coring operation.

Full-depth, nominally 4-inch diameter cores were removed from each of the eight traffic lanes, identified as Lanes 1 through 4 for each direction of travel (numbered west to east). At the time of the collapse, the new overlay was completed in Southbound Lanes 1 and 2 and Northbound Lanes 3 and 4. The existing overlay had been removed but not replaced on Southbound Lanes 3 and 4, and the existing overlay was still in place on Northbound Lanes 1 and 2. The core locations are referenced relative to the median for the east-west direction and referenced relative to a specific deck expansion joint for the north-south direction.

The concrete deck thickness was measured at each core location. The average total deck thickness for each traffic lane of the main truss spans is shown in Table 5.1. The total thickness measurements include the overlay, when present. Variations in existing overlay thickness were observed as shown in Figures 5.2 through 5.4. The total deck thickness for the approach Spans 5 and 9 varied between 7 and 9.5 inches.

Table 5.1 - Main Truss Span Deck Thickness Summary

Location	Deck Surface	Average Deck Thickness (in)
SB Lanes 1, 2	New overlay completed	8.9
SB Lanes 3, 4	No overlay in place	7.0
NB Lanes 1, 2	Existing overlay in place	8.6
NB Lanes 3, 4	New overlay completed	8.8

5.2 Concrete Deck and Pier Properties

In addition to the deck core samples, thirty, nominally 4-inch diameter cores were removed from the main span truss piers. Cores were extracted from the side faces of the pier columns by ACS, as accessible from the surrounding grade or atop the pier wall. The cores ranged in length from approximately 4 inches to 28 inches. Table 5.2 lists the location and number of cores extracted from the piers as well as the number sent for testing to WJE and FHWA-TFHRC. Several of the cores extracted from the piers were not suitable for testing due to the presence of reinforcing steel or fractures, or were too short to obtain the proper length-to-diameter ratio for testing. Cores not sent to either testing party remain at Bohemian Flats with MnDOT. Figure 5.5 shows the removal of a concrete core from Pier 8W.

Table 5.2 - Pier Core Locations

Pier	Cores Removed	FHWA	WJE	MnDOT
5E	4	2	1	1
5W	4	2	1	1
6E	1	1	-	-
6W	6	4	2	-
7E	2	-	2	-
7W	3	1	1	1
8E	5	1	3	1
8W	5	2	-	3
Total	30	13	10	7

Density and compressive strength testing was performed by WJE on selected deck concrete cores in accordance with *ASTM C642 Standard Test Method for Density, Absorption, and Voids in Hardened Concrete*, *ASTM C42 Standard Test Method for Obtaining and Testing Drilled Cores and Sawed Beams of Concrete* and *ASTM C39 Standard Test Method for Compressive Strength of Cylindrical Concrete Specimens*, respectively. The cores were tested in the as-received moisture condition. Additional testing by FHWA-TFHRC determined density, compressive strength, compressive modulus of elasticity, and coefficient of thermal expansion of selected deck and pier concrete cores in accordance with *ASTM C127 Standard Test Method for Density, Relative Density (Specific Gravity), and Absorption of Coarse Aggregate, ASTM C39 Standard Test Method for Compressive Strength of Cylindrical Concrete Specimens, ASTM C469 Standard Test Method for Static Modulus of Elasticity and Poisson's Ratio of Concrete in Compression* and *AASHTO TP-60 Standard Method of Test for Coefficient of Thermal Expansion of Hydraulic Cement Concrete*, respectively.

The density of the concrete cores taken by WJE varied between 145.7 lb/ft^3 to 156.7 lb/ft^3. The density of the concrete deck as determined by FHWA-TFHRC was 148 lb/ft^3 and for the pier concrete was 149 lb/ft^3. Due to the varying proportions of structural deck and overlay with different mix designs and densities, FHWA-TFHRC estimated the density to be 150 lb/ft^3 for the structural deck concrete and 140 lb/ft^3 for the overlay concrete, assuming 3% air void content, for the purpose of calculating the self-weight of the deck for the analysis. WJE utilized these same properties for its analysis.

The average compressive strength of the concrete pier cores determined by WJE was 9,600 psi (ranging between 6,410 and 10,920 psi). The strength determined by FHWA-TFHRC was 9,700 psi with standard deviation of 1,000 psi. The average compressive strength of two deck concrete cores tested by FHWA-TFHRC was 8,300 psi.

The average modulus of elasticity as determined by FHWA-TFHRC from seven pier cores was 5,330 ksi with a standard deviation of 300 ksi. The average modulus of elasticity of two deck cores was 4,820 ksi. The average coefficient of thermal expansion for two concrete deck cores tested by FHWA-TFHRC was 5.3 x 10^{-6} in./in./°F.

The strength of all cores are uniformly above the design strength and do not indicate any strength deficiencies or abnormalities with the concrete. In addition, the other concrete properties evaluated were within normal ranges.

5.3 Steel Properties

5.3.1 Gusset Plates

Steel samples measuring approximately 1 ft-6 in. by 2 ft-5 in. were removed from the upper south edge of both the east and west gusset plates at Nodes U10W and U10E and tested by FHWA-TFHRC. From each of the four samples, the following test specimens were machined: Charpy V-notch specimens (measuring 0.39 in. x 2.17 in. x 0.39 in. thick), fracture toughness (CT) specimens (overall dimensions measuring 2.46 in. x 2.40 in.), and tension specimens (measuring 1 ft 4 in. x 2 in.). The tension and CT specimens were the full thickness of the gusset plate. Due to the gusset plate shape, it was not possible to determine the rolling direction; therefore, all specimen types were removed from both the longitudinal direction (north-south direction) and transverse direction (up-down direction). The typical specimen layout on each gusset sample prepared by FHWA-TFHRC is shown in Figure 5.6.

Tensile testing was performed according to *ASTM E8-04 Standard Test Methods for Tension Testing of Metallic Materials* and included two longitudinal and two transverse test specimens per plate sample. The testing was performed at room temperature using the ASTM-specified lower bound loading rate of 0.02 in./min. or approximately 22 ksi/min. Static yield strength was determined based on procedures specified in the *Structural Stability Research Council (SSRC) Technical Memorandum No. 7* [45]. The average static yield and tensile strengths for the longitudinal and transverse specimens are 51.1 ksi and 79.7 ksi and 52.2 ksi and 81.0 ksi, respectively. The average strength and elongation per plate and orientation are tabulated in Table 5.3. A typical stress-strain curve generated from test data is shown in Figure 5.7. The test results for the U10 gusset plate samples show all exceeded the minimum specified yield strength of 50 ksi for ASTM A441 material.

A series of Charpy V-notch (CVN) tests were performed to determine the toughness of the material in comparison with current AASHTO material specifications. Charpy V-notch testing was performed according to *ASTM E23-07 Standard Test Methods for Notched Bar Impact Testing of Metallic Materials* and included one set of three samples for each orientation per plate sample. The testing was performed at 50 degrees F. Test results shown in Table 5.4 indicate an average overall test result of 61.0 ft-lb@50°F and 28.5 ft-lb@50°F for specimens in the longitudinal and transverse directions, respectively. A distinct difference in toughness was observed between the orthogonally oriented specimens indicating that the longitudinal direction was most likely the rolling direction of the plates. Historic test results have shown the longitudinal (parallel to plate rolling) test results to be about two times the transverse test results.

During the design and construction of the I-35W Bridge, there were no AASHTO toughness requirements for bridge steels. Today, AASHTO CVN requirements for fracture critical applications would require 25 ft-lb@40°F for Zone 2 (lowest anticipated service temperature = -30 degrees F). *ASTM A673-07-Standard Specification for Sampling Procedure for Impact Testing of Structural Steel* specifies that CVN

tests be done with samples oriented in a direction parallel to rolling (L-T direction). Therefore, the gusset plate CVN test results in the longitudinal direction, though performed at a temperature 10 degrees F higher than specified, exceed the Zone 2 toughness requirements for fracture critical plates and would have been acceptable for use.

Tearing resistance testing using compact tension (CT) specimens was performed according to *ASTM E1820-08 Standard Test Method for Measurement of Fracture Toughness* and included two specimens for each orientation per plate sample. The CT tests were performed at approximately 75 degrees F which was about 20 degrees F below the steel temperature at the time of the collapse. All of the CT tests failed through stable ductile tearing with no brittle fracture observed. As with the CVN tests, there was a difference in behavior between the longitudinal and transverse specimens with the longitudinal specimens having greater fracture energy.

Table 5.3 - Tension Test Averages for U10 Gusset Plates

Plate I.D.	Specimen Orientation	0.2% Offset Yield F_y (ksi)	Static Yield, F_y (ksi)	Ultimate Strength Stress, F_u (ksi)	% Elongation (8 in)
WE[1]	Longitudinal	52.8	51.4	79.9	23
WW[2]		51.6	50.4	77.6	23
EW[3]		51.9	50.6	79.6	23
EE[4]		53.8	51.9	81.5	22
WE[1]	Transverse	54.4	52.9	81.5	20
WW[2]		53.0	51.7	80.9	19
EW[3]		52.8	51.4	80.0	17
EE[4]		54.2	52.8	81.6	17

Notes:
[1] WE = West truss, east side gusset plate
[2] WW = West truss, west side gusset plate
[3] EW = East truss, west side gusset plate
[4] EE = East truss, east side gusset plate

Table 5.4 - Charpy V-Notch Average Test Results for U10 Gusset Plates

Plate I.D.	Specimen Orientation	Absorbed Energy (ft-lb @ 50°F)	Notes
WE[1]	Longitudinal	55.1	[1] WE = West truss, east side gusset plate
WW[2]		60.6	[2] WW = West truss, west side gusset plate
EW[3]		64.4	[3] EW = East truss, west side gusset plate
EE[4]		63.7	[4] EE = East truss, east side gusset plate
WE[1]	Transverse	27.6	[1] WE = West truss, east side gusset plate
WW[2]		28.4	[2] WW = West truss, west side gusset plate
EW[3]		26.5	[3] EW = East truss, west side gusset plate
EE[4]		31.5	[4] EE = East truss, east side gusset plate

5.3.1 Truss Members

Samples were removed from each of the five truss members framing into the two U10 and U10′ connections. From these samples, 72 tensile samples conforming to the same ASTM testing procedures used for the gusset plate tests were removed from each of the plates comprising the member samples (4 samples from box-shaped members and 3 samples from H-shaped members). The tensile specimens were oriented in the longitudinal direction for each member and cut from the full thickness of the plates.

Three material grades of plate were specified for the truss members: ASTM A36, ASTM A441 and ASTM A242. Test results show that 62 of the specimens were within the original M.H.D. material specifications for yield and ultimate tensile strength. The remaining 10 test results were within 9 percent of the minimum specified yield strength. Figures 5.8 to 5.10 show plots of the tensile testing results. A previous study by others which reviewed the variation in tensile plate data found that one standard deviation from the specified requirements was equal to 4 percent for tensile strength and 8 percent for yield strength [46]. Given the statistical scatter and the purposely selected minimum specified load rate which can reduce results by an additional two percent below mill test results, the plate material tested is consistent with the specifications.

5.3.3 FT10 Members

Five member samples from FT10 were removed for tensile testing. The sample members removed represented the various rolled shapes used in the floor truss. Three tensile specimens (web, bottom flange, and top flange) were machined from each of these samples. As shown highlighted in yellow in Table 5.5, several of the samples were below the minimum-specified yield strength and tensile strength of 36 ksi and 60 ksi, respectively. However, as discussed above, these values are considered typical, particularly those results from rolled flanges which have a tendency to be lower than results from the web portion of a member.

Table 5.5 - Floor Truss 10 Tensile Test Results

Member	Plate	Steel Grade	Thickness (in)	Fy (ksi)	Fu (ksi)
U13-U14	Top	36	0.576	33.95	64.16
	Bottom	36	0.576	37.41	65.22
	Web	36	0.345	33.84	63.51
U4-L4	Top	36	0.493	34.43	55.38
	Bottom	36	0.493	32.71	54.56
	Web	36	0.315	36.96	58.79
U3-L4	Top	36	0.618	36.67	62.12
	Bottom	36	0.618	35.65	62.55
	Web	36	0.368	35.58	59.30
L2-L4	Top	36	0.796	46.53	77.16
	Bottom	36	0.796	38.08	71.58
	Web	36	0.495	36.27	68.25
L2-U3	Top	36	0.856	36.02	72.46
	Bottom	36	0.856	36.00	72.56
	Web	36	0.545	46.05	73.03

5.4 Fractographic Examination

A sample of the fracture surface in L10W-L11W just south of Node L11W was removed and examined using close optical and SEM methods by NTSB and by Fisher. A report titled *Materials Laboratory Factual Report No. 08-004* prepared by NTSB dated April 18, 2008 summarizes the findings [47].

The sample obtained was approximately 8 inches in length along the north fracture surface of the west side plate of L10W-L11W. An uncharacteristic fracture feature was identified by NTSB at this location. Corrosion product was present on the fracture surfaces upon removal of the member from the collapse debris. Clear lacquer was applied to the fracture surface to prevent further corrosion. The lacquer was later removed by NTSB prior to microscopic examination. Refer to Figure 5.11 for an overall and close-up view of the sample prior to cutting and removing from the member.

The gusset plate and side plate were deformed adjacent to the fracture, and NTSB reported the fracture in the side plate generally displayed brittle features with chevron markings indicating upward propagation from the lower region of the side plate. The non-characteristic fracture surface (1-1/2 inches in length) was located approximately 9 inches from the bottom of the member. The fracture surface below this area was identified by NTSB as ductile fracture which intersected the lower two rows of rivets at the south edge of the gusset. The fracture surface above this area was identified as brittle fracture as previously mentioned.

SEM examination by Fisher confirmed the characteristic brittle and ductile fracture surfaces on either side of the non-characteristic fracture surface. The isolated non-characteristic fracture surface shows evidence of rubbing or abrasion. This surface was further examined and identified by Fisher to contain ductile shear dimple features near the brittle fracture boundary. Refer to Figure 5.12. The orientations of the dimples were found to be consistent and indicative of a shear direction nearly parallel to the plate surface. Based on these observations, the uncharacteristic fracture surface is a continuation of the ductile tear region and not an independent crack.

Figure 5.1. Concrete coring of bridge deck.

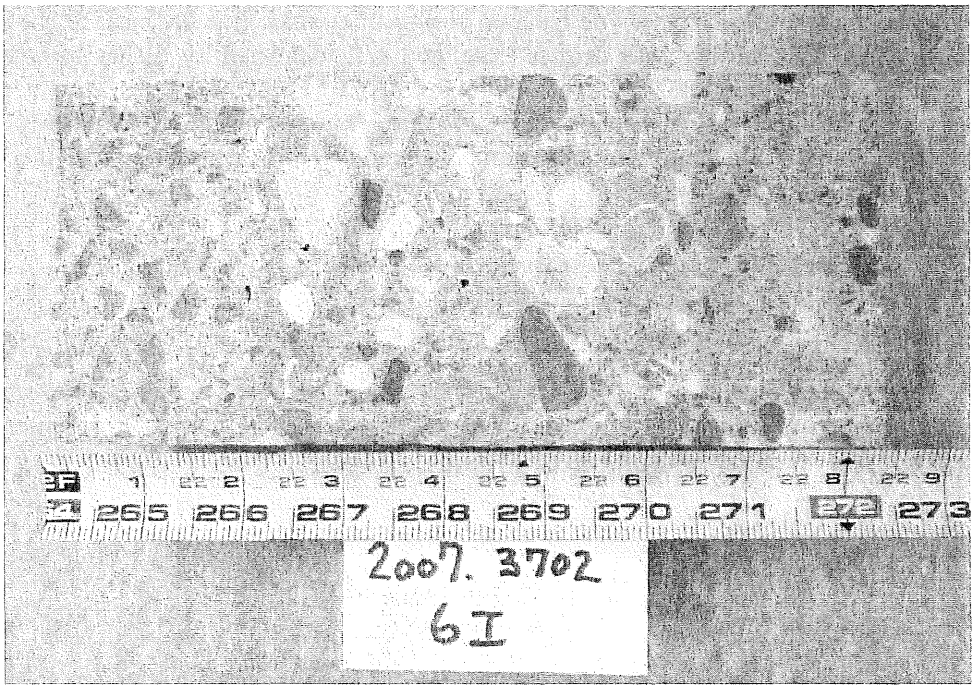

Figure 5.2. Core 6I showing existing 2 inch overlay. Total core length equals 8.5 inches.

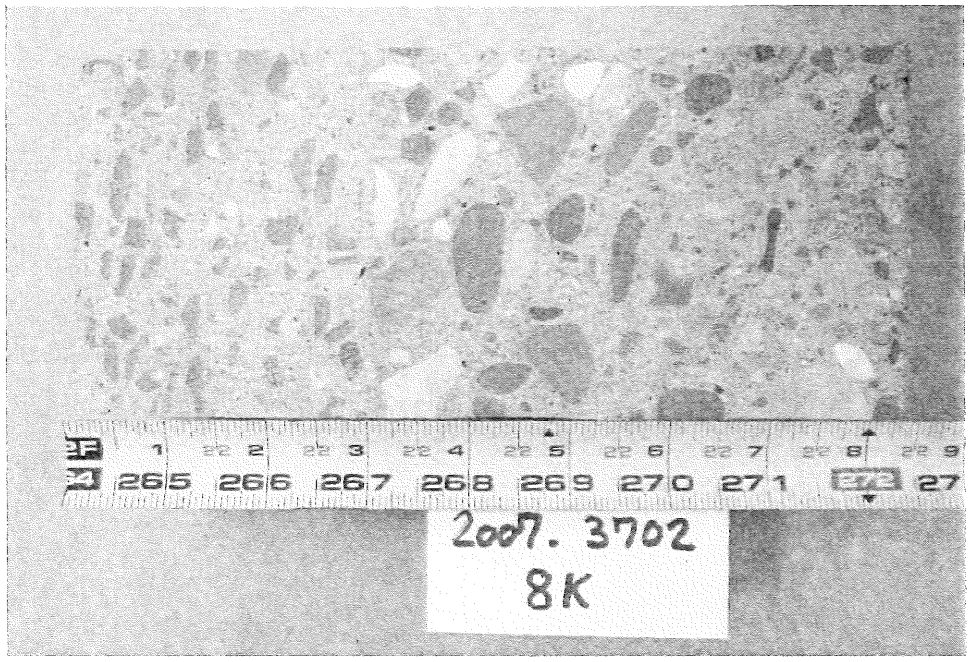

Figure 5.3. Core 8K showing existing 3 inch overlay. Total core length equals 8.375 inches.

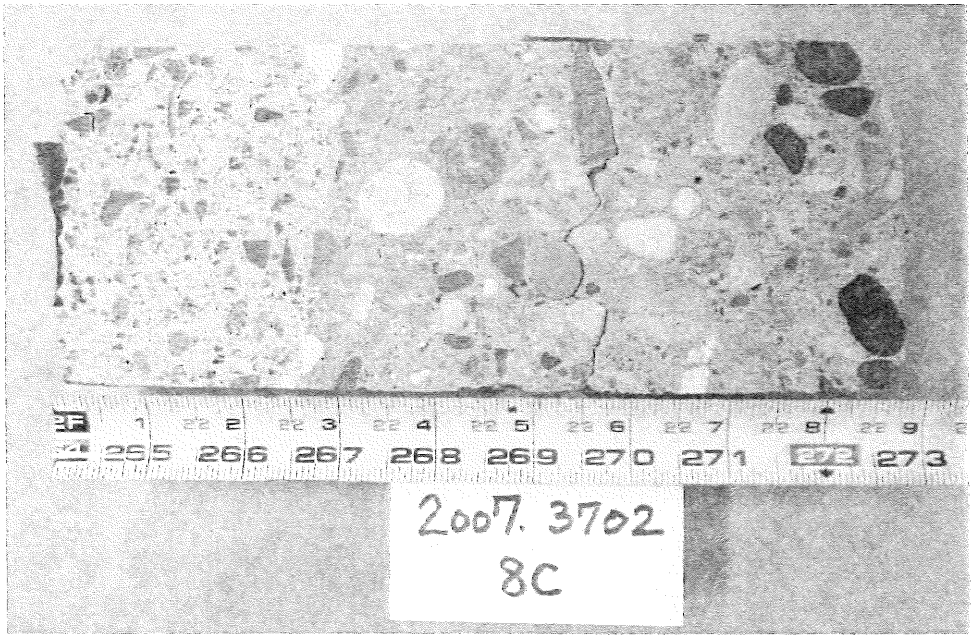

Figure 5.4. Core 8C showing new 2.75 inch overlay. Total core length equals 8.875 inches.

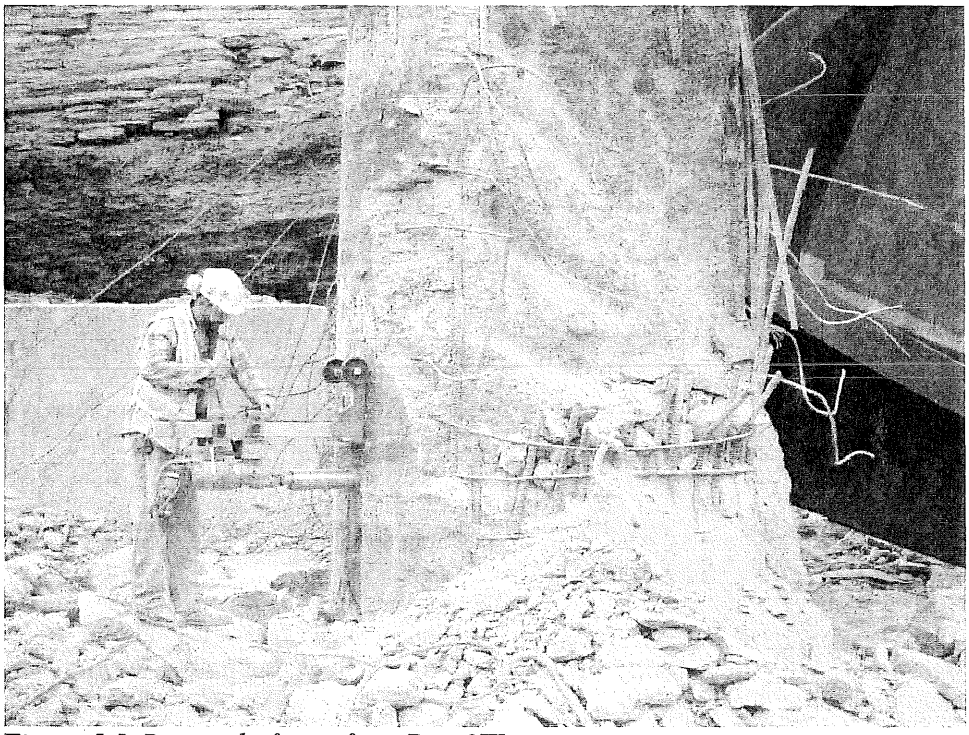

Figure 5.5. Removal of core from Pier 8W.

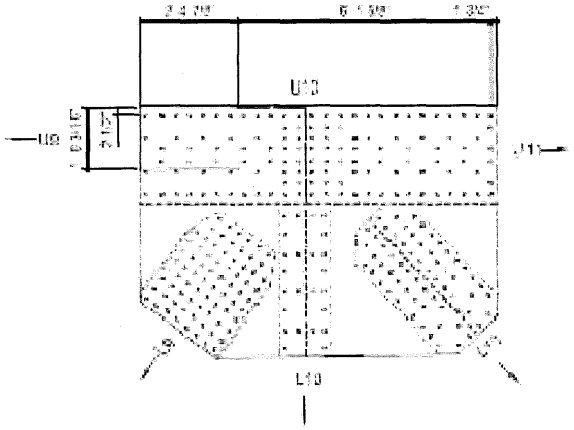

EAST SIDE GUSSET PLATE: ~~A4~~

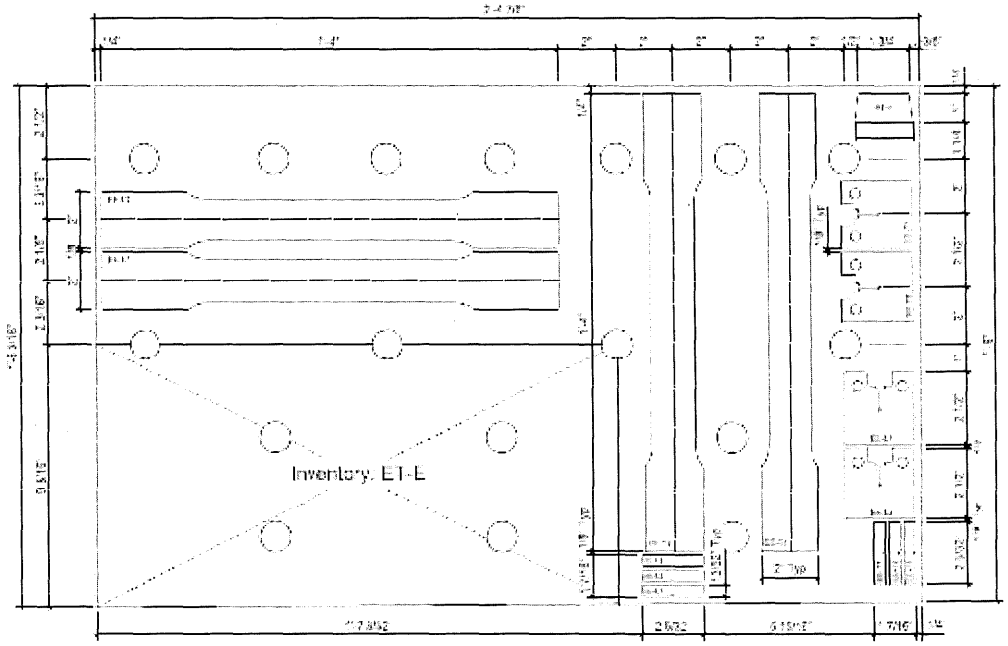

SPECIMEN LAYOUT

Figure 5.6. Overall view and close-up of steel testing specimen locations from gusset plate (east gusset plate of east truss shown). Drawing supplied by FHWA.

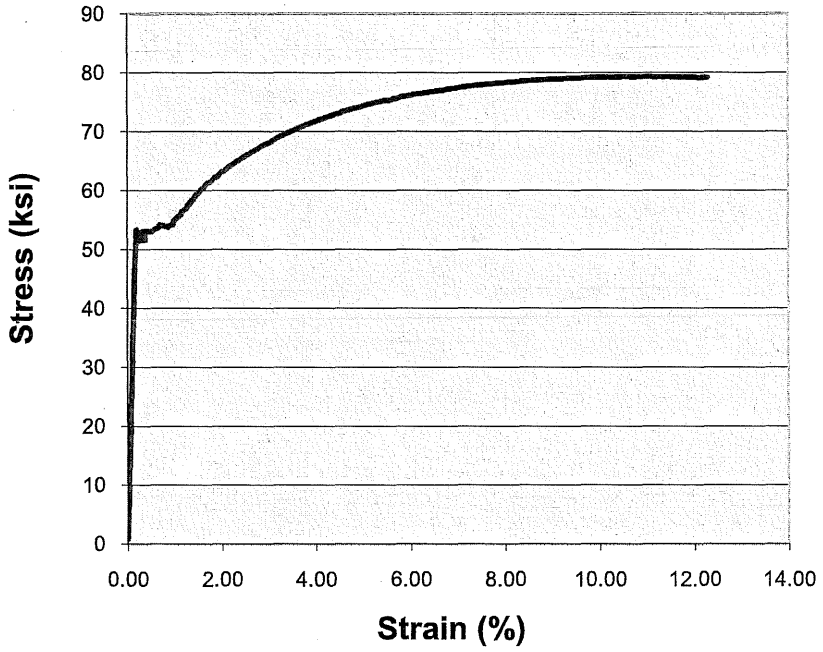

Figure 5.7. Typical stress-strain curve for gusset plate tensile test (west truss, east gusset plate, specimen 2 shown).

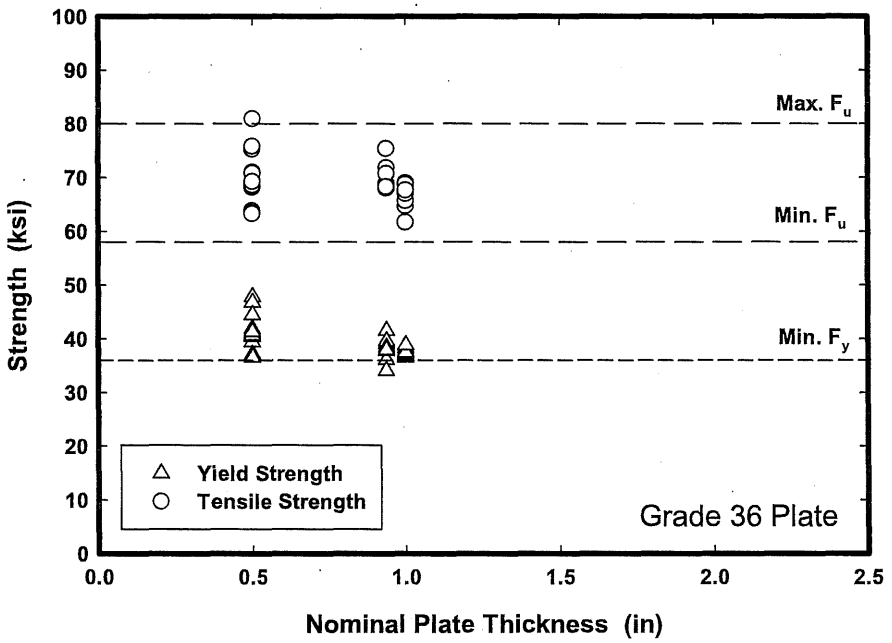

Figure 5.8. Tensile test results for truss members with ASTM A36 material (figure courtesy of FHWA).

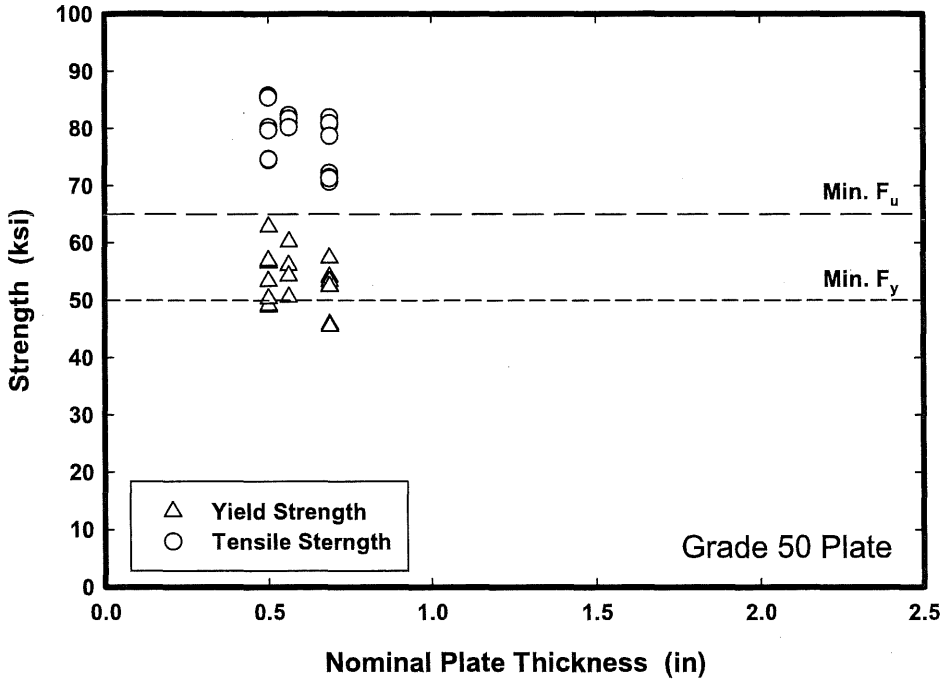

Figure 5.9. Tensile test results for truss members with ASTM A441 material (figure courtesy of FHWA).

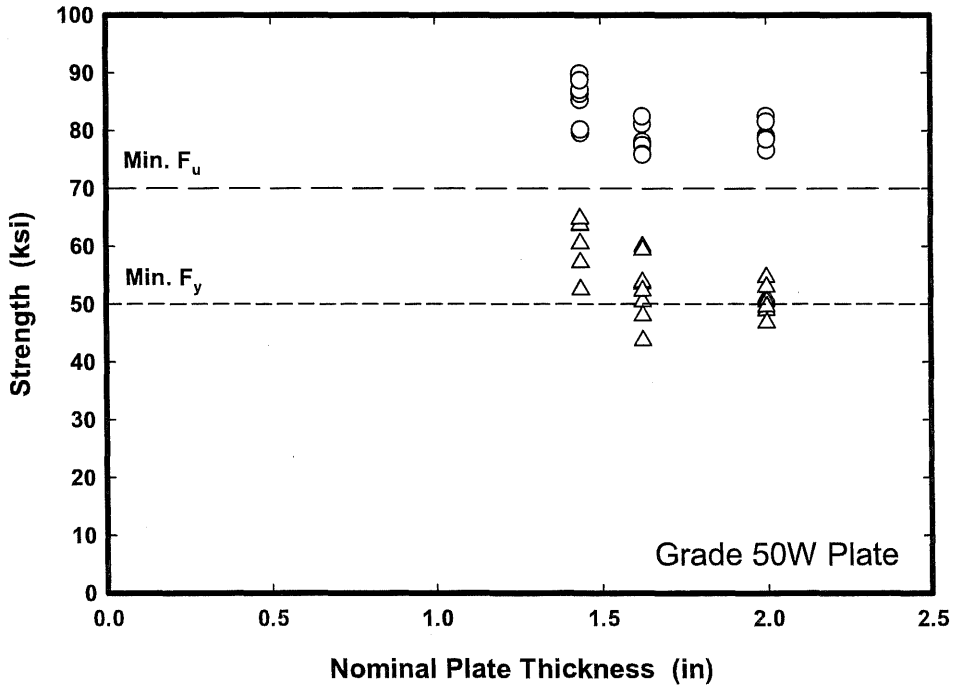

Figure 5.10. Tensile test results for truss members with ASTM A242 material (figure courtesy of FHWA).

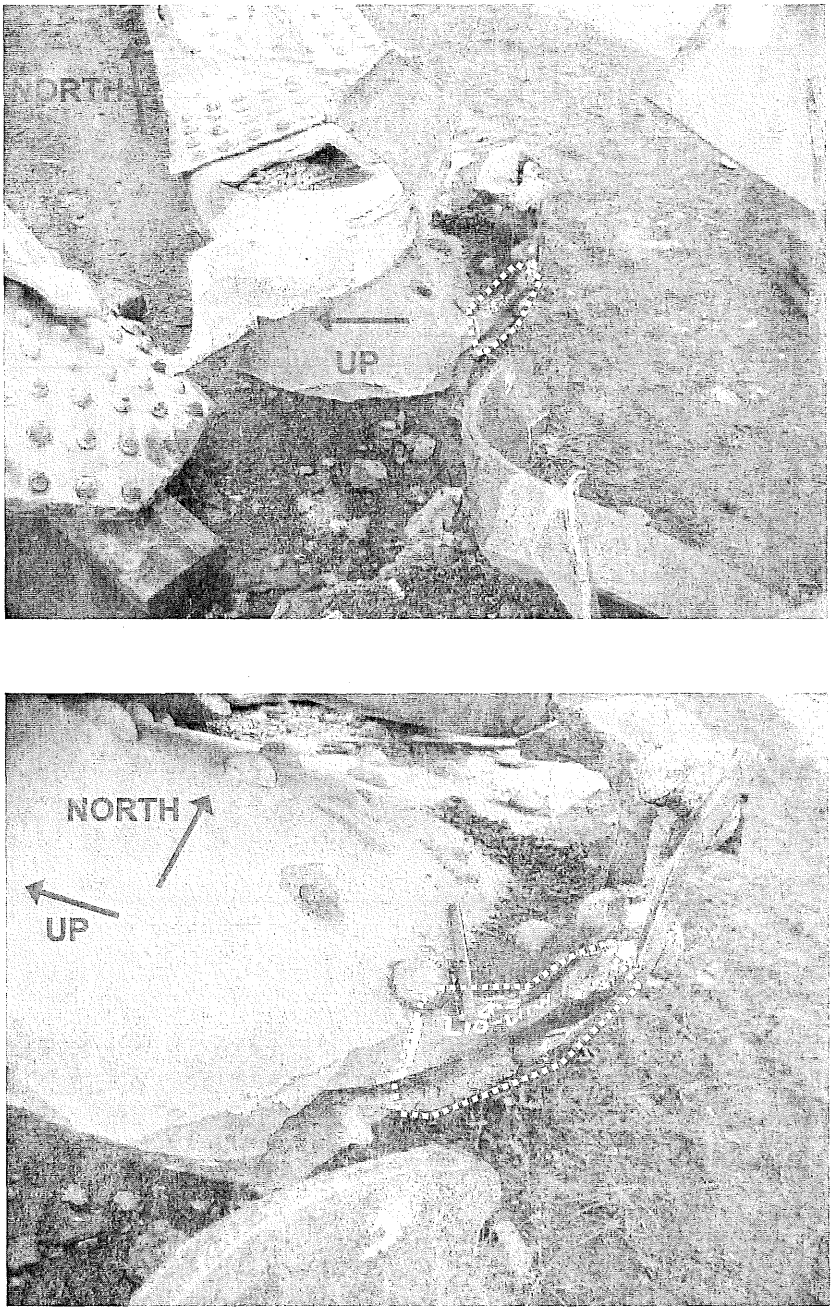

Figure 5.11. Overview and close-up of sample removed from west side plate of L10W-L11W for fracture examination by NTSB and Fisher (outlined).

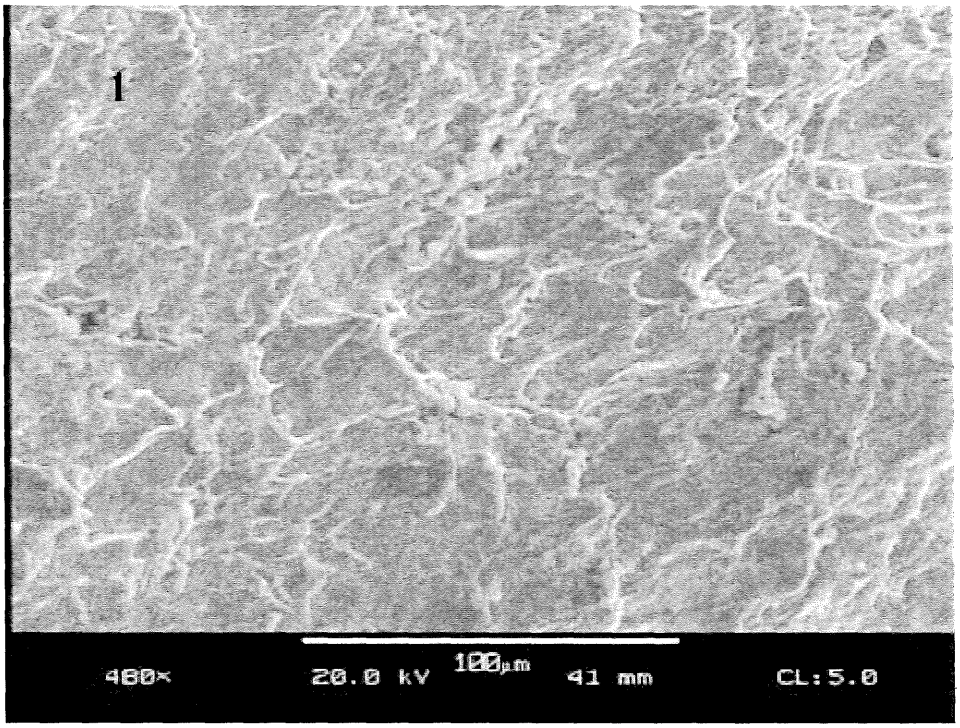

Figure 5.12. Ductile shear dimples observed in location of non-characteristic fracture surface (courtesy Figure 4 of Fisher report).

6 STRUCTURAL ANALYSIS

Structural analysis techniques were used to quantify the overall performance of the bridge and certain individual components under various loading conditions.

6.1 Conditions at Failure

At the time of the collapse, significant bridge loads included:

- Weight of structural steel
- Weight of concrete deck and deck features (e.g. barrier walls, parapet walls, etc.)
- Weight of construction materials and equipment
- Weight of vehicles

Estimates of these loads and the manner in which they were determined are summarized in Chapters 2 and 5 of this report. In order to quantify the extent to which these loads affected specific structural elements, they were incorporated into various structural analysis models. Structural analysis models were also used to investigate other issues related to the collapse, such as: local deformations of overloaded members, thermal effects, and material and geometric nonlinearities.

6.1.1 Initial Calculations

Since preliminary site observations suggested significant weaknesses at the U10 and U10′ nodes, initial structural analysis efforts focused on these regions. Rough estimates of the member dead load forces acting at a typical U10 node were established by increasing the original design dead load to account for the subsequent overlay and deck features. These forces were used to estimate critical dead load shear stresses on the gusset plate; which were found to be substantially higher than the allowable shear stress allowed by the 1964 AASHO, the governing code at the time the bridge was designed. The U10 gusset plates were then checked against the original design loads, and it was found that shear stress exceeded the allowable stress by a factor of almost 2.0.

Before the comprehensive study of superimposed loads was completed, additional hand calculations were used to estimate the ultimate strength of the U10 node. These calculations were based the following assumptions:

- The U10 node became unstable when the loading in the L9-U10 member created a yield mechanism in the gusset plates. While some degree of local strain hardening may have occurred before the ultimate capacity was achieved, yield strength (rather than ultimate strength) provides a more accurate representation of the average stress mobilized in the plastic portions of the gusset plate failure mechanism.
- Limit state performance was defined by Von Mises yield criteria and assumed tensile yield strength of 55 ksi (no material test results were available at the time).

These hand calculations indicated the gusset plates at a U10 node could sustain, at ultimate strength, about 2480 kips of axial load in the compression diagonal (L9-U10 member). The original design drawings specify a service load of 2288 kips in this member. Subsequent tension testing of gusset plate material indicated that the actual yield strength was closer to 51 ksi. Since the limit state calculations had assumed the steel yield strength was 55 ksi, the original estimated capacity of 2480 kips was factored by 51/55 to obtain a revised gusset plate capacity of 2300 kips in the L9-U10 member.

Given the major design deficiency in the U10 and U10′ gusset plates, simple, design-type hand calculations were used to check the remaining main truss gusset plates against original design loads. This process revealed deficiencies in the L11 and L11′ gusset plates that were similar in magnitude to the U10/U10′ deficiencies. Follow-up limit state calculations (again, assuming a steel yield strength of 55 ksi) indicated that the L11 gusset plates were capable of sustaining about 2200 kips of axial load in the most heavily loaded diagonal (U10-L11 member), which in this case was a tension member. Multiplying this value by 51/55 to reflect test-based steel properties that later became available, indicated the ability to carry an ultimate U10-L11 load of about 2040 kips. The original design drawings show a service load of 1975 kips in this member.

6.1.2 Finite Element Modeling of Entire Bridge

In order to provide more accurate estimates of the demands in critical structural elements, a three dimensional finite element model of the three-span-deck truss portion of the bridge, as well as the multi-girder approach spans, was constructed using SAP2000 software, a proprietary finite element modeling program commonly used to analyze structural systems. The initial SAP2000 model was created and checked by engineers at TranSystems, who then turned the model over to WJE. WJE engineers also verified the model and made various modifications during the process of evaluating bridge performance.

The SAP2000 bridge models included all main truss, floor truss, and lateral system members. They also included the deck and deck stringers. Additional SAP2000 models were created to evaluate the performance of certain bridge components. Member geometry and connectivity were based on the original design documents, while deck thickness was based on field measurements. Unless noted otherwise, expansion bearings were assumed to operate as designed and permit unrestrained thermal movements of the superstructure. Relevant material properties were as specified in the original design documents and verified by field sample testing. Connections between members of the main trusses and floor trusses were typically modeled as fixed, reflecting the flexural continuity provided by the gusset plates. However, for purposes of making operating rating calculations for the bridge (discussed later in this report), connections between members of the main and floor trusses were modeled as pinned, as this produced slightly higher axial force demands in some members. Figures 6.1 and 6.2 show overall views of the SAP2000 bridge model.

6.1.2.1 Model Verification

The accuracy of the SAP2000 bridge finite element modeling was thoroughly checked in a number of ways. Using structural loads consistent with those assumed in the original design, member forces and support reactions were compared to values listed in the original design drawings. This exercise indicated that the model was performing well, as the member forces obtained from the model were typically very close to the original design values. Table 6.1 compares key member dead load forces for the main span of the west truss predicted by the model with those listed on the original design plans.

Table 6.1 - Comparison of Model Forces for West Truss with Original Design Loads

Member ID	Original Design Dead Load (kips)	Dead Load Predicted by Model (kips)	Ratio of Predicted to Original
U8-L8	2527	2498	0.99
U8-L9	1560	1522	0.98

Member ID	Original Design Dead Load (kips)	Dead Load Predicted by Model (kips)	Ratio of Predicted to Original
L9-U10	1680	1696	1.01
U10-L11	1432	1378	0.96
L11-U12	1215	1200	0.99
U12-L13	834	764	0.92
L13-U14	214	256	1.20
L8-L9	2543	2546	1.00
L9-L11	559	559	1.00
L11-L13	1311	1222	0.93
U8-U10	1551	1527	0.98
U10-U12	486	387	0.80
U12-U14	1899	1673	0.88
Pier 6 Reaction	3660	3659	1.00
Pier 7 Reaction	3589	3604	1.00

For member L13-U14, the dead load predicted by the model is 20 percent greater than that indicated on the original drawings, but the actual magnitude of the difference is only around 40 kips, which is relatively small. For the upper chord members near the middle of the main span (U10-U12 and U12-U14), the dead load predicted by the model is somewhat less than that indicated on the design drawings, likely due to composite action of the concrete deck at this location. The effects of composite action were probably not considered when determining truss forces during the original design.

A check conducted by TranSystems during initial model development involved the simulation of test loads that were applied as part of a previous study conducted by engineers from the University of Minnesota (U of M study). The U of M study measured strains in several main truss members, including one L9-U10 diagonal, as moving truck test loads were applied. TranSystems applied loading of identical magnitude and distribution to their model, which predicted peak L9-U10 member strains that were about 89 percent of the U of M study measured values. Since strain values measured in the U of M study included the effects of the loading being applied dynamically (and possibly traffic in other lanes), it is not surprising that they exceed the simulated strains by the amount indicated. The 11 percent difference is well within the range of AASHTO impact factors that are commonly used to account for dynamic load effects when designing bridges.

The application of AASHTO truck and lane loadings in the open traffic lanes (for purposes of determining an operating rating at the time of collapse, as discussed later in this section) was also checked against hand calculations of stresses in critical members of the main trusses and floor trusses. Numerous other hand calculations were performed to verify the predicted forces in critical members of the model under various loading conditions.

6.1.2.2 Gravity Load Effects

Using the SAP2000 model and NTSB estimates of the superimposed loading at the time of the collapse, corresponding forces were determined for the members of the deck truss. With two exceptions, east and west main truss member forces were less than the original governing service loads shown on the design drawings. The two exceptions were the L9-U10 compression diagonal and the U8-L9 tension diagonal in

the west truss, which carried axial loads that were about 2 percent and 1 percent greater than the original design service loads, respectively. A comparison between original design service loads and the loads at collapse as predicted by the SAP2000 model for key main truss members is presented in Table 6.2. As shown in this table, the main truss members in the southern half of the main span were typically more heavily loaded than the corresponding members in the northern half; and for all exceptions, the loading was relatively low.

The most critically loaded floor truss member was the FT10-L4-U5 compression diagonal. The SAP2000 load in this member was 213 kips, which was about 6 percent greater than the original design service load. The loads in the remaining main span floor truss members were less than the corresponding design service loads.

Table 6.2 - Comparison of West Truss Forces at Collapse with Original Design Service Loads

Member	Original Design Service Load (kips)	Load at Collapse Predicted by Model (kips)	Ratio of Collapse Load to Original Service Load
U6-L7	1635	1573	0.96
L7-U8	1647	1518	0.92
U8-L8	3320	3308	0.99
U8-L9	2088	2109	***1.01***
L9-U10	2288	2340	***1.02***
U10-L11	1975	1856	0.94
L11-U12	1725	1538	0.89
U12′-L13′	1256	995	0.79
L13′-U14′	552	350	0.63
L5-L7	1696	1469	0.87
L7-L8	3407	3351	0.98
L8-L9	3420	3373	0.99
L9′-L11′	919	673	0.73
L11-L13	2011	1694	0.84
L13-L13′	2975	2419	0.81
U6-U8	2436	2337	0.96
U8-U10	2147	1983	0.92
U10-U12	924	616	0.67
U12′-U14′	2790	2265	0.81

Since preliminary analyses showed that the U10/U10′ and the L11/L11′ gusset plates were substantially under-designed, the SAP2000 collapse-level forces acting on them were compared to hand calculated ultimate capacity estimates. The axial load in the critical L9-U10 compression diagonal (west truss) at Node U10 at the time of the collapse was approximately 2340 kips. This represents about 102 percent of the estimated U10/U10′ node capacity. The axial load in the critical U10-L11 tension diagonal (west truss) at Node L11 was about 1856 kips; which represents about 91 percent of the estimated strength of the as-built L11/L11′ connections. Of the total load in the critical U10-L11 member at the time of the collapse, more than 85 percent was dead load, which means that less than 15 percent was due to

superimposed loads consisting of construction loading and traffic. For a total load of 91 percent of capacity, 15 percent superimposed loads represents 13.7 percent of total capacity. Since failure at Node L11 would require an additional load of about 9 percent of capacity, the L11 as-designed capacity to carry superimposed load was approximately 66 percent greater than the superimposed load that existed at the time of the collapse, while the critical U10 node had no additional capacity.

For the U10 gusset plates, the critical diagonal member was in compression. Since the hand calculations did not include consideration of plate buckling under the high compressive and shear stresses that existed at the limit state, these calculations tended to overestimate the actual ultimate capacity. For the L11 gusset plates, the critical diagonal member was under tension and therefore unaffected by issues related to buckling. Therefore, the difference between the criticalities, as designed, of the two nodes was even greater than the stated stress ratios indicate.

As described in Chapter 4, the L11/L11′ gusset plates exhibited corrosion pitting along a line parallel to and just above the tops of the lower chord members; particularly the gusset plates located on the insides of the nodes. Thickness measurements on the most heavily deteriorated L11/L11′ plates indicated local reductions in thickness of up to 0.16 inch (about 32 percent). Where conditions allowed thickness measurements to be made over a large portion of the pitted area, the overall net section loss of the most severely affected plates was less than 20 percent. The uppermost row of rivets connecting the gusset plate and lower chord was parallel to this line of deterioration and was subject to a nearly identical loading. The holes originally drilled in the gusset plate to accommodate these rivets resulted in a 24 percent net section loss along this line. Therefore, the net section loss along the area of notable pitting had not reached the point where it was as great as the reduction in section along the adjacent fastener line. This simple comparison indicates that corrosion had not yet become severe enough to significantly affect the plate's ultimate strength.

The loads sustained by the U10 gusset plates at the time of the collapse were close to their estimated ultimate strengths. Also, no other primary structural elements were as severely loaded. Therefore, the preliminary structural analyses indicated that the collapse initiated with the failure of the gusset plates at one of the U10 nodes; most likely the west one, which was carrying the greater load.

6.1.2.3 Thermal Effects

The design of the 3-span deck truss system included roller bearings at three of the four supporting piers (Piers 5, 6 and 8). The Pier 6 design detail is shown in Figure 6.3; while components of the actual bearing can be seen in Figure 6.4. Roller bearings were used at all but one support pier to allow volume changes to occur without causing significant restraining forces at the piers. Since deterioration can impair the ability of roller bearings to move freely, piers with deteriorated roller bearings may resist volume change movements in the supported structure. If this situation arises, longitudinal forces will develop at all piers that do not have freely rolling bearings and associated forces will be imparted to the supported structure.

The condition of the Pier 6 bearings and comments made in the URS report indicated that the Pier 6 bearings may not have been operating freely at the time of the collapse. Accurately quantifying volume change restraint forces requires knowledge of the degree of restraint provided and the state of the structure (in terms of temperature, position and loading) each time the state of restraint changed. This information does not exist for the I-35W Bridge. However, the potential effects of thermally-induced restraint forces can be estimated by making assumptions regarding restraint and temperature changes consistent with the bridge's structural configuration, the age and condition of its bearings, and local climatic conditions.

In order to estimate the possible significance of volume change restraint forces in key structural elements, a SAP2000 model was created with longitudinal restraint at all main pier bearings and longitudinal springs at all piers to approximate the compliance of the substructure. This model was then subjected to a variety of temperature change scenarios consistent with weather conditions at the time of the collapse. First, the entire structure was subjected to a 40 degree F temperature increase. This represents general mid-day, summer conditions relative to the cooler evenings. Next, the bottom chord members of the west truss were subjected to an 80 degree F temperature increase while the temperature of the rest of the structure was increased 40 degree F. This represents mid to late afternoon conditions where solar radiation is intense enough to substantially warm painted steel surfaces that become exposed to direct sunlight. Table 6.3 summarizes the temperature change conditions that were evaluated and the associated changes in critical member forces.

As indicated in Table 6.3, the magnitudes of the thermal restraint forces are small relative to total member loads. However, these force changes represent a significant fraction of the forces generated by superimposed loads (e.g. traffic and construction loading). Also significant is the fact that the orientation of thermal restraint forces is such that, as temperatures increase, they tend to reduce demands on critical elements framing into Node U10. This means that, for a given state of bearing restraint, an increase in temperature would shift loading away from the L9-U10 members (i.e. out of the critical load path and into another, less critical one). As long as the L9-U10 members remained critical (i.e. as long as the shift in load was not so drastic as to make other elements of the structure more critical), this type of load shift could have a proportional increase on the bridge's ultimate ability to carry superimposed loads. Ductility represents a potentially mitigating factor to this effect. At one extreme, (i.e. with all needed ductility), a thermally-induced shift in load would have had no impact on ultimate capacity. This is due to the fact that sufficient ductility would have allowed Node U10 to reach its ultimate strength and then simply deform inelastically as needed while all remaining load paths were fully mobilized, assuming they too had sufficient ductility. Thus, the maximum capacity of the structure would be achieved regardless of the initial thermal conditions. At the other extreme (i.e. with little or no ductility), the critical U10 node would have failed almost immediately after reaching its ultimate strength. In this case, thermally-induced changes in Node U10 member forces could have substantially affected bridge capacity. Since critical Node U10 demands decreased with increasing temperatures (with restraint at the roller bearings); this effect would have increased capacity during warmer periods. Conversely, cooling of the structure would have decreased capacity. Slippage of the Pier 6 bearings would have had an effect similar to cooling. For example, if restraint-related forces had reduced demands on the U10 gusset plates, subsequent slippage of the bearings would quickly increase U10 demands.

Table 6.3 - Impact of Temperature Increase on Member Forces in West Main Truss

Member	Load at Collapse, Unrestrained (kips)	Load at Collapse, Piers Restrained, No Temperature Effects (kips)	Change in Force, 40°F Temp. Rise in Entire Structure (kips)	Change in Force, 80°F Temp. Rise in West Bottom Chord, 40°F Temp. Rise in Rest of Structure (kips)
L9-U10	2340 (C)	2221 (C)	62 (T)	136 (T)
U10-L11	1856 (T)	1684 (T)	90 (C)	183 (C)
U8-U10	1983 (T)	1555 (T)	257 (C)	168 (C)
U10-U12	616 (C)	853 (C)	157 (C)	23 (T)
L11-U12	1538 (C)	1499 (C)	26 (T)	79 (T)

Member	Load at Collapse, Unrestrained (kips)	Load at Collapse, Piers Restrained, No Temperature Effects (kips)	Change in Force, 40°F Temp. Rise in Entire Structure (kips)	Change in Force, 80°F Temp. Rise in West Bottom Chord, 40°F Temp. Rise in Rest of Structure (kips)
L9-L11	648 (C)	1346 (C)	329 (C)	896 (C)
L11-L13	1694 (T)	857 (T)	404 (C)	1066 (C)
Horiz. Shear, U10 Gusset	2599	2408	-100	-191
Horiz. Shear, L11 Gusset	2342	2203	-75	-170

6.1.2.4 Failure Sequence

The portion of the main truss span bounded by the four U10/U10′ nodes comprised a rectangle (in plan) that was supported at each corner by the U10/U10′ nodes. When support at one corner was compromised, the associated deflection caused significant increases in the adjacent corner loads and a decrease in the load at the opposite corner. To demonstrate this effect, the west truss L9-U10 diagonal was shortened (using a local temperature change) in the SAP2000 finite element model representing conditions at the time of the collapse. This shortening represented the initial stages of the failure of the U10 gusset plates and the associated decrease in distance between the U10 and L9 nodes. Table 6.4 summarizes the effects of a 0.42 inch and a 2 inch shortening of the west truss L9-U10 diagonal on the load in the other L9-U10 and L9′-U10′ diagonals. As indicated in Table 6.4, a 0.42 inch shortening of the west truss L9-U10 member increases the force in the east truss L9-U10 member to a level comparable to the initial west truss value. A 2 inch shortening causes forces in the east truss member to exceed 2500 kips. This analysis indicated that failure of one U10 node would be followed almost immediately by failure of the other. After both U10 nodes were compromised; vertical displacement of the south end of the U10/U10′ rectangle resulted in large increases in the framing forces at the north end, including added stresses in the U10′ gusset plates. This phenomenon led quickly to failure of the U10′ gusset plates, and the complete loss of adequate support at all four corners of the U10/U10′ rectangle. This sequence is consistent with the widely viewed security camera footage of the collapse, which indicates that the two U10 nodes failed nearly simultaneously and were followed shortly thereafter by the failure of the U10′ nodes.

Table 6.4 - Effects of Shortening L9-U10 Member at West Truss on Member Forces

Case	L9-U10, West (kips)	L9-U10, East (kips)	L9′-U10′, West (kips)	L9′-U10′, East (kips)
No Shortening	2340	2247	2108	2102
Δ = -0.42 in.	2203	2304	2121	2091
Δ = -2 in.	1699	2517	2168	2047

6.1.3 Localized Finite Element Modeling of Critical Components

6.1.3.1 Description

In order to further investigate limit state behavior at the U10 node, models of this node and associated members were constructed using Abaqus finite element software. These models were used to evaluate limit state performance characteristics of the U10 components with greater accuracy than could be achieved via hand calculations. A schematic view of an Abaqus U10 model is shown in Figure 6.5.

Since field measurements indicated close conformance with the shop drawing details, geometric features of the modeled components were based primarily on the shop drawings. However, variances from the

shop drawings, such as deformations visible in photographs taken before the collapse, were incorporated in some models. Material properties representing design and collapse conditions were based on testing performed by FHWA on samples of steel taken from U10 gusset plates. The steel stress-strain curve used in the models is shown in Figure 6.6. This relationship was used in conjunction with Von Mises total stress criteria to define material stiffness in non-linear models. A model constructed to evaluate the effect of using high strength (F_y = 100 ksi) plate used a simple elastic-plastic stress strain curve.

At first, several two-dimensional models were used to investigate the sensitivity of the response to various parameters and modeling assumptions. Modeling parameters investigated included the effect of net section, rivet modeling, mesh size and material properties such as yield strength and Poisson's ratio; in addition to the investigation of different boundary conditions, out of plane distortion and loading algorithms. Other investigated parameters included the effect of number of integration points through shell element thickness, the modeling of contact, and friction.

In general, a 0.5 inch element size was used to mesh the gusset plates, while 1 to 3 inch elements were used to mesh the other members. Four-node thick shell elements with reduced integration and hourglass control (S4R) were used to model all plates. The effect of the mesh size on predicted capacity was investigated by using a smaller mesh size equal to half of the regular mesh size (0.25 inch for the gusset), but the effect on the actual predicted capacity was negligible. The analyses were generally performed using five integration points through the thickness of the shell element, as using seven integration points did not cause a meaningful difference in the results.

The final models used to assess Node U10 performance were three-dimensional, and included modeling of the framing members to the next node. These models accounted for the effects of material and geometric nonlinearities. Member axial forces and boundary displacements were applied in proportion to forces and displacements obtained from the SAP2000 model of the complete bridge.

Photographs of U10 gusset plates were taken as part of a study that was completed early in 2007. These photos indicated visible out-of-plane distortion along the vertical edges located between the L9-U10/L9′-U10′ members and the adjacent upper chords. A reproduction of one such photograph is provided as Figure 6.7. To evaluate the significance of this condition, an initial out-of-plane plate distortion was created in some of the models.

Models incorporating properly designed gusset plates were also evaluated. These included replacement of the original gusset plates with either similar thickness plates of higher strength (F_y = 100 ksi) steel, or 0.875 inch thick plates with F_y = 50 ksi steel.

6.1.3.2 Results

In all cases, the models indicated that the maximum total load that could be sustained is limited by the capacity of the gusset plates in the vicinity of the L9-U10 member. In other words, ultimate capacity is defined by the inability of the L9-U10 member to sustain additional compression. Figure 6.8 shows a typical Abaqus plot of Von Mises stresses in the various elements that were modeled, shortly before the ultimate strength is reached. As indicated, achievement of ultimate strength results in high local stresses and strains (i.e. beyond yield) near the tip of the L9-U10 member, and essentially yield level stresses in much of the gusset plate below the top chord. Given that the stability of the gusset plates in the vicinity of the L9-U10 member is the controlling factor, L9-U10 axial force is used to characterize the capacities of the various models. The models without any initial distortion in the gusset plates indicated a maximum achievable L9-U10 axial force of 2470 kips compared with 2300 kips based on the hand calculations.

To evaluate the significance of edge distortion similar to that shown in Figure 6.7, models were created with the vertical edges of the plates distorted to a similar shape. The distortion was defined by applying an out-of-plane load to the edges of both plates (either inward - toward bridge centerline; or outward - away from bridge centerline). The resulting plate shapes were used as the starting points for several gravity load analyses. The magnitude of the initial (i.e. no load) distortion was selected so as to produce a peak out-of-plane deformation amplitude of about 0.5 inches at 95 percent of the ultimate load (i.e. conditions similar to those shown in Figure 6.7). When both plate edges were initially distorted inward, the maximum L9-U10 axial force was about 2390 kips. The maximum plate edge distortion amplitude at 95 percent of the ultimate load was about 0.5 inches, and the maximum plate edge distortion at the ultimate load was about 0.8 inches. When both plate edges were initially distorted outward, the maximum L9-U10 axial force was about 2470 kips. The maximum plate edge distortion amplitude at 95 percent of the ultimate load was about 0.4 inches, and the maximum plate edge distortion at the ultimate load was about 0.8 inches. In both cases, the top of the L9-U10 member was moving in the direction of the initial plate edge distortion as the peak load was achieved.

In order to provide perspective concerning the significance of the U10 gusset plate design errors, an Abaqus model was created using stronger 0.5 inch thick plates (F_y = 100 ksi; F_u = 100 ksi); and another model was created using 0.875-inch thick plates with material properties consistent with original design specifications (the stress-strain relationship shown in Figure 6.6 was used). These combinations were selected as two practical options for satisfying original design requirements. Loading was applied incrementally in proportion to the forces caused by the original design loads plus the subsequent deck load additions. In all other respects, the model was identical to the edge-distorted model described above. L9-U10 force-displacement (where displacement refers to the axial movement of the end of L9-U10 relative to the Node U10 work point) curves for each case are shown in Figure 6.9. Figure 6.9 also shows a force-displacement curve for the as-designed condition. The data represented in Figure 6.9 clearly show that, in both cases, the ultimate strength was much greater than what was provided by the as-designed conditions. For the 0.875-inch thick plates, the finite element modeling predicted an ultimate capacity of approximately 4500 kips. For the 0.5-inch thick plates of stronger material, the modeling indicated an expected capacity of approximately 3900 kips. Both of these alternate gusset plate designs would have provided Operating Rating Factors much greater than 1.0 for the loading present at the time of collapse (2340 kips).

6.1.4 Load Distribution, Magnitude and Duration Issues

At the time of the collapse, the most critically loaded members of the main truss (i.e. those comprising Node U10 of the west truss) sustained forces that were essentially at or below the service loads listed on the original design drawings. The estimated 2340 kip axial load carried by critical member L9-U10 consisted of the following:

- 2010 kips dead load (85.9 percent)
- 290 kips construction load (12.4 percent)
- 40 kips traffic load (1.7 percent)

Roughly 1.5 inches of deck concrete had been removed from the closed lanes where the construction loading was located. Therefore, to compare conditions at the time of collapse to normal conditions, the L9-U10 loading represented by this material should be subtracted from the construction load and added to the dead load (i.e. a portion of the 290 kip construction load represents material that was to replace the

overlay that had been removed from this area). When this is done, the resulting breakdown of the 2340 kip failure load becomes:

- 2075 kips dead load (88.7 percent)
- 225 kips construction load (9.6 percent)
- 40 kips traffic load (1.7 percent)

In 1999 and 2000, the U of M conducted load tests that included instrumentation of the L9-U10 diagonal of the west truss. This testing measured the stresses induced by the passing of traffic, including a controlled series of loaded dump trucks. In their March 2001 report, the U of M investigators reported a peak live load stress of about 1.4 ksi in the west truss L9-U10 diagonal. This level of stress was caused by a 3 by 3 group of nine loaded dump trucks (GVW of about 51 kips each), traveling in the three innermost lanes of the four southbound lanes. Apparently, the U of M study also included several weeks of general live load monitoring which indicated similar peak live load stress values. Assuming the reported 1.4 ksi stress range represents the average stress on the member cross section, the corresponding axial load is about 176 kips; which is about two thirds of the 265 kips (approximately 2.1 ksi) associated with the net superimposed loading at the time of collapse.

The difference between the U of M test loading and the collapse loading is more substantial than the difference in magnitudes indicates. The primary reason for this is that the U of M superimposed loads were applied by moving vehicles, while the superimposed loads at the time of collapse were essentially static. This distinction is significant for two reasons. First, the strength of mild steel is sensitive to strain rate: the greater the rate of strain, the larger the strength. The U of M loading was provided by trucks travelling at "highway speed." If the ultimate strength of the gusset plates is represented by a yield stress of 51 ksi, 88.7 percent of which is "consumed" by dead load; this leaves approximately 6 ksi of gusset plate strength available to sustain traffic load. Therefore, every ksi of strength increase associated with dynamic loading provides a 17 percent increase in traffic load capacity.

The second factor that makes dynamic loads less critical than equal magnitude static loads is the fact that the U10 failure mechanism was relatively ductile. A ductile mechanism can sustain demands in excess of capacity as long as they are of sufficiently short duration. Therefore, the structure was capable of sustaining moving truck loads that exceeded even its dynamic capacity. In contrast, static loading that exceeds static capacity, even by a very small margin, will eventually cause failure.

6.2 Operating Conditions and Operating Rating Calculations

As described in Chapter 2, the bridge repair contractor placed construction material and equipment weighing approximately 577 kips on the main span of the bridge prior to the collapse. In order to evaluate the effect of this load, SAP2000 models were used to develop peak member forces associated with the contractor's construction loads acting together with the existing dead load and AASHTO HS20-44 truck or lane loads in the active lanes. Initially, the live load impact factor for AASHTO loadings was conservatively set at 1.3 for all members. The construction loads considered in this effort included the loading in place at the time of the collapse as reported by the NTSB. When determining critical loads for the floor trusses most affected by the stockpiled granular material (i.e. Floor Trusses 9 and 10), the water truck was repositioned so as to sit directly above each truss. These forces were then used in conjunction with lower bound member capacities (calculated by multiplying the critical service loads listed on the original design drawings by the original design factor of safety) to establish AASHTO Load Factor Design (LFD) Operating Rating Factors (ORF). Since connections are required to at least sustain member

design forces with the same factor of safety, using original design loads to establish nominal member capacities precludes any need to check connections. The AASHTO LFD Operating Rating Factor reflects the maximum live load that a structure can carry as a fraction of the live load used to calculate element forces. If element forces are determined using the minimum required live loads specified by AASHTO, an ORF less than one indicates a deficiency, while an ORF greater than one indicates reserve capacity.

For a properly designed bridge, this simple load rating methodology is inherently conservative. This is because actual component capacities are typically greater, often substantially so, than the minimum required capacities. This load rating methodology must be supplemented with capacity calculations based upon actual member properties when it indicates an unacceptable ORF or when deterioration has reached a point where the ability to sustain original design loads becomes questionable.

All members of the main trusses were found to have LFD ORFs greater than 1.0 under the combined effects of construction loads in the closed lanes and AASHTO lane or truck loadings in the open lanes. Put another way, the Operating level factored demands for each member of the main trusses were found to be less than the computed capacities. Similarly, all floor truss members affected by the construction loading in Span 7 also had LFD ORFs greater than 1.0. The U1-L2 diagonal in Floor Truss FT1 had an LFD ORF of slightly less than 1.0 using the simple and conservative approach outlined above, but was found to be well above 1.0 using actual member capacity. This condition indicated that the original floor truss design loads may have been underestimated at some locations; likely due to the fact that the original design did not account for two factors:

- Three dimensional behavior of the structure - Because the main trusses deflect under load, and because the amount of deflection varies along the bridge, the reactions of the stringers on the floor trusses also vary. The floor trusses located near the piers have stiffer support from the trusses than those further away from the piers; which means they attract more than their tributary share of the adjacent stringer loads.
- Stringer continuity - At each expansion joint, deck stringers are flexurally discontinuous. The floor trusses located one stringer span away from the joints (i.e. first interior supports) carry more than half of the common span loads.

For floor trusses that are not significantly affected by these issues, the simplified LFD ORFs are greater than 1.0.

Since stringer design moments were not specified on the original drawings, nominal capacities were calculated using current AASHTO LFD procedures, conservatively ignoring lateral support provided by the concrete deck. All stringers, including those directly beneath the mounded aggregate piles in Span 7, were found to have LFD ORFs greater than 1.0.

As load rating procedures are to reflect actual conditions, significant corrosion and other detrimental effects of being in service need to be considered when establishing the nominal strengths of affected components. When the element is a connection or connection component, the easiest way to incorporate the effects of deterioration is to reduce the nominal strengths of affected members by a proportional amount. This approach is conservative because it assumes that the actual strength of the connection is the minimum possible permitted by AASHO/AASHTO. If this procedure yields acceptable ORFs, no additional analyses are needed. If this procedure yields unacceptable ORF values, the next step would be to establish ORFs starting with the average of member design loads and actual capacities (AASHO required connections to be able to sustain the average of the design load and the actual strength of the

associated members). Of the two improperly designed gusset plates (i.e. U10/U10′ and L11/L11′), only the L11/L11′ nodes had sustained enough corrosion to warrant further consideration for load rating. As described in Chapter 4, the L11/L11′ gusset plates exhibited pitting along a line parallel to and just above the tops of the lower chord members; particularly the plates located on the insides of the nodes. Thickness measurements on the most heavily deteriorated L11/L11′ plate indicated an average net section loss of about 10 percent along this line. The uppermost row of rivets connecting the gusset plate and bottom chord paralleled this line of deterioration and was subject to a nearly identical loading. The holes originally drilled in the gusset plate to accommodate these rivets resulted in a 24 percent net section loss along this line. Therefore, the section loss along the areas of notable pitting had not reached the point where it was as great as the reduction in section along the adjacent fastener line. Consequently, it is unlikely that the pitting had a significant impact on the plate's ultimate strength. Nonetheless, operating level load rating calculations were performed assuming the following:

- Along the zone of pitting, the pair of gusset plates at each L11/L11′ node sustained an average net section loss of 10 percent
- At each L11/L11′ node, the ability of each pair of gusset plates to carry any type of loading was reduced by 10 percent
- The original strength of the gusset plates exactly matched the original member design loads (i.e. the original connection strength was less than the minimum permitted by AASHO)

Based on these assumptions, factored member loads (using a load factor of 1.3 for operating conditions) were compared to 90 percent of the corresponding minimum nominal strengths (i.e. 0.9 x 1.8 x design load, where the minimum factor of safety is taken as 1.8). In each case, ORFs for the L11/L11′ members under the collapse loading were greater than 1.0, indicating acceptable performance. For pre-construction or post-construction operating conditions (i.e. all lanes open), this procedure also indicated acceptable ORFs for all members. Even using this conservative load rating procedure, ORFs do not fall below 1.0 until the entire connection (i.e. both plates, in all critical areas) loses almost 20 percent of its original capacity.

In summary, for all of the main span structural members affected by the construction loads, a simple and conservative evaluation indicated acceptable performance under the imposed loads. This same approach also indicated acceptable performance under the operating conditions that existed before the recent repair program was initiated. Furthermore, in each case, actual loading and element conditions could have been accounted for without analyzing any connections.

6.3 Pre-collapse Structural Evaluations

In 1999 - 2001, the U of M performed a fatigue evaluation of the main truss spans. The evaluation included measurement of live load stress ranges in several members, inspection of potential fatigue sensitive details, and analysis of truss performance under various loading conditions. The study concluded that the live load demands on the bridge were not severe enough to cause fatigue damage. This conclusion was supported by live load strain measurements, analyses, and field observations of some of the most fatigue sensitive details. The U of M study did not include evaluation of any of the main truss gusset plate connections.

In 2006 - 2007, URS performed a fatigue and redundancy evaluation of the bridge. This study also concluded that fatigue did not appear to be a significant issue for this structure. The redundancy portion of the URS study consisted of evaluating the effects of losing individual members, and identifying those

members whose loss would likely cause the structure to collapse. The conclusions of the URS study included the recommendation that MnDOT implement one of three "equally viable" retrofit approaches. The most conservative approach consisted of installing cover plates on the members that had been identified as fracture critical. Another approach consisted of intensive examination of weld details in the fracture critical members and removal of measurable defects that were found. The final approach consisted of a combination of the first two. The URS study did not include evaluation of the main truss gusset plate connections. Furthermore, had the most conservative of the URS recommended retrofit programs been implemented, the capacities of the deficient U10/U10′ nodes would not have been increased. Therefore, implementing any or all of the URS recommendations would not have addressed the deficiency that caused the August 1, 2007 collapse.

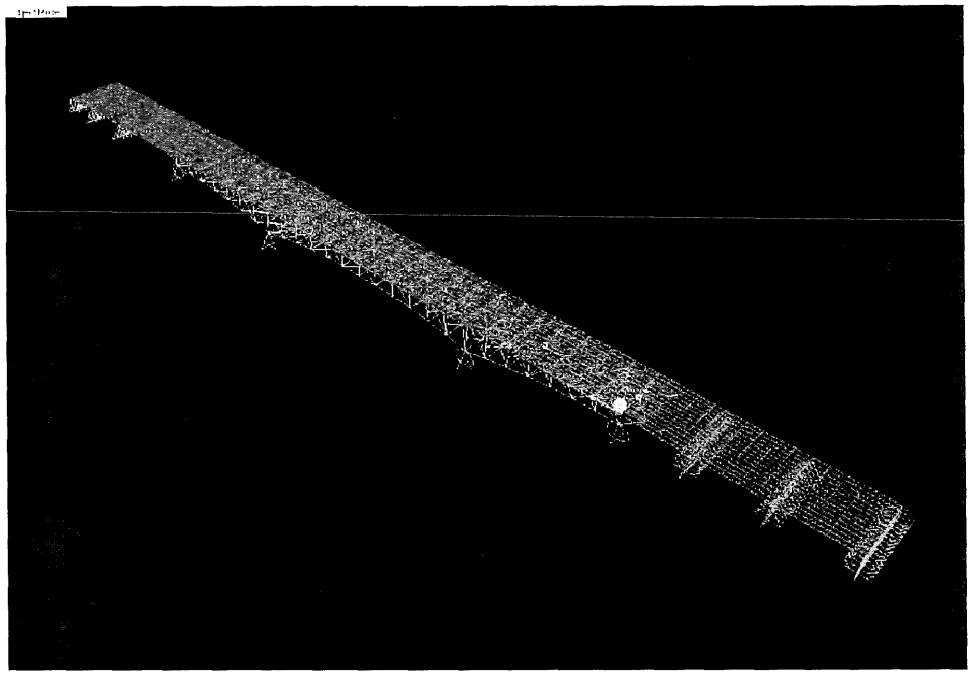

Figure 6.1. Overall view of SAP 2000 finite element model.

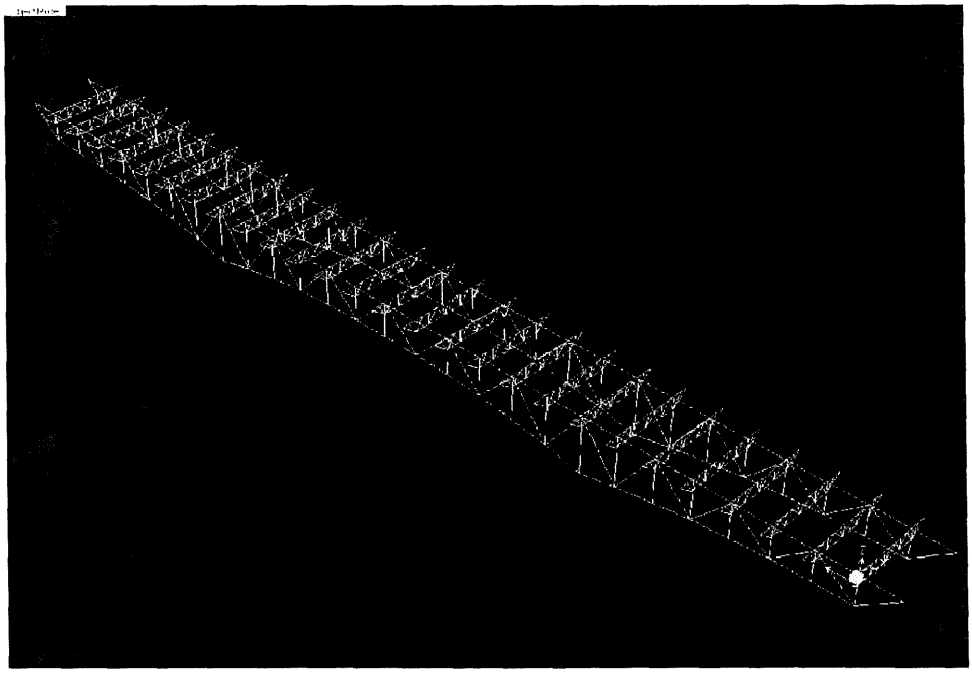

Figure 6.2. Main truss and floor truss framing in SAP 2000 model.

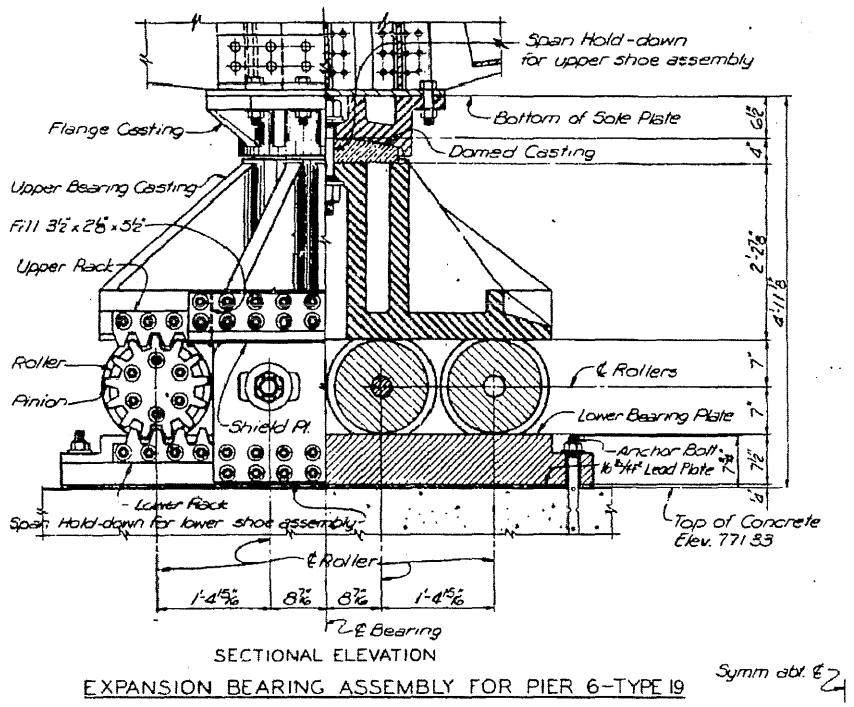

Figure 6.3. Original design detail, Pier 6 expansion bearing.

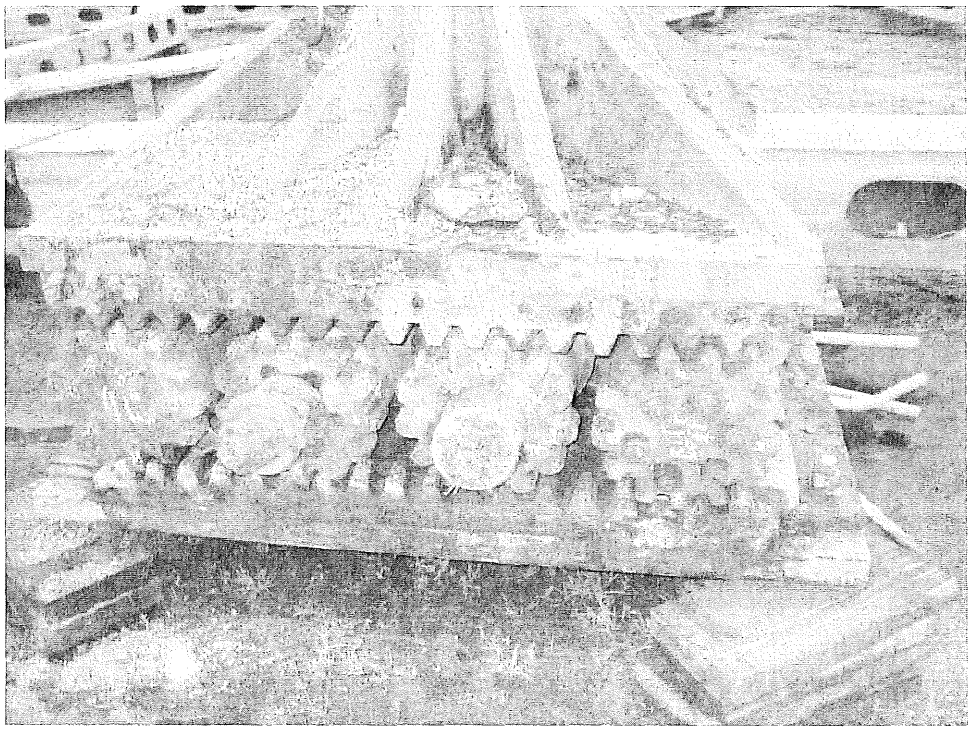

Figure 6.4. Re-assembled Pier 6 bearing.

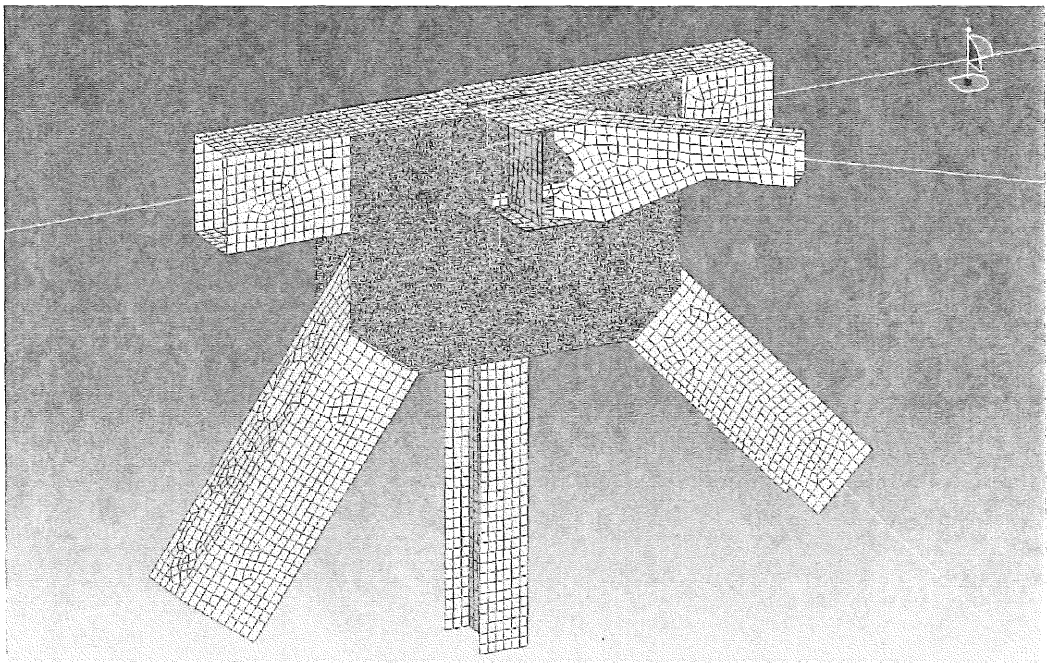

Figure 6.5. Schematic view of Node U10 as modeled in Abaqus software program.

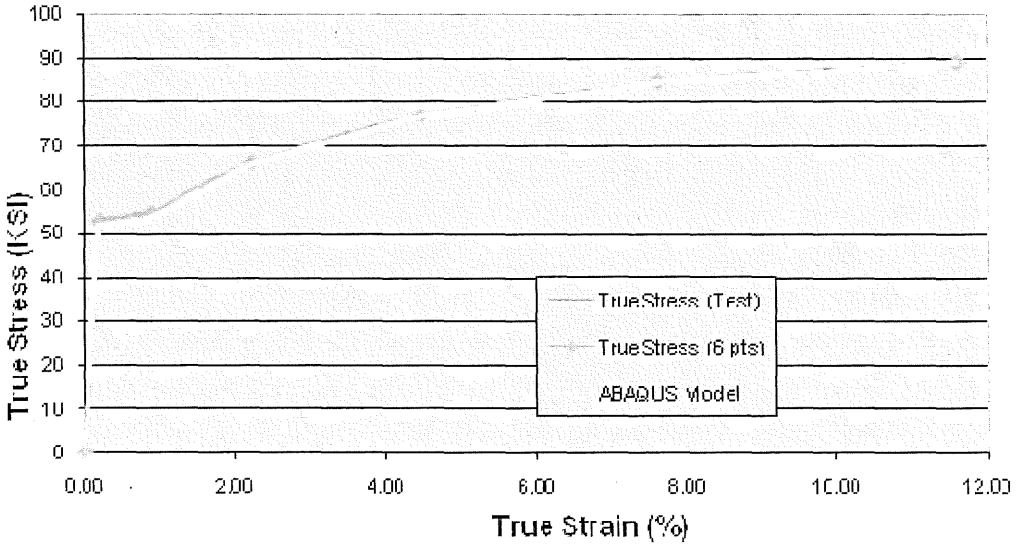

Figure 6.6. Stress-strain relationship used in Abaqus modeling.

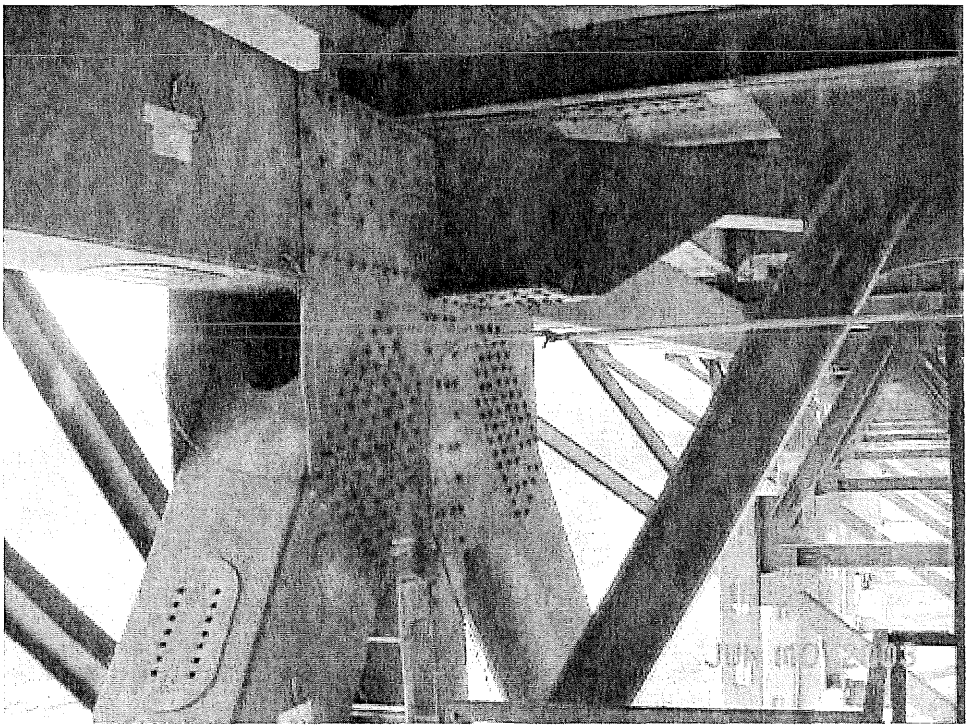

Figure 6.7 URS photograph of Node U10W, looking northwest, showing bowing in gusset plate.

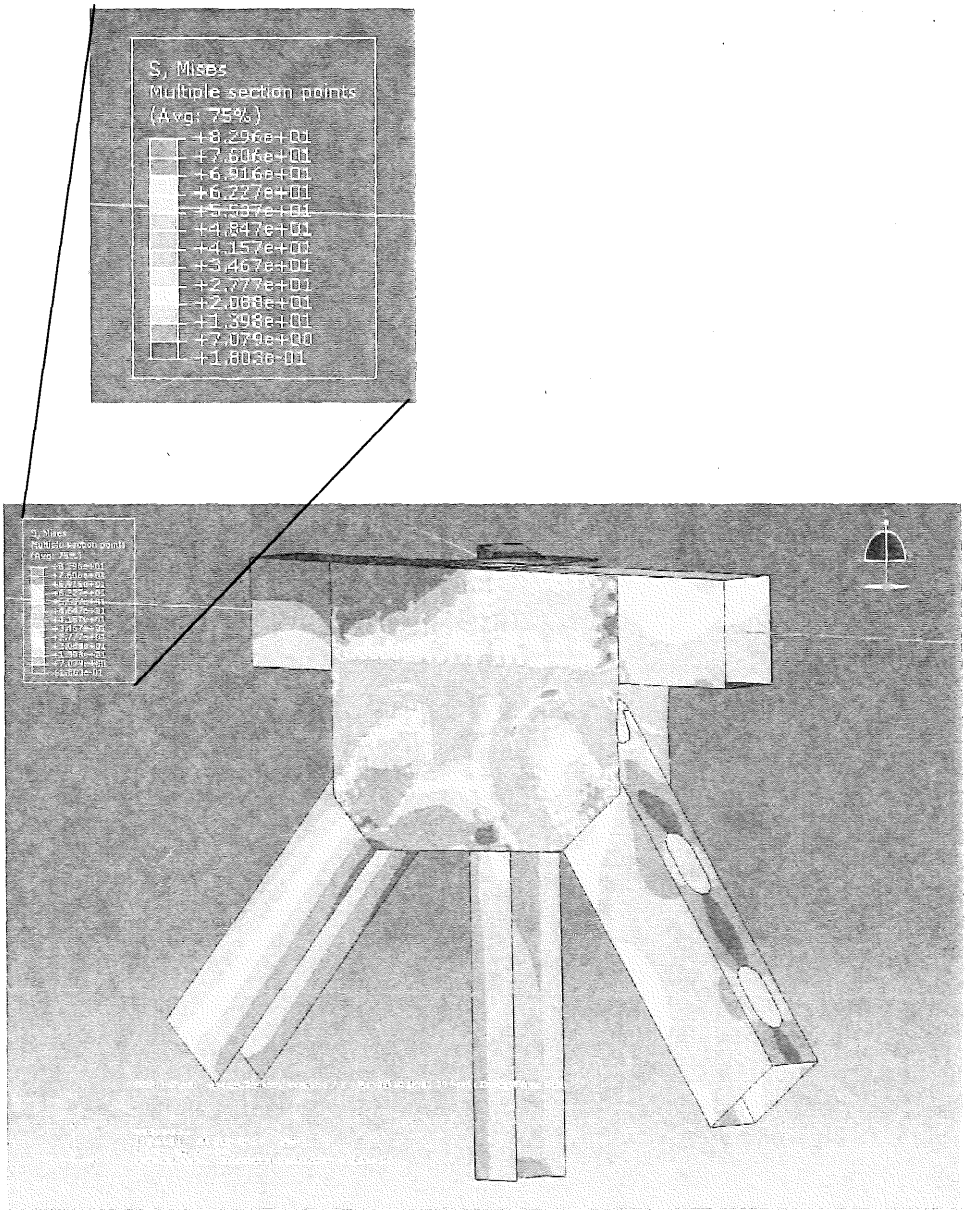

Figure 6.8. Abaqus plot showing stress levels at Node U10.

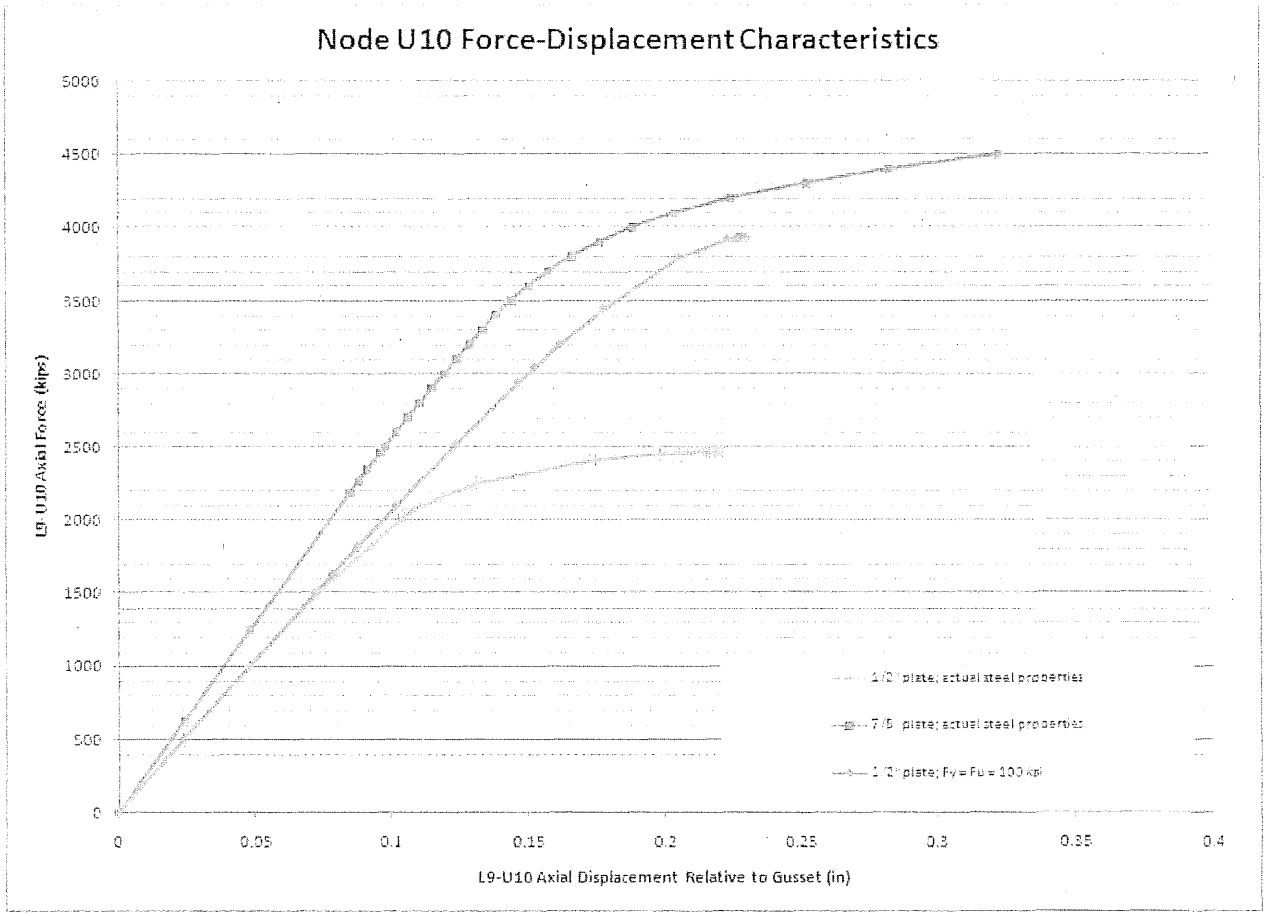

Figure 6.9 Load-displacement relationship for various configurations of U10 gusset plate.

7 DISCUSSION

7.1 Conditions at Failure

7.1.1 Loading

The forces in the various bridge structural components at the time of the collapse were dominated by gravity-related loads. These included: self weight, construction loads and vehicular traffic. With few exceptions, truss member loads at the time of the collapse were less than the service-level loads indicated on the original design drawings. In each case where the actual load exceeded the corresponding original service-level design load, the actual load was substantially less than the minimum permissible nominal strength associated with the original design criteria. In all cases, component forces at the time of the collapse were such that a properly designed element would have had an LFD Operating Rating Factor greater than 1.0. This is not surprising considering:

- The total main span construction load combined with main span 1964 AASHO design lane loads in the four active lanes was only about 80 percent of the main span design live load
- The main span construction loading in the four closed lanes was about 60 percent of the design live load for these lanes
- The total main span shear force at Pier 6 due to construction loading combined with 1964 AASHO design lane loading in the four active lanes was about 95 percent of the shear caused by the original design live load
- The loading superimposed on Floor Truss FT10 under construction loading plus 1964 AASHO design lane loading in the four active lanes was less than the original FT10 design live load

By any reasonable measure, the loading in place at the time of collapse was less than what the bridge could have safely carried if the deficient gusset plates at U10 and L11 had been properly designed. It is true that the demands placed on some members at the time of the collapse were likely greater than the demands sustained under normal service conditions. The construction loading minus the weight of the old overlay material that had been removed represented the equivalent of about seven AASHTO HS20 truck loads in the two closed lanes of the southwest quadrant of the main span. Having this much superimposed static weight concentrated in two lanes of the southwest quadrant of the main span would have been unlikely under normal conditions. However, if it had been properly designed, the bridge would have been able to safely support these loads.

The fact that the construction load was essentially static (rather than applied via moving vehicles passing by) was also unusual. The dead load carried by the critical elements, both at the time of the collapse and in the previous years, represented a large fraction of available capacity. Therefore, small changes in strength, such as those associated with static versus dynamic loading, would cause a relatively large change in live load capacity. Conversely, the static nature of the construction loads made them significantly more severe than moving loads of a comparable magnitude.

7.1.2 Capacity Provided by Original Design

Examination of the structural framing that existed at the time of the collapse indicated conformance with the original design documents. In addition, the main structural elements of the truss system were found to be in good condition. While there was visible corrosion-related section loss in some elements, in no instance was the deterioration sufficient to cause concern regarding the ability of a properly designed element to sustain applicable traffic loading with an appropriate factor of safety.

Evaluation of the truss system structural components revealed two major design flaws: a deficient gusset plate design for the U10/U10′ nodes; and a deficient gusset plate design for the L11/L11′ nodes. In each case, the nominal capacity provided by the plates was about half of the nominal capacity required by applicable AASHO design provisions. Since these design provisions required a nominal factor of safety of slightly less than 2.0; a nominal capacity deficiency of 50 percent suggests that the expected ultimate strength would be close to the service level design load. This is consistent with the fact that, at the time of the collapse, the west truss L9-U10 compression diagonal (which framed into the U10 node) was carrying about 100 percent of its original design load, and was the most critically loaded member framing into any of the U10/U10′ or L11/L11′ nodes.

Analysis indicated that the U10 gusset plates were more critically loaded than any other components of the main truss, and that the estimated loading at the time of the collapse was very close to the computed ultimate capacity. Preliminary hand calculations, revised to reflect measured steel strength in lieu of the original assumed value, indicated an ultimate L9-U10 axial capacity of 2300 kips. Relatively sophisticated finite element analyses of a U10 node and associated framing indicated an ultimate strength of about 2390 kips. The best estimate of the L9-U10 axial load at the time of the collapse lies between 2300 and 2400 kips.

The design of the L11/L11′ gusset plates was deficient by a similar degree to that of the U10/U10′ gusset plates, and the L11/L11′ plates had been affected by corrosion. However, relative to actual capacity, the L11/L11′ plates were less severely loaded at the time of collapse. This is due mainly to the following facts:

- The critical members framing into the L11/L11′ nodes were less affected by the construction loads.
- The most heavily loaded diagonal member at the L11/L11′ nodes was in tension.
- The corrosion-related section loss sustained by the L11/L11′ gusset plates was less severe than the section loss due to drilling the original fastener holes along a comparably loaded parallel plane.

Furthermore, post-collapse examination of the L11/L11′ gusset plates indicated that they were essentially intact until the lower chord of the truss hit the river bottom; and L11/L11′ nodes visible in the collapse video were still intact after the collapse began.

Since properly designed U10/U10′ and L11/L11′ gusset plates would have had approximately twice the nominal strength as those actually provided (with or without distorted edges), it is clear that a properly designed main span deck truss structure would have been able to carry the loading that existed at the time of collapse. Put another way, had the deficient U10/U10′ gusset plates been properly sized, they could have sustained a nearly 50 percent loss of capacity (e.g. from severe corrosion) and remained capable of supporting the loads that existed at the time of collapse. The L11/L11′ gussets could have sustained even greater loss. Furthermore, had these plates met the original design requirements, the main span deck truss structure would have been able to sustain the construction loads that existed at the time of the collapse along with AASHTO HS20 lane loading in the active lanes, with an appropriate factor of safety.

As indicated in Chapter 2, some of the original gusset plate design calculations were made available for review. The calculations related to the U10 gusset plates are based only on their function as chord splice elements. This is significant because the gussets do far more than splice chords; which means other design considerations might require a gusset to be thicker/stronger. For example, the calculations related to Node U10 show that 0.5 inch thick gusset plates are adequate for splicing the top chord. However, 0.5 inch thick gussets are not adequate for handling the forces in the web members at U10, and this can be

shown using an extremely simple web/chord shear flow calculation. Information contained in the calculations that were made available for review indicated various possibilities as to how the deficient plate size came to be shown in the design documents. However, given the limited scope of the original calculations, it was not possible to positively identify the source of the error. We believe that Sverdrup-designed bridges contemporary to the I-35W Bridge should be carefully reviewed for similar problems.

7.1.3 Thermal Restraint Effects

The evaluation of potential thermal restraint effects indicated that the bridge's ability to carry superimposed load may have been sensitive to climatic conditions. For fully locked roller bearings, increasing the temperature of the entire structure in the SAP2000 model by 40 degrees F reduced the force in the critical L9-U10 member by 62 kips. Since this comprises about 23 percent of the member force caused by superimposed loading at the time of collapse, such a temperature change could have increased the bridge's ability to carry superimposed loads by a similar proportion. Increasing the temperature of the west truss bottom chord by 40 degrees relative to the rest of the structure decreased the L9-U10 force in the west truss by 75 kips, which represents 28 percent of the force caused by superimposed loading at the time of the collapse. Compromised roller bearings and the associated restraint forces could have resulted in a substantial increase in the bridge's ability to carry superimposed loads at the time the construction material was being placed on the deck.

Unfortunately, enhanced capacity caused by restrained thermal expansion would have been a temporary condition, lasting only as long as the increased temperature and bearing restraint were maintained. Therefore, either cooling of the structure or bearing slippage would have reduced bridge capacity. Since the collapse occurred in the early evening, a decrease in the intensity of solar radiation may have resulted in cooling of the west truss relative to its afternoon peak (the ambient air temperature remained relatively constant during this time). This would have increased the demands in the U10 gusset plates. Slippage of the Pier 6 roller bearings would have had a similar effect. Therefore, if the bridge structure was still realizing a net heat gain at the time of collapse, the buildup of restraint forces in the Pier 6 bearings could have caused them to slip, which would have quickly increased Node U10 demands. In each case, thermal effects acting in combination with some restraint at the Pier 6 bearings could have temporarily increased bridge capacity, allowing it to carry the full construction loads and traffic for a few hours.

The overall impact of thermally-induced changes in member force was mitigated to some degree by the ductility of the U10 failure mode. Non-linear analysis of Node U10 indicated the gusset plates were capable of sustaining substantial plastic strains (i.e. that, in terms of strain, the Node U10 gusset plate failure was very ductile). However, ductility of Node U10 as defined by its ability to sustain inelastic deformations along the longitudinal axis of L9-U10 (i.e. the type of deformation needed to permit redistribution of forces within the truss) was limited; which means the Node U10 failure mode did not allow for the magnitude of load redistribution needed to fully mobilize alternate load paths. Therefore, any thermally-induced changes in the L9-U10 member force would have had a nearly proportional change in bridge capacity, likely making the ultimate capacity somewhat dependent on temperature. Although there is insufficient information to accurately quantify the extent to which thermal and restraint effects influenced the structure on the day of the collapse, they could have caused significant fluctuation in Node U10 demands.

7.1.4 Failure Scenario

Observations of the collapsed structure indicated that the deck truss spans separated into three sections along the 10 and 10′ node lines. Generally speaking, truss members located north of the plane defined by

the U10 and L9 nodes and south of the plane defined by the U10′ and L9′ nodes went into the river while the rest stayed with the wreckage on either bank. This fact, along with the essentially vertical movement of the portion that fell into the river (there was very little twist or rotation) indicated that the collapse initiated with a failure in either a U10 node, an L9 node, or in one of the L9-U10 members, followed closely by similar failures at the other three locations. The following observations confirm that the collapse started with failure of one of the U10 nodes:

- The U10 gusset plates had failed, separating into multiple pieces while the L9 gusset plates did not.
- The L9-U10 members showed no signs of compression overload.
- Gusset plate remnants at the upper ends of each L9-U10 member indicated that out-of-plane gusset plate buckling occurred at the U10 nodes.

Each L9-U10 and L9′-U10′ member sustained some degree of top and bottom plate splitting caused by a main truss upper chord side plate pushing down between the L9-U10 side plates following gusset plate failure. This along with the last of the bulleted items listed above indicates that failure of the critical U10/U10′ gusset plate initiated in the area surrounding the end of the compression diagonal. At each U10/U10′ location, the compression diagonal essentially broke free of the node, while the remaining members stayed connected long enough to be pulled down through it for some distance before additional plate fractures allowed the node to come completely apart. The conditions observed at the U10/U10′ nodes and associated members are consistent with the analytical findings previously discussed.

Like the U10/U10′ nodes, the L11/L11′ nodes were under-designed by a factor of about 2. Unlike the U10/U10′ nodes, they appeared to remain intact until after the collapse was in progress. Observation of these nodes indicated that the web members – including what had been the tension diagonals – were driven into the corresponding nodes when the bottom chords hit the river bed, at which time the gusset plates sustained some fractures. These observations of the L11/L11′ nodes are consistent with the analytical findings.

Although most of the truss span framing was severely distorted during the collapse, and many connections sustained complete or partial fractures, there was no visible evidence to indicate that the collapse initiated at any location other than the U10 nodes. With the exception of the FT10U10 top chord fracture discussed in Chapter 4, the most critically loaded floor truss elements and associated connections that were affected by the construction loading were found intact during the recovery efforts. Where members and connections were severely distorted, the observed deformation appeared consistent with one or more of the following three mechanisms:

- Distortion caused by relative movement between collapsing sections
- Impact with the ground or river bed
- Impact with a pier

Falling of the center section (i.e. bounded by the U10/U10′ nodes) relative to the adjacent framing damaged framing elements that had connections to both sections. When the center section hit the river bed, the inertia of the deck and supporting members caused large impulsive forces to develop throughout the truss system. Similar levels of forces were generated in Spans 6 and 8 when members struck the tops of piers or the ground.

Observations of the Span 6 framing indicated that, during the collapse, it moved many feet to the north, and rotated via its northern end moving to the east. Both of these global movements were due to a

northward pull from the section that fell into the river and related effects. Framing members such as stringers and bottom chords provided continuity between the falling center section and the adjacent Span 6 section after the U10 nodes came apart. As a result, the falling center section pulled Span 6 to the north. Since Span 6 was not connected to either of the supporting piers or the approach roadway, it was relatively free to move. After coming off of the bearings on Pier 5, the truss fell causing an impact between the U0-L1 members and the pier top. A similar phenomenon occurred at Pier 6, where loss of the bearings allowed the L7-L8 chord sections to fall onto the tops of the pier columns. On the east truss, this impact was severe enough to locally damage the chord element and to completely fail its connection to the L7 and L8 nodes. As this L7-L8 element was no longer supported at its ends, it could no longer carry the weight of the structure above. As the east truss dropped relative to the west truss, the framing system at Pier 6 rotated east.

While the Span 8 framing also moved towards the river, the amount of movement was less than that experienced by Span 6. This is most likely due to the fact that Span 8 was connected to Pier 7 via fixed bearings. However, the movement of Span 8 was sufficient to compromise vertical support at Pier 8, which allowed the Span 8 to drop to the ground.

7.1.5 Other Failure Scenarios

As discussed above, the failure of the bridge initiated at the U10 gusset plates due to a significant error during the original design. During the investigation, no evidence was uncovered that suggested the collapse initiated elsewhere in the structure, or from a cause other than the initial design error for the U10 gusset plates. During the course of our investigation, WJE was asked about several hypothetical failure scenarios. Comments related to these scenarios are summarized below.

- There is no evidence that the bridge collapse was the result of an act of domestic or international terrorism. The Department of Homeland Security quickly ruled out terrorism as a probable cause in the days immediately after the collapse, and subsequent investigation and analysis confirmed this assessment.
- There is no evidence indicating that scour underneath Pier 6 or Pier 7 played any role in the collapse. The river was not at flood stage at the time of the collapse, and there had not been any significant flood events in the months prior to the collapse. No evidence of scour was detected during the investigation of the collapse and the demolition of the structure.
- There is no evidence that the anti-icing system installed on the bridge played a role in the collapse. While anti-icing operations can expose structural elements to corrosive substances which can hasten the rate of corrosion in steel members, there was no evidence that this anti-icing system significantly affected the elements that dominated the structure's response to the collapse loading. As discussed in Chapters 6 and 7, the observed corrosion at the L11/L11′ gusset plates was not significant enough to make these plates more critical than the U10 gusset plates. Sporadic corrosion-related deterioration was noted elsewhere throughout the structure, mainly at or near expansion joints in the deck. As noted in Chapter 4, several of the lateral bracing connections to the main truss elements had experienced significant or total section loss. However, this corrosion did not reduce the ability of the structure to carry the collapse loading.
- There is no evidence that effects from normal traffic loads over the life of the bridge had a structurally significant effect on the overall capacity of the bridge, or contributed in any way to the collapse. There appears to be no correlation between the average daily traffic counts on the bridge, the overload permit policy, and the cause of the collapse.

- There is no evidence that ground subsidence or seismic activity played any role in the failure. Survey measurements of pier positions indicated very little post-construction movement. The portions of Piers 7 and 8 that did experience substantial movement clearly did so as a result of the collapse.
- There was no evidence that fatigue cracking contributed to the collapse. Several cracked tack welds had been previously documented and were observed. A thorough post-collapse inspection of all tension and stress reversal elements found no indications of crack extension into the truss members and no sign of fatigue damage in the critical gusset plates.

7.2 Pre-Collapse Inspections and Evaluations

7.2.1 Previous Studies

Before the August 1, 2007 collapse, the bridge had been the subject of various structural evaluations. These included: the U of M study of 1999 - 2001, the 2003 - 2007 URS study, and various inspection and load rating efforts conducted by the MnDOT. Neither of these evaluations included explicit assessment of the U10 gusset plates. The U of M study evaluated fatigue sensitivity of the truss members which is unrelated to connection strength. While the URS study included evaluation of truss response to member failure, and therefore, required consideration of connection strength; the URS approach did not include evaluation of actual connection details. Instead, they assumed the connections met the minimum requirements of the original design code which, for a properly designed bridge, is appropriate.

7.2.2 Observed Deterioration

As discussed in Chapter 4, mainly isolated areas of deterioration were identified in the various pre-collapse inspections performed by others. Notable deterioration included corrosion pitting in the L11/L11′ gusset plates, and numerous fatigue cracks in the steel beams comprising the north and south approach spans. During previous inspections performed by MnDOT and URS, no cracking or defects of concern were identified in the main truss framing.

Although the condition of the roller bearings at Piers 5, 6 and 8 had degraded to a point where their ability to move freely and accommodate thermal movements of the bridge had been somewhat compromised, the associated restraint would have increased the bridge's capacity at the time of the collapse.

The most critical area of corrosion-related section loss occurred at some of the L11/L11′ bottom chord gusset plates. However, the associated reductions in plate section remained less than the reduction caused by drilling rivet holes along adjacent – and comparably loaded – sections of the affected plates. Furthermore, acceptable load ratings could be computed using conservative assumptions to quantify member and connection strengths (including the effects of corrosion), without analyzing connection components. While this approach will overlook connection design errors, load rating efforts are not intended to check the original design of members or their connections. This is due to the fact that the presumption of proper design is established as soon as a bridge is opened to traffic.

If actual member capacity is used to establish a load rating, as opposed to conservatively using the capacity required by design, and if this capacity exceeds the minimum connection strength requirement; then the rating process must include explicit evaluation of the capacities of the member's connections. As previously discussed, acceptable rating factors for both collapse and normal operating conditions could be established without relying on actual member strengths.

When a connection has been damaged (e.g. by the effects of corrosion), it may become necessary to evaluate its actual capacity. However, even in this case, a conservative load rating can be established by simply assuming the capacities of the associated members are reduced in proportion to the degree of connection damage. As previously discussed, this conservative approach indicated acceptable L11/L11′ load ratings for the normal pre-collapse operating conditions as well as the conditions that existed at the time of the collapse. In other words, the corrosion sustained by these elements was not sufficient to require explicit determination of connection strength as part of a typical pre-collapse load review.

7.3 Summary

When the I-35W Bridge failed, the demand on the deck truss structure was dominated by its own weight, with the weight of construction material and equipment that had been placed on it and the weight of traffic playing significantly smaller roles. This demand was much less than the minimum required capacity as defined by the original design code, and less than a properly designed structure would have been able to safely carry.

Among other things, evaluation of the collapsed structure revealed the following:

- The U10 node was constructed as indicated in the design documents.
- The as-built capacity of the U10 gusset plates was much less than the capacity required by the governing design code.
- At the time of the collapse, the U10 gusset plates had not experienced any significant damage or deterioration.
- The as-built capacity of the U10 gusset plates was essentially identical to the demands that existed at the time of the collapse.
- Although other elements of the structure had experienced significant deterioration at the time of the collapse, and although other elements of the structure lacked the strength required by the original design code; at the time of the collapse, the U10 gusset plates were the most critically loaded elements in the deck truss structure.

Failure of the I-35W Bridge began with the failure of gusset plates that connected the web members to the chord members at one of the U10 nodes of the deck truss. The west U10 gusset plates were more heavily loaded than the east U10 gusset plates at the time of collapse, which makes them the likely initiation point. However, the difference in loading between the east and west U10 nodes was small enough that normal variation in such things as material properties and joint geometry could have made the less heavily loaded east U10 gusset plates slightly more critical than the west U10 gusset plates. In either case, failure of one was followed very quickly by failure of the other, which then led to the complete collapse of the deck truss system.

ACKNOWLEDGEMENTS

An investigation to determine the cause of the collapse of the I-35W Bridge was undertaken on August 2, 2008 for the Minnesota Department of Transportation on behalf of the Governor of Minnesota by Wiss, Janney, Elstner Associates, Inc. (WJE) of Northbrook, Illinois.

Throughout the investigation, personnel of the Bridge Office were very helpful. In particular, the support provided by Ed Lutgen and Dustin Thomas was timely and invaluable. Furthermore, the information provided by MnDOT's survey crews was appreciated. WJE would also like to acknowledge the efforts of the NTSB and FHWA investigators on this project. The collaborative efforts of all investigators helped to facilitate this investigation.

During the course of the field investigation the support and assistance of Terry Zoller and Eric Embacher of MnDOT construction were invaluable. Personnel of the Carl Bolander and Sons Company and Armstrong Crane and Rigging, Corporation were very cooperative. Their efforts in providing access to the site, member removal, assisting with the truss lay down area, and making their equipment and work force available to WJE requests were especially helpful and appreciated.

WJE would also like to recognize the assistance of Dr. John W. Fisher, Dr. Robert Connor, and the engineers from TranSystems Corporation during the investigation. Besides the authors of this report, the WJE project staff contributing to this report included Mark Chauvin, Wade Clarke, Jennifer Dimig, Kristin DuChateau, Jonathan Lewis, Terrence Paret, and Raymond Tide.

REFERENCES

[1] T.H. 35W State of Minnesota Department of Highways, Bridge No. 9340 Contract B Design Drawings, Sverdrup & Parcel and Associates, Inc., St. Louis, Missouri, June 18, 1965. Sheets 1 to 94,

[2] *Fatigue Evaluation of the Deck Truss of Bridge 9340,* O'Connell, H.M., Dexter, R.J., and Bergson, P.M, Department of Civil Engineering, University of Minnesota, Minneapolis, Minnesota, March 2001, 82 pgs.

[3] *Draft Report Fatigue Evaluation and Redundancy Analysis, Bridge No. 9340, I-35W Over Mississippi River*, URS Corporation, Minneapolis, Minnesota, July 2006, 295 pgs.

[4] *Executive Summary, Evaluation and Redundancy Analysis, Bridge No. 9340, I-35W Over Mississippi River*, URS Corporation, Minneapolis, Minnesota, January 2007, 4 pgs.

[5] *1961 AASHO Design Specification and 1961, and 1962 Interim Specifications.*

[6] *Minnesota Highway Department (M.H.D.) Standard Specifications for Highway Construction*, 1964

[7] *Specifications for Welded Highway and Railroad Bridges, D2.0-63 the Fifth Edition* American Welding Society

[8] *Preliminary Engineering Report, Bridge No. 9340, T.H. 35W Over Mississippi River, Minneapolis, Project I-35W-3-(47)112*, Sverdrup & Parcel and Associates, Inc., St. Louis, Missouri, April 1963, 24 pgs.

[9] Prel. Computations, Minnesota Br. 9340, Minneapolis, Sverdrup & Parcel, Dec. 1962 to March 1963

[10] Joint U12 Detail, Sverdrup & Parcel and Associates, Inc. Minnesota Bridge No. 9340, December 12, 1963

[11] Job 2083 Minn Br. #9340 Truss Design Computations, Sverdrup & Parcel, Sept. 1963 to March 1964, Sheets 1 to 223

[12] Deck Truss Spans Elevation and Details showing proposed steel grades, Sverdrup & Parcel and Associates, Inc., 1963, Modified in 1965

[13] Minnesota Bridge No. 9340 Computations for Truss Details, Sverdrup & Parcel, Nov. 1963, 21 pgs.

[14] *Comments of Meeting with Minnesota Bridge Department Relative to Structural Steels*, March 3, 1964, 3 pgs.

[15] *Memorandum for Record*, Conference in St. Paul, March 4 and 5, 1964 on Minnesota Bridge 9340, Mannes, A. K., Sverdrup & Parcel and Associates, Inc., March 11, 1964, 2 pgs.

[16] *Manual for Condition Evaluation of Bridges*, American Association of State Highway and Transportation Officials, Washington, D.C.

[17] *Guide Specifications for the Strength Evaluation of Existing Steel and Concrete Bridges*, American Association of State Highway and Transportation Officials, Washington, D.C.

[18] Construction Plan for Repair of Bridge 9340 and 9340A, Minnesota Department of Transportation, March 17, 1977, Sheets 1 to 10

[19] Pier No. 11 Pier Cap Repair, Bridge No. 9340, July 16, 1985, 1 sheet

[20] Structural Vulnerability Assessment of Critical Highway Structures for State of Minnesota, FHWA Engineering Assessment Team, December 2003

[21] Minnesota Department of Transportation, Construction Plan for Deck Repair, Bridge 9340, January 30, 1998, Sheets 0 to 61

[22] Minnesota Department of Transportation, Approach Span Steel Repair Details, Bridge No. 9340, January 4, 1999, Sheets 1 to 3

[23] Minnesota Department of Transportation, Bridge Overlay Drawings, February 7, 2007, Sheets 1 to 119

[24] *Bridge Support Strain Monitoring of Bridge 9340 - TH 35W over Mississippi,* Maxim Technologies, Inc., Twin City Testing, St. Paul, Minnesota, January 8, 1997, 8 pgs.

[25] *Bridge No. 9340 - Load Test Results*, Bergson, Paul, Department of Civil Engineering, University of Minnesota, Minneapolis, Minnesota, December 21, 1998

[26] *Meeting Minutes*, Bridge #9340, Minnesota Department of Transportation, Office of Bridges and Structures, Kivisto, Paul, November 5, 1998

[27] *Initial Inspection Report for: Fatigue Evaluation, Bridge 9340, 35W Over Mississippi River*, URS, Minneapolis, Minnesota, June 9th - June 13, 2003, 99 pgs.

[28] *Second Inspection Report for: Fatigue Evaluation, Bridge 9340, 35W Over Mississippi River*, URS, Minneapolis, Minnesota, November 17 - 18, 2003

[29] *Highway Factors Group On-Scene Investigation Report,* NTSB No. HWY-07-MH-024, National Traffic Safety Board, Office of Highway Safety, Washington, D.C., 2008

[30] Letter to Mr. Dave Rayburn at NTSB, Dorgan, D., Minnesota Department of Transportation, February 21, 2008

[31] Email from Lutgen, E., MnDOT, to McGormley, J., WJE, Re: Approach span load rating, August 8, 2008

[32] Minneapolis Fire Department table of passages over Bridge No. 9340, August 13, 2007

[33] *Standard Specifications for Construction*, Minnesota Department of Transportation, 2005

[34] *I-35W & Mississippi River Bridge Anti-Icing Project Operational Evaluation Report*, Minnesota Department of Transportation, Office of Metro Maintenance Operations, Johnson, C., Rpt No. 2001-22, July 2001, 34 pgs.

[35] Email from Niemann, T, MnDOT to Lilly, J. and Beck, C., MnDOT, Re: Thickness measurements of galvanized bridge components on the I-35W bridge, October 13, 2005

[36] *Geologic and Hydrologic Aspects of Tunneling in the Twin Cities Area, Minnesota*, Geologic Sections and Engineering Characteristics of Quaternary Units, Miscellaneous Investigation Series, Map I-1157, Plate 5, Mossler, J. H., and Olsen, B. M., Minnesota Geologic Survey, U.S. Department of the Interior, Geologic Survey, Reston, VA, 1979

[37] *Minnesota at a Glance, Earthquakes in Minnesota*, Chandler, V. W., Minnesota Geologic Survey, Regents of the University of Minnesota, St. Paul, Minnesota, 1994, 4 pgs.

[38] IRIS Earthquake Browser, http://www.iris.washington.edu/servlet/eventserver/map.do

[39] *Geologic and Hydrologic Aspects of Tunneling in the Twin Cities Area, Minnesota*, Hydraulic Properties and Tunneling Constraints, Miscellaneous Investigation Series, Map I-1157, Plate 7, Madsen, E. L., and Norvitch, R. F., Minnesota Geologic Survey, U.S. Department of the Interior, Geologic Survey, Reston, VA, 1979

[40] Inspection of MnDOT Storm Drain Tunnels Beneath I-35W Bridge, August 6 and 7, 2007, City of Minneapolis, Department of Public Works, Field Services - Sewer & Storm Drains, Ervin, R., Minneapolis, MN

[41] Weather Underground KMNMINNE17 Weather Data, University of Minnesota, Minneapolis, Minnesota, August 1, 2007

[42] Weather Data for Lower St. Anthony Falls, Minnesota, National Climatic Data Center, U.S. Department of Commerce, August 1, 2007

[43] *Structural Vulnerability Assessment of Critical Highway Structures for State of Minnesota*, Final Report, FHWA Engineering Assessment Team, December 2003, selected sections

[44] *Materials Laboratory Factual Report No. 08-096*, NTSB No. HWY-07-MH-024, National Traffic Safety Board, Office of Research and Engineering, Materials Laboratory Division, Washington, D.C., September 2008, 13 pgs.

[45] *Structural Stability Research Council Technical Memorandum No. 7: Tension Testing,* October 23, 1986.

[46] *Standard Specification for General Requirements for Rolled Structural Steel Bars, Plates, Shapes, and Sheet Piling, A6-02*, Appendix X2. Variation of Tensile Properties in Plates and Structural Shapes, ASTM International, West Conshohocken, Pennsylvania, 2005.

[47] *Materials Laboratory Factual Report No. 08-004,* NTSB No. HWY-07-MH-024, National Traffic Safety Board, Office of Research and Engineering, Materials Laboratory Division, Washington, D.C., April 18, 2008